Constitutive expression of the AR corepressor, Hey1, from a nonreplicating adenovirus, sensitises prostate cancer cells to chemotherapeutic agents through multiple pathways.

Sweeney, Katrina Gabrielle

Constitutive expression of the AR corepressor, Hey1, from a non-replicating adenovirus, sensitises prostate cancer cells to chemotherapeutic agents through multiple pathways

Katrina Gabrielle Sweeney

A thesis submitted for the degree of Doctor of Philosophy

June 2013

Viral Gene Therapy Group
Centre for Molecular Oncology
Barts Cancer Institute
Barts and The London School of Medicine and Dentistry
Queen Mary, University of London
Charterhouse Square
London
United Kingdom

Declaration

The material presented in this thesis is the result of original work carried out by the author, Katrina Gabrielle Sweeney, at the Centre for Molecular Oncology, Barts Cancer Institute, Barts and The London School of Medicine and Dentistry, Queen Mary, University of London. All external sources have been properly acknowledged

Acknowledgements

First and foremost I would like to thank my supervisor Dr Gunnel Halldén for providing me with the opportunity to carry out this project after working as a research assistant in the Viral Gene Therapy Group prior to undertaking this PhD. During the course of the PhD she imparted, without fail, sound advice and endless encouragement, which I will always be grateful for; with her guidance I gained in confidence in my abilities as a researcher.

I am also grateful to all the members of Gunnel's research group, past and present, Dr Stephan Leitner, Dr Chiat Cheong, Dr Daniel Öberg, Dr Gioia Cherubini, Dr Maria Ekblad, Dr Virginie Adam, Dr Enrique Miranda, Hector Maya Pineda, Constantia Pantelidou, Jennelle Francis and Heike Muller - for their ideas, critical appraisal and technical help throughout my time here. I have learned an incredible amount about research and without you all I would not have accomplished the vast undertaking that is a PhD. I would especially like to express my appreciation to Dr Daniel Öberg who instructed me on the intricacies of adenovirus cloning while in the lab and remotely, once back in his native Sweden; your encouragement knew no bounds. A special thank you to Dr Virginie Adam for her friendship and advice even when far away in Philadelphia - whiling away long hours in tissue culture together cemented our friendship for many years to come. I also had the opportunity of supervising three students, NaRa, Ana and Ash who produced great data including wonderful western blots. Being able to pass on technical know-how as well as helping in guiding their projects provided me with valuable experience that I will take with me to my next role.

I am very thankful to Professor Nick Lemoine for allowing me to work and then study at Barts Cancer Institute. I feel privileged to have been able to amass a small fraction of the knowledge from the numerous talented individuals who work here. I would also like to recognize the department Lab Manager, Vipul Bhakta for his tireless efforts at keeping out department organised as well as Dr Guglielmo Rosignoli for his technical expertise in flow cytometry. I would like to thank my fellow PhD students and colleagues – those that are still current and those who have moved on: Sab, Lynsey, Katrina P, Lynda, Kate, Emma,

Margot, Eiman, Delphine and many others. Your friendship and support has made my time here all the more fantastic.

Finally I would like to thank my mother, Laila, for looking after me and being there for me when times got difficult. I could not have done this without you.

Abstract

Androgen receptor (AR) cell signalling is active in most castration-resistant prostate cancer (PCa) tumours and suppression is hypothesized to impede cell proliferation. Hey1, a corepressor of AR is being investigated as a therapeutic transgene for late-stage PCa. A replication-defective recombinant adenovirus deleted for E1 and E3 and expressing Hey1 under a CMV promoter was constructed (Ad5Hey1). A dual luciferase reporter system demonstrated that Ad5Hey1 repressed AR activity in a dose dependent manner in mibolerone-stimulated 22Rv1 cells. Ad5Hey1 was cytotoxic in both AR-positive 22Rv1 and LNCaP and AR-negative DU145 cells. The doses required to kill 50% of cells (EC_{50}) were comparable to those of AdE1A12S expressing the cytotoxic E1A12S gene from an identical vector.

The mechanisms of Ad5Hey1-induced cell killing were investigated in 22Rv1 and DU145 cells. Using RNA interference towards AR or p53 in 22Rv1 cells we concluded both proteins were required for optimal cell killing by Ad5Hey1. In DU145 cells, with non-functional p53, Ad5Hey1 decreased levels of phospho-STAT3 and total STAT3 suggesting Ad5Hey1 might inhibit STAT3 signalling while the JAK1/2 inhibitor, AZD1480 was ineffective at sensitising DU145 cells to Ad5Hey1. Preliminary data therefore suggests Ad5Hey1 may interfere with JAK/STAT signalling in these cells.

Cell-killing efficacy with Ad5Hey1 in combination with cytotoxic drugs currently used in the clinic for the treatment of late-stage PCa, mitoxantrone and docetaxel, resulted in a synergistic enhancement of cell death in 22Rv1 and DU145 cells. LNCaP cells were also sensitised to the drugs. Characterisation of the mode of cell killing demonstrated augmented mitochondrial membrane depolarisation and caspase-3 activation when combined with docetaxel in all cell lines and with mitoxantrone in 22Rv1 and LNCaP cells, typical of apoptotic death. In DU145 cells, the combination of Ad5Hey1 with mitoxantrone decreased the proportion of apoptotic cells suggesting cells are dying by alternative cell death mechanisms.

In this thesis I have demonstrated that Ad5Hey1 potently eliminates PCa cells both in the presence and absence of functional AR or p53, and that cell killing is

improved in combination with cytotoxic drugs. I demonstrate that the mechanisms by which Ad5Hey1 acts as a cell death enhancer is mainly through cooperation with drugs on apoptotic pathways while other factors such as inhibition of survival are also involved. In conclusion, these data suggest that it is feasible to develop a future replication-selective adenovirus expressing Hey1 as a cytotoxic transgene to improve antitumour efficacy *in vitro* and *in vivo,* especially in combination with apoptosis-inducing drugs.

Abbreviations

5-FC: 5-flurocytosine

5-FU: 5-fluorouracil

ACTH: Adrenocorticotropic hormone

Ad5: adenovirus type 5

ADT: androgen ablation therapy

AF: activation factor

AR: androgen receptor

ARA: AR-associated

ARE: androgen-response elements

ARNT: aryl hydrocarbon receptor nuclear transporter

ATCC: American Type Tissue Culture Collection

Bak: Bcl-2-antagonist/killer-1

DAPI: 4’,6-diamidino-2-phenylindole

Bax: Bcl-2-associated X protein

Bcl-2: B-cell lymphoma 2

bHLH: basic helix-loop-helix

Bid: BH3 interacting death protein

BMP: bone morphogenic protein

bp: base-pair

BRCA: breast cancer antigens

CAB: complete androgen blockade

CAR: coxsackie adenovirus receptor

CARNs: castration-resistant Nkx3.1-expressing cells

CBP: (CREB)-binding protein

CD: cluster of differentiation

CDK: cyclin dependent kinase

c-FLIP: cellular FLICE-inhibitory protein

ChIP: chromatin immunoprecipitation

CMV: cytomegalovirus

CPA: cyproterone acetate

CPE: cytopathic effect

CR: conserved region

CREB: cAMP response element binding protein

CRPC: castration resistant prostate cancer

CtBP: C-terminal Binding Protein

CTLA-4: cytotoxic T-lymphocyte-associated antigen 4

DBD: DNA-binding domain

DHEA-S: dehydroepiandrosterone-sulfate

DHT: dihydrotestosterone

DISC: death-inducing signalling complex

DLL: Delta-like proteins

DMEM: Dulbecco's Modified Eagle medium

DNA: deoxyribonucleic acid

DRE: digital rectal exam

GAPDH: glyceraldehyde-3-phosphate dehydrogenase

GST: glutathione S-transferase

GBM: glioblastoma multifome

EC_{50}: effective concentration dose required to kill 50% of cells

EGF: epidermal growth factor

EMT: epithelial mesenchymal transition

ERK: extracellular-signal-regulated kinases

ERSPC: European Randomized Study of Screening for Prostate Cancer

FasL: Fas ligand

FBS: fetal bovine serum

FDA: Federal Drug Administration

FGF: fibroblast growth factor

FITC: fluorescein

FSH: follicle-stimulating hormone

GFP: green fluorescence protein

h: hours

HAT: histone acetyltransferase

HDAC: histone deacetylases

HGPIN: high-grade prostatic intraepithelial neoplasia

HER2/neu: human epidermal growth factor receptor 2

HES: hairy and enhancer of split protein

HEY: Hairy/enhancer of split with YPRW-like motif protein

hKh2: human glandular kallilrein-2

HDM2: human double minute 2

HPC-1: hereditary prostate cancer locus-1

HRPC: hormone refractory prostate cancer

HSPG: heparan sulfate proteogylcans

HSP: heat shock protein

IGF-1: insulin-like growth factor 1
IHC: immunohistochemistry
IL: interleukin
ITR: inverted terminal repeat
JAK: Janus kinase
kDa: kiloDalton
LBD: ligand-binding domain
LH: luteinizing hormone
LHRH: luteinizing hormone-releasing hormone
LSD1: lysine specific demethylase
MAGE-11: melanoma antigen gene protein-A11
MAPK: mitogen-activated protein kinase
Mcl-1: myeloid cell leukaemia sequence 1
MED: Mediator
MEF: mouse embryonic fibroblast
MEK: MAPK extracellular kinase
MFI: mean fluorescence intensity
MHC: major histocompatibility complex
min: minutes
mRNA: messenger RNA
miRNA: micro RNA
MLP: major late promoter
mTOR: mammalian target of rapamycin
MTS: 3-(4,5-dimethylthiazol-2-yl)-5(3-carboxymethoxyphenyl)-2-(4-sulphophenyl)-2H-tetrazolium
N: number of times an experiment was repeated
NCoR : nuclear receptor coreprepssor
NF-κB: nuclear factor-κB
NLS: nuclear localisation signal
NTD: N-terminal domain
OriR : Origin of Replication
PCa: prostate cancer
PCR: polymerase chain reaction
pfu: plaque forming unit
P/CAF: p300/CBP-associated factor
pH3: phospho-histone 3+
PI3K: phosphatidylinositide 3-kinase

PIC: preinitiation complex

PIN: prostatic intraepithelial neoplasia

PMS: phenazine methosulphate

ppc: particles per cell

pRB: retinoblastoma tumour suppressor protein

PolyQ: polyglutamine

PSA: prostate specific antigen

PTEN: phosphatase and tensin homologue deleted on chromosome 10

Puma: p53 upregulated modulator of apoptosis

QPCR: quantitative polymerase chain reaction

RNA: ribonucleic acid

RPMI: Roswell Park Memorial Institute medium

RGD: arginine-glycine-aspartic acid

RTK: receptor tyrosine kinase

SIRT1: sirtuin 1

Skp2: S phase kinase associated protein 2

SMRT: silencing mediator of retinoic acid

SNP: single nucleotide polymorphism

Src: sarcoma-related kinase

SRC: steroid-receptor-coactivator

STAT: signal transducer and activator of transcription

T-ALL: T-cell lymphoblastic/lymphoma

TAU: transactivation domain

TBP: TATA-binding protein

$TCID_{50}$: tissue culture infectious dose 50%

TGF-β: transforming growth factor-β

TIF2: transcription intermediary factor 2

TMRE: tetramethylrhodamine ethyl ester percholate

TRAPP: transactivation/transformation domain-associated protein

TRAMP: transgenic adenocarcinoma of the mouse prostate

TRAIL: TNF-related apoptosis-inducing ligand

TSA: trichostatin A

VA: virus associated RNA

VCAM-1: vascular cell adhesion molecule 1

VDAC: voltage-dependent anion channel

vp: virus particle

Contents

List of Figures

List of Tables

1. Introduction

1.1. Prostate cancer

1.1.1. The normal prostate

The prostate gland is located beneath the bladder and surrounds the urethra. In the presence of foetal androgens, the embryonic prostate develops from the embryonic urogenital sinus, which is composed of urogenital sinus epithelial cells and mesenchymal cells (Schulz, Burchardt et al. 2003). Interactions between these two cell types are obligatory for prostate development. Mesenchymal cells express the androgen receptor (AR) and upon stimulation by testosterone, paracrine signalling from the mesenchymal cells induces epithelial bud formation, growth and branching and promotes epithelial differentiation into secretory epithelial cells (Cunha, Hayward et al. 2003). Reciprocal signalling from epithelial cells results in spatial patterning and smooth muscle differentiation in the mesenchymal cells, which develops into mature prostatic stroma (Cunha, Hayward et al. 2003). The embryonic prostate remains quiescent until puberty when, under the stimulation of testosterone, the prostate gland grows to consist of 30-50 branched ducts lined with glandular epithelium (Giles 2010). The function of the prostate is to secrete factors required for sperm motility and viability. It also protects the male urinary and reproductive system from pathogens (Giles 2010).

The adult prostate gland is composed of a fibromuscular stromal compartment surrounding glandular epithelial acini. The glandular epithelial compartment is composed of multiple differentiated cell types including basal, secretory luminal and neuroendocrine cells (Figure 1). The glandular compartment is made up of the large peripheral zone and the smaller central zone, which makes up 95% of the gland. Approximately 70% of prostate cancers develop in the peripheral zone (Schulz, Burchardt et al. 2003). In the adult prostate, the cells within the stromal compartment are responsible for inducing and maintaining epithelial differentiation. AR-expressing stromal cells respond to androgen thus stimulating the production and secretion of growth factors, which in turn signals

to epithelial cells to induce either intermediary transit-amplifying cells to progress through the cell cycle or repress apoptosis of secretory luminal cells (Litvinov, De Marzo et al. 2003). Luminal secretory cells express high levels and respond to androgen stimulation by producing and secreting of prostatic-specific differentiation proteins such as prostate specific antigen (PSA) and human glandular kallilrein-2 (hKh2) which influence proliferation and differentiation of stromal cells (Litvinov, De Marzo et al. 2003). It is a matter of debate whether basal cells express AR, however, an alternatively spliced AR variant termed AR3 has recently been detected in basal cells and stromal cells of benign prostate tissue. It is not known whether this variant has any influence on paracrine and autocrine signalling within the prostate (Guo and Qiu 2011). In the normal prostate, AR has been shown to function as a growth suppressor wherein AR-negative intermediate epithelial cells transgenically induced to express AR were inhibited to proliferate *in vitro* after androgen stimulation even in the presence of growth factors (Whitacre, Chauhan et al. 2002). Moreover, AR induces differentiation of transit-amplifying cells to a terminally differentiated phenotype through a mechanism related to AR up-regulation of p27 cyclin-dependent kinase inhibitor and repression of the S phase kinase associated protein 2 (Skp2) (Litvinov, De Marzo et al. 2003).

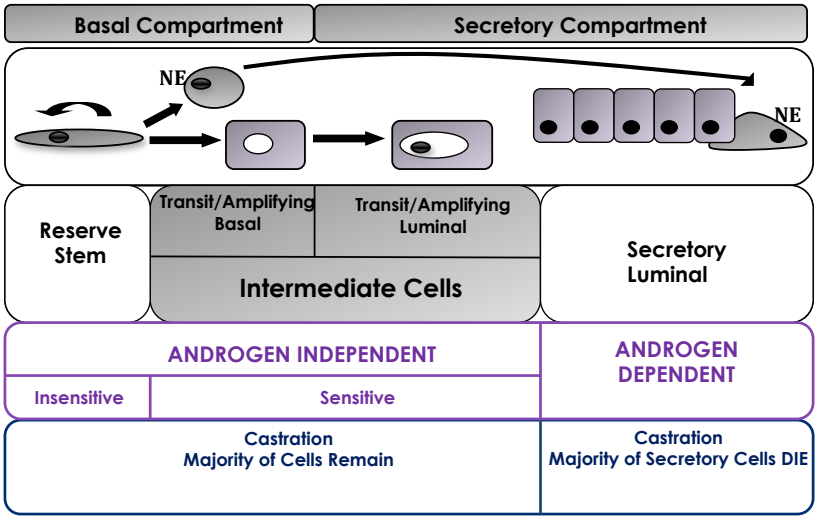

Protein Marker expression				
AR	-/+		-/+	+
p63	+		-	-
Bcl-2	+		+	-
p27	+	-	-/+	+
Cytokeratin	5 & 14	5, 8, 14 & 18		8 & 18

Figure 1. Model of prostatic epithelial cell compartmentalisation

The epithelial compartment consists of several types of cells: stem cells, basal, intermediate, neuroendocrine and luminal secretory which bear defining cytokeratin profiles and differ in expression in a number of proteins including AR, p63, Bcl-2, and p27. +, expression of marker, -,lack of expression marker, NE (neuroendrocrine). Figure adapted from (Litvinov, De Marzo et al. 2003). Stem cells are located in the basal epithelial layer and give rise to a progenitor (transit-amplifying) cells, which either remain in the basal layer or differentiate and move into the secretory epithelial layer becoming terminally differentiated secretory luminal cells or neuroendocrine cells (Litvinov, De Marzo et al. 2003). Controversy exists about the hierarchical arrangement of prostatic stem and linear-specific progenitor cells. In this figure a linear arrangement is shown, however other models have been proposed (Taylor, Toivanen et al. 2010).

1.1.2. Natural progression of PCa

Since the majority of prostate cancer (PCa) begins in the peripheral zone and retains some glandular structure, these are categorised as adenocarcinomas. The earliest precursor of PCa is detected as prostatic intraepithelial neoplasia (PIN) defined as a thickening of the epithelial layer with basal and secretory luminal layers becoming less distinct with cells expressing both basal and secretory markers such as cytokeratins, AR and PSA (Schulz, Burchardt et al. 2003). Most adenocarcinomas arise from high grade PIN (HGPIN) that in turn arises from low grade PIN. While cell proliferation remains low in PIN, PCa is thought to occur due to low rate in apoptosis since the rate of cell growth

remains low during PCa development (Schulz, Burchardt et al. 2003). Both PCa and HGPIN have phenotypic and morphological characteristics that are similar to secretory luminal cells but have retained features of basal epithelium cells such as expression of anti-apoptotic protein B-cell lymphoma 2 (Bcl-2), DNA replication and self-renewal capacity (Litvinov, De Marzo et al. 2003).

PCa develops with a number of different foci occurring within the gland, which vary according to the amount of cellular dysplasia, tissue disorganisation and heterogeneity (Schulz, Burchardt et al. 2003). One third of PCas remain indolent with respect to growth and have no clinical symptoms however others are more aggressive, becoming locally invasive and spreading beyond the tissue capsule and/or metastasise to lymph nodes and distant organs such as the bone, liver and lung (Schulz, Burchardt et al. 2003). During the initial stages of PCa development, AR no longer functions as a growth suppressor. In contrast to normal prostate, the secretory luminal cells express higher levels of AR resulting in enhanced growth rather than terminal differentiation. During the initial stages of PCa, cell growth is still dependent on the binding of androgen to the AR receptor. However due to the heterogeneous nature of PCa, some cells will express AR that do not require androgen stimulation for growth. Androgen ablation therapy (ADT), discussed later on in this chapter, will only induce apoptosis in androgen-dependent cells (Figure 1) but will not eliminate androgen-independent PCa cells and this will eventually result in castration resistant prostate cancer (CRPC) phenotype (Figure 1) (Litvinov, De Marzo et al. 2003).

1.1.3. Aetiology of PCa

PCa is the second cause of male cancer mortality in the United Kingdom (UK) and in 2010, 40975 new cases of PCa were recorded in the UK and 10721 people died from it (www.cancerresearchuk.org). PCa incidence is strongly correlated to age; in the UK between 2008 and 2010, approximately 75% of cases were diagnosed in men over the age of 65 while only 1% of cases were diagnosed in the under-50 age group (www.cancerresearchuk.org). The highest incidence is in the 75-79 age group with 794 cases per 100000 men (Williams, Hughes et al. 2011).

As with many other cancers, PCa is a multifactorial disease and no definite cause has been demonstrated and both environmental factors and genetic predisposition play roles in PCa development (Kral, Rosinska et al. 2011). More than 85% of PCa are sporadic while only 10-15% are classified as familial or hereditary. PCa has become a significant problem in Western industrialized countries and immigrant studies have indicated that genetic causes can be partially attributed to this observation. The most important locus implicated in familial PCa was hereditary prostate cancer locus-1 (HPC-1) for which RNASEL was the candidate protein product of this locus. Carriers of mutant RNASEL develop PCa under the age of 65 and have a more aggressive cancer (Kral, Rosinska et al. 2011). In addition to Breast Cancer Antigens (BRCA) 1 and 2 providing information as to a genetic predisposition for breast and ovarian cancer, mutations in these genes in men are also associated with a higher risk of hereditary PCa. Mutations in BRCA1 are often related to men younger than 65 years developing PCa (Kral, Rosinska et al. 2011) and a germline mutation in BRCA2 has been associated with an increased susceptibility to PCa and may account for 2% of PCa cases in men less than 55 years of age (Edwards, Kote-Jarai et al. 2003).

The incidence and mortality of PCa also vary between countries; men in Asia have a low risk of developing PCa whereas men have a higher risk in the United States of America (USA) and Western Europe. Scandinavia has the highest incidence of PCa. This suggests that race and ethnicity are PCa risk factors. In the USA, the highest reported incidence of PCa from one ethnic group was in African-American men. The incidence in white and African-American men was 156 and 248 per 100000 respectively and the difference in mortality rate was 25 and 59 per 100000 respectively (Jemal, Siegel et al. 2008). African American men also have a worse staging, tumour grading and more aggressive phenotype compared with Caucasian men (Robbins, Torres et al. 2007). One study confirmed the association of genetic variants of chromosome 8q24 were linked to a high incidence of PCa in African populations (Robbins, Torres et al. 2007). Genomic profiling of human PCa has demonstrated certain chromosome regions including regions p and q on chromosome 8 harbour PCa susceptibility genes. Mutations and sequence variants of genes in these regions have been reported to be associated with PCa risk and frequent genomic rearrangements are observed within these regions in prostate tumours (Shen and Abate-Shen 2010). Epidemiological studies have also shown that men of African descent

have a higher incidence of polymorphism for the gene encoding 5α-reductase, the enzyme responsible for converting the androgen, testosterone to the more potent AR ligand, dihydrotestosterone (DHT). This polymorphism results in higher 5α-reductase enzyme activity and men of Asian descent who have a low risk of developing PCa also have a lower incidence of this polymorphism (Makridakis, Ross et al. 1997).

Genomic profiling of human PCa has identified alterations in copy number and chromosomal rearrangements associated with prostate tumourigenesis. Somatic alterations have been identified by comparative genomic hybridisation as amplifications in chromosome 8q and losses in 3p, 8p, 10q, 13q and 17p. Key regulatory genes implicated in the development of PCa have been mapped to within these chromosome regions include Nkx3.1 at 8p21, phosphatase and tensin homologue deleted on chromosome 10 (PTEN) at 10q23, c-Myc at 8q24 and CPY17 at 10q24. Chromosomal rearrangements have also been implicated as a novel pathogenic mechanism for PCa development. In 15% of high-grade PIN lesions and 50% of localised PCa cases, the TMPRSS2-ERG fusion is detected and leads to the overexpression of the transcription factor ERG from the androgen-regulated TMPRSS2 promoter. The fusion of these to genes is thought to arise by androgen stimulation (Tomlins, Rhodes et al. 2005; Bastus, Boyd et al. 2010).

Additionally, lifestyle factors and in particular diet have also been implicated in contributing to PCa incidence. In the Western diet, there is an absence of protective elements such as selenium, folate and phytoestrogens from the diet while the ingestion of high levels fat, dairy and red meat have been found to be risk factors (Schulz, Burchardt et al. 2003). This has been demonstrated in Japanese men in the USA who had a higher risk of developing PCa compared with their counterparts in Japan, a country that has a lower rate of PCa incidence (Sim and Cheng 2005). Antioxidants such as vitamin E, β-carotene present in tomatoes and selenium have also been associated with a reduction in cancer risk when ingested by PCa patients. They operate as a reactive oxygen species that prevent DNA damage and mutation during oxidative stress that would otherwise result in cellular transformation (Chan, Gann et al. 2005). In autopsy studies, the Innuit population of Greenland had a very low prevalence of latent prostate carcinoma compared to other populations (including Asian populations). This was attributed to the high intake of omega-3 fatty acids and

selenium in their diet, reiterating significance of certain dietary components that are protective against prostate cancer (Dewailly, Mulvad et al. 2003). Other lifestyle factors determining the development of PCa include physical fitness. Epidemiological studies found that men who are physically active (measured by fitness) have between a 30 and 60% reduced risk of developing PCa compared with men who were physically inactive (Oliveria and Christos 1997).

1.2. PCa treatment

1.2.1. Diagnosis and PCa staging

Historically, diagnosis for PCa has been carried out using the digital rectal exam (DRE) and/or serum levels of PSA, an androgen-regulated serine protease present in the semen and used as a biomarker for PCa progression. However early stage PCa detection using PSA is lacking due to reduced specificity between levels of PSA in a normal individual vs. a PCa patient. Examination of histopathological biopsies from the prostate gland confirms the diagnosis. The Gleason Score, which measures the extent of tumour differentiation, is the most common method of grading PCa where a score of between 2 and 10 is given (2 is the least aggressive while 10 is the most aggressive form). This score is the sum of the two most common patterns of tumour growth (grades 1-5). Local staging (T staging) of the cancer is carried out by the DRE, PSA levels and tumour grade and from this the risk of patients possessing locally advanced PCa are established (Bjartell 2006; Damber and Aus 2008). In the UK, patients are categorised into risk groups to estimate the post-treatment outcome for the particular treatment used. Low risk patients with PSA ≤ 10ng/ml, Gleason score of ≤ 6 and staged at T1c to T2a or who have a life expectancy of less than 10 years are actively monitored as the first choice of treatment. Those patients with a longer life expectancy or in a higher risk group (intermediate risk: PSA 10-20ng/ml, Gleason score of 7 and with T2b staged disease or high risk: PSA ≥ 20ng/ml, Gleason score of 8 and T2c stage) are recommended a curative treatment (Damber and Aus 2008). In the USA, an aggressive screening policy has been adopted and this is often attributed to a reduced mortality rate for PCa. The updated outcome from the European Randomized Study of Screening for Prostate Cancer (ERSPC) concluded PSA-based screening reduced the risk of

death from PCa by 21% in the screening group but that this was linked to a high risk of over-diagnosis wherein 1410 men would need to be screened and 48 cases of PCa to be treated to prevent one death (Heidenreich 2012; Schroder, Hugosson et al. 2012). The recent identification of 23 susceptibility loci through single nucleotide polymorphism (SNP) genotyping of >25000 PCa samples may be valuable biomarkers for PCa screening in the future (Eeles, Olama et al. 2013).

1.2.2. Treatment of localised and locally advanced PCa

Treatment options and regimens for PCa depend on clinical stage, Gleason score and PSA levels at time of presentation and patients can undergo a number of different treatments depending on their assessed risk of developing PCa. Previously, in the UK, “watchful waiting” was symptom-guided treatment management for early PCa however surgery provided a survival advantage over this treatment option (Bill-Axelson, Holmberg et al. 2005). Nevertheless, watchful waiting is a treatment option for patients with localised PCa with limited life expectancy (Heidenreich 2012), 2012 #100}. Another conservative method of treating PCa is with “active surveillance,” patients undergo PSA screening and prostate biopsies and are treated at thresholds defining disease progression (Heidenreich 2012).

Approximately 25% of patients present with localised PCa and for these patients curative procedures are mainly single-modality treatments such as radical prostatectomy or radiotherapy (external-beam radiotherapy or brachytherapy). As PCa is driven in part by testosterone, ADT or androgen ablation therapy (see section 1.2.3) aims to reduce circulating testosterone and is used at all stages of the disease. AR antagonists are also used as initial treatment options and aim to inhibit AR activity within PCa cells. Patients presenting with higher Gleason scores and rising PSA levels can benefit from radiotherapy in conjunction with ADT and locally advanced PCa (extracapsular extensions of the tumour) are treated with combined treatment; either surgery and adjuvant radiotherapy or radiotherapy with ADT (Heidenreich 2012).. Recurrence of PCa after definitive treatment is also treated with ADT as a salvage treatment.

An alternative treatment for patients with localised PCa is cryosurgery ablation, a minimally invasive alternative to surgery. However long-term results are lacking and 5-year disease-free survival is inferior to that achieved by radical prostatectomy in low-risk PCa patients. Other minimally invasive experimental treatment options include high-intensity focused ultrasound, which heats malignant tissue to above 65°C thereby destroying it by coagulative necrosis (Heidenreich 2012).

Despite technical advances in surgery, radiotherapy as single modality treatments or combined with hormone therapy, between 27-53% of patients develop local or distant recurrences within 10 years of initial therapy and 16-35% of patients receive second-line treatment within 5 years of initial treatment (Heidenreich 2012). Treatment failure is defined as rising PSA level (Pound, Partin et al. 1999). Localised failure is characterized with a late PSA increase (>12months after treatment), long PSA-doubling time and a less aggressive disease at diagnosis having been made. Systemic failure is classified as a rapid PSA doubling time with significant pathological changes. Patients with local failure with a life expectancy of between 5 and 10 years are often offered a second treatment such as radiotherapy if their first-line treatment was surgery (Simmons, Stephenson et al. 2007). Men who received radiotherapy as their initial treatment have the option of salvage radical prostatectomy, brachytherapy, cryotherapy or ultrasound. Patents who are at risk of systemic failure are treated with hormonal therapy (Heidenreich 2012).

1.2.3. Treatment of advanced androgen-dependent PCa

Historically ADT was the mainstay therapy for advanced PCa. Charles Huggins pioneered ADT in 1941 when he demonstrated that lowering testosterone by surgical castration or injection of oestrogens resulted in a major regression of PCa and relief in symptoms (Huggins 1941). In recent years there has been a move towards increasing the use of hormonal treatment in younger patients with earlier disease (non-metastatic) or recurrent disease after definitive treatment as a single agent or multi-modal approach. However, for patients with metastatic PCa, ADT is usually the first-line treatment. In more advanced forms (CRPC),

although it can effectively alleviate symptoms, it does not extend life (Heidenreich 2012).

Testosterone release is regulated by the hypothalamic-pituitary-gonadal axis. Luteinizing hormone-releasing hormone (LHRH) when released in a pulsatile fashion stimulates the anterior pituitary gland to release luteinizing hormone (LH) and follicle-stimulating hormone (FSH). LH induces the Leydig cells in the testes to secrete testosterone (Choi and Lee 2011). In prostate cells, testosterone is converted to the more potent androgen, DHT. By inhibiting secretion of testicular androgens or DHT prostate cells are deprived of androgenic stimulation and undergo apoptosis. There are several approaches treating androgen-dependent PCa: testosterone lowering therapy, antiandrogenss and complete androgen blockade.

1.2.3.1. Testosterone lowering therapy

Otherwise known as medical castration, LHRH agonists such as leuprolide (Lupron®; Eligard®) mimic LHRH by inhibiting LH production by continuous pituitary stimulation, overcoming the pulsatile release of LHRH (Allen, O'Shea et al. 1983; Choi and Lee 2011). Shutdown of testosterone production is however initially preceded with a surge of LH and testosterone (known as a “flare”) resulting in a temporary increase in PCa growth and worsening of symptoms. The flare effect can be inhibited if non-steroidal antiandrogens are given before the LHRH agonist. In contrast, LHRH antagonists (e.g. abarelix and degarelix) competitively bind to LHRH receptors in the pituitary gland (Mongiat-Artus and Teillac 2004) and decrease LH, FSH and testosterone without the “flare” effect.

1.2.3.2. Antiandrogens

There are two classes of antiandrogens, steroid and non-steroidal. Both are classed as AR antagonists as they compete with endogenous androgens for binding to ligand-binding domain (LBD) of the AR and to prevent AR transcription activity. Steroidal androgens include cyproterone acetate (CPA), which has partial agonist activity. It can also activate the progesterone and glucocorticoid receptors and is therefore not used as a first-line treatment. Non-steroidal antiandrogens include flutamide, nilutamide and bicalutamide

(Casodex®) and were developed to circumvent off-target effects of steroidal antiandrogens. The exact mechanism by which AR antagonists block AR transcriptional activity remains elusive and recent studies have demonstrated the mechanism-of-action to be more complicated than simply competitive binding with DHT for AR binding. It has been suggested that bicalutamide mediates recruitment of AR corepressors (Masiello, Cheng et al. 2002; Shang, Myers et al. 2002; Hodgson, Astapova et al. 2005). Later, AR antagonist activity was proposed to be independent of AR coactivator-to-corepressor ratio and rather due to the failure of bicalutamide-liganded AR to recruit coactivators (Hodgson, Astapova et al. 2007). Bicalutamide was approved in 1995 by the Federal Drug Administration (FDA) and is the most commonly used antiandrogen. It has a 2-fold increased affinity to AR compared with flutamide and nilutamide, a longer half-life (>1 week) and significantly decreased toxicities (Schellhammer, Venner et al. 1997).

1.2.3.3. Combined androgen blockade

Although medical castration reduces serum testosterone levels by 95%, intraprostatic androgen is maintained due to circulating androgen of adrenal origin being converted into DHT. Adrenal androgens can be inhibited with the addition of antiandrogens to medical castration treatments. This approach is known as complete androgen blockade (CAB) (Hellerstedt and Pienta 2002). Systemic reviews and meta-analyses at a follow up of 5-years shows that the combined approach provides a small survival advantage (<5%) versus monotherapy (Heidenreich 2012). Antiandrogens as a monotherapy are better tolerated with fewer side effects (sexual dysfunction, hot flashes, weight gain, diabetes mellitus and coronary heart disease and decrease bone mineral density) than other androgen lowering approaches or CAB and is of benefit to patients treated with radiotherapy for locally advanced disease (Iversen, Tyrrell et al. 2000). However monotherapy was found to be inferior in patients with metastatic disease (Tyrrell, Kaisary et al. 1998) and a trend towards decreased survival in patients with early, localised disease (Iversen, Tyrrell et al. 2000). A limitation for all currently approved antiandrogens is that a certain proportion of patients will respond to selective discontinuation of the drug termed “androgen withdrawal syndrome” resulting in a decline in PSA and regression of the tumour

which is indicative of antiandrogens serving as AR agonists (Kelly and Scher 1993; Schellhammer, Venner et al. 1997).

1.2.3.4. Novel antiandrogens

Due to the shortcomings of currently available antiandrogens, extensive research has focused on the development of novel AR antagonists. One such second-generation antiandrogen, enzalutamide (formerly MDV-3100), was approved by the FDA in 2012 for the treatment of patients with CRPC previously treated with chemotherapy after enzalutamide demonstrated a significant survival benefit in patients compared with placebo (Scher, Fizazi et al. 2012). Based on a non-steroidal thiohydantoin agonist, RU59063, it is able to bind AR with 8-fold higher affinity compared with bicalutamide and does not activate wild-type AR or T877A or W741C AR mutants. Inhibition of AR-mediated transcription and cell growth in AR over expressing cell lines was superior to bicalutamide and induced tumour regression in LNCaP/AR xenografts model. Whereas bicalutamide causes AR to translocate to the nucleus and bind to androgen-response elements (ARE) within DNA, enzalutamide is less efficient at doing so and a significant fraction of AR remains in the cytosol with nucleus-localised enzalutamide-bound AR not binding to DNA (Tran, Ouk et al. 2009). Most strategies involve targeting the C-terminal LBD of the AR, however Sadar *et al* have identified a compound (EPI-001) derived from marine sponge extracts, which targets the N-terminal domain (NTD). EPI-001 is able to inhibit regulation of androgen-regulated genes and significantly prevented ligand-dependent and –independent transactivation of the AR as well as blocking constitutively active ΔLBD-AR mutants. Mechanistically, EPI-001 reduces the interaction of AR with AR-target genes and it decreased the interaction of AR coactivators p300/CBP and RAP74 thereby blocking protein-protein interactions required for stabilisation of AR on ARE. EPI-001 is still at the preclinical stage of development and was found to supress growth of LNCaP xenografts in non-castrated mice and resulted in regression of an orthotopic LNCaP xenograft in castrated mice (Andersen, Mawji et al. 2010; Sadar 2011).

1.2.4. Treatment of castration resistance cancer

Despite achieving castrate levels of serum testosterone <50ng/dL or <1.7nmol/L prostate cancers that are progressing are considered castrate resistant (CRPC). CRPC however is still sensitive to low levels of androgens, derived by the conversion of weak adrenal androgens to testosterone or *de novo* androgen synthesis from cholesterol. As a result, patients are receptive to secondary hormone manipulations such as LHRH agonists, CAB, antiandrogen withdrawal and corticosteroids, which inhibit adrenal androgen synthesis (described below).

After 12-18 months the tumour cells develop resistance and once men have developed metastatic CRPC, cytotoxic therapy is a treatment option alongside adrenal androgen suppressants. However, this form of PCa is the final stage of the disease and the goal is symptom palliation as opposed to cure. In this section current treatment options will be described as well as novel approaches which are currently in development.

1.2.4.1. Steroid biosynthesis inhibitors

Conventional hormonal therapies have focused on agents that block androgen signalling by either decreasing circulating testosterone or through competition for binding with the AR. Medical castration, reduces serum testosterone to 10ng/ml but does not affect the levels of the androgens produced in the adrenal glands such as dehydroepiandrosterone-sulfate (DHEA-S) (Chen, Clegg et al. 2009). Adrenal-derived androgens are synthesised from their respective precursors pregnenolone and progesterone, into DHEA-S and androstenedione by the cytochrome P450 CYP171A enzyme after which synthesis of testosterone and DHT from these weak androgens occurs in peripheral tissue, including PCa tumours (Cai and Balk 2011). Strategies for inhibiting adrenal androgen synthesis have involved blocking adrenal androgen production at several stages. Adrenocorticotropic hormone (ACTH) stimulates the conversion of cholesterol to pregnenolone. By administering glucocorticoids (e.g. prednisone) ACTH-mediated stimulus is inhibited resulting in a decrease in adrenal androgen production. Currently glucocorticoids are administered as an adjunct to chemotherapy. A non-selective inhibitor of P450 such as

ketoconazole was administered in combination with androgen withdrawal in a phase III trial and resulted in a longer time to PSA progression compared with androgen withdrawal alone. However, there was no difference in overall survival (Small, Halabi et al. 2004). In contrast, abiraterone, a pregnenolone analogue, which binds specifically and irreversibly to CYP17A1, has afforded more success compared with ketoconazole. The FDA approved it in 2011 as a second-line treatment for CRPC after docetaxel treatment (Danila, Morris et al. 2010; Reid, Attard et al. 2010; Fizazi, Scher et al. 2012) and approval was further expanded in 2012 for use as a first-line therapy for chemotherapy-naïve patients (de Bono, Logothetis et al. 2011; Ryan, Smith et al. 2013). However despite the relative success of abiraterone, patients in the initial Phase I/II trials have progressed as a result of AR activation. The recurrence of AR activity in these patients has been suggested to be as a result of increased activity of steroid compounds upstream of CYP171A in the steroidogenesis pathway, which may activate mutated AR proteins. It has been postulated that abiraterone may in fact become an agonist due to the steroid backbone structure of the compound (Chen, Clegg et al. 2009).

1.2.4.2. Chemotherapy

In the early 1990s, metastatic CRPC was considered a chemo-refractory disease. The chemotherapeutic drugs, mitoxantrone, estramustine and docetaxel are approved by the FDA for first-line treatment of metastatic CRPC. A landmark TAX-327 trial comparing docetaxel and mitoxantrone in combination with prednisone showed improved survival in the arm where patients received docetaxel every three weeks compared with weekly docetaxel or mitoxantrone (Berthold, Pond et al. 2008). In the Southwest Oncology Group (SWOG) 99-16 trial docetaxel/estramustine and mitoxantrone/prednisone regimens were compared (Petrylak, Tangen et al. 2004). Docetaxel was reported to be superior to mitoxantrone in terms of median survival and time to progression although no objective tumour response differences were found. However it is more toxic than mitoxantrone and only improves median survival by 2 months (Tannock, de Wit et al. 2004). Patients who have failed doxetaxel treatment can be offered cabazitaxel, a novel taxane approved by the FDA in 2011 for the treatment of CRPC with prednisone (Galsky, Dritselis et al. 2010). It differs from docetaxel in that it is a poor substrate for the multi-drug resistant P-glycoprotein efflux pump

overexpressed in taxane-resistant tumours (Mita, Denis et al. 2009). Mitoxantrone decreases the length and severity of pain despite it having no effect on overall survival (Tannock, Osoba et al. 1996). Patients who fail first-line chemotherapy have limited treatment options and mitoxantrone is used for palliative care in men with CRPC. As docetaxel and mitoxantrone are first-line treatments for metastatic CRPC our research group have combined these drugs with adenoviral mutants to improve viral potency and tumour efficacy for the treatment of CRPC (Oberg, Yanover et al. 2010; Radhakrishnan, Miranda et al. 2010; Miranda, Maya Pineda et al. 2012).

1.2.4.2.1. Docetaxel

Docetaxel is semi-synthetic analogue of paclitaxel and has high affinity to β-tubulin monomers thereby stabilising microtubules and arresting their depolymerisation (Ringel and Horwitz 1991). Stabilisation of microtubules prevents cell processes such as mitosis, endosomal uptake, secretion and transport required for growth and proliferation. The therapeutic response of docetaxel (and paclitaxel) is mediated through apoptosis and mitotic catastrophe (Jordan, Wendell et al. 1996; Morse, Gray et al. 2005). Mitotic catastrophe, a process considered to be an irreversible trigger to cell death, occurs as a result of aberrant mitosis or missegregation of chromosomes following cell division. In androgen-independent PCa cells, DU145 and PC3, docetaxel induced G2/M arrest, which preceded mitotic exit followed by apoptosis (Fabbri, Amadori et al. 2008). Docetaxel-induced apoptotic cell death is thought to occur as a result of inactivation of the Bcl-2 protein through phosphorylation (Haldar, Chintapalli et al. 1996; Herbst and Khuri 2003). Other mechanisms of anti-neoplastic action by docetaxel include anti-angiogenic activity possibly by inhibiting angiogenic growth factors such as vascular endothelial growth factor (VEGF) (Herbst and Khuri 2003).

1.2.4.2.2. Mitoxantrone

Mitoxantrone is a synthetic derivative of anthracycline originally synthesised in 1979 and alongside doxorubicin, belongs to a class of agents known as the anthracenediones. It has numerous modes of action, possessing antiviral, antibacterial, immunomodulatory, and antitumor activity (Fox 2004). Its anti-

tumour activity may be attributed to its inhibitory effects on DNA synthesis, intercalation into DNA and inducing DNA strand breaks (Durr, Wallace et al. 1983). These abnormalities are ascribed to the function of mitoxantrone as a topoisomerase IIA inhibitor, an ATP-dependent nuclear enzyme that catalyzes changes in DNA tangles and supercoiling by cleaving and rejoining of DNA strands. It is implicated in processes such as DNA replication, recombination and chromatin reorganization. Mitoxantrone inhibits topoisomerase II by stabilizing the enzyme during the transient “cleavage complex” form and inhibits religation of cleaved DNA strands. As a consequence, high levels of enzyme-mediated single-strand and double-strand DNA breaks are generated ultimately resulting in activation of cell death responses (Fortune and Osheroff 2000; Pommier, Leo et al. 2010). Mitoxantrone also inhibits cell proliferation by delaying cell cycle progression resulting in a G2/M arrest (Durr, Wallace et al. 1983; Fox 2004) and in PCa cells resulted in accumulation of cells in G2/M (Miranda, Maya Pineda et al. 2012) suggesting it has a role as a cytostatic agent; one study demonstrated it had high affinity to tubulin and inhibited microtubule polymerization (Ho, Law et al. 1991). In addition, mitoxantrone displays broad immunosuppressive action, inhibiting proliferation of T- and B-lymphocytes and macrophages. It also induces apoptosis in antigen-presenting cells and reduces proinflammatory cytokine secretion (Fox 2004) and is therefore used to treat adult acute myeloid leukaemia and multiple sclerosis.

1.2.4.3. Novel therapies for CRPC

Development of novel therapeutic agents has also focused on immunomodulatory therapy. One such treatment is Provenge (sipuleucel-T), which was approved by the FDA for asymptomatic or minimally symptomatic metastatic CRPC after the IMPACT trial found an increased survival advantage of 4.1 months over placebo (Plosker 2011). By procuring the patient’s own antigen-presenting cells and co-culturing them with prostatic acid phosphatase and infused back into the patient, a T-lymphocyte mediate immunity is elicited against the PCa tumour. Recently, cytotoxic T-lymphocyte-associated antigen 4 (CTLA-4) has emerged as a promising target. Ipilimumab, a human monoclonal antibody, which specifically blocks CTLA-4 from binding to its ligands CD80/CD86, was able to downregulate T-lymphocyte responses leading to a sustained immune response against the prostate tumour. This agent as

completed phase II trials in patients with CRPC in combination with radiotherapy (Slovin, Higano et al. 2013).

1.3. Progression to castration resistant prostate cancer

Patients with androgen-dependent PCa will initially respond positively to ADT. At the cellular level, androgen ablation results in cell death and cell cycle arrest of prostatic secretory epithelial cells resulting in tumour regression. Clinically, 80-90% of patients with localised PCa will respond to androgen ablation treatment with AR inhibition detected by a decrease in serum PSA levels and improvement in clinical symptoms. However ADT ultimately fails and patients progress to a CRPC phenotype which is commonly associated with overexpression of AR as well as expression of AR target genes such as PSA and the TMPRSS2:ERG fusion indicating AR signalling is intact (Ruizeveld de Winter, Janssen et al. 1994; Gregory, Hamil et al. 1998; Wang, Cai et al. 2008). Initial indications of tumour progression to CRPC were found to be associated with an increase in serum PSA levels prior to tumour recurrence despite continued androgen ablation (Klotz 2000).

It is not clear when and how castration resistance arises within PCa tumours. Two models have been proposed. The “adaption” model suggests that during androgen ablation, androgen-dependent cells are converted to a castration-resistant phenotype through genetic and epigenetic mechanisms thus conferring a survival advantage to the CRPC cells. In support of this theory, the mechanisms underlying molecular changes during long-term androgen ablation were first investigated by Kokontis and Liao who observed an increase in AR mRNA and protein expression in an LNCaP sub-line after prolonged culture in androgen-depleted medium (Kokontis, Takakura et al. 1994). Chen *et al* provided a causal link between AR and emergence of a castration-resistant phenotype when it was demonstrated that an increase in AR mRNA and protein was both necessary and sufficient to produce resistance to antiandrogen therapy in animal models (Chen, Welsbie et al. 2004). In addition, antiandrogens such as bicalutamide and flutamide behaved as partial AR agonists in cells overexpressing AR (Chen, Welsbie et al. 2004). The consequence of this is

observed in patients who exhibit “androgen withdrawal syndrome” after the cessation of antiandrogen treatment (discussed in 1.3.2.2).

The “clonal selection” model proposes CRPC emerges from the selection of a previously rare quiescent population of castration-resistant cells within an androgen-dependent tumour. Following androgen deprivation, androgen-dependent cells would be eradicated leaving the castration-resistant cells to proliferate (Isaacs and Coffey 1981). The “adaptive” model reflects the more accepted viewpoint for the primary route for CRPC however the two models are not mutually exclusive and increased AR activity may be selected prior to ADT. Recently, castration-resistant Nkx3.1-expressing cells (CARNs); a rare androgen-independent population have been identified. CARNs are strictly luminal and demonstrated bi-potential and self-renewal capacity and may be putative cancer stem cells. Inducible PTEN and Nkx3.1 deletion in the CARN population of castrated mice resulted in HGPIN and PCa lesions, which were devoid of basal cells and exhibited enhanced proliferation (Wang, Kruithof-de Julio et al. 2009).

Once PCa progresses to CRPC inappropriate AR signalling continues to sustain growth and prevent apoptosis. A number of mechanisms have been identified by which AR activity is maintained and can be either ligand-dependent or ligand-independent. Furthermore, CRPC cells have developed AR-independent mechanisms to achieve androgen-independence involving up-regulation of cell survival and growth pathways and inhibition of apoptotic signalling. Several pathways are likely to contribute to the development of CRPC. To provide context for the AR-dependent mechanisms, the structure and function of the AR will first be described before discussing the mechanisms that contribute to the development of CRPC.

1.3.1. The androgen receptor

The AR belongs to the steroid receptor subclass of the nuclear receptor superfamily. The gene is located at Xq11-12 and consists of 8 exons encoding a protein 919 amino acids in length (Figure 2); exon 1 encodes the NTD and is highly flexible with minimum secondary structure. Exons 2 and 3 code for the DNA-binding domain (DBD), which is made up of 3 α-helices organised into two

zinc-finger-like motifs. These are important for AR dimerization and recognition of specific DNA sequences within the AREs located within the regulatory regions of target genes. Exons 4-8 encode the hinge region and the C-terminal LBD and are central for recognition and binding of androgens. Activation of the AR is mediated through two activation domains; activation factor-1 (AF-1) located in the NTD and AF-2 situated in the LBD. AF-1 is the major domain responsible for transactivation activity of the AR. The bipartite nuclear localisation signal flanks the DBD and hinge region (Bennett, Gardiner et al. 2010; van de Wijngaart, Dubbink et al. 2012).

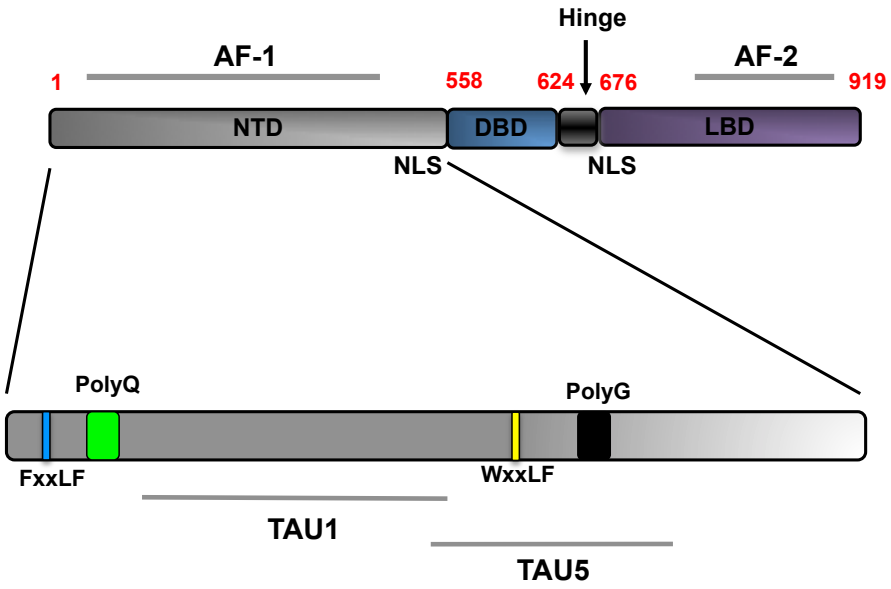

Figure 2. Functional domains of the androgen receptor

There are four structurally and functionally distinct domains; The N-terminal transactivation domain (NTD) is responsible for transcriptional activation. It consists of the activation function 1 (AF-1) region within which transactivation unit (TAU) 1 and TAU5 reside. The DNA binding domain (DBD) is located C-terminal to the NTD and adjacent to the small hinge region. The C-terminal ligand-binding domain (LBD) contains AF-2 which allows for binding with FxxLF-like motifs present in many coactivators. The nuclear localization signal (NLS) flanks the DBD and the hinge region. Within the NTD two FxxLF-like motifs are present capable of binding to AF-2. Also within the NTD are amino acid stretches containing polymorphic tri-nucleotide repeat, CAG and GGC, which encode poly glutamine (polyQ) and poly glycine (polyG) tracts respectively. Numbers in red signify the amino acid number. Adapted from (van de Wijngaart, Dubbink et al. 2012).

Prior to activation, the AR is diffuse throughout the cell, an unstable protein held inactive by chaperone proteins. Heat shock protein (HSP)90 binds to the LBD maintaining AR in a conformation that allows access for ligands to bind. Upon androgen binding, AR is activated and AR-induced transcription occurs by series of steps. Ligand binding induces a conformational change in 12 α-helices of the LBD with helix-12 changing position to form a lid over the ligand-binding socket thus stabilising the ligand within the LBD cavity. This in turn exposes a

hydrophobic groove in the AF-2 domain to serve as a docking site for LxxLL motifs (where x is any amino acid) present in AR coativators (e.g. p160-family member, steroid-receptor-coactivator 1; SRC1) and corepressors (e.g. nuclear receptor coreprepssor; NCoR) (Liao, Chen et al. 2003). The AR LBD disassociates from HSP90 and the AF-2 domain binds intra-molecularly to the LxxLL-like motif, FxxLF in the NTD (Klokk TI and Slagsvold T 2006). AF-2 binding to FxxLF motifs occurs with higher affinity than binding to LxxLL-containing motifs suggesting the N/C interaction is required for receptor stability and prevents coactivator from binding until the AR is bound to DNA (Li, Fu et al. 2006). Ligand binds to the monomeric form of AR however dimerization is facilitated by inter-molecular interactions between D-box regions in the second zinc-finger of the DBDs (Verrijdt, Haelens et al. 2003). It is thought this interaction is required for inter-molecular N/C interaction, which may occur once the AR enters the nucleus (van Royen, van Cappellen et al. 2012). Dimerization of AR molecules via inter-molecular forces are thought to be necessary for AR binding to promoters containing AREs of varying affinities, although AR DBD mutants are able to stimulate high affinity AREs suggesting AR monomers are also functionally active (van Royen, van Cappellen et al. 2012).

DNA binding is mediated through the first zinc-finger within the DBD containing the P-box, which interacts with the DNA major groove. Recognition sequences within the AREs are organized into spaced inverted or direct repeats of the core sequence 5'-TGTTCT-3' (Denayer, Helsen et al. 2010). On binding to AREs, the N/C interaction is dissolved and this enables recruitment of cofactors including the basal transcription complex, chromatin modification enzymes with histone acetyltransferase (HAT) activity and histone deacetylases (HDAC) activity as well as coactivators and corepressors (Bennett, Gardiner et al. 2010). As mentioned above, AF-1 in the NTD has the main transactivation potential and has been mapped to two domains, transactivation domain 1 (TAU1) and TAU5. Transactivation of full-length AR is primarily mediated through TAU1 however it is TAU5 is responsible for the constitutive activation of LBD-truncated AR mutants (Jenster, van der Korput et al. 1995). Dissection of TAU5 identified the WxxLF motif to be responsible for the ligand-independent activity and functions as an autonomous transactivation domain. Conversely, it inhibits ligand-dependent activity of full-length AR through N/C interaction with the LxxLL motif in AF-2. This indicates TAU5 as a negative regulatory domain in the context of ligand-dependent AR activity (Dehm, Regan et al. 2007). As well as regulating

the N/C interaction, these motifs also compete with LxxLL motif-containing AR coregulators for LBD binding in the presence of ligand. The TAU5 domain also mediates recruitment of SRC1. This interaction is regulated indirectly by TAU1 although it binds neither SRC1 nor co-operates with TAU5 (Callewaert, Van Tilborgh et al. 2006).

1.3.2. AR-dependent mechanisms of PCa recurrence

Several pathways lead to the aberrant activation of AR in CRPC (Figure 3): (i) AR amplification, (ii) AR gain-of-function mutations that broaden ligand specificity and/or alter AR coactivator recruitment (iii) alternative splicing which renders the AR constitutively active, (iv) alterations in relative AR coregulator levels, (v) increased intratumoural *de novo* synthesis of androgens and (vi) activation of proliferation and cell survival pathways by growth factor and cytokine stimulation enhancing AR transcriptional activity independent of ligand activation.

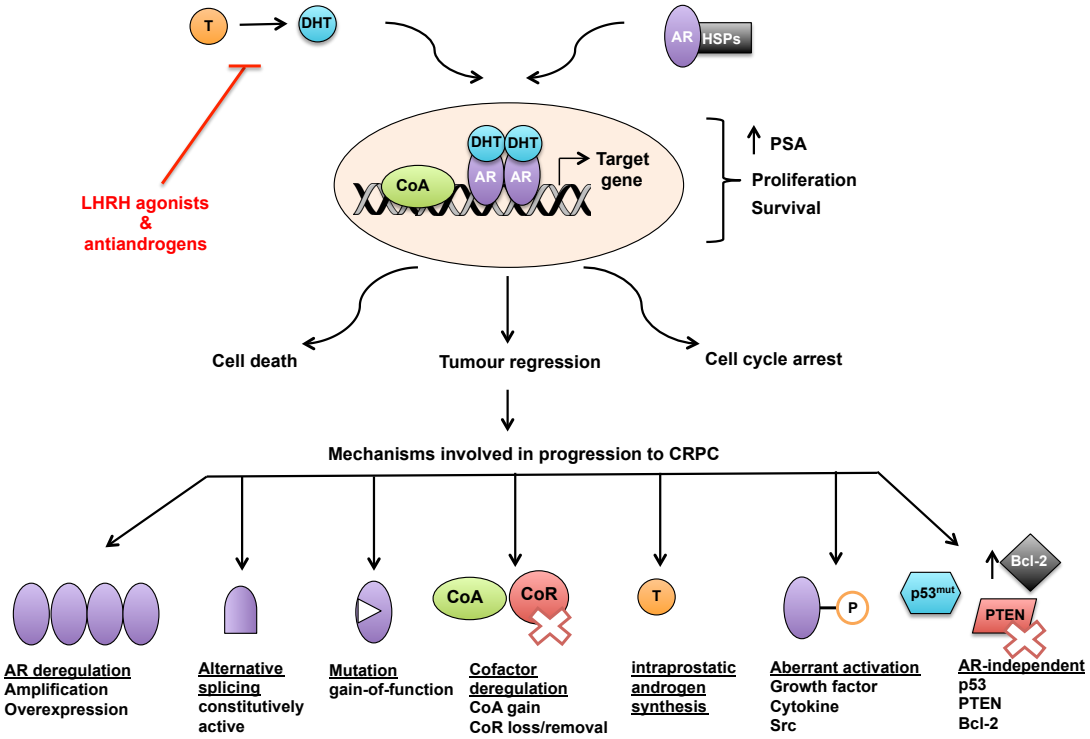

Figure 3. Possible pathways to CRPC involve AR reactivation (ligand-dependent and –independent) and AR-independent mechanisms

Prostate tumours evade androgen ablation therapy and adapt to low levels of androgen by reinstating AR activity through a number of mechanisms. Deregulation of tumour suppressor pathways and activation of oncogenic pathways also contribute to a CRPC phenotype. Adapted from (Knudsen and Kelly 2011).

1.3.2.1. AR amplification

Enhanced AR expression can arise from a number of mechanisms. AR gene amplification has been detected in approximately 30% of patients with recurrent

PCa (Koivisto, Kononen et al. 1997). The outcome of a recent study with a median follow-up of 12 years assessing AR levels from tumour samples derived prior to the start of treatment revealed that increased levels of AR present within the tumour nuclei correlated with increased risk of death from PCa (Donovan, Osman et al. 2010). Mechanistically, it is believed overexpression of AR reduces the amount of ligand needed for AR-mediated proliferation and survival and as consequence sensitises cells to the effects of residual prostatic androgens. LNCaP-ARhi, a LNCaP cell line stably expressing four to six times higher levels of AR than the parental cells were more sensitive to stimulation by 1nM DHT resulting in enhanced proliferation compared with the control cells and which also correlated with increased expression of cell cycle-associated genes (Waltering, Helenius et al. 2009).

However few studies have addressed the process of how AR overexpression occurs. An unexpected link between AR expression and the retinoblastoma tumour suppressor protein (pRB) has provided a potential mechanism of loss of AR regulation during the development of CRPC. It was demonstrated that pRB was able to act as a transcriptional repressor at the AR gene with suppression of pRB resulting in an increase in AR expression *in vivo* and which was correlated to increased E2F1 expression. These findings were further validated using clinical specimens from patient with CRPC; pRB loss was found to be overrepresented in CRPC and this significantly inversely correlated with AR levels (Sharma, Yeow et al. 2010). It has also recently been demonstrated that ligand-bound AR is able to mediate a negative feedback loop on its own activity. In VCaP cells (derived from vertebral metastasis in a patient with CRPC), AR was able to enhance its own expression at low androgen levels through binding at an enhancer element within the second intron of the AR gene. Conversely, high levels of androgen resulted in ligand-bound AR functioning as a transcriptional repressor at this site resulting in the recruitment of the transcriptional coregulator, lysine specific demethylase (LSD1) and demethylation of histone mark, H3K4me1,2 (Cai, He et al. 2011).

1.3.2.2. AR gain-of-function mutations

The acquisition and selection of AR mutations and alternatively spliced isoforms during androgen ablation provide PCa cells with a mechanism of circumventing

growth regulation at low androgen levels and by activation by other ligand types. The precise frequency of somatic AR mutations during the development of CRPC is unclear due to cellular heterogeneity within tumours, variations in tumour staging and difficulty of accessing metastatic samples. However Marcelli *et al*. observed that patients in the early stages of PCa had no AR mutations whereas the frequency increased to 20% in localised metastatic samples and this escalated further to 50% in more distant metastatic samples suggesting AR mutations play a role in tumour progression (Marcelli, Ittmann et al. 2000). More recently, an assessment of AR mutations in circulating tumour cells showed AR alterations were present in 20 out of 35 patients highlighting the incidence of mutations may be higher in cells with metastatic potential (Jiang, Palma et al. 2010).

The number of different somatic AR mutations that have been found in patients with PCa tissues currently stands at 159 and are catalogued in the Androgen Receptor Gene Mutations Database (Gottlieb, Beitel et al. 2012). Gain-of-function mutations are found either localised within region of the LBD (~45%) or a significant minority (~30%) are located in exon 1 of the AR (Gottlieb, Beitel et al. 2012). A large numbers of variant AR transcripts have been detected in PCa cell lines, CRPC xenografts and tissue specimens. These AR splice variants encode truncated AR isoforms, which retain NTD and DBD but lack the LBD and several are able to induce ligand-independent activation of ARE-driven reporters in the absence of androgens (Guo and Qiu 2011).

The first AR mutation to be identified was a missense mutation resulting in the substitution of threonine for alanine at position 877 (T887A). This mutation is also found in the LNCaP cell line, established from lymph node metastases from a patient treated with hormonal therapy (Horoszewicz, Leong et al. 1980). X-ray crystallography studies mapped the amino acid substitution within the ligand-binding pocket of the AR resulting in an altered size and shape of the binding pocket thus decreasing ligand specificity (Sack, Kish et al. 2001). As consequence, in addition to androgen-mediated activation, this promiscuous receptor can bind other steroid hormones (progestins and oestrogens) and antiandrogens (CPA and flutamide) (Veldscholte, Berrevoets et al. 1992). It is noteworthy to mention that the T877A mutation does not respond in the same way to other antiandrogens such as bicalutamide. Of 24 tumour samples examined from patients with metastatic PCa, 25% expressed this mutation

(Gaddipati, McLeod et al. 1994). A study a year later by Taplin and co-workers revealed that the frequency of mutations at amino acids 877 and 874 increased in metastatic PCa tumours derived from patients who had previously been treated with orchiectomy or LHRH agonist (Taplin, Bubley et al. 1995). The clinically observed Flutamide Withdrawal Syndrome where some patients treated with flutamide experience increasing PSA levels and worsening symptoms may have arisen from the selection of cells containing a flutamide-activated mutant AR. In support of this theory, AR mutations developing in response to flutamide treatment was demonstrated when 5 out of 16 patients with bone metastases receiving androgen blockade with flutamide were found to have T877A mutations, which were stimulated to grow *in vitro* when flutamide was added. This was in contrast with patients not treated with flutamide harbouring different AR mutations (Taplin, Bubley et al. 1999).

The AF-2 domain appears to be a hot spot for other mutations namely T877S and H874Y, which also exhibit broadened ligand specificity. The T877S AR mutant similarly shows altered an altered ligand-binding pocket in terms of size and shape (Matias, Donner et al. 2000). In the case of the H874Y mutation, the substitution of tyrosine at position 874 instead strengthens the interaction of helix 12 with the ligand-binding groove thus setting it in an active confirmation even when non-optimal ligands bind (McDonald, Brive et al. 2000). This particular mutation has also confers enhanced recruitment of p160 coactivators which also contributes to its enhanced activity (Duff and McEwan 2005). As demonstrated above with flutamide-based therapy, treatment with other AR antagonists similarly selects for mutations and results in these agents functioning as agonists. The W741C has been frequently found in bicalutamide-treated patients and was induced in LNCaP cells when cells were cultured long-term in the presence of bicalutamide (Haapala, Hyytinen et al. 2001; Hara, Miyazaki et al. 2003). The androgen-dependent KUCaP-1 xenograft, derived from the liver metastatic tissue of a patient treated with bicalutamide also harbours the W741C mutation. After castration, KUCaP-1 tumours regressed and did not grow. However when treated with bicalutamide after castration, these tumours regrew and only regressed two months after bicalutamide withdrawal (Terada, Shimizu et al. 2010).

The hinge and the N-terminal region of the AR have also been found to harbour mutations. As these domains are not involved in ligand binding, these alterations

impact on AR activity in other ways. AR mutations R629Q and K630T were identified from patients who had undergone ADT or who was treatment-naïve respectively and reside in the hinge region, which spans the DBD and NLS. Despite these mutants demonstrating a reduced nuclear localisation, they exhibit increased transcriptional activity. Mutational analysis of the hinge region revealed that deletion of amino acid residues 629-636 increased the transactivation potency of various reporters with the AR p160 coactivator, transcription intermediary factor 2 (TIF2) potentiating the effect compared with when the region was present. The deletion also enhanced the N/C interaction indicating this critical area serves to inhibit aberrant AR activation. These results suggest that mutations, which occur with this region, may increase the affinity of the AF-2 domain to interacting partners such at the NTD, TIF2 and other coactivators resulting in enhanced AR activity (Haelens, Tanner et al. 2007).

There have been comparatively fewer studies assessing N-terminal mutations. One example was the identification of dual somatic missense mutations within the N-terminal polyglutamine (PolyQ) tract. This resulted in two leucine residues disrupting the tract thereby reducing the N/C interaction but unexpectedly, increasing AR activity compared with wild-type AR. The AR coactivator, AR-associated (ARA) protein, ARA24 has been demonstrated to interact with the CAG repeat within the PolyQ tract thus increasing stability and folding of the tract and leading to enhanced transcriptional activity of the AR (Hsiao, Lin et al. 1999; Buchanan, Yang et al. 2004).

NTD AR variants were found to be prevalent in CRPC patients in a recent study by Steinkamp and co-workers. They compared AR variants in metastases obtained from patients treated with bicalutamide or flutamide with lymph node metastases from hormone-naïve patients (Steinkamp, O'Mahony et al. 2009). Of 26 recurring mutations, the majority were located in the NTD and occurred in multiple tumours. One mutation, W435L, replaced the WxxLF motif in TAU5 for an LxxLF motif. As a result, this mutation strengthened the intramolecular N/C interaction leading to an enhancement of transcriptional activity. The mechanism by which this mutation increased AR activity has not been clarified however the authors postulate it may be as a result of increased ligand-dependent activity due to altered competition with the FxxLF motif or greater interactions with coactivators due to LxxLF-mediated binding. Another N-terminal mutation,

E255K, resulted in increased protein stability and nuclear localisation in the absence of androgen (Steinkamp, O'Mahony et al. 2009).

Synthesis of truncated AR variant proteins through alternative splicing has recently emerged as a mechanism of resistance towards androgen ablation therapy. Since 1994, when 110kDa and 87kDa isoforms of the AR were first described in human genital skin fibroblasts, numerous alternatively spliced AR variants have been cloned and identified. The various isoforms have distinct functions, however many exhibit constitutively active, transactivation activity. This has been attributed to the TAU5 domain in the NTD region of the AR (Dehm, Regan et al. 2007). Dehm *et al*. reported three AR splice variants from the androgen-independent human PCa cell line, 22Rv1, derived form the relapsed CRW22 xenograft (Dehm, Schmidt et al. 2008). One variant produced a full length AR with a duplicated exon 3 (AR 1/2/3/CE3) and the other variants resulted in truncated isoforms (AR 1/2/2b and AR 1/2/3/2b), which lack a LBD but possess a novel exon 2b. Exon 2 encodes the first zinc finger of the DBD and this was sufficient for AR to bind to ARE on DNA thereby rendering the truncated isoforms constitutively active and promoting growth independent of androgen stimulation (Dehm, Schmidt et al. 2008). Another AR isoform, designated AR3 (containing the NTD and DBD regions only) has been revealed to be a principal constitutive isoform in PCa cell lines (including 22Rv1 cells) and was identified in human PCa tissue from two independent studies. Expression levels of AR3 have also been correlated to recurrence of PCa and survival time with depletion of androgen resulting in overexpression (Guo and Qiu 2011). Other AR variants that are implicated in the development of CRPC include AR^{v567es} (exons Δ5-7), which is constitutively active and in the absence of ligand, binds to and stabilises wild-type AR resulting in enhanced activity. AR^{v567es} VCwas initially identified from a number of different human PCa xenografts, termed the LuCaP series, derived from men with CRPC who have undergone ADT. Enhanced expression of this variant was found in the castration-resistant xenografts compared to androgen-dependent tumours. Later it was found that 10 out of 13 CRPC patients had a minimum of one metastasis that was positive for AR^{v567es} (Sun, Sprenger et al. 2010). Both AR3 and AR^{v567es} regulate a distinct set of gene targets compared with those regulated by wild-type AR, which may be of significance for tumour initiation and progression (Guo and Qiu 2011).

1.3.2.3. Altered expression of AR coregulators

Besides mutations altering the activity of the AR which in some circumstances lead to the aberrant recruitment of coactivators, it also been recognised that the expression levels of AR coregulators can also be deregulated in a subset of PCas. On example is the overexpression of SRC1 and TIF2. Increased expression of these coactivators was found to correlate with disease progression and was higher in patients with recurrent PCa who had failed hormone therapy compared with androgen-dependent PCa samples (Gregory, He et al. 2001). Enhanced SRC1 and TIF2 expression was also associated with the regrowth of androgen-dependent CWR22 human prostate xenograft after castration and also paralleled an increase in AR expression in this tumour model (Gregory, He et al. 2001). A later study correlated SRC1 expression with increased tumour aggressiveness in localised androgen-dependent PCa samples. *In vitro* studies confirmed the role of SRC1 in AR-mediated cell growth since knockdown of SRC1 in androgen-dependent LNCaP cells and androgen-independent subclone of LNCaP, C4-2 resulted in reduced growth and a decrease in AR-mediated gene regulation (Agoulnik, Vaid et al. 2005). Another coactivator that has been linked with PCa development is Tat-interactive protein 60kDa (TIP60). This was found to accumulate in the nucleus of specimens derived from patients with CRPC compared with a more diffuse distribution in specimens of primary PCa. Moreover, in the xenograft CWR22 tumours and LNCaP cells, TIP60 was upregulated and localised to the nucleus after androgen withdrawal (Halkidou, Gnanapragasam et al. 2003). However due to the divergent nature of PCa, clinical results such as those described might not necessarily be representative. A recent microarray analysis comparing gene expression patterns between normal and tumour tissue found SRC1 to be elevated in two data sets but decreased in one and TIF2 to be elevated in one but not in another. TIP60 was decreased in the majority of data sets (Chmelar, Buchanan et al. 2007).

In addition to upregulation of certain coactivators there is evidence that deregulation of AR corepressors may influence PCa development and progression. An example of AR antagonists converting to agonists is through the modulation of AR corepressor activity. In the presence of AR antagonists, interleukin (IL)-1β signalling from infiltrating macrophages resulted in TAB2, a component of the NCoR repressor complex, releasing NCoR from the AR

transcriptional complex thereby de-repressing AR activity (Zhu, Baek et al. 2006). This finding is of significant clinical relevance since IL-1β is effectively converting AR antagonists into agonists (Zhu, Baek et al. 2006). As will be described section 1.4.1.2, cyclin D1 functions as an AR corepressor. Studies from a murine model have shown that cyclin D1 expression decreases as a function of disease development (Maddison, Huss et al. 2004). Characterisation of cyclin D1 status in patient samples found that increased cyclin D1 expression correlated with primary PCa compared with benign tissue and differential cellular distribution of cyclin D1 was associated with different grade of tumours; cytoplasmic in low grade tumours and nuclear in higher grades (Comstock, Revelo et al. 2007). Another AR corepressor, Notch effector protein, Hey1, is deregulated in PCa. Expression of both Notch and its ligand Jagged1 are repressed as a result of androgen stimulation while Hey1 localisation in PCa is either downregulated or excluded from the nucleus in PCa specimens (Belandia, Powell et al. 2005; Wang, Leow et al. 2006). Together this indicates a possible mechanism of reduced Hey1 signalling in PCa. This will be discussed in further detail in section 1.5.3.4.

1.3.2.4. Intraprostatic androgen synthesis

Another mechanism by which PCa cells adapt to ADT is through enhanced activity of enzymes that convert weak adrenal androgens (DHEA-S and androstenediol) into testosterone and DHT thus providing the necessary levels of agonist to re-establish AR activity. Analysis of metastatic tissue derived from patients with CRPC through a "warm autopsy" program distinguished higher testosterone levels in CRPC samples relative to control tissues. In parallel, gene expression studies have identified increased expression of enzymes involved in the conversion of weak adrenal androgens to testosterone in CRPC bone metastases compared with primary PCa samples (Cai and Balk 2011).

PCa cells can either take up weak adrenal androgens from the blood stream or synthesise androgens *de novo* from cholesterol as was demonstrated in LNCaP xenografts model (Locke, Guns et al. 2008). LNCaP, PC3 and DU145 were all found to express CYP11A1 and CYP171A, both of which are integral to the steroidogenic pathway indicating PCa cells can divert to alternative methods when testosterone is low. These levels of these enzymes have also been found

to increase in castration resistant LNCaP sub-lines (Dillard, Lin et al. 2008). Despite demonstrating that *de novo* androgen synthesis occurred in cell lines and xenografts, testosterone levels were still low and PCa cells may produces DHT through a “back door” pathway. However since testosterone levels are high in clinical CRPC patients it is therefore questionable whether *de novo* synthesis occurs in CRPC patients to adequate levels that will lead to activation of the AR. However, in support of this theory, mRNA levels for CYP11A1 and CYP171A were detected in metastatic CRPC bone marrow samples (Stanbrough, Bubley et al. 2006). Nevertheless it is still to be defined to what extent *de novo* androgen synthesis plays are role in activating AR whereas circulating adrenal androgens provide a significant source of substrate to convert to testosterone and DHT.

1.3.2.5. Growth factor- and cytokine-mediated activation of AR

It has been well documented that signalling cascades initiated by growth factors such as epidermal growth factor (EGF), insulin-like growth factor 1 (IGF-1) and cytokines like IL-6 can stimulate AR activity. These can activate transcriptional activity of AR independently of androgen or can sensitise AR to low concentrations of androgen. Initial experiments demonstrated stimulation by EGF and IGF-1 could crosstalk with AR signalling when ectopically expressed AR in DU145 cells mediated AR-dependent reporter gene transcription. Antagonising AR with bicalutamide in the presence of EGF blocked transactivation thus demonstrating the requirement of AR (Culig, Comuzzi et al. 2004). Since this study, a number of groups have related the upregulation of members of the EGFR-family with enhanced AR activity. For example, ectopic expression of human epidermal growth factor receptor 2 (HER2/neu) in LNCaP cells resulted in activation of the AR pathway through AKT-mediated phosphorylation of AR (Wen, Hu et al. 2000). It was then proposed that the heterodimerisation of HER2 with HER3 resulted in optimal AR activity through increased AR stabilisation and DNA binding thereby increasing AR transactivation. Inhibition of HER2 rather than EGFR resulted in decreased AR activity suggesting HER2 was responsible for modulating AR function (Mellinghoff, Vivanco et al. 2004). In the clinic, overexpression of EGF and EGF receptor has been detected in patients with metastatic PCa and has been associated with progression to CRPC (Di Lorenzo, Tortora et al. 2002). The result of growth factor stimulation results in activation of several downstream signalling cascades including the mitogen-activated protein kinase (MAPK) pathway. Of the many downstream effectors of the MAPK pathway, the sarcoma-related kinase (Src) and the p42/44 extracellular-signal-regulated kinases (ERK) 1 and 2, have been shown to stimulate AR activity (Lonergan and Tindall 2011). Treatment of LNCaP cells with EGF resulted in phosphorylation of AR on a number of tyrosine residues, which were inhibited by Src kinase inhibitors (Guo, Dai et al. 2006). Mass spectrometry identified Y534 as a primary site on the AR for enhanced activity since mutation of this residue reduced Src-induced phosphorylation. This may be significant for the progression of PCa since expression levels of phospho-Y534 and phospho-Src were greater in castration-resistant PCa tumours compared with hormone-naïve PCa or normal prostate samples (Guo, Dai et al. 2006). Activation of ERK1 and ERK2 has also

been correlated with tumour progression in PCa. The relationship between ERK1/2 activity and AR signalling was revealed when C4-2 cells, in steroid-depleted conditions, were treated with the MAPK extracellular kinase (MEK) inhibitor, U0126, which blocks ERK1/2 activity. As a consequence of MEK inhibition, stimulation of the AR target genes, PSA and TMPRSS2 were decreased suggesting that the autocrine growth factor signalling influences AR activity in the absence of androgens. The reduction of AR activity by U0126 was attributed to a reduction in the interaction of AR and its coactivator, SRC1 as well as a decrease of MAPK-mediated phosphorylation of SRC1, which is important for interaction with another AR coactivator, cAMP response element binding protein (CREB)-binding protein (CBP) (Agoulnik and Weigel 2008).

As mentioned above, growth factors and their cognate receptor tyrosine kinase (RTK) also activate the phosphatidylinositide 3-kinase (PI3K)/AKT pathway, an important regulator of cell survival. PI3K mediates production of the second messenger, phosphoinositol (3,4,5) triphosphate (PIP_3). This recruits the threonine/serine kinase, AKT that acts downstream via mammalian target of rapamycin (mTOR) to regulate growth, proliferation and apoptosis. Initially activation of AKT was thought to correlate simply with increased AR activity through phosphorylation of AR. However, later it was appreciated the crosstalk between the pathways was more complex since AKT was found to block or enhance AR activity in a cell passage number-dependent manner (Lin, Hu et al. 2003). Carver *et al* have recently determined that the PI3K/AKT and AR pathways regulate each other through complex reciprocal feedback mechanisms (Carver, Chapinski et al. 2011). They and others have shown that HER2 and HER3 are activated when the PI3K/AKT pathway is blocked (Carver, Chapinski et al. 2011; Chandarlapaty, Sawai et al. 2011). In LNCaP cells, treatment with either BEZ235 (a dual PI3K and mTORC1/2 inhibitor) or siRNA against AKT resulted in enhanced HER3 and AR expression which was blocked with the addition of a HER family kinase inhibitor. Conversely inhibition of AR activity using either MDV3100 or siRNA against AR resulted in enhanced AKT activity through the downregulation of the androgen-regulated FKBP5 protein, a chaperone protein for the AKT phosphatase PHLPP (Carver, Chapinski et al. 2011).

IL-6 is a pleiotropic cytokine produced by a number of different cell types including prostate, immune and osteoblast cells. It mediates differentiation of

lymphocytes, cell proliferation, cell survival and apoptotic signals. Depending on the cell type, it can transduce and activate MAPK and PI3K/AKT signalling cascades however it generally induces phosphorylation of the signal transducer and activator of transcription (STAT) protein, STAT3. In normal cells, IL-6 signalling is strictly regulated and therefore transient. IL-6 binds to the IL-6 receptor, which is composed of the immunoglobulin (Ig)-like ligand-binding subunit, gp80 and the signal-transducing gp130 subunit. This results in autophosphorylation and activation of the Janus kinase (JAK) family of proteins (particularly JAK2 but also JAK1 and TYK2) which then bind to and phosphorylate STAT3 inducing dimerization and translocation to the nucleus. STAT3 homodimers then bind to consensus sequences within the enhancer regions of target genes and in conjunction with other transcription factors, drive gene expression. Targets genes include c-Myc, Bcl-2, Bcl-xL and cyclin D1 (Hodge, Hurt et al. 2005).

IL-6 was implicated in PCa progression after elevated levels of serum IL-6 were detected in patients with CRPC and was associated with decreased survival. Furthermore, the IL-6 receptor is overexpressed in LNCaP, DU145 and PC3 cells and has been correlated with progression to CRPC (Yang, Wang et al. 2003; Lonergan and Tindall 2011). Initial studies suggesting AR could be regulated by IL-6 stimulation were derived from DU145 cells transfected with an AR expression vector and ARE-dependent reporter gene construct. Treatment with IL-6 resulted in AR-dependent gene transcription, which could be blocked with bicalutamide or tyrosine kinase inhibitors to MAPK, protein kinase A or C (Hobisch, Eder et al. 1998). In agreement with these results, IL-6 treatment of LNCaP cells in androgen-depleted conditions also increased levels of PSA mRNA and augmented PSA secretion (Hobisch, Eder et al. 1998). The potential mechanisms that mediate the interaction between IL-6 and AR signalling have been studied by a number of groups. Through the activation of the MAPK pathway, AR coactivator, p300 has been implicated in mediating AR transactivation. This was revealed after p300 depletion either by E1A-dependent sequestration or siRNA against p300 resulted in a reduction of AR activity in androgen-deprived LNCaP cells (Debes, Schmidt et al. 2002). In a separate study, the yeast Gal4 system identified that the NTD of AR was activated after IL-6 treatment of LNCaP cells and blocked by protein kinase inhibitors against MAPK and JAK (Ueda, Mawji et al. 2002). More specifically, the JAK kinase inhibitor, AG490 also inhibited MAPK phosphorylation as well as STAT3

phosphorylation indicating the JAK/STAT pathways plays a central role in mediating IL-6-dependent activation of AR NTD. This theory was supported when STAT3 was found to bind to the AF-1 region of AR (Ueda, Bruchovsky et al. 2002).

It should be emphasised, activation of cell proliferation and survival pathways such as MAPK, PI3K/AKT and JAK/STAT do not always impinge on AR activity and through interactions with each other and other signalling cascades will contribute to the development of a more malignant PCa phenotype by mechanisms independent of AR.

1.3.3. AR-independent mechanisms of PCa recurrence

The cellular mechanisms described so far require PCa cells to express the AR to achieve androgen independence however; complementary or alternative pathways have been ascertained that can circumvent AR.

Many of the pathways resulting in tumour development and progression described above have involved deregulation of proliferation. In addition, defective apoptosis also plays a significant role in tumourigenesis. The anti-apoptotic protein, Bcl-2 is frequently expressed in PIN and CRPC. In an LNCaP xenograft model, castration-resistant tumours expressed Bcl-2 and blocking Bcl-2 with antisense oligonucleotides delayed the development of androgen-independent tumours indicating Bcl-2 may bypass the signal for apoptosis normally generated during androgen ablation (Liu, Corey et al. 1996; Gleave, Tolcher et al. 1999). In advanced PCa, Bcl-2 was expressed in 70% of androgen-independent tumours and 34% of bone metastases in castration-resistant patients suggesting Bcl-2 expression is an important factor in facilitating PCa cells to survive in an androgen-depleted environment (Feldman and Feldman 2001; Gurumurthy, Vasudevan et al. 2001). Bcl-xL another anti-apoptotic protein is overexpressed in PCa and is associated with higher Gleason scores (Castilla, Congregado et al. 2006).

In addition to the activation of oncogenic pathways, inactivation of tumour suppressor genes also contributes to PCa progression. Inactivation of p53 is

considered an important step in tumourigenesis of many cancers including PCa. The involvement of p53 in the progression of PCa progression was demonstrated using the mouse prostate reconstitution (MPR) model (Thompson, Park et al. 1995). PCa was identified in all mice heterozygous and homozygous for p53 mutations while no metastasis were found in wild-type p53 mice (Thompson, Park et al. 1995). *In vivo*, LNCaP cells stably expressing dominant negative form of p53 readily formed tumours in castrated mice while parental LNCaP xenografts did not suggesting mutant p53 can contribute to the CRPC phenotype (Burchardt, Burchardt et al. 2001). It is widely accepted that p53 in DU145 is non-functioning in terms of the classical p53 signalling pathway. This has been attributed to two separate mutations on the different chromosome alleles resulting in co-expression of two mutant proteins with different amino acid substitutions (section 2.2, Table 5) (Isaacs, Carter et al. 1991). Characterisation studies of the DU145-derived, p53-mutant proteins in p53-deficient cells, demonstrated that alone these proteins possessed properties that closely resembled wild-type p53 since they did not have dominant-negative effects against wild-type p53 (Gurova, Rokhlin et al. 2003). Co-expression of these mutants neutralized the other's growth suppressive effects and converted the Fas-sensitive phenotype of p53-null, PC3 cells to a Fas-resistant one by downregulating Fas receptor (FasR) expression (Gurova, Rokhlin et al. 2003).

As discussed above, the PI3K/AKT pathway has been correlated with progression to CRPC. Loss of the major negative regulator of this pathway, tumour suppressor gene, PTEN has been detected in approximately 25% of primary tumours and 79% of CRPC samples and correlates with advanced PCa and high Gleason score (Lonergan and Tindall 2011). Knockdown of PTEN in PCa cell lines and conditional deletion in mice have established that a loss of PTEN expression promotes resistance to androgen ablation therapies (Gao, Ouyang et al. 2006).

1.4. Androgen receptor signalling

1.4.1. Androgen receptor regulators

Approximately 200 AR regulators have been identified and are categorised as coactivators or corepressors. The relative levels of coactivators versus corepressors modulate the activity of AR thereby regulating the cell's response to changes in hormone levels. They do not typically bind DNA but function at AR target gene promoter and/or enhancer regions to: (i) assist DNA binding, (ii) induce chromatin remodelling and acetylation/deacetylation of chromatin via the recruitment of HAT and HDACs respectively (iii) control cofactor binding to the AF-2 coactivator binding groove by regulating the AR N/C interaction and (iv) recruit general transcription factors associated to facilitate the assembly of the preinitiation complex (PIC) (Figure 4). Many of the coregulators perform multiple functions and bind to other cofactors to either enhance either activation or repression of AR transcription (van de Wijngaart, Dubbink et al. 2012). A summary of the mechanisms of action for the coregulators discussed in this section is listed in Table 1.

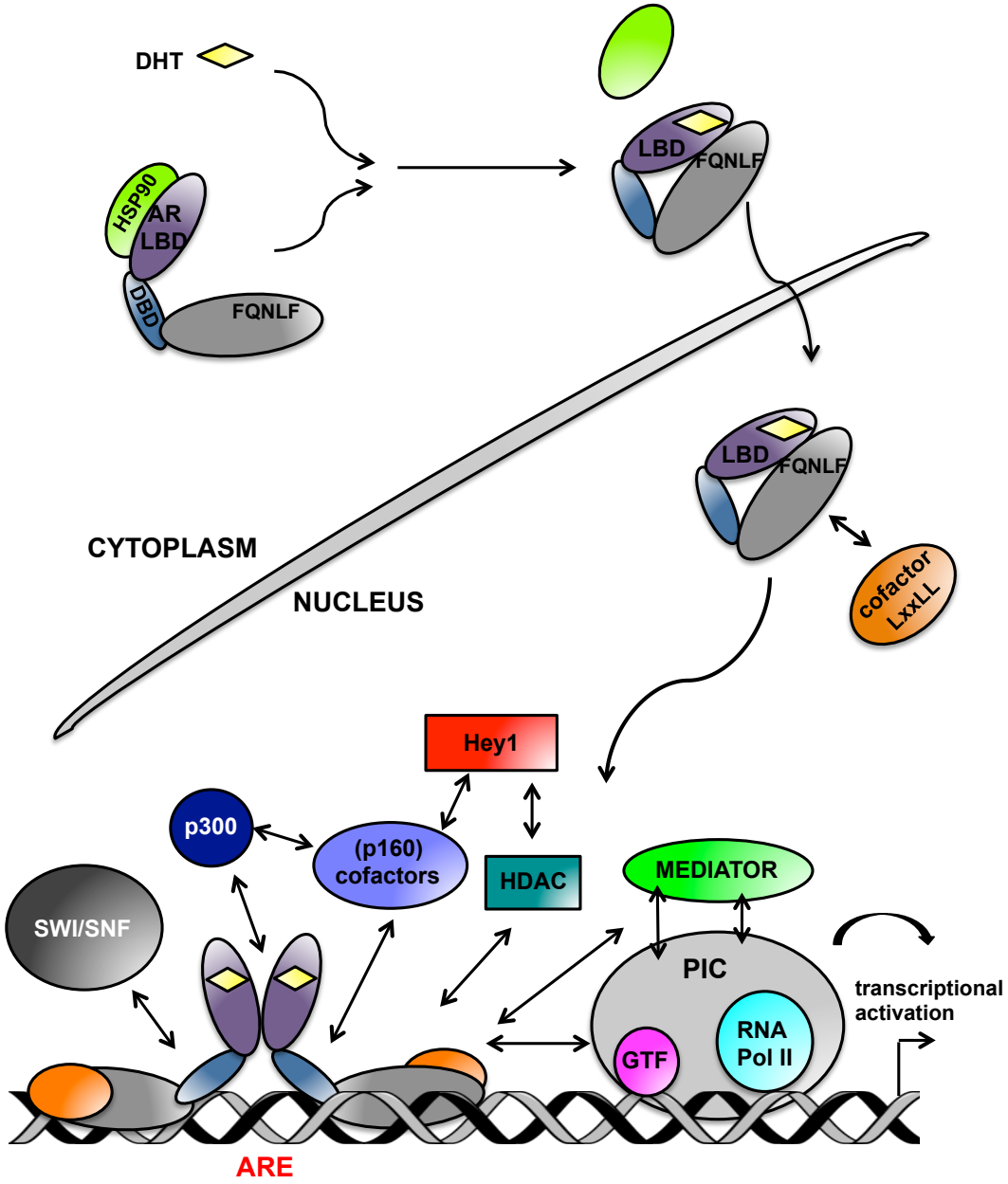

Figure 4. Schematic diagram illustrating AR activation and protein-protein interactions regulating AR transcriptional activity

Upon ligand binding to the LBD, intra-molecular N/C interaction occurs (as well as intermolecular binding, not shown). On binding to the ARE, the N/C interaction is disrupted resulting in interactions with cofactors guiding the recruitment of complexes that modulate chromatin remodelling and initiate transcription. AR LBD, androgen receptor ligand binding domain; ARE, androgen response element; DHT; dihydrotestosterone, GTF: general transcription factors, RNA pol II; RNA polymerase II, PIC; preinitiation complex. Adapted from (van de Wijngaart, Dubbink et al. 2012).

1.4.1.1. AR coactivators

The best-characterised coactivators of the AR are p300 and CBP protein and the p160/SRC-family proteins, both of which are overexpressed in PCa. p300

levels from tissue samples of patients who underwent prostatectomy correlated with proliferation *in vivo* and was associated with larger tumour volumes. *In vitro*, p300 levels increased under androgen deprivation resulting in a growth advantage. SRC1 has been found to be overexpressed in 50% of androgen-dependent PCa samples compared with benign or normal prostate tissue and increased levels of SRC3 correlated to tumour grade in localised disease (Lonergan and Tindall 2011).

AR transcriptional activation by p300/CBP arises from its dual role as a scaffold protein and its function as a HAT protein. It serves to link DNA-binding AR to basal transcription machinery and functions as a surface for nucleation of transcription factors (Iyer, Ozdag et al. 2004). Its HAT activity results in acetylation of lysine residues in histone proteins thereby reducing the interaction between histones and the DNA and allowing access for the basal transcription machinery (Iyer, Ozdag et al. 2004). The molecular features of p160/SRC proteins (SRC1, TIF2 and SRC3) augment transcriptional activity of AR as well as providing a structural base for recruiting other coregulators. SRCs contain three distinct structural domains, the N-terminal basic helix-loop-helix-PAS (bHLH-PAS) domain required for protein-protein interactions, a central region which contains LxxLL motifs for AR interaction and a C-terminal portion containing transcriptional activation domains (AD1 and AD2). AD1 binds p300/CBP proteins and AD2 interacts with proteins with histone methyltransferase activity. C-terminal regions of SRC1 and SRC3 also possess intrinsic HAT activity (Xu, Wu et al. 2009). SRC1 was found to enhance AR activity via two independent interactions. A weak interaction was found between its LxxLL motifs and the AF-2 region whereas a stronger interaction was observed between the glutamine-rich motif and AF-1 (Bevan, Hoare et al. 1999; Powell, Christiaens et al. 2004). Recruitment of p300/CBP and the intrinsic HAT activity of SRC1 further potentiated AR–mediated transcription resulting in chromatin acetylation which promoted the recruitment of another class of AR coactivator, chromatin remodelling complexes (e.g. SWI/SNF) which also loosen DNA-histone interactions (Smith, Onate et al. 1996; Becker and Horz 2002). Similarly, p300 was recently found to enhance AR transcriptional activity when AR was in a complex with the coregulator melanoma antigen gene protein-A11 (MAGE-11) and TIF2. MAGE-11 interacted with the FxxLF motif of the AR-NTD via a F-box domain and also bound to the N-terminal region of p300 with AR transcriptional activity dependent on p300 HAT activity. The AR N/C interaction

is thought to be critical in mediating AR transcriptional activity as mutation of AF-2 disrupted FxxLF motif binding and AR function. This suggests binding of MAGE-11 to FxxLF increases coactivator binding, providing better accessibility to LxxLL motifs in TIF2 (Askew, Bai et al. 2010).

Direct modification of AR at the post-transcriptional level also regulates transcriptional activity. p300 and p300/CBP-associated factor (P/CAF) proteins have been found to directly acetylate the ^{630}KLKK^{633} motif within the hinge region of the AR and is necessary for maximum activation of the AR (Fu, Wang et al. 2000; Lavery and Bevan 2011). Another protein involved in acetylating AR is the TIP60, which contains a HAT domain capable of acetylating several types of histone proteins, AR and possibly chromatin. In addition it also interacts with AR-LBD via a LxxLL motif in its C-terminus (Lavery and Bevan 2011). Ubiquitination of the AR by ubiquitin E3 ligase protein, RNF6 recruits and stabilises further AR coregulators. RNF6 induces polyubiquitination of K845 within the AF-2 domain thereby recruiting coactivator, ARA54 (Xu, Shimelis et al. 2009). This protein binds to the C-terminus portion of the AR and mediates ligand-dependent AR (Kang, Yeh et al. 1999). Mutating K845 abolished ARA54 binding to a subset of AREs indicating RNF6 has a role in promoter specificity of AR target genes (Xu, Shimelis et al. 2009). Other coactivators however have a stabilising function so AR may interact with the basal transcription machinery. One such multi-subunit complex is Mediator (MED) also known as TRAP/DRIP/ARC, which bridges the AR (via its LBD) to general transcription factors and RNA polymerase II via an LxxLL motif in the TRAP220/DRIP205 protein residing within the complex (van de Wijngaart, Dubbink et al. 2012).

1.4.1.2. AR corepressors

Two well-characterised AR corepressors are nuclear receptor corepressor (NCoR) and the related silencing mediator of retinoic acid (SMRT), which mediate disruption of AR N/C interaction and competition with SRC/p160 coactivators to repress AR activity. NCoR and SMRT are large scaffold proteins and contain LxxLL-like motifs, which interact with AR and bind to AF-2. Recruitment of these corepressors is dependent upon the conformational change induced by ligand binding either by AR antagonists such as flutamide or bicalutamide or by agonist binding (Liao, Chen et al. 2003; Hodgson, Astapova

et al. 2005). Disruption of AR N/C protein interactions and binding of coactivators assist in repression of AR activity, Since AR-NTD is the main region mediating transcriptional activation; this suggests corepressors recruited to this region are key for repressing AR function. NCoR has been found to interact strongly with the AR-NTD region thereby preventing SRC1 from interacting with the NTD region. Mutagenesis studies showed that NCoR interacted with an area distinct from FxxLF motif and TAU5, regions required for AR N/C interaction (Hodgson, Astapova et al. 2005). On the other hand, TAU5 has been defined as a SMRT binding region, the degree to which SMRT could repress AR activity increased proportionaly with the number of CAG repeats in the polyQ tract (Buchanan, Need et al. 2011). It is generally believed the transcriptional competence of AR correlates to the number of CAG repeats; an increase in the polyQ region inhibiting p160-mediated coactivation of the AR (Irvine, Ma et al. 2000). Increasing the amount of SMRT in the assay abolished SMRT-mediated AR repression as a result of cofactor competition suggesting a functional link between CAG repeat length and AR activity with a balance between corepressor and coactivator occupancy for the LBD and NTD-binding (Buchanan, Need et al. 2011). Another copressor that abrogates N/C interaction is cyclin D1, which binds directly to the FxxLF motif within the AR-NTD region preventing the conformational changes required for AR stabilisation on chromatin. Its ability to bind HDAC3 was also important for AR inhibition (Petre, Wetherill et al. 2002). Human checkpoint protein hRad9 also abrogates the N/C interaction due to its high affinity C-terminal FxxLF motif competing with LxxLL-like motifs in coactivators (Wang, Hsu et al. 2004).

NCoR or SMRT further inhibit AR transcriptional activity due to the presence of at least two independent repressor domains in these proteins, which recruit primarily HDAC3 complexes (Fischle, Dequiedt et al. 2002). This results in deacetylation of lysine residues of histone proteins, tightening between nucleosomes and DNA leading to chromatin condensation and promoter inaccessibility. Other corepressors that require HDAC activity include protein inhibitor of activated STAT (PIASγ) and cyclin D1 since trichostatin A (TSA) an inhibitor of class I/II HDACs restored AR activity (Burd, Morey et al. 2006). Other corepressors such as ErbB3-binding protein (EBP1) and TG-interacting factor (TGIF) mediate their effect through Sin3, a protein that provides structural support for Sin3/HDAC complexes and other DNA-remodelling enzymes by directing Sin3 complexes to specific gene targets (Burd, Morey et al. 2006). AR

is equally susceptible to deacetylation as it is to acetylation; HDACs directly repress AR activity by deacetylation. HDAC1 has been reported to interact with the DBD/LBD region and is required for AR repression. Sirtuin 1 (SIRT1) a class 3 HDAC is also able to regulate AR activity through direct deacetylation and could also abrogate p300-enhanced AR N/C interaction possibly by disrupting acetylation of the AR hinge region (Lavery and Bevan 2011). In summary, HDACs play a significant role in facilitating repression of AR while the corepressors lend specificity to the regulation of AR transcriptional activity.

Table 1. List of selected AR coregulators that directly modulate AR transcriptional activity

Reviewed by the following: (van de Wijngaart, Dubbink et al. 2012) (Lavery and Bevan 2011) (Burd, Morey et al. 2006). ND, not determined

Name	Function	Coactivator/ corepressor	Region in AR to which coregulator binds
SRC1, TIF2, SRC3	HAT (SRC1 and SRC3) Recruitment of HATs	coactivator	TAU5 and AF-2
TIP60	HAT Chromatin remodelling	coactivator	AR-LBD
p300/CBP/PCAF	HAT	coactivator	Indirect
SWI/SNF complex	Chromatin remodelling	coactivator	AR-LBD (via BAF57 subunit)
MAGE-11	Inhibition of N/C interaction	coactivator	FxxLL in AR-NTD
RNF6	E3 ubiquitin-protein ligase	coactivator	Indirect
TRAPP20/MED1	Recruitment of preinitiation complex	coactivator	AR-LBD
NCoR	Recruitment of HDACs Inhibition of N/C interaction Competition with coactivators	corepressor	AF-2 AF-1
SMRT	Recruitment of HDACs Inhibition of N/C interaction Competition with coactivators	corepressor	AF-2 TAU5
Hey1, 2, L	Recruitment of HDACs Competition with coactivators	corepressor	AF-1
$PIAS_Y$	Recruitment of HDACs	corepressor	ND
SIRT1	HDAC	corepressor	ND
HDACs (class I and II)	HDAC	corepressor	ND
Cyclin D1	Inhibition of N/C interaction Recruitment of HDACs Competition with coactivators	corepressor	FxxLF in AR-NTD
hRAD9	Inhibition of N/C interaction	corepressor	AR-LBD
EBP1	Recruitment of HDACs	corepressor	ND
TGIF	Recruitment of HDACs	corepressor	ND

1.4.2. AR corepressor Hey1

Drosophila hairy and Enhancer of split [E(spl)] bHLH proteins belong to bHLH super-family of DNA-binding transcription factors and all share the tandem arrangement of a bHLH and Orange domain (Figure 5). Mammalian counterparts have six E(spl) proteins, (hairy and enhancer of split) Hes1-6 and three Hairy/enhancer of split with YPRW-like motif proteins (Hey) proteins Hey1, 2 and L. Hes and Hey proteins are effectors genes which are expressed as a result of the Notch signalling pathway, a principal regulator of gene expression. All function as DNA-binding transcriptional repressors and regulate a variety of biological functions (Davis and Turner 2001; Fischer and Gessler 2007). These will be discussed in further detail in relation to the Hey family proteins in section 1.5.1.1

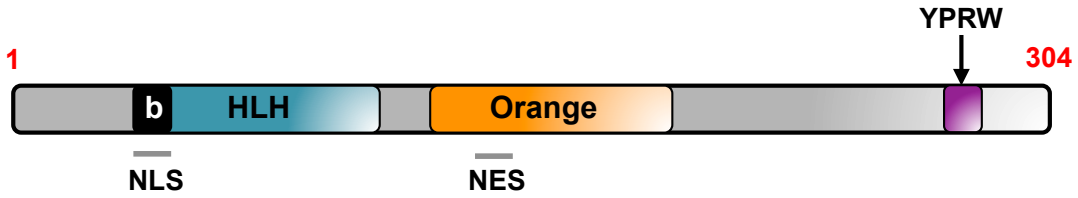

Figure 5. Protein domain structure of Hey1

The N-terminus consists of a DNA-binding basic domain (b), which contains an invariant glycine residue and is contiguous with the α-helix-loop-helix (HLH) region. The latter serves as a dimerization domain for homodimer/heterodimer formation as well as for other additional protein interactions. It is followed by two more α-helical stretches (the Orange domain), which functions as an additional interface for protein interactions. At the C-terminus resides a conserved YRPW motif. The NLS and nuclear export sequence (NES) are located in the basic and orange domain respectively (Villaronga, Lavery et al. 2009; Lavery, Villaronga et al. 2011). Diagram adapted from (Fischer and Gessler 2007).

1.4.2.1. Hey1, a bHLH –Orange transcriptional repressor

The preferred DNA binding site for Hey1 proteins is the class B E-box sequence, CACGTG. N-box binding for Hey1 and Hey2 (which is the preferred sequence for Hes proteins) is very weak although binding to class C E-box sites (CACGCG) occurs when heterodimer Hey2/Hes1 is formed (Fischer and Gessler 2007). The HLH and orange domains mediate protein-protein interactions facilitating the recruitment of cofactors such as HDACs and/or Sin3A complexes and interactions with transcription factors often converting these into transcriptional repressors (Fischer and Gessler 2007). In contrast to

the Hes family of proteins, which recruit corepressors TLE/Groucho via their C-terminal WRPW motif, Hey proteins are unable to bind TLE proteins due to the tyrosine to tryptophan (Y → W) exchange (Fischer and Gessler 2007). Instead, the transcriptional repressive activity of Hey proteins has been mapped to the bHLH domain. This activity was found to be associated with direct interaction with the mSin3A complex, which could indirectly recruit HDAC1. Transcriptional repression by Hey1 was also attributed to bHLH-mediated interaction with the NCoR corepressor (Iso, Sartorelli et al. 2001). In another study, Hey2 repressed its own gene expression by a HDAC1/II-independent mechanism and was later found to recruit SIRT1, an HDAC insensitive to TSA (Nakagawa, McFadden et al. 2000; Takata and Ishikawa 2003). In addition to HDAC-associated complexes, Hey proteins have also been demonstrated to interact with other transcription factors. For example, Hey1 was found to bind to the aryl hydrocarbon receptor nuclear transporter (ARNT) and was proposed to inhibit ARNT-dependent transcription from the VEGF promoter by mediating the release of the ARNT complex from DNA (Chin, Maemura et al. 2000). Both Hey1 and Hey2 have been reported to mediate repression of Myo-dependent transcription of the myogenin promoter through the sequestration of MyoD-E47 complexes rendering them inactive. This repression was mapped to the Orange domain in Hey2 since neither the C-terminal or bHLH regions were required to mediate repression (Sun, Kamei et al. 2001). This illustrates the ability of Hey proteins to physically interact and antagonise the activity of other transcription factors. In fact, there have been few instances that implicate a role of DNA binding for Hey protein function. One such case is the binding of Hey1 to a putative E-box sequence within the proximal promoter of IL-6 resulting in repression of IL-6 transcription (Hu, Chung et al. 2008). Microarray expression and ChIPseq analyses studies in Hey1-inducible cell lines indicated Hey proteins act as direct transcriptional repressors and mutagenesis of putative class B E-box binding sites supported the notion of direct DNA binding. However only a fraction of Hey proteins bound box-E sequence sites suggesting Hey proteins can bind a more relaxed consensus sequence or depend on interacting proteins (Heisig, Weber et al. 2012). The microarray analysis also identified cases of gene activation. Since no direct Hey binding was associated with these genes, activation must be mediated by indirect/secondary mechanisms (Heisig, Weber et al. 2012).

1.4.2.2. Hey-family proteins are AR corepressors

Characterisation of Hey1 as an AR corepressor commenced after Hey1 was identified to interact with the bHLH-PAS domain of SRC1 in a yeast two-hybrid screen (Belandia, Powell et al. 2005). Glutathione S-transferase (GST) pull down assays determined Hey1 could interact with the AF-1 region on the AR and repressed AF-1-mediated transcriptional activity. This repressive function of Hey1 was mapped to two distinct domains, the C-terminal portion and the N-terminal bHLH region. Treatment with TSA completely reversed the repressive effects of a Hey1 mutant lacking the HLH domain but only partially reversed the repressive activity of full length Hey1 or C-terminal truncated Hey mutants indicating HLH-mediated repression was both class I/II HDAC-dependent and –independent (Belandia, Powell et al. 2005). Results from other studies suggest Hey and Hes proteins can recruit HDAC1 using the bHLH domain and the C-terminus while SIRT1 binds only to the bHLH domain (Takata and Ishikawa 2003; Elagib, Xiao et al. 2004; Fischer, Klattig et al. 2005). This model presents a reasonable explanation for the Hey1-mediated AR repression. Hey1-mediated repression required both bHLH and C-terminal domains since the isolated domains failed to inhibit transcription from androgen-responsive promoters (Belandia, Powell et al. 2005). More recently, HeyL was found to be more potent than Hey1 or Hey2 in repressing AR activity and was not dependent on class I/II HDAC activity (Lavery, Villaronga et al. 2011). HeyL was also found to interact with the AF-1 region of AR and repressed its activity through this region too. Mutational analysis of AF-1 determined that deletion of either TAU1 or TAU5 decreased repression of AR by HeyL. However, deletion of TAU5 resulted in a comparatively smaller decrease of repression than deletion of TAU1 suggesting TAU1 transactivation activity is the main region of AR which HeyL affects (Lavery, Villaronga et al. 2011). As discussed above, competition between coactivator and corepressor is also an important regulatory mechanism for AR activity. The functional significance of Hey1/HeyL or SRC1 binding to AF-1 is evident since both Hey1 and HeyL were able to compete with SRC1 for binding to AF-1 thereby blocking SRC1/AR interaction or sequestering SRC1 away from transcriptional complexes (Belandia, Powell et al. 2005; Lavery, Villaronga et al. 2011).

1.5. Notch signalling

1.5.1. The Notch signalling pathway

The Hey family of transcriptional repressor proteins are canonical targets of Notch signalling, an evolutionarily conserved local cell signalling pathway. Notch signalling regulates a variety of developmental processes that include cell fate specification, stem cell renewal, differentiation, proliferation, apoptosis, adhesion, epithelial mesenchymal transition (EMT), migration and angiogenesis (Moreno 2010). The Notch protein functions at the cell surface, receiving extracellular signals and in the nucleus, regulating gene expression. In mammals there are four Notch proteins (Notch 1-4) and five ligands, three Delta-like proteins (DLL 1, 3 and 4) and two Jagged proteins, Jagged1 and Jagged2 (Ranganathan, Weaver et al. 2011). Figure 6 summarises the activation of the Notch signalling pathway. In addition to the Hey protein family, downstream targets of Notch signalling include the Hes family of proteins, cyclin dependent kinase (CDK) inhibitor p21, cyclin D1, c-Myc, Bcl-2 as well as Notch receptors and ligands (Ranganathan, Weaver et al. 2011).

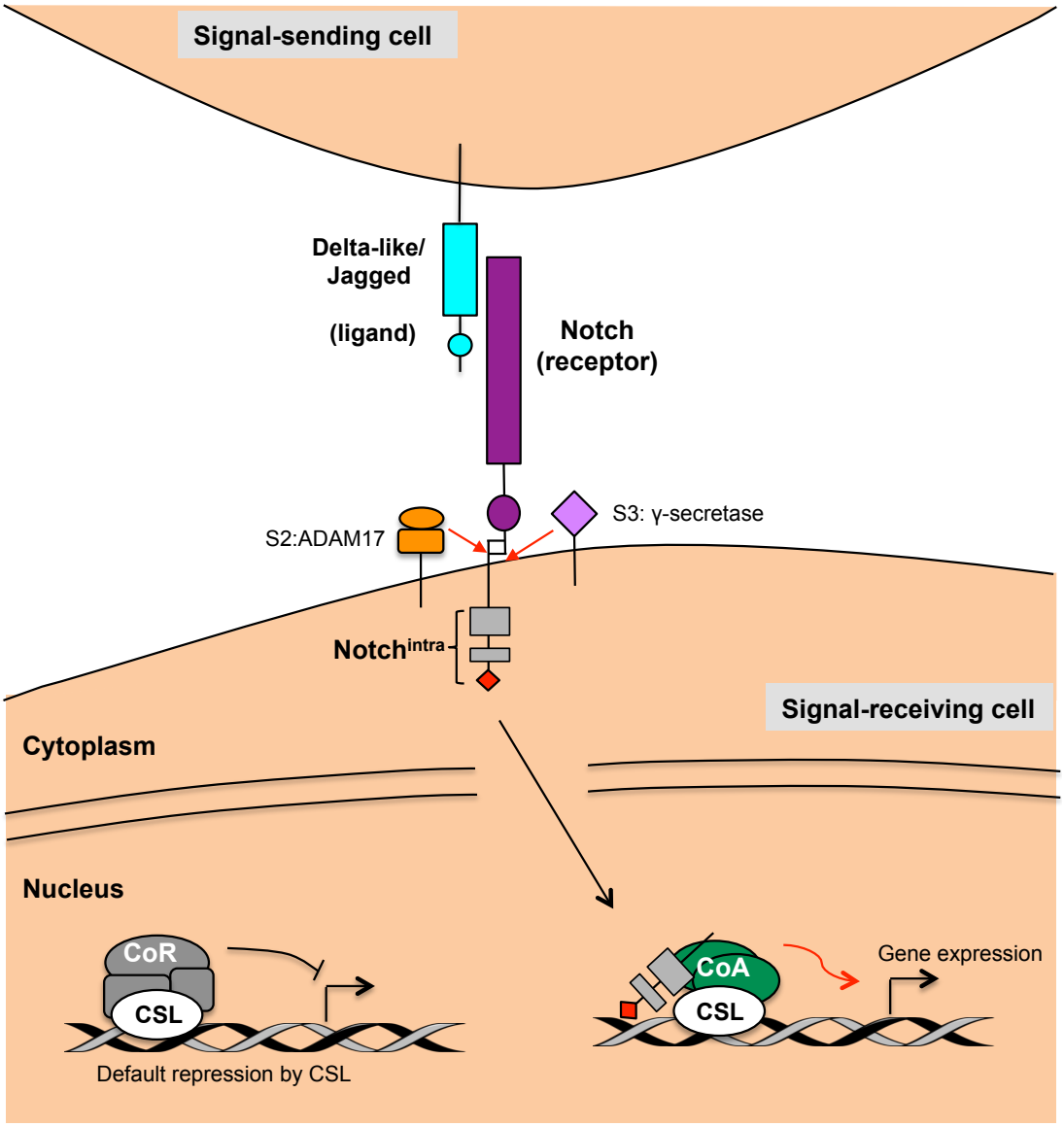

Figure 6. A basic outline of Notch signalling

Delta-like and Jagged ligands and Notch are transmembrane proteins. Engagement of a Notch receptor with its ligand expressed on neighbouring cells initiates two successive cleavages in the signal-receiving cell: firstly by ADAM metalloproteinases at site S2 followed by intramembranous cleavage at site S3 by the protease γ-secretase. The S3 cleavage liberates the intracellular domain of Notch (Notch^{intra}) and subsequently translocates to the nucleus. Prior to Notch activation, the transcriptional repressor, C protein binding factor 1/Suppressor of Hairless/Lag1 (CSL) is bound to DNA along with other corepressors (CoR) such as SMRT/NCoR and HDAC1. Notch^{intra} binds to CSL thus displacing the CoR complex and recruits coactivators (CoA) of the Mastermind-like (MAML) family, p300/CBP and other HATS converting the CSL complex into a transcriptional activator complex and driving Notch target genes. Target genes include Hes1, Hey1, cyclin D1, p21, c-Myc and Bcl-2 as well as Notch receptors and ligands. The activity of Notch^{intra} is transitory since the signal is terminated with phosphorylation of the C-terminal PEST domain (red diamond) within Notch^{intra}. This is followed by ubiquitination and Notch^{intra} is targeted for proteasomal degradation. Adapted from (Lai 2004) (Ranganathan, Weaver et al. 2011).

1.5.1.1. Hey proteins are Notch effector proteins

In 2000, the Hey family of transcriptional repressor proteins in mouse and human were cloned and characterised as a subfamily of bHLH superfamily and shortly afterwards were identified as downstream effector proteins of Notch signalling alongside the Hes proteins (Steidl, Leimeister et al. 2000). The Hey genes are involved in transducing Notch signalling in a number of embryonic development pathways namely the cardiovascular system, angiogenesis, neurogenesis, gliogenesis and bone development (Davis and Turner 2001). Hey proteins are implicated in a wide-range of processes however it is beyond the scope of this thesis to comprehensively describe them all and so only key aspects in the biological activities of the Hey proteins will be discussed.

All three Hey genes are active and expressed in the endocardium of the developing heart and blood vessels. A series of knockout mice have been generated to understand the molecular effects of Notch signalling in the heart. *Hey1*$^{-/-}$ and *HeyL*$^{-/-}$ mice are viable and show no apparent pathology (Fischer, Klamt et al. 2004; Fischer and Gessler 2007). However, *Hey2*$^{-/-}$ mice die within 10 days of birth from defects in the ventricle septum and the combined loss of *Hey1* and *Hey2* results in embryonic death. These defects in double *Hey* null mice recapitulate phenotypes in Jagged1 and Notch1 knockout mice indicating Hey proteins are essential transducers of Notch signalling (Gessler, Knobeloch et al. 2002; Fischer, Klamt et al. 2004). Moreover, the combined *Hey1/HeyL* knockout animals have the same cardiac phenotypes as *Hey2*$^{-/-}$ mice suggesting all three Hey genes perform similar functions with partial redundancy between the family members (Fischer and Gessler 2007). Functional redundancy between the different Hey members at the target gene level was recently determined *in vitro* using ChIPseq analysis (Heisig, Weber et al. 2012). This may also be the case in the context of androgen signalling since no additive effects were observed with HeyL-induced repression of AR transcriptional activity when Hey1 or Hey2 were combined with HeyL (Lavery, Villaronga et al. 2011).

Hey1 has also been identified as a direct target of signalling induced from bone morphogenic protein (BMP) receptors. BMPs are members of the transforming growth factor-β (TGF-β) superfamily and play an important role in regulating osteoblast differentiation and bone formation. Hey1 is upregulated in the early

stages of osteogenic differentiation of mesenchymal stem cells *in vitro* and enhanced mineralisation of the bone matrix *in vivo* in response to BMP9. This is proposed to occur in synergy with Runx2, another Notch target (Sharff, Song et al. 2009).

1.5.2. Notch signalling and cancer

Mutations in signalling pathways required for embryonic development often lead to the development of cancer. The presence of mutations or deregulation of the Notch pathway has been associated with a range of cancers. The prototypical Notch-associated cancer is human acute T-cell lymphoblastic/lymphoma (T-ALL) which was originally associated with a chromosome translocation resulting in the expression of $Notch1^{intra}$ under the control of the T-cell receptor β promoter. This aberration is however rare and the majority of T-ALL have gain-of-function mutations in Notch1 resulting in abnormal downstream signalling (Ranganathan, Weaver et al. 2011). A causative role of Notch signalling in the development of T-ALL is well established however evidence indicating that Notch signalling directly contributes to tumourigenesis of epithelial tissue remains elusive. While genetic alterations in Notch genes in solid tumours are uncommon, Notch signalling appears crucial in a number of tumours, including prostate, breast, colon, pancreas and cancers of the central nervous system (Ranganathan, Weaver et al. 2011).

The outcome of altered Notch signalling is dependent on its normal function in a given tissue as well as interactions with the tumour microenvironment and crosstalk with other signalling pathways. Inappropriate activation of Notch signalling in tumourigenesis of solid tumours may occur by either the loss of negative regulators, indicating Notch has a tumour suppressor function or the deregulated expression of Notch receptor and ligands leading to aberrant activation of the pathway (Ranganathan, Weaver et al. 2011). Recent studies using T-ALL models have indicated Notch drives tumourigenesis by promoting cell cycle progression directing transcription of cyclin D1, c-Myc and Skp2. In glioma cells, Notch overexpression is observed which results in crosstalk and activation of the EGFR pathway since siRNA-mediated knockdown of Notch resulted in downregulation of EGFR as well as downstream signalling components including PI3K/AKT pathway, Ras and cyclin D1 (Xu, Qiu et al.

2010). In addition to activating cell proliferation and survival pathways, apoptosis is also inhibited as a consequence of a deregulated Notch pathway. In certain tumour types, PTEN activity is inhibited due to enhanced expression of the PTEN negative regulator, Hes1. As a consequence, enhanced PI3K/AKT signalling occurs which leads to the phosphorylation of the p53 negative regulator, HDM2 resulting in p53 inhibition (Nair, Somasundaram et al. 2003). In T-ALL, Notch activation also leads to the repression of the HDM2 negative regulator, $p14^{ARF}$ (Beverly, Felsher et al. 2005).

In contrast, a tumour suppressor function for Notch has also been ascertained in a number of different tumour types. One of the first indications of this was in mouse keratinocytes where inactivation of Notch1 resulted in spontaneous and chemical-induced carcinogenesis in mouse skin (Nicolas, Wolfer et al. 2003). Inducible inactivation of Notch1 was also able to cause regenerative hyperplasia in mouse liver indicating loss of Notch signalling contributed factor to cancer progression in the liver. Consequently, overexpression of $Notch1^{intra}$ in a hepatocellular carcinoma model sensitised cells to p53-mediated apoptosis as a result blocking the AKT-HDM2 pathway and preventing proteasomal degradation of p53 (Wang, Qi et al. 2009; Ranganathan, Weaver et al. 2011). A further example comes from Ewing's sarcoma, which develops in part, as a result of down-regulated Jagged1 expression and inhibition of Notch signalling as a result of EWS-FLI1, a fusion gene that has arisen from a chromosome translocation. Tumours retain wild-type p53 although it is poorly expressed as a consequence of the EWS-FLI1 oncogene. Knockdown of EWS-FLI1 was able to reactivate Notch signalling as demonstrated by Hey1 expression and increased p53 activity (Ban, Bennani-Baiti et al. 2008; Dotto 2009). The implication of Hey1 as regulator of p53 expression will be discussed later in this chapter.

1.5.3. Notch signalling and PCa

1.5.3.1. Notch signalling in normal prostate development

Notch signalling along with other developmental pathways including the AR, TGF-β, fibroblast growth factor (FGF), Hedgehog and Wnt play critical roles in

normal prostate development. Notch signalling regulates embryonic prostate development and postnatal prostate maturation. This was first shown using a Notch1-GFP transgenic mouse model where GFP was under the control of the Notch1 promoter. *In situ* hybridization demonstrated Notch1 activation was found in all cells of the epithelium at postnatal 3 days, however activity was down-regulated overtime and in the adult, GFP expression was only associated with the basal layer of prostate epithelium (Shou, Ross et al. 2001). The suggestion that Notch1 expression may be a significant characteristic of prostate progenitor cells was studied further using a transgenic mouse model that allowed the selective elimination of Notch1-expressing cells with a prodrug-converting enzyme under the control of the Notch1 promoter. The ablation of Notch1-expressing cells resulted in inhibition of branching morphogenesis, growth and differentiation and prevented androgen-induced regrowth after castration (Wang, Shou et al. 2004). These data indicate Notch signalling elements are differentially expressed in the prostatic epithelium during postnatal prostate maturation and crucially, define Notch signalling in prostate development and regrowth. Furthermore it was subsequently established that Notch signalling is required for normal prostate epithelial proliferation and differentiation (Wang, Leow et al. 2006). Modulating Notch activity in early postnatal rat ventral prostates *ex vivo* with γ-secretase inhibitors resulted in reduced branching morphogenesis while staining with p63, an epithelial cell marker, revealed prostates treated with γ-secretase inhibitors exhibited less luminal and basal segregation. Prostates treated with inhibitors displayed a highly proliferative phenotype as well as co-expression of cytokeratin 8 and 14, markers that are normally mutually exclusive and are associated with luminal and basal cells respectively (Wang, Leow et al. 2006). This suggests Notch is essential for controlled prostate proliferation as well as effective differentiation.

1.5.3.2. Notch signalling and PCa development

Together with the requirement of Notch activity in normal prostate functioning, Notch signalling was also implicated as having a role in malignant prostate epithelial cells. In the transgenic adenocarcinoma of the mouse prostate (TRAMP) model, Notch1 was elevated in malignant prostate and metastatic epithelial cells. In PCa cells lines, Notch1 mRNA was expressed whereas Notch ligand expression was undetectable. By expressing constitutively active forms of

Notch1 in these cells Notch signalling was reactivated and resulted in cell growth inhibition (Shou, Ross et al. 2001). Later, the same group utilised a conditional Notch1 knockout mouse model and demonstrated Notch1 deletion was associated with a hyperplastic phenotype and prostate epithelial cells were in a predifferentiation development stage as indicated by the co-expression of cytokeratin 8 and 14 (Wang, Leow et al. 2006). This suggested disruption of Notch signalling might contribute to tumourigenesis since the Notch1 knockout model resembled the early stages of prostatic neoplasia (Wang, Leow et al. 2006). Analysis of microarray data in the Gene Logic database found Notch1 and its effector, Hey1 to be significantly lower in prostate adenocarcinoma compared with adjacent normal prostate tissue supporting the notion that Notch may play a tumour suppressive role (Wang, Leow et al. 2006). A more recent study concluded a similar outcome; Notch signalling was significantly downregulated in prostate adenocarcinoma foci since cleaved Notch1 was undetectable and Hey1 expression low compared with adjacent benign tissue (Whelan, Kellogg et al. 2009).

In contrast another study found Notch1 ligand, Jagged1 to be overexpressed in human prostate tumour samples (Santagata, Demichelis et al. 2004). Previously, Jagged1 had been identified as an androgen-responsive gene in lymph node-derived LNCaP cells and this led to the interrogation of the comparative Jagged1 protein levels in benign tissue or tumour tissue from localised PCa or hormone- and refractory-metastatic PCa using immunohistochemistry (IHC). Jagged1 was significantly more highly expressed in localised PCa compared with benign tissue and in metastatic PCa compared with localised or benign tissue. Furthermore, increased Jagged1 expression correlated with PCa recurrence suggesting Jagged1 is involved in cancer progression (Santagata, Demichelis et al. 2004). In agreement with this, down-regulation of Jagged1 in PCa cell lines correlated with inhibition of cell growth (Zhang, Wang et al. 2006). Notch1 is also overexpressed in osteoblastic prostate cancer metastatic cells compared with non-skeletal metastatic LNCaP and PC3 cells. Clinical samples of osteoblastic PCa metastases also express Notch1 (Zayzafoon, Abdulkadir et al. 2004). Together this suggests Jagged1 and Notch1 are associated with PCa metastases and it is possible Jagged1-mediated Notch1 activation could stimulate metastasis. In support of this hypothesis, inhibition of Notch signalling with a γ-secretase inhibitor or Notch1 siRNA in a Notch-induced metastatic cells reduced PCa cell motility or invasion

respectively (Scorey, Fraser et al. 2006; Bin Hafeez, Adhami et al. 2009). In a different study, an increase in apoptosis and a decrease in migration and invasion were reported when Notch1 or Jagged1 activity was blocked. This effect was associated with inactivation of AKT, mTOR and nuclear factor-κB (NF-κB) (Wang, Li et al. 2010). These data suggest Notch may play an oncogenic role in PCa progression since inhibiting Notch signalling resulted in the growth inhibition of PCa cells. Nevertheless, Shou *et al* reported that introduction of constitutively active components of Notch signalling blocked cell growth while inhibitors of Notch activation enhanced proliferation. Furthermore, human PCa samples also demonstrate loss of Notch1 signalling as shown by a decrease in Hey1 and/or cleaved Notch expression suggestive of a tumour suppressor function. These contradictory findings for Notch signalling playing a tumour suppressor or oncogenic role may reflect the heterogeneity of PCa and Notch may play different roles within different tumour types at different stages of cancer progression (Leong and Gao 2008).

1.5.3.3. Hey1 and cancer

It is unsurprising that the essential and recognised role of Hey proteins in embryonic development translates to their association with the development of cancer. There is now a growing body of evidence that Hey1 is deregulated in cancers. The Hey1 gene is located on chromosome 8q21, which is amplified in a significant proportion of prostate tumours (DeMarzo, Nelson et al. 2003). *In situ* hybridisation of primary tumour microarrays revealed Hey1 to be upregulated in glioma and expression in glioblastoma multifome (GBM) correlating positively with tumour-grade and survival (Hulleman, Quarto et al. 2009). pRb plays a crucial role in neurogenesis with neural precursor cells from *pRb*$^{-/-}$ mouse embryos exhibiting an increase in S-phase population and deregulated E2F activity. This underscores the alteration of the pRB/E2F pathway found in gliomas. Deregulated E2F activity was demonstrated to directly regulate Hey1 expression through E2F-binding sites present in the *Hey1* promoter. Moreover, ectopic expression of Hey1 in neural stem cells induced proliferation while knocking down Hey1 reduced growth suggesting Hey1 is an important factor in formation of GBM (Hulleman, Quarto et al. 2009).

Notch signalling has been implicated in modifying the EMT programme during embryogenesis and the signals responsible for stimulating EMT have also been associated with tumour invasion and metastasis. Fundamentally, EMT is a process by which cells from a primary epithelial tumour become mesenchymal and with that lose cell-adhesion and become motile. This model provides a method by which single cell carcinoma cells from primary epithelial tumours disseminate and facilitate metastasis. TGF-β signalling is involved in inducing EMT during development and is also reported to promote EMT in cancer cells allowing spread to other sites *in vivo* (Yang and Weinberg 2008). Hey1 has been identified as a direct target gene of TGF-β/SMAD signalling (Zavadil, Cermak et al. 2004). TGF-β stimulation of epithelial cells of mammary gland, kidney and epidermis resulted in Hey1 expression in a biphasic manner during the onset of EMT. The first phase of Hey1 expression was directed by SMAD3/4 activating transcription from the Hey1 promoter while the second delayed wave of gene activation required Notch-dependent signalling with TGF-β signalling through SMAD3 and ERK/MAPK resulting in the expression of Jagged1. Silencing of Hey1 or Jagged1 blocked TGF-β-induced EMT preventing disassembly of E-cadherin adherens junctions (Zavadil, Cermak et al. 2004). This suggests that the coordinated expression of Hey1 by Notch and TGF-β signalling pathways are important for EMT, a process also observed in advanced tumourigenesis.

The role of Hey1 functioning as a tumour suppressor was derived after a genome-wide screen for potential p53 regulators revealed Hey1 as positive regulator of p53. Overexpression of Hey1 in HCT116p53$^{+/+}$ cells resulted in increased p53 activity due to a decrease in human homolog of murine double minute 2 (HDM2) expression at the transcriptional level thus blocking HDM2-mediated degradation of p53. Hey1 was found not to bind to E-box or N-box sequences within the HDM2 promoter suggesting repression by Hey1 was independent of its DNA-binding abilities (Huang, Raya et al. 2004) and more likely to be a consequence of recruiting other HLH proteins, corepressors or HDAC proteins to the transcription complex. Evidence of Hey1 as a tumour suppressor was attained after ectopic expression of Hey1 in zebrafish increased p53 levels and induced apoptosis. In avian embryos, overexpression of Hey1 resulted in truncation of developing wings. Furthermore, Hey1 was able to overcome Ras- and Myc-induced transformation of mouse embryonic fibroblast (MEF) cells in a p53-dependent manner but was ineffective in supressing

transformation in p53-deficient MEFs (Huang, Raya et al. 2004). Hey1-dependent p53 activation was later demonstrated in Ewing's sarcoma when knockdown of the EWS-FL1 fusion protein reactivated Notch signalling resulting in Hey1 expression, enhanced p53 activity and cell cycle arrest (Ban, Bennani-Baiti et al. 2008).

Recent studies investigating the ability of Hey1 to activate p53 signalling have been extended to include Hey1 with a naturally occurring non-synonymous polymorphism (SNP) present in 1% of the population. This SNP results in a leucine substitution to methionine at codon 94 (L94M) in the bHLH domain of Hey1. The SNP resulted in L94M acting as a coactivator of AR and was also unable to stimulate a p53-responsive reporter gene (Villaronga, Lavery et al. 2009). Functional differences between Hey1 and L94M were examined by stably expressing inducible Hey1 or L94M in human osteosarcoma U2OS cells. Induction of Hey1 expression was found to inhibit cell proliferation and induce growth arrest concomitant with an increase in p53 expression whereas expression of L94M did not perturb cell homeostasis. Furthermore Hey1-mediated increase in p53 activity was able to sensitise U2OS cells to cisplatin or doxorubicin in contrast to L94M, which had no effect on the sensitivity of cells to the cytotoxic drugs (Villaronga, Lavery et al. 2009). These results may have important implications in the outcome of cellular response to anticancer drugs for patients with this polymorphism. Since half of human cancers express wild-type p53, it has been postulated that L94M could contribute to oncogenic transformation in a proportion of tumours.

1.5.3.4. Hey1 and PCa

As discussed previously, Hey1 expression as assessed by microarray and IHC found Hey1 to be significantly down regulated compared with normal tumour-adjacent prostate tissue (Wang, Leow et al. 2006; Whelan, Kellogg et al. 2009). Wang *et al* also assessed the level of other Notch signalling components; Notch receptors (Notch 2, Notch3, and Notch4), Notch ligands (DLL1, Jagged1 and Jagged2) and downstream target genes (Hes1, Hes4, Hes6 and Hey2) and found equivalent mRNA levels to be expressed between normal and cancerous PCa tissue (Wang, Leow et al. 2006) implying Hey1-mediated Notch signalling may play a potential role in inhibiting prostate tumourigenesis. In contrast,

another study did not report a change in total Hey1 protein levels in cancerous prostate tissue but reported a difference in the subcellular localisation of Hey1. In 8 out of 10 PCa tumours, Hey1 protein expression was confined to the cytoplasm whereas in 13 out of 14 benign prostatic hyperplasia tissue samples, Hey1 was detected in both the cytoplasmic and nuclear compartments with the majority showing greater nuclear Hey1 expression (Belandia, Powell et al. 2005). Later, another study determined HeyL was also excluded from the nucleus in human PCa tumour specimens with a concomitant increase in cytoplasmic expression in contrast to benign samples, where HeyL expression was exclusively nuclear (Lavery, Villaronga et al. 2011). These observations have led to the proposal that exclusion of Hey1 from the nucleus results in a reduction of this transcriptional repressor in the nucleus and consequently a decrease in the repression of target genes (Belandia, Powell et al. 2005; Powell, Brooke et al. 2006). The aberrant localisation of Hey1 and HeyL to the cytoplasmic compartment may be a mechanism to circumvent the repressive effects of nuclear Hey proteins and contribute to the development of androgen-independence (Powell, Brooke et al. 2006; Lavery, Villaronga et al. 2011). Manipulation of the NLS sequence within Hey1 provided an insight into its effects on AR transcriptional activity when localised in the cytoplasm. Mutation of the NLS converted Hey1 to an AR transcriptional coactivator whereas the coactivation function of the Hey1 mutant, L94M was not altered (Villaronga, Lavery et al. 2009). This suggests that the mislocalisation of Hey1 and HeyL through undetermined mechanisms might contribute to disease progression thereby enhancing AR transcriptional activity. We and others have screened PCa AR-positive cells for Hey1 and HeyL expression and have found very low levels of mRNA transcripts for these proteins suggesting a loss of expression may have occurred during malignant progression (Lavery, Villaronga et al. 2011)(Dr S.C. Cheong, unpublished observations).

1.6. Adenoviruses

1.6.1. Adenovirus classification

Adenoviruses were first isolated in 1953 from human adenoids. They form part of the *Adenoviridae* family of viruses which can be divided into four genera: *Mastadenovirus*, *Aviadenovirus*, *Atadenovirus* and *Siadenovirus*. These classifications are based on the hosts for the viruses; viruses of the *Mastadenovirus* infect mammals, *Aviadenovirus* infect birds while the other two genera have a broader host range, which include reptiles and amphibians (Davison, Benko et al. 2003). Human adenoviruses fall into the *Mastadenovirus* genus and more than 52 different human adenovirus serotypes have been identified. These have been classified into seven different species according to biological, physiochemical and genetic properties (Table 2). Human adenoviruses are not considered to be highly pathogenic and generally cause self-contained disease such as respiratory infections, haemorrhagic cystitis and gastroenteritis. Ocular infections are also a principal cause of viral conjunctivitis. However, the incidence of adenoviral infections causing life-threatening disease is on the increase due to immunocompromised individuals as a consequence of transplantation in conjunction with immunosuppressive therapy and the HIV epidemic (Lenaerts, De Clercq et al. 2008). The most widely studied are adenoviruses from Group C, the closely related serotypes 2 and 5 (Ad2 and Ad5) and for this reason have been most commonly used for the development of viral gene therapy vectors (other serotypes have also been used).

Table 2. Classification human adenoviruses based on biological and physiochemical properties.

Species	Serotypes	Receptors(s)	Tropism	Disease
A	12, 18, 31	CAR, FIX, FX	Cryptic (enteric and respiratory)	Mainly asymptomatic
B1	3, 7, 16, 21, 50	CD46, DSG-2, FX, CD80, CD86	Respiratory, ocular	Respiratory and ocular diseases
B2	11, 14, 34, 35	CD46, DSG-2, FX, CD80, CD86	Renal, ocular, respiratory	Respiratory diseases
C	1, 2, 5, 6	CAR, FIX, FX, Lf, DPPC, VCAM-1, HSPG, MHC1-α2	Respiratory, ocular, lymphoid,	Ocular diseases
D	8-10, 13, 15, 17, 19, 20, 22-30, 32, 33, 36-39, 42-49, 51	SA, CD46, CAR, fx	Ocular (enteric)	Ocular diseases
E	4	CAR	Ocular, respiratory	Respiratory and ocular diseases
F	40, 41	CAR	Enteric	Gastroenteritis
G	52	ND	Enteric	Gastroenteritis

CAR; Coxsackie adenovirus receptor, CD; cluster of differentiation, DPPC; diapalmitoyl phosphatidylcholine, FIX; coagulation factor IX, FX; coagulation factor X, HSPG; Heparan sulfate proteoglycans, Lf; lactoferrin, MHC1-α2; major histocompatibility complex 1- α2 domain, SA; sialic acid, VCAM-1; vascular cell adhesion molecule 1, ND; Not determined, DSG-2; Desmoglein-2 (Wang, Li et al. 2011). Based on a table within Arnberg 2009.

1.6.2. Adenovirus structure

1.6.2.1. The viral capsid

Adenoviruses are non-enveloped, lytic, double-stranded DNA viruses. They have an icosahedral morphology made up of three primary capsid proteins and four minor proteins (Figure 7). The homotrimeric hexon protein is the most abundant with 240 on the faces and edges of the capsid, with a penton base residing at each of the 12 apices. From each penton base extends a trimeric fiber protein composed of three polypeptide (p) IV molecules consisting of of an N-terminal tail, a central shaft and a C-terminal knob region. The N-terminal region is attached to the penton via non-covalent interactions. Also associated with penton are five copies of the minor capsid protein, pIIIa which is located at

the base of the penton. Other minor capsid proteins, pVI and pVIII bind hexon proteins on their underside although their exact locations have been difficult to resolve. pVIII is thought to provide a bond between hexons and the rest of the capsid while pIX stabilises interactions between adjacent hexons. Core proteins include pV and pVII, which associate with the viral DNA. The specific functions of pV remain unclear however in Ad5-infected cells it is directed to the nucleus and nucleolus and may facilitate dissociation of core proteins along with pre-pVII thereby revealing the viral DNA for replication/transcription. pVII, may play a role in mediating of nuclear import of the viral DNA, dampening early viral transcription and facilitating viral assembly at the end of the adenoviral life cycle. The function of another core protein, Mu is largely unknown however it can duplicate the nucleolar functions of pV and as part of a precursor (preMu) it may modulate the shift between early protein and late protein expression. The virion also contains approximately 10 copies of the adenovirus cysteine proteinase associated with viral DNA within the core. The protease is an essential feature of the virion; a defective mutant could not advance beyond initial stages of infection. In the latter stages of infection it is also required for cleaving structural proteins during virion maturation. Another core protein, IVa2 present in only a few copies, binds to the left hand end of the viral DNA and the major late promoter (MLP) via repeat sequences in the DNA. It mediates encapsidation along with pVII and the non-structural protein, L4 22K. IVa2 also regulates the switch to late transcription. The final structural protein, the terminal protein (TP) is covalently attached to the 5' DNA termini. TP is made from precursor, pTP and serves as a primer for DNA replications as well as mediate binding of the viral genome to the nuclear matrix (Shenk 2001; Russell 2009).

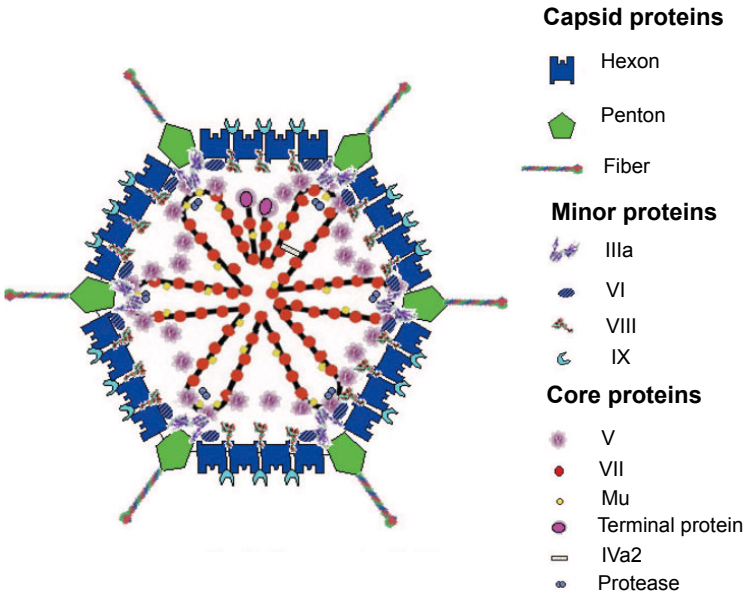

Figure 7. Adenovirus structure

A schematic representation of the structure based on cryo-electron microscopy and crystallography. Image taken from Russell 2009.

1.6.2.2. Genome organisation

In 1984, Ad2 was the first adenovirus genome to be completely sequenced and Ad5 followed in 1992 and is 35935 base pairs (bp) in length. The linear, double-stranded DNA molecule is characterised by inverted terminal repeats (ITR) which allow single stranded DNA to circularise by complementary base pairing with ITR sequences. This is important in forming panhandles, which is required for the replication of viral DNA (Shenk 2001). The genome also contains two origins of replication and one is present in each ITR. Additionally, a *cis*-acting packaging sequence situated at the left terminus, which interacts with structural proteins to direct the encapsidation of progeny virion (Shenk 2001).

Adenovirus transcription can be categorised as a two-stage event, early and late occurring before and after DNA replication respectively (Figure 8). The viral chromosome is subdivided into five early transcription units (E1A, E1B, E2, E3 and E4), which prepare the infected cell for efficient viral replication and modify the host immune response to the infected cells. Two delayed early units (IX and IVa2) are expressed shortly after the early genes and regulate transcription of late genes. The late genes are transcribed into a primary transcript from the major late promoter which its then processed into five families (L1 to L5). All

viral genes are transcribed by RNA polymerase II with the exception of virus-associated (VA) I and II genes. These are transcribed by RNA polymerase III and are expressed as short RNA molecules during the translation of viral mRNA (Shenk 2001). The functions of the viral genes are summarised in Table 3.

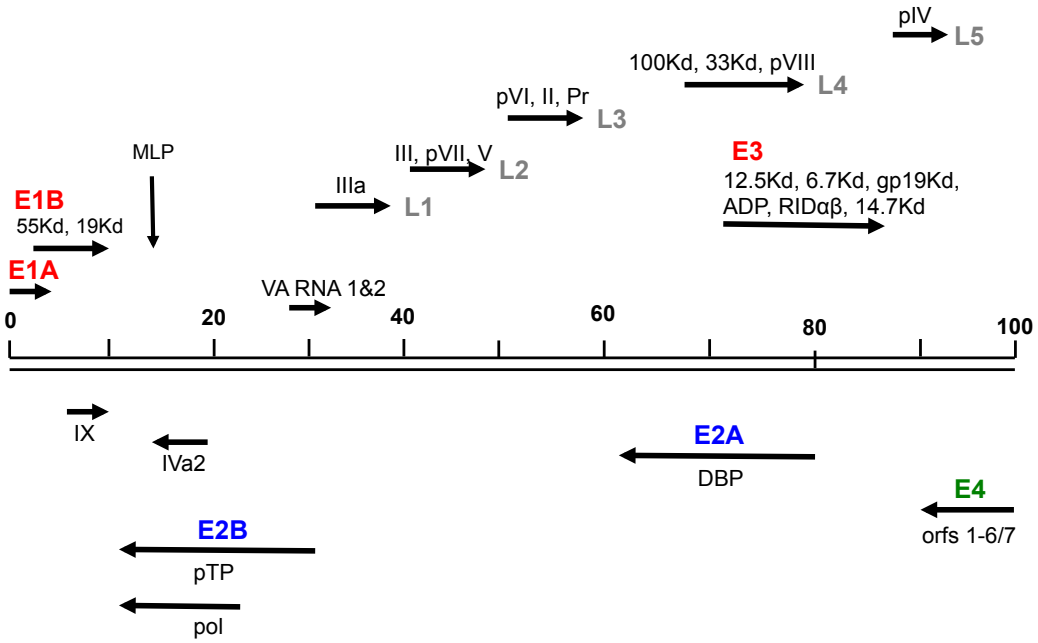

Figure 8. A schematic map of transcription of the Ad5 genome

The early genes (E1A, E1B and E3) which are involved in preparing the infected cell for DNA replication and modulating the immune response to the infected cell are outlined in red. The early genes E2A and E2B are involved in regulating viral DNA replication and are defined in blue. The last set of early genes (E4) have a disparate set of functions are outlined in green. The late genes are defined in grey and are transcribed from the MLP as one primary transcript which is subsequently processed by differential poly(A) site utilisation and splicing. The structural proteins encoded are termed II to IX. Arrows indicate the direction of transcription and both strands of DNA are transcribed. Adapted from Russell 2000.

Table 3. Protein products of Ad5 encoded genes and their functions

Gene	Protein	Function
E1A	E1A12S	• Binds many cellular proteins including pRB (p107 &p130), p300/CBP & STAT1 • Represses transactivating function of E1A13S through p300 binding • Activates p53
	E1A13S	• Transactivates viral genes • Binds to cellular proteins TBP, Sp1, CREB, DR1 • Essential for viral replication
E1B	E1B19Kd	• Anti-apoptotic Bcl2 homolog
	E1B55Kd	• Binds to and blocks p53 activity • Binds to and actively represses transcriptional activity of p53 • Together with E4orf6, stimulates late viral nuclear export; inhibits host cell mRNA export • Together with E4orf6 degrades cellular proteins in a E3 ubiquitin ligase complex
E2A	Polymerase	• Viral polymerase with 5'-to-3' polymerase activity and 3'-to-5' exonuclease activity
	DNA-binding protein (DBP)	• Chain elongation for DNA replication
E2B	Pre-terminal protein (Pre-TP)	• Covalently bound to 5' DNA termini • Primer for DNA replication • Attachment to nuclear matrix
E3A	12.5Kd	• Unknown
E3A	6.7Kd	• Unknown
E3A	gp19Kd	• Binds to MHC and sequesters it in the endoplasmic reticulum preventing presentation of viral antigens in infected cell
	Adenovirus death protein (ADP)	• Promotes viral release
E3B	10.4/14.5Kd RID	• Mediate internalisation of FAS receptor • Inhibits pro-apoptotic phospholipase A2
E3B	14.7Kd	• Inhibits FAS & TNF ligand-induced apoptosis by interacting with caspase-8 in FLICE • Inhibits pro-apoptotic phospholipase A2 • Bind to and blocks pro-apoptotic FIP proteins
E4	Orf 1	• Facilitates transformation
	Orf 2	• Unknown
	Orf 3	• Interacts with E1B55K
	Orf 4	• Inhibits E1A activation of E2F
	Orf 6	• Interacts with E1B55K for late viral RNA export • Shuts off cellular mRNA processing
	Orf 6/7	• Modulates E2F activity; transactivates E2A promoter by binding to E2F-binding sites

Gene	Protein	Function
Delayed early gene	IX	• Stabilises hexon-hexon interactions
	IVa2	• Activates late viral gene transcription • Mediates encapsidation process
L1	IIIa	• Bridges hexon and hexon interaction between facets
L2	III	• Penton base
	V	• Binds to penton base and may bridge the capsid and core • Facilitates final uncoating stages of capsid proteins. May participate with pre-VII
	VII	• Mediates localisation of virion to nucleus • Diminishes early transcription • Facilitates viral assembly at the end of lytic cycle
L3	II	• Associates in trimers to form hexon capsomere
	Protease	• Essential for uncoating during virion internalisation • Cleaves precursor polypeptides generating mature and infectious virus particles
	VI	• Stabilises hexon-hexon interactions • Bridges interaction between capsid and core • Mediates escape of virion from endosome during infection process
L4	100K	• Stimulates late viral translation • Participates in association of hexons during virion assembly
	VIII	• Stabilises hexon-hexon interactions • Bridges interaction between capsid and core
L5	IV	• Associates in trimers to form penton • Mediates attachment of virion to cell surface receptors
VA RNA	VA1 & VA2	• Blocks α- and β- interferon anti-viral response by inhibiting PKR activation • Prevents PKR-mediated protein synthesis shutoff
Mu		• Modulate E2 gene expression to switch from early to late viral transcription • Condenses viral chromatin during packaging of virion particles

Data summarised from Russell 2000; Gallimore and Turnell 2001; Shenk 2001; Wiethoff, Wodrich et al. 2005; Russell 2009

1.6.3. Adenovirus life cycle

1.6.3.1. Virus attachment, internalisation and trafficking to the nucleus

Adenovirus infection *in vitro* is a two-step process; firstly the distal C-terminal fiber-knob domain docks onto a cellular receptor. The coxsackie adenovirus receptor (CAR), a member of the immunoglobulin superfamily has been found to serve as a high-affinity receptor for all human adenovirus species except species B and G (Table 2). Adenoviruses from species B and D use CD46, CD80 or CD86 and the recently identified desmoglein (previously called receptor X) as cellular receptors and from species D use both CD46 and CAR. Ad5 has been shown to have numerous docking receptors including heparan sulfate proteogylcans (HSPG), the α2 domain of the class I MHC and the vascular cell adhesion molecule 1 (VCAM-1) (Table 2). *In vivo*, adenovirus has been shown to bind more physiologically relevant receptors such as complement-4 binding protein (C4BP), coagulation factor IX (FIX) and factor X (FX). Bridging/docking receptors include sialic acid, lactoferrin and O-linked sulfate side chains on HSPGs

Following the fiber-CAR interaction the second interaction requires an arginine-glycine-aspartic acid (RGD) motif within the penton protein to interact with cellular integrins ($\alpha_V\beta_3$ or $\alpha_V\beta_5$) which is essential for subsequent internalisation of most adenoviruses except those of species F which do not contain a RGD motif. Binding of RGD to integrins result in integrin clustering, which subsequently initiates downstream signalling cascades resulting in PI3K/AKT activation. This triggers the Rho family of GTPases and reorganisation of the actin cytoskeleton for clathrin-mediated endocytosis. Other intracellular signalling pathways activated are the extracellular signal-related kinase (ERK1/2) cascade resulting in clustering of CAR and increasing the activation status of β-integrin subunits as well as the p38/MAPK pathway resulting in an increase in IL-8 production indicative of activation of the host defence system (Russell 2000; Coughlan, Alba et al. 2010).

Disassembly of Ad5 occurs very soon after attachment as the fiber is released from the virion at the cell surface. The process of endocytosis allows for further

disassembly and acidification to pH4.6-6.0 induces conformational changes to the structure of the virion while proteolytic capsid maturation are thought to be essential for endosomal escape. Virus escapes from the endosome before the formation of the lysosome however the exact mechanism of endosome penetration has yet to be elucidated (Shenk 2001). Wiethoff *et al* demonstrated that pVI possessed 95% membrane lytic activity *in vitro* and consequently proposed that after hexons, penton, pIIIa and pVI are disassembled in the acidic endosome, pVI dissociates from the hexons and associates with the endosome membrane resulting in membrane disruption and release of the uncoated virions into the cytoplasm (Wiethoff, Wodrich et al. 2005). Once in the cytoplasm, the nucleocapsid-hexon core associates with cellular proteins including importins, histone H1 and HSP70. Transport to the nucleus occurs by way of the microtubule network using the microtubule-associated motor, dynein. pVII is thought to be the primary viral mediator of import to the nucleus (Russell 2009).

1.6.3.2. Viral gene transcription

As discussed in section 1.6.2.2, adenovirus transcription can be described as a two-phase event separated into early and late. There are three primary objectives of early gene transcription: firstly to induce S phase in the host cell thereby providing an optimal setting for viral replication, secondly allow expression of immunomodulatory viral genes to protect the cell from antiviral defences and lastly to enable synthesis of viral gene products required for DNA replication (Shenk 2001).

The E1A gene is the first transcription unit to be expressed after the viral chromosome enters the nucleus. A constitutively active promoter controls expression of the E1A unit leading to the synthesis of E1A12S (243 amino acids) and E1A13S (289 amino acids) during the early phases of infection. These contain identical 5' and 3' ends but differ in the central region due to differential splicing. Three highly conserved regions (CR)1, CR2, CR3 and CR4 are present in the E1A gene of human adenoviruses and along with conserved residues in the N-terminal region, facilitate protein-protein interactions with cellular proteins (Figure 9) (Shenk 2001). E1A12S and E1A13S differ only the presence of the CR3 region in E1A13S protein. The CR3 region within E1A13S acts as a strong activation domain, essential for activation of early viral

promoters and binds proteins involved in transcriptional activation including TATA-binding protein (TBP), MED23, a subunit of the MED complex and CREB. As a consequence, stabilisation of preinitiation complexes (PICs) with RNA polymerase II is allowed to occur at early adenoviral promoters. E1A13S protein is produced during the early phases of infection and is more efficient than E1A12S at transactivating early gene expression due to the presence of the CR3 domain (Shenk 2001; Berk 2005). Transactivation capabilities of E1A12S (and therefore E1A13S) are mediated through TATA motifs and E2F-binding sites. E1A12S can alleviate transcriptional repression directed by Dr1 (a protein which binds to and inhibits TBP) by binding to and requisitioning Dr1 from TBP. The E2F-binding sites present in the adenovirus E1A and E2 promoters are activated through indirect E1A12S modulation. Both E1A proteins bind to the pRB via the CR1 or CR2 domain thus relieving the inhibitory effect of pRB on transcriptional activity of E2F. E2F-mediated transcription affects viral gene expression and influences cellular gene expression; most notably genes important for S phase and cell growth (Shenk 2001). The presence of E1A is however not an absolute requirement for the transcription of early viral genes in some cell types since an E1A-deleted mutant, *dl*312 was shown to replicate in HeLa cells to a similar extent as wild-type when infected at a high multiplicity of infection. The discovery of E2F and E4F sites in the viral E2 and E4 promoter respectively indicated cellular transcription factors could bind early viral promoters and stimulate low levels of transcription initiation in the absence of E1A (Shenk 2001).

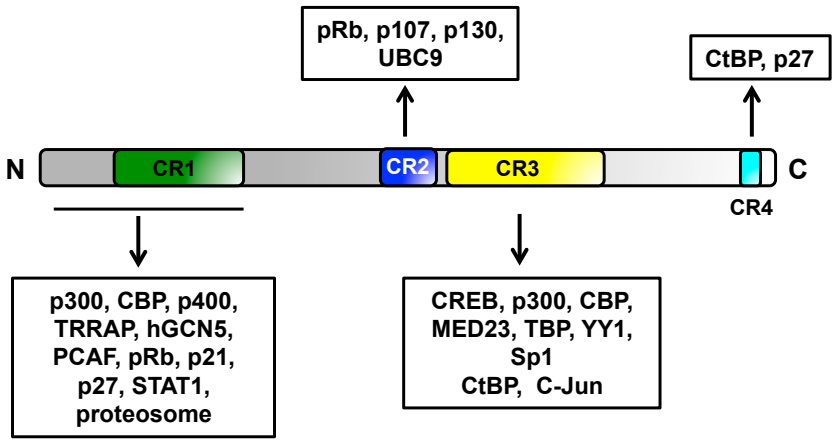

Figure 9. Schematic diagram of the protein domain structure of E1A13S

Cellular proteins bind to conserved regions (CRs) of E1A and through conserved residues present within the N-terminus. Listed are the main E1A-interacting proteins although this is not an exhaustive compilation.

1.6.3.3. Activation of the host cell

1.6.3.3.1. E1A-stimulated S phase induction

The protein products of early adenoviral genes modulate cellular metabolism to make the cell more receptive to virus replication. As illustrated in Figure 9, E1A interacts with many cellular proteins to generate the optimal cell environment for viral DNA replication. The most significant interactions for E1A are with pRb-pocket proteins and the p300/CBP proteins.

Entry into S phase is stimulated by primarily through E1A-binding to pRb via the CR2 domain. pRb, regulates the key effectors of proliferation, the transcription factor E2F family of proteins. When bound to E2F, pRb functions to inhibit E2F-1 transcriptional activity and maintains cells in G1. In response to growth stimulus, hypophosphorylated pRb is phosphorylated sequentially by cyclin/CDK complexes resulting in the release of E2F allowing it to activate transcription of genes required for DNA synthesis (Munro, Carr et al. 2012). E1A bypasses the regulatory signals applied by growth factor stimulation and competes with E2F for access to the pocket domain in pRB or related proteins, p107 and p130 via its CR2 domain. Binding is mediated through a LxCxE-motif in CR2 interacting with same domain to which pRb binds E2F-1. CR1 can also weakly interact with pRb and plays an auxiliary role stabilising CR2–pRb interaction and is necessary for driving the cell cycle into mitosis (Berk 2005). Independent of E2F sequestration, pRb functions as a transcriptional repressor through its interactions with multi-subunit HDAC-containing complexes as well as binding to members of the SWI/SNF transcriptional regulators, hBRM and BRG1 to promoter complexes resulting in cell cycle arrest. E1A binding to pRB disrupts these interactions thereby modifying the transcriptional repression applied by these pRB-containing complexes (Gallimore and Turnell 2001). In addition to disrupting pRB-E2F complexes, E1A binds to CDK inhibitors p21 and p27 preventing them from binding to and inhibiting G1 cyclin-CDK complexes (Shenk 2001).

A second pathway by which E1A enables cell cycle progression is through binding to p300 and CBP proteins. E1A binds to the transcriptional adapter motif (TRAM) of p300/CBP primarily through the CR1 and the N-terminal region

(O'Connor, Zimmermann et al. 1999). More recently the CR3 domain has also been shown to bind p300/CBP (Pelka, Ablack et al. 2009). p300/CBP proteins are multidomain proteins and as mentioned earlier in this chapter, exhibit intrinsic histone acetylase activity. They recruit other HAT proteins e.g. p300/CBP-associated factor (P/CAF) and serve as coactivators to numerous gene-specific transcription factors. Whether E1A inhibits HAT activity of p300/CBP is controversial and context-specific repression or elevation of HAT activity has been observed. In the context of S phase entry, p300/CBP acts as a coactivator of p53. By redirecting p300/CBP activity away from active sites of transcription the ability of p53 to induce cell cycle arrest through the transcription of CDK inhibitors or apoptosis via the expression of pro-apoptotic proteins is antagonized (Shenk 2001). However, this by itself does not stimulate S phase progression, it has been reported inhibition of p300 leads to an increase in c-Myc expression hence driving quiescent cells into S phase. This is thought to occur by E1A binding to p300 causing dissociation of p300, YY1 and HDAC3 from chromatin alleviating transcriptional repression of c-Myc promoter (Kadeppagari, Sankar et al. 2009). However HAT activity is crucially required for some of E1A functions; for example transcriptional activation of the viral E3 or E4 promoter is dependent on the recruitment of p300/CBP to E1A13S through its CR3 domain and was inhibited by the presence of E1A12S possibly by sequestering p300/CBP from the larger E1A protein (Pelka, Ablack et al. 2009). This suggests the transcriptional activity of p300/CBP depends on the ratio of E1A12S and E1A13S present with the CR1 domain of E1A12S repressing CR3-mediated transcriptional activity.

In addition to directing or sequestering p300/CBP towards or away from active sites of transcription, recruitment of p300/CBP may serve to facilitate acetylation of E1A itself. Acetylation of E1A at K239 or K285 on E1A12S and E1A13S respectively occurs proximal to the C-terminal Binding Protein (CtBP)-binding site. Mutation of this lysine residue blocked CtBP binding *in vitro* and disrupted E1A/CtBP interaction *in vivo* (Zhang, Yao et al. 2000). CtBP functions as a transcriptional repressor interacting directly with HDACS. The CR4 domain of E1A may disrupt this interaction by competing with HDACS for binding thereby requisitioning CtBP from transcriptional multimeric complexes (Sundqvist, Sollerbrant et al. 1998). Therefore, analogous to E1A-mediated inhibition of pRB-dependent repression, the CR4 domain might derepress cellular genes by sequestering CtBP. Conversely; E1A may repress cellular genes by tethering

CtBP to their promoter region possibly to counteract the activation capability of E1A-p300/CBP complexes (Berk 2005). Another mechanism by which E1A regulates the acetylation of histones is through the binding of chromatin remodeller, p400, a SWI2/SNF2 DNA-dependent ATPase that alters DNA-histone interactions (Gallimore and Turnell 2001). It exists in multimeric protein complexes alongside transactivation/transformation domain-associated protein (TRAPP), which itself is a key component of several multiprotein HAT complexes such as TIP60 and hGCN5 (Berk 2005). Both p400 and TRAPP/hGCN5 have been associated with c-Myc activity. E1A-mediated stabilisation of c-Myc has been connected with its interaction with p400 and an E1A mutant unable to bind p400 did not stabilise c-Myc. p400 is known to induce c-Myc and E1A promotes the association between p400 and c-Myc reducing ubiquitin-mediated degradation of c-Myc thereby promoting the formation of p400-c-Myc complexes on promoters of c-Myc-target genes (Chakraborty and Tansey 2009). Equally, TRAPP also binds to the N-terminus of c-Myc promoting transcriptional activation through recruitment of HAT complexes. By means of the N-terminus of E1A, TRAPP and/or hGCN5 are sequestered resulting in reduced transcriptional activation of c-Myc and E2F thereby redirecting transcriptional coactivators to viral and cellular promoters (Lang and Hearing 2003). This is in conflict with the requirement of c-Myc activity for cell cycle progression, however inhibition of p300/CBP by E1A may alleviate p300/CBP-imposed repression on the c-Myc promoter (Berk 2005).

The multidomain structure of E1A therefore allows recruitment of several binding proteins to form multi-component complex. E1A binding to pRB and p300/CBP are both required to drive quiescent cells into S phase and for cells to pass the G2/M checkpoint to progress into mitosis. Additionally, through differential regulation of p300/CBP and other binding proteins such as p400, the c-Myc pathway is also activated to drive cells into S-phase providing E1A with two methods of activating transcriptional networks that control cell growth.

1.6.3.3.2. E1A-mediated induction of apoptosis by p53-dependent and –independent mechanisms

In the absence of the E1B-encoded anti-apoptotic proteins, E1B55K and E1B19K, E1A induces apoptosis by stabilisation of p53 and through p53-

independent mechanisms. However, the functional significance of this in the context of the viral lifecycle remains unclear. Apoptosis undoubtedly occurs as a defence mechanism against E1A-mediated perturbation of cell cycle regulation. It has long been recognised that expression of E1A induces p53-dependent apoptosis as a result of E1A binding to p300/CBP and pRB for which at least three mechanisms have been proposed (Figure 10) (Debbas and White 1993; Lowe and Ruley 1993; Grand, Grant et al. 1994; Sabbatini, Lin et al. 1995; Querido, Teodoro et al. 1997).

Firstly, E1A binding to pRB through either the CR1 or CR2 domains promotes E2F-dependent transcription of the potent tumour suppressor, $p14^{ARF}$. $p14^{ARF}$ facilitates the accumulation of p53 by sequestering and directing the degradation of the p53-antagonist, HDM2 through the ubiquitin/proteasome pathway (de Stanchina, McCurrach et al. 1998; Deng, Kloosterbooer et al. 2002). Intriguingly, E1A was later found to bind to $p14^{ARF}$ and could compete with the HDM2 for binding to $p14^{ARF}$ (Shen, Zhang et al. 2011). $p14^{ARF}$ also promoted ubiquitination and proteasomal degradation of E1A independent of p53 and HDM2 status and inhibited E1A-dependent entry into S phase. This suggested E1A might have evolved the ability to prevent $p14^{ARF}$–HDM2 interaction thus blocking $p14^{ARF}$-mediated p53 stabilisation. Therefore, E1A has a mechanism of overcoming p53-dependent host anti-viral response by fine-tuning its own replication activity (Shen, Zhang et al. 2011).

Secondly, E1A binding via its N-terminus and CR1 domain to the TRAM motif of p300/CBP can disrupt p53-HDM2 complexes since p300 binds to HDM2 and is important for HDM2-mediated degradation of p53 (Grossman, Perez et al. 1998). Later, studies revealed that E1A binding of p300 prevented the intrinsic ubiquitin ligase activity of p300 to polyubiquitinate p53 and with HDM2 mediate the degradation of p53 (Grossman, Deato et al. 2003). Reports have shown accumulation of p53 and induction of apoptosis by E1A12S is prevented by deletions in the N-terminus and CR1 domain which confer pRb and p300/CBP binding supporting the notion that a complex of E1A, pRb and p300 are involved in p53-dependent apoptosis (Querido, Teodoro et al. 1997). Another study however revealed that the CR1 domain was required for the interaction between E1A and MDMX (a HDM2-related, p53-binding protein) (Li, Day et al. 2004). This resulted in the stabilisation of p53 in a $p14^{ARF}$-independent manner and

protected MDMX from HDM2-mediated nuclear export and degradation of p53 (Li, Day et al. 2004).

Thirdly, p53 stabilisation can be induced by the interaction between E1A and 26S proteasome. The 26 proteasome consists of a 20S proteasome and the 19S regulatory complex. Through N-terminal interactions, E1A binds to S4 and S8 ATPases that make up the 19S regulatory complex. E1A inhibits the ATPase activity of S4, which acts as a "gatekeeper" for ubiquitin-tagged proteins however the consequence of E1A binding to S8 has yet to be established. Therefore E1A functions to inhibit entry of proteins into the proteasome and more specifically, can impede the proteasomal-mediated degradation of p53 (Turnell, Grand et al. 2000). Other studies have inferred that p400 is crucial for efficient E1A-mediated cell death. In normal fibroblasts, E1A mutants that lacked p300 binding were dispensable for inducing $p14^{ARF}$, p53 and apoptosis whereas deletion of the p400-binding region was defective in stimulating apoptosis (Samuelson, Narita et al. 2005).

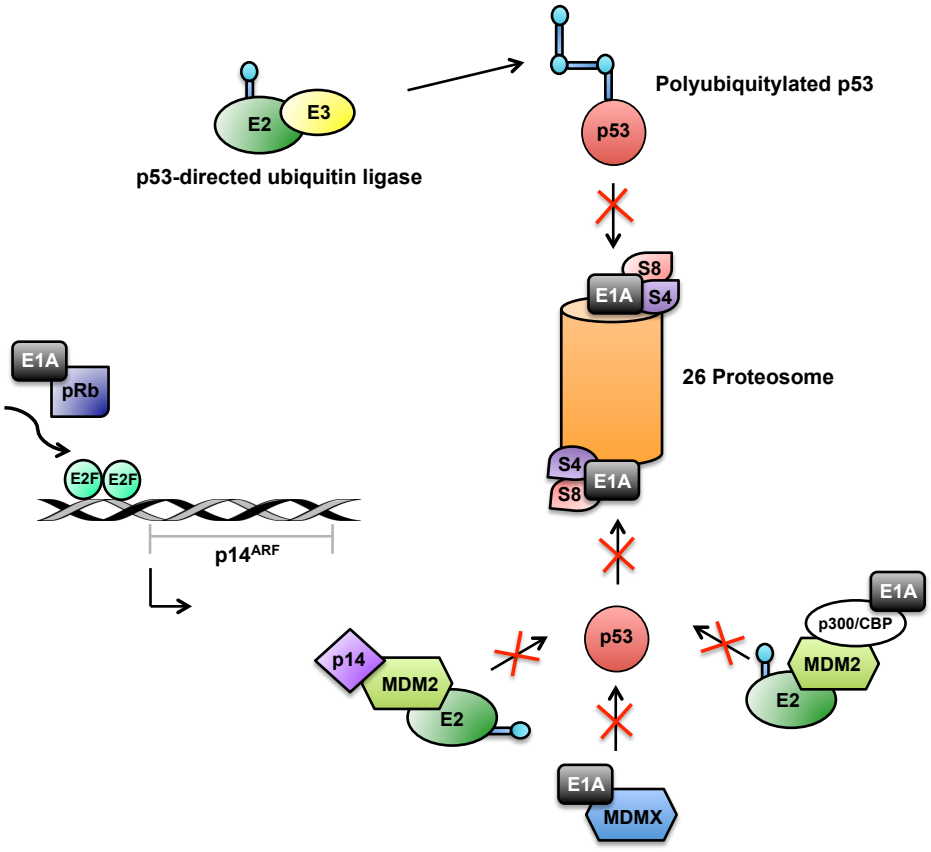

Figure 10. Mechanisms of E1A-mediated stabilisation of p53

E1A targets and inhibits several regulatory components important in p53 degradation. Adapted from Gallimore and Turnell 2001.

Besides p53-dependent apoptosis, E1A expression induces cell death in p53-deficient cells and E1A deletion mutants similarly confirmed the requirement of pRb- and p300-binding to E1A for this to occur. The mechanism of cell death implicated a mitochondrial-mediated cell death mechanism since apoptosis was significantly blocked with the addition of caspase inhibitors or co-expression with E1B19K or Bcl-2 (Putzer, Stiewe et al. 2000). Therefore presumably, E1A-mediated inactivation of pRb in p53-deficient cells may also result in E2F transcriptional activation resulting in expression of $p14^{ARF}$. Several lines of evidence indicate $p14^{ARF}$ exerts its tumour suppressive function independent of p53. For example, $p14^{ARF}$ interacts with and inhibits c-Myc function via a p53-independent mechanism, preventing c-Myc from activating target genes involved in hyperproliferation and transformation (Qi, Gregory et al. 2004). In addition, overexpression of $p14^{ARF}$ in p53-deficient cells has been shown to induce proapoptotic Bcl-2-associated X protein (Bax)/Bcl-2-antagonist/killer-1 (Bak)-dependent apoptosis (Hemmati, Guner et al. 2006). Interactions of the N-terminus and CR1 domain of E1A with other cellular proteins have also been determined and include upregulation of the p53-related protein TAp73 resulting in activation of the p53/p73 pro-apoptotic target, p53 upregulated modulator of apoptosis (Puma) (Klanrit, Flinterman et al. 2008). Furthermore, binding of E1A to p400 has also been implicated in downregulating the EGFR in cancer cells with p400 binding important in E1A-induced apoptosis (Flinterman, Mymryk et al. 2007).

Another mechanism of E1A-induced, p53-independent apoptosis is through the inhibition of antiapoptotic proteins. A screen of Bcl-2 family proteins during virus infection revealed that E1A down-regulated mRNA and protein levels of Bcl-2 family member, myeloid cell leukaemia sequence 1 (Mcl-1). This decrease was accounted for by a virus-induced DNA damage response resulting in increased proteasome-mediated turnover of Mcl-1. As a consequence, Mcl-1-dependent suppression of the proapoptotic Bak protein was relieved leading to Bak activation and subsequent oligomerisation with the proapototic protein, Bax resulting in outer mitochondrial membrane pore formation and apoptosis (Cuconati, Mukherjee et al. 2003).

E1A is also able to sensitise cells to TNF-α receptor mediated apoptosis. Host anti-viral production of TNF-α results in stimulation of the extrinsic apoptotic

pathway as well as the NF-κB-mediated survival pathway. Since a pro-survival pathway is elicited, TNF-α-induced cell death requires the inhibition of NF-κB-dependent anti-apoptotic gene expression for TNF-α to induce apoptosis. The mechanism of E1A-dependent sensitisation was found to be as a result of down-regulating the antiapoptotic cellular FLICE-inhibitory protein (c-FLIP), which functions to blocks activation of capspase-8 at the death-inducing signalling complex (DISC). E1A prevented c-FLIP expression by preventing transcription of c-FLIP mRNA and also promoting ubiquitination and proteasomal-degradation of c-FLIP proteins (Perez and White 2003).

1.6.3.3.3. Viral-mediated inhibition of adenovirus-induced apoptosis

As a consequence of E1A-induced deregulation of the cell cycle, E1A induces apoptosis through p53-dependent and –independent mechanisms. The presence of foreign DNA also induces the DNA damage response pathway. To ensure a productive lifecycle, adenoviruses have evolved mechanisms to counter these pathways. E1B55K and E1B19K the principle proteins encoded by E1B neutralise the effects of p53-dependent and p53-independent apoptosis (Shenk 2001).

E1B19K is a functional homolog of cellular anti-apoptotic protein, Bcl-2 and inhibits p53-dependent and –independent apoptosis. As discussed in the previous section, during a productive infection, E1A is able to sensitise cells to killing by death receptor ligands, TNF-α, Fas ligand (FasL) and TRAIL, which is blocked when E1B19K is expressed (White 2001). Moreover, infection of an E1B19K-deleted mutant resulted in premature cell death of normal cells after treatment with TNF resulting in attenuation of viral replication (Cuconati, Degenhardt et al. 2002). E1B19K is able to bind Bax and Bak although only the interaction with Bak appearing to be constitutive. Upon TNF-α treatment, active caspase-8 cleaves BH3-interacting death protein (Bid) to tBid, which subsequently binds to and activates Bax and Bak. Binding of tBid to Bax induces a conformational change in Bax resulting in E1B19K binding. As a consequence, E1B19K is able to block mitochondrial pore formation by binding to both Bax and Bak preventing the release of apoptogenic factors and propagation of the intrinsic apoptotic pathway (White 2001).

E1B55K functions to inhibit p53-dependent cell cycle arrest and apoptosis. This is mediated through high affinity binding of E1B55K to the transcriptional activation domain of p53 thereby preventing coactivators from binding p53 (Shenk 2001). Additionally, E1B55K contains a C-terminus repression domain which when mutated was unable to inhibit p53-mediated transcriptional activation despite retaining the ability to bind p53 like wild-type E1B55K. This suggests by binding to p53, E1B55K converts p53 into a repressor of p53-target genes (Berk 2005). E1B55K is also found in a complex with viral encoded protein, E4orf6, which together are bound to E3 ubiquitin ligases to form a high molecular weight ubiquitin ligase complex. Two known substrates for

E1B55K/E4orf6 ubiquitin ligase complex include p53 and the cellular Mre11-Rad50-Nbs1 (MRN) complex, involved in the processing of double-stranded DNA breaks prior to repair (Berk 2005). It is believed E1B55K mediates substrate recognition, since it is able to bind to p53 or the MRN complex and together with E4orf6 targets these proteins for proteasome-mediated degradation. Degradation of certain cellular proteins thus promotes efficient viral replication by abrogating p53-mediated apoptosis and preventing the activation of the DNA damage response that would result in concatamer formation of viral DNA and prevention of viral assembly (Schwartz, Lakdawala et al. 2008).

1.6.3.3.4. Viral mechanisms to counter the host immune defence

In response to adenoviral infection, the innate and adaptive immune responses are induced. The activation of the innate immune response involves upregulation of NF-κB, a key regulator of the antiviral response and activates transcription of cytokines such as interferon (IFN) (type I and II) and TNF-α as well as adhesion molecules. Adenoviruses encode three gene products that ensure persistence of the adenovirus within the host. E1A proteins and VA RNA I, which have generally been found to inhibit the cellular response to IFN and products encoded by the E3 region which protect infected cells from cytotoxic lymphocyte (CTL) and TNF-α-mediated cell killing (Shenk 2001).

IFN is released early during viral infection and binds to cell receptors and activates cellular JAK/STAT pathway with the result of STAT proteins binding to interferon response elements (ISREs) and stimulating the transcription of RNA receptor, protein kinase R (PKR) and other immunomodulators. E1A inhibits the function of IFN by blocking transcription of IFN- and NF-κB-target genes, which can be attributed to E1A competing for binding with p300/CBP. This in turn represses the transactivation function of members of the STAT family, STAT1 and STAT2 together with p65, a coactivator of the transcription factor NF-κB (Bhattacharya, Eckner et al. 1996; Zhang, Vinkemeier et al. 1996; Gerritsen, Williams et al. 1997). Additionally, E1A can bind STAT1 via its N-terminus, independent of the p300-binding region, blocking STAT1-dependent gene activation. These findings indicate that E1A can target STAT1-dependent events by several mechanisms (Look, Roswit et al. 1998). Another mechanism of

impeding the IFN response is through the inhibition of PKR. Upon binding to double-stranded RNA, the kinase activity of PKR is activated resulting in the phosphorylation of the α-subunit of eukaryotic initiation factor 2 (eIF2). This prevents the exchange reaction of eIF-2-GDP to eIF-2-GTP resulting in inhibition of protein translation during viral infection. However, the conserved secondary structure adopted by VAI enables it to bind competitively with PKR and inhibit its kinase activity thus preventing symmetrical transcription of viral DNA from activating PKR (Shenk 2001).

The protein products encoded by the E3 region are primarily involved in protecting infected cells from the immune system however the adenoviral death protein (ADP) is associated with mediating viral release at the end of the lytic cycle. The E3 and E2 promoters contain binding sites for cellular transcription factors NF-κB and nuclear factor-interleukin-6 (NF-IL6) respectively underpinning the intricate mechanisms adenoviruses have evolved to protect infected cells from host immune responses (Shenk 2001). Recognition and lysis of virus-infected cells by CTLs requires the recognition of virus antigen in a complex with major histocompatibility complex class I proteins on the cell surface. E3A viral-encoded protein, E3gp19K is a transmembrane protein that localises in the endoplasmic reticulum (ER) where it binds to the heavy chain of the major histocompatibility complex (MHC) class I proteins and prevents the transport of peptide antigens to the cell surface and subsequent detection by CTLs. It also binds and inhibits the transporter associated with antigen presenting (TAP), an ER-membrane protein whose function is to transport processed peptides from the cytosol into the ER lumen (Shenk 2001). On the other hand, evasion of immune surveillance can also be mediated by E1A sequestering CBP resulting in downregulation of the MHC class II protein expression (Kretsovali, Agalioti et al. 1998). E3B products, 10.4 and 14.5Kd (also known as the receptor internalisation and degradation complex (RID)-α/β) block TNF and FasL-induced apoptosis elicited by CTL-bearing FasL or TNF-α engagement by triggering internalisation and degradation of the respective death domain receptors (Shenk 2001). FasL and TNF-induced apoptosis is also blocked by the interaction of E3B-encoded 14.7Kd protein with the downstream effector, caspase-8/FLICE or through binding and inhibiting the pro-apoptotic FIP proteins which are ordinarily involved in keeping NF-κB associated with its inhibitor, IκBα (Shenk 2001).

1.6.3.4. Viral genome replication

Viral genome replication proceeds after the products of the early genes have established optimum conditions for DNA synthesis and products encoded from the E2 region required for DNA replication have accumulated. DNA replication endures until the host cell dies. ITRs are located at either end of the DNA strands and contain the replication origin comprised of *cis*-acting sequences. Within this sequence, three functional domains have been defined; domain A recruits viral encoded pTP and DNA polymerase while domains B and C bind cellular proteins, nuclear factor (NF)I and NFIII respectively to increase initiation efficiency of DNA synthesis. pTP binds covalently to the 5' termini of the DNA strands and serves as primer for DNA replication and maintains the integrity of the ITR sequence during multiple rounds of replication. pTP also interacts with the nuclear matrix and this is thought to anchor adenovirus DNA replication complexes near suitable cellular factors. pTP binds DNA polymerase which possesses 5'-to-3' polymerase activity and 3'-to-5' exonuclease, proofreading function. Once initiation of DNA synthesis has occurred, chain elongation is driven by the DNA-binding protein (DBP) enabling the DNA polymerase to be highly processive. The DBP is also required to maintain DNA strand separation. Another cellular factor, NFII, identified as having topoisomerase activity, may also assist in DNA replication to overcome problems in DNA topology that occur after extensive replication (Shenk 2001).

1.6.3.5. Viral assembly and release

Soon after DNA replication begins, transcription of a large transcript encoding the late genes occurs. Through a complex series of splicing reactions, mRNAs grouped into five families (L1 to L5) are generated and encode the structural components of the progeny virions as well as the components required for the maturation and encapsidation process (Table 3). The MLP controls the expression of the late genes and at the beginning of the lifecycle transcription occurs at a low level. However, after DNA replication ensues it becomes several hundred-fold more active. The shift in late gene expression from the MLP is controlled by the cellular transcription factor, USF/MLTF, which binds to a site upstream of the MLP after DNA synthesis begins with the viral protein, IVa2

cooperating with USF/MLTF to regulate the transition from early to late viral transcription (Shenk 2001).

Once DNA replication is initiated and late viral mRNA are synthesised, the accumulation of cellular mRNAs in the cytoplasm is halted. This is attributed to late viral cycle function of E1B55K, which is able to facilitate shutdown of host protein synthesis. This occurs as a consequence of E1B55K-mediated export of the viral L4-100K protein. Once L4-100K has been exported out of the nucleus, it is able to inhibit the translation of capped cellular mRNA by preventing the phosphorylation and activation of the cellular initiation factor eIF-4F, which normally contributes to cellular mRNA translation (Cuesta, Laroia et al. 2000). On the other hand, viral mRNA translation is enabled due to the selective export of viral mRNA into the cytoplasm by the E1B55K/E4orf6 complex. E1B55K exhibits an intrinsic RNA-binding activity while E4orf6 contains a nuclear export sequence and shuttles between the nucleus and the cytoplasm. Viral mRNA is preferentially translated as they are not capped unlike cellular mRNA and possess a unique 5'-non-coding region termed the tripartite leader sequence. This 5'-UTR region allows the 40S ribosome to translate the mRNA using "ribosomal jumping" without requiring the helicase activity of eIF-4F that is required for cellular mRNA translation (Shenk 2001).

The accumulation of synthesised viral DNA and structural proteins initiates viral assembly. Hexon monomers are assembled intro trimers with L4-100Kd serving as a scaffold while trimeric fiber structures and pentameric penton bases assemble more slowly. The hexon and penton capsomeres then accumulate in the nucleus where the packaging sequence within the DNA allows for DNA-capsid recognition resulting in the viral genome entering the empty capsid. IVa2 binds to viral DNA and plays a role on encapsidation along with L1 52/55Kd and pVII. The L3 encoded protease functions later in the assembly process and cleaves pVI, pVII, pVIII and pTP to stabilise the particle and render it infectious (Shenk 2001).

Virus encapsidation is accompanied by changes to the nuclear infrastructure and permeabilisation of the nuclear membrane. Subsequent escape and spread of progeny virus occurs through the disruption of intermediate filaments, which include the cleavage of cytokeratins K7 and K18 by the viral protease preventing further polymerisation. Together with host protein synthesis shutoff, the cell is

incapable of replacing components of the cytoskeleton and consequently the structural integrity of the cell is compromised. The E3 ADP facilitates cytolysis of the cell. The mechanism by which this occurs is unclear however the localisation of ADP to the nuclear envelope and Golgi was lost in adenoviruses with mutated ADP. This correlated with regions important for N- and O-linked glycosylation resulting in lower protein stability and reduced lytic behaviour (Tollefson, Scaria et al. 2003).

1.7. Oncolytic adenovirus therapy

Adenoviruses have been engineered as novel targeted anticancer agents. The intrinsic nature of viruses to infect, replicate and lyse cells causing cell death and release of viral particles to infect neighbouring cells make them ideal candidates for further development. Ad5 in particular is an attractive vector for genetic manipulation (see section 1.6.1). The adenoviral genome is genetically stable and does not integrate into the host. This prevents complications with insertional mutagenesis, which can occur with lentivirus or gammaretrovirus-based-vectors, which have been used as gene delivery tools. However, insertional mutagenesis is unlikely to cause a problem in cancer cells which are already deregulated. The small size of its genome also enables easy modifications and can be exceeded by up to 5% by transgene-insertions. Engineered vectors can subsequently be produced in large quantities of high-titre stocks (10^{12}pt/ml) in the laboratory and good manufacturing practice (GMP) conditions. Ad5 is able to infect and replicate in cycling and non-cycling cells since the E1 gene is able to induce S phase. A rapid lytic lifecycle is completed within 18-24h and in a single replication cycle, up to 10000-fold amplification of progeny virus can be released.

1.7.1. Tumour selectivity

Since wild-type adenoviruses target most epithelial cells as well as cancer cells this requires adenoviruses to be engineered to ensure tumour selectivity. One approach has been to engineer adenoviruses to complement mutations in cancers (for example proteins involved in cell cycle and apoptosis) with loss-of-function mutations within the adenovirus genome that are essential for virus propagation in normal cells but are dispensable for replication in cancer cells with deregulated regulatory pathways (Figure 11). Complementation therefore renders the adenovirus selective for cancer cells and will be referred to hereafter as replication-selective oncolytic viruses.

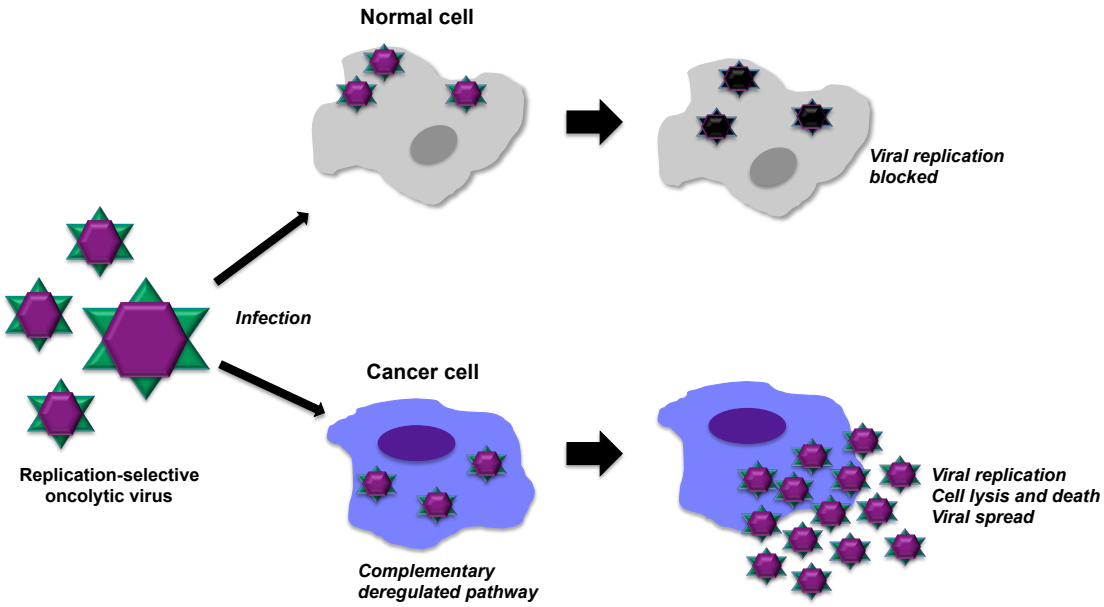

Figure 11. Schematic diagram of cancer-selective killing by oncolytic adenoviruses

Oncolytic adenoviral mutants contain gene deletions that are complemented in deregulated cancer cells resulting in a productive viral lifecycle thereby killing cancer cells and allowing virus spread. Normal cells do not support viral replication since the viral mutants lack essential proteins for cell cycle progression and inhibition of apoptosis. Adapted from Choi, Lee et al. 2012.

During a productive wild-type adenovirus infection, E1A induces p53 accumulation as discussed in section 1.6.3.3.2. To counteract this effect, E1B55K represses p53-mediated transactivation and together with E4orf6 promote p53 degradation thereby preventing cell-cycle arrest and apoptosis. Replication-selective adenoviruses were initially based on the deletion of the E1B55K gene and resulted in the development of the archetypal oncolytic virus, *dl*1520 (Bischoff, Kirn et al. 1996) (also known as ONYX-015). This virus was designed to complement cancer cells with non-functional p53 either through direct p53 mutation or mutations in upstream or downstream p53 regulators and effectors such as $p14^{ARF}$ and Bax respectively. By deleting E1B55K, ONYX-015 is unable to degrade p53 during viral replication thereby restricting replication in normal p53-expressig cells but able to replicate in p53-deficient cells. Further investigations into the selectivity of ONYX-015 found that the mutant was unable to efficiently replicate in some p53-deficient cell lines or cell lines mutated in p53-related genes (e.g. $p14^{ARF}$) (Goodrum and Ornelles 1998; Edwards, Dix et al. 2002). In contrast, it was also found to replicate in certain cells retaining wild-type p53 (Goodrum and Ornelles 1998; Rothmann, Hengstermann et al. 1998). Furthermore the mutant was shown to replicate in p53-expressing normal cells overriding G1/S and G2/M checkpoints, retarding mitosis thus resulting in the accumulation of aneuploid cells (Cherubini, Petouchoff et al. 2006). Selectivity of

ONXY-015 was later attributed to the unique ability of certain tumour cells to efficiently export late viral mRNA in the absence of E1B55K. As discussed in section 1.6.3.3.3, another function of E1B55K together with E4orf6, is to mediate the export of viral mRNA while shutting off protein synthesis of cellular proteins. In tumour cells that are not able to facilitate the export of viral mRNA transcripts, the absence of E1B55K would severely attenuate the replication of ONYX-015. This caveat in ONYX-015 replication-selectivity may go towards partially explaining the reported attenuation in replication of virus compared with wild-type virus and therefore suboptimal antitumour efficacy (O'Shea, Johnson et al. 2004).

Nevertheless, 18 Phase I and II trials have been conducted with ONYX-015 establishing safety for all routes of administration for a variety of indications. However, administration as a single agent ONYX-015 did not show therapeutic efficacy. Less than 15% of cases resulted in clinical benefit in patients with head and neck cancer who received intratumoural injection of ONYX-015 (Nemunaitis, Khuri et al. 2001) and only when combined with standard chemotherapy could this oncolytic virus attain an objective response (Khuri, Nemunaitis et al. 2000). In a Phase III trial in China, a 79% response rate was achieved in patients receiving a near identical mutant, H101 (Oncorine, Shanghai Sunway, China) by intratumoural injection in combination with cisplatin or 5-fluorouracil (5-FU) compared with 40% with patients receiving chemotherapy alone (Xia, Chang et al. 2004). The favourable outcome in this trial resulted in the licensing of H101 in China for the treatment of head and neck squamous cell carcinoma in 2005 (Garber 2006) and revealed the potential of oncolytic adenoviral therapy as a promising anticancer agent. However, long-term follow-up data and survival benefits have not been reported.

Since ONYX-015 did not show clinical efficacy as a single therapy, this highlighted the requirement for further improvements of oncolytic adenoviruses. Enhanced response rates in combination with chemotherapy suggested that optimising combination therapies could increase efficacy while reducing the toxic side effects associated with chemotherapy treatment. Extensive knowledge of adenoviral biology and the historical use of replication-defective adenoviral vectors for cancer gene therapy defined the following strategies to engineer cancer-selective oncolytic mutants: (i) Restricting adenoviral replication using tissue/tumour-specific promoter and/or enhancer elements, (ii) retargeting

adenovirus attachment and infection and (iii) arming adenoviruses with therapeutic transgenes. These modifications have been based on viral backbones derived from ONYX-015 or more recently replication selective oncolytic adenoviruses with complementation-specific deletions in other areas of the adenoviral genome specifically deletions in the E1ACR2 gene and/or the E1B19K gene.

1.7.1.1. Tissue/tumour-specific promoter/enhancer elements for PCa

Controlling the expression of viral genes involved in replication provides another approach for ensuring oncolytic viruses selectively replicate in a specific tissue or tumour type. Since E1A is the first viral gene to be expressed, the expression of this gene has been placed under the control of an exogenous promoter active in a particular cancer. An early example is CG7060, in which a PSA promoter/enhancer element was inserted between the native E1A promoter and the E1A coding region. This resulted in replication of CG7060 being elevated in tissue with high levels of PSA expression (Rodriguez, Schuur et al. 1997). CG7060 was proven to be safe with evidence of decreases in PSA levels in a Phase I clinical trial for patients with recurrent localised PCa (DeWeese, van der Poel et al. 2001). Further modifications of this virus yielded CG7870, which uses a rat probasin promoter and a minimal PSA enhancer/promoter to drive E1A and E1B expression respectively. Furthermore, this virus contains an intact E3 region required for modulating the immune response and preventing premature elimination of infected cells. In Phase I /II trials, intraprostatic delivery of CG7870 was well tolerated in patients with localised disease while intravenous delivery for metastatic CRPC resulted in a decrease of PSA levels and 27% patients were free from progression at 6 months. Despite this, significant efficacy was not reported (Small, Carducci et al. 2006). No further trials have been described for either CG7060 or CG7870.

Other tissue specific promoters used to direct replication of oncolytic adenoviruses to tumour cells include osteocalcin (for bone metastases of PCa) and the human telomerase reverse transcriptase (hTERT) promoter, which restricts viral replication to telomerase-positive cancer cells. One such oncolytic

adenovirus is OBP-301 where E1A expression is under the control of the hTERT promoter (Huang, Watanabe et al. 2008).

1.7.1.2. Retargeting and detargeting of adenoviruses

CAR is known to serve as a receptor for efficient infection *in vitro* of adenoviruses species A, C, D, E and F but not species B. Adenoviral vectors (mainly Ad2 and Ad5) have been shown to be inefficient at infecting cells *in vivo* due to neutralisation by pre-existing antibodies. A growing body of evidence has also indicated CAR may not be the primary receptor for *in vivo* binding. For example, species C adenoviruses infect cells in the airway, liver and lymphocytes, which express either none or very little CAR mRNA and ablation of CAR-binding from adenoviral vectors do not change their biodistribution *in vivo*. Furthermore, interaction between the fiber and CAR has been suggested to be involved in virus escape from the cell rather than attachment (Arnberg 2009). Therefore, *in vivo*, it is likely attachment of adenovirus to receptors other than CAR is also required for efficient viral infection. A number of examples include: CD46, which is expressed on the apical region of epithelial cells in the respiratory tract, lactoferrin, which has been found to facilitate Ad5 transduction through bridging interaction with cell surface receptors and HSPGs which are ubiquitously expressed (Arnberg 2009).

The peptide motif, RGD is required for interaction with several integrins known to act as co-receptors for adenovirus infection. Efficient retargeting of oncolytic adenoviruses has been possible via the modification of the “knob” domain within the fiber region of Ad5, which binds CAR. CAR-independent pathways mediated infection *in vitro* when a cysteine-enriched RGD motif, RGD•4C was incorporated into the H1-loop of the fiber-knob domain (Krasnykh, Dmitriev et al. 1998). This alteration has been integrated into a number of oncolytic adenoviruses to improve transduction. For example, alternative complementation mutant viruses with a small deletion in the E1ACR2 region such as Ad5Δ24RGD•4C has been retargeted to infect cells expressing intergrins which are more widely expressed on cancer cells (Pesonen, Diaconu et al. 2012). This oncolytic virus was determined to be safe in a Phase I for recurrent ovarian cancers and is currently being investigated in a Phase I trial for the treatment of recurrent gliomas (http://clinicaltrials.gov/NCT00805376). As

well as conferring higher tropism for cancer cells it also selectively replicates in cells with deregulated G1/S checkpoints and pRb signalling pathways due deletion of the CR2 domain in the E1A gene. The ΔCR2 mutants do not bind pRB preventing the formation of E1A/pRb complexes and blocking S phase initiation. In cells with deregulated cell cycle control the E1ACR2 region is surplus to requirements and a productive replication will ensue whereas these mutants are severely attenuated in non-proliferating cells. Adenoviral mutants with a small deletion in the E1ACR2 region such as *dl*922/947 and AdΔ24 (Fueyo, Gomez-Manzano et al. 2000; Heise, Hermiston et al. 2000) have shown greater efficacy compared with *dl*1520 mutants *in vivo* (Lockley, Fernandez et al. 2006; Radhakrishnan, Miranda et al. 2010; Bhattacharyya, Francis et al. 2011). Retargeting using the RGD-motif has also been employed by a more advanced version of OBP-301, OBP-405, which exhibited increased transfection efficiency in CAR-negative tumours as well as mediating CAR-dependent virus entry. It prolonged survival of mice with lung xenografts and selective replication was also determined in distant uninjected tumours demonstrating that retargeting increased target range by increasing infection efficiency (Taki, Kagawa et al. 2005).

Another approach to retargeting is fiber knob switching. By incorporating an alternate subtype's binding domain into a subtype2/5-based vector the chimeric adenovirus is able to bind to receptors that are overexpressed on the cell surface of cancer cells. One example is Ad5/3-Cox2L-Δ24 where the Ad5 fiber gene was substituted with the fiber gene of Ad3. This resulted in the chimeric virus binding to the CD46 receptors, which are highly expressed on tumour cells (Pesonen, Nokisalmi et al. 2010). Additional modifications include a 24bp deletion in the E1ACR2 gene with E1A gene expression under the control of the cyclooxygenase 2 promoter. This triple-modified oncolytic adenovirus was found to be safe for compassionate use in patients with refractory or progressive solid tumours with anti-tumour activity in 61 patients (Pesonen, Nokisalmi et al. 2010). An alternative version designated ICOVIR-7 has the same E1ACR2 deletion under the control of an E2F-1 promoter designed to confer tumour-selectivity and increase E2F dependency on E1A expression. Enhanced infection efficiency was conferred by a RGD•4C motif in the fiber-knob region. Both viruses were demonstrated safe for the compassionate treatment of patients with refractory or progressive solid tumours and conferred anticancer activity (Nokisalmi, Pesonen et al. 2010). The use of alternate adenovirus serotypes

such as Ad3 may have improved potency in certain preclinical models due to affinity to CD46 receptors and lack of pre-existing antibodies to this serotype (Hallden and Portella 2012).

Other means of achieving precise selectivity is by harnessing the high affinity and specificity found in antibodies. This adapter-based approach involves retargeting the oncolytic adenovirus to an alternative surface antigen on the cell surface. Bispecific targeting moieties have been developed wherein one site of the protein is directed against the viral capsid protein and the other site is specific towards a cell surface molecule. Previously, bispecific adapters have been complexed with the virus before administration and have shown good selectivity and affinity. However this strategy only allows for a single-round of infection as the amount of adapter protein is limited. To overcome this, replication selective oncolytic adenoviruses has recently been engineered to express the bispecific adapters themselves. One such virus (AdΔ24-425S11) encodes an anti-EGFR single chain Fv antibody fragment (scFv) 425 and anti-adenovirus fiber knob (scFV s11) and demonstrated enhanced infectivity and anti-cancer properties on EGFR-positive, CAR-negative tumour cells and retained native binding to CAR and intergrins (van Beusechem, Mastenbroek et al. 2003).

Other strategies have focused on combining retargeting modifications with the additional complexity of detargeting adenovirus vectors, which display tropism for the liver. Although efficacy can be attained with intratumoural administration, substantial challenges are encountered to attain efficacy after systemic delivery. Following intravenous delivery, oncolytic adenoviruses interact with high affinity to erythrocytes via CAR binding in conjunction with antibodies and complement thereby trapping virus in the circulation. Adenovirus binding to CAR also facilitates agglutination of erythrocytes resulting in reduced tumour delivery *in vivo* (Coughlan, Alba et al. 2010). In terms of liver tropism, Ad5, via its knob domain has been shown to bind a variety of coagulation factors such as FIX, FVIII and FX as well as components of the complement system such as C4 binding protein (C4BP). These interactions as well as binding with HSPG or low-density lipoprotein receptor on the surface of hepatocytes allow Ad5 to transduce these cells (Arnberg 2009). The interaction between adenovirus and the vitamin K-dependent zymogen, FX has been mapped to the hexon protein, providing a bridge for hepatocyte transduction and may be the major mode by

which Ad5 enters hepatocytes giving rise to the toxic side effects within the liver which is associated with systemic delivery of adenoviral vectors. Kupffer cells, the resident macrophages of the liver are also able to sequester adenovirus through opsonization of adenovirus with antibodies and/or complement thereby reducing the levels of the virus in circulation (Coughlan, Alba et al. 2010). Interactions between adenovirus and cells of the immune system also enhance clearance of the virus and most adults will have neutralizing antibodies against adenoviruses. Therefore in recent years it has been recognised that detargeting adenoviruses from their native receptor binding is as important as developing engineered adenoviruses with enhanced tumour cell specificity if systemic delivery and targeting of metastatic sites will be possible.

One approach to overcome erythrocyte and liver binding uses polyethylene glycol (PEG) conjugated to the surface of the adenovirus resulting in a “stealth” adenovirus. PEGylated adenoviruses show increased plasma circulation, reduced liver toxicity and decreased innate immune responses. However on its own, PEGylation reduces CAR-mediated endocytosis due to steric hindrance from the PEG chains resulting in low transduction efficiency (Choi, Lee et al. 2012). Therefore, to overcome this limitation, PEGylated adenoviruses require retargeting and moieties such as RGD peptides or folate ligand have been investigated (Choi, Lee et al. 2012). Recently, a replication-selective adenovirus (DWP418) assessed in Phase I trials was modified to generate a tumour targeted and PEGylated oncolytic virus (Kim, Sohn et al. 2011). Tumour-specific replication was controlled with the presence of the hTERT promoter. Potency was further enhanced with the deletion of the antiapoptotic E1B19K gene and inserting the relaxin gene in the E3 region. Retargeting was achieved using PEG conjugated to the human Her2/neu-specific MAb (Herceptin) and DWP418-PEG-HER was found to specifically kill Her2/neu expressing cells. After intravenous injection, enhanced anti-tumour activity was demonstrated compared with the non-targeted, naked adenovirus and accumulated in the tumour tissue at 58.0×10^4-fold higher levels than the naked adenovirus. Liver uptake of the DWP418-PEG-HER was significantly lower than naked adenovirus with 3.7×10^5-fold less accumulation (Kim, Sohn et al. 2011). Another approach for increased tumour transduction is the use of mesenchymal stem cells (MSCs), which have intrinsic cancer tropism. Intravenous administration of MSCs preloaded with oncolytic adenovirus facilitated the delivery of virus to orthotopic breast and lung tumours, increasing the survival of mice. This method

has been evaluated in patients with refractory neuroblastoma (Pesonen, Kangasniemi et al. 2011).

1.7.1.3. Arming oncolytic adenovirus with therapeutic transgenes

Although oncolytic adenoviruses can kill tumour cells through complementation deletions in the genome or the introduction of tumour-specific promoters, potency can be further enhanced with the introduction of a transgene. These so-called “armed” replication selective oncolytic adenoviruses have the advantage of amplifying the therapeutic gene with the virus so that each virus progeny will have inherited the transgene, infect neighbouring cells thus augmenting the potency of the oncolytic adenovirus. The insertion of a transgene into a replication selective oncolytic adenovirus also has the advantage of tumour cell-specific restriction of the transgene decreasing the possibility of side effects from expression in normal cells.

There have been many approaches to engineering armed oncolytic adenoviruses with insertion of transgenes being primarily expressed from the E1B or E3 regions of replicating adenoviruses either under the control of the corresponding viral promoter or after the insertion of tumour-specific/heterologous promoters. Various types of transgenes have been inserted into oncolytic adenoviruses representing a variety of strategies for tumour eradication. It is beyond the scope of this thesis to discuss all of these strategies, which include enhanced cell killing, modulation of the tumour environment and stimulation of the immune response to the tumour. Here I will focus on the recent developments of oncolytic adenoviruses containing prodrug-converting enzymes currently in clinical trials, promising targeting strategies that involve micro RNA (miRNA) as well as the insertion of tumour suppressor genes.

1.7.1.3.1. Prodrug-converting enzymes

Insertion of a non-mammalian prodrug-converting enzyme into a tumour-selective adenovirus augments efficacy when a non-toxic prodrug is administered. This is converted to a toxic drug only in infected cells that express

the enzyme. Furthermore, cell killing is potentiated by the "bystander effect" when the toxic metabolite from the infected cell diffuses to neighbouring cells in the tumour through gap junctions. Another advantage of this approach is that it also avoids toxic effects of systemic administration of other types of cytotoxic therapy. A variety of pro-drug converting enzymes have been introduced into replication selective adenoviruses, however only recent outcomes will be described here.

Ad5-$_{Y}$CD/*mut*TK$_{SR39}$-*rep*-ADP is a second-generation suicide gene therapy replication-selective adenovirus deleted in the E1B55K region. It utilizes double-suicide gene therapy by expressing yeast cytosine deaminase fused to an improved mutant herpes simplex virus thymidine kinase enzyme under the control of the cytomegalovirus (CMV) promoter, which converts non-toxic 5-flurocytosine (5-FC) to 5-FU and ganciclovir to monophosphorylated nucleotides respectively. The ADP under the control of CMV promoter replaces the E3 region for enhanced viral spread (Freytag, Barton et al. 2007). This virus is currently being evaluated in Phase II/III trials in newly diagnosed PCa patients in combination with 5-FC, ganciclovir and radiotherapy (http://clinicaltrials.gov/NCT00583492) after a Phase I trial in patients with localised recurrent PCa in combination with radiotherapy demonstrating safety and initial efficacy (Freytag, Movsas et al. 2007).

Another variety of pro-drug converting enzyme is the *Escherichia coli* nitroreductase (NTR). This has been incorporated into a replication-defective (E1 and E3-deleted) adenovirus (CTL102). Delivery of prodrug CB-1954 generates a highly toxic DNA cross-linking agent in infected cells. In a Phase I/II trial in patients with localised PCa, CTL102 was delivered by intraprostatic injection and CB-1954 administered systemically, decreases in PSA levels were demonstrated in 14 out of 19 patients (Patel, Young et al. 2009). This result suggests NTR enzymes could be incorporated into replication-selective adenoviruses.

1.7.1.3.2. Small RNAs

Micro RNA (miRNA) binding sites have been incorporated into replication selective adenoviruses with the aim of attenuating viral potency at sites of

normal tissue e.g. the liver but retaining wild-type efficacy at sites that do not express the relevant miRNA. Four copies of the hepatocyte-selective mir-122 binding site were inserted at the 3'UTR of the E1A gene transcriptional cassette in wild-type adenovirus. Reporter gene expression with E1A fused to luciferase showed mir-122 binding sites reduced E1A expression up to 80-fold in murine hepatocytes following intravenous administration. In tumour cells, the virus retained full anti-tumour activity without the associated toxic effects of replication in the liver (Cawood, Chen et al. 2009). Similar findings were demonstrated with another mutant, which used six tandem repeats of the mir-122 binding site, which was also tumour selective for neuroendocrine tumours. Arrested replication of this mutant was demonstrated in normal liver cells demonstrating mir-122-mediated detargeting in the liver (Leja, Nilsson et al. 2010). This suggests tissue-specific miRNAs may be utilized to inhibit inappropriate E1A expression in certain cells types thereby reducing toxic effects.

1.7.1.3.3. Tumour suppressor protein, p53

Insertion of transgenes that have a direct cytotoxic effect is another way of improving potency. A variety of cytotoxic genes have been studied, the encoded products killing cells by a number of different mechanisms. These include overexpression of the viral ADP, which enhances the release and spread of the viral progeny and TNF-related apoptosis-inducing ligand (TRAIL), a transmembrane protein, which is able to kill tumour cells by initiating an apoptotic cascade and also improves viral release and spread *in vivo* (Cody and Douglas 2009). Another strategy is to induce apoptosis by expressing a tumour suppressor protein. p53 is an attractive candidate since 50% of human cancers are deficient in functional p53. Gene transfer of p53 has been found to be toxic in many cancer cell types. In one study, a E3-deleted mutant expressing p53 from the fiber transcription unit via an internal ribosomal entry site was demonstrated to enhance oncolysis, viral release and spread in lung cancer cell lines without attenuating replication and was more potent than a mutant retaining ADP. It was also found to be less cytotoxic in normal fibroblasts (Sauthoff, Pipiya et al. 2002). Another study included p53 in the E3 region of a Δ24-mutant adenovirus. This virus was found to kill more efficiently in a variety of tumour cells with different p53 status *in vitro. In vivo*, it demonstrated enhanced anti-tumour efficacy in xenografts models of primary glioma (van

Beusechem, van den Doel et al. 2002; Geoerger, Vassal et al. 2004). More recently, a triple-deleted-mutant expressing p53 (SG600-p53) Δ24-deleted and where E1B was under the control of a hTERT promoter, demonstrated superior anti-tumour potency in xenografts models of human non-small cell lung cancer (Wang, Su et al. 2008). However limitations to p53-based therapy exist and certain cell lines are resistant to the effect of p53-mediated enhanced oncolysis. This arises from the presence of p53 regulators such as HDM2, which is overexpressed in certain cancers including PCa. The intrinsic nature of adenovirus to regulated p53 via E1B55K can also attenuate p53 expression. To overcome this restriction, p53 variants have been developed that are unaffected by HDM2- and E1B55K-mediated degradation. Sauthoff *et al*, using their previous oncolytic construct developed a p53 mutant that was impervious to HDM2 and E1B55K-mediated degradation. Although it demonstrated improved p53 stability and enhanced cell killing *in vitro*, anti-tumour efficacy *in vivo* was not substantially different to the control virus suggesting that in the case of this oncolytic construct, the presence of E1B19K and E1A were opposing p53 function (Sauthoff, Pipiya et al. 2006). These studies indicate that introducing a potent tumour suppressor protein and transcription factor such as p53 into tumours enhances the efficacy of replication-selective adenoviruses. However this approach is not without its drawbacks. In designing a strategy to express proteins with a tumour suppressor function, the mutations required to create replication-selective adenoviruses need to be considered so as to complement transgene's mode of action. This is essential since overlap exists between the signalling pathways used by the virus for replications and pathways activated by the transgene to mediate growth arrest and/or apoptosis. In the case of the transcriptional repressor, Hey1, AR and HDM2 are two targets that Hey1 potentially uses to regulate cell proliferation and apoptosis. Since these pathways are deregulated in cancer, Hey1 is an attractive candidate to harness as a transgene for oncolytic therapy.

1.7.1.4. AdΔΔ, an optimised replication-selective oncolytic adenovirus

As discussed above, incorporating other modifications to increase cancer specificity has enhanced the potency of replication selective mutants. The majority contain deletions in either E1B55K or E1ACR2 genes for selective

replication in cancer cells. Since *dl*1520-based mutants resulted in attenuated replication and aberrant replication of *dl*922/947-based mutants occurred in normal cells (Heise, Hermiston et al. 2000), further improvements were required to enhance potency and specificity of replication-selective adenoviruses. A further advancement in adenoviral genetic engineering has entailed deleting the anti-apoptotic gene E1B19K gene. As described within section 1.6.3.3.3, E1B19K inhibits p53-dependent and –independent apoptosis in virally infected cells by preventing receptor-induced induced apoptosis by binding Bax and Bak thus preventing oligomerisation of Bax/Bak and mitochondrial pore formation (White 2001). Deletion of E1B19K is complemented in cancer cells due to frequent inactivation of apoptotic pathways while replication is hindered in normal cells since the absence of E1B19K prevents viral spread by TNF-induced apoptosis (White 2001; Liu, Hallden et al. 2004). Numerous studies have demonstrated enhanced efficacy of wild-type and adenoviral mutants when combined with a variety of cytotoxic drugs compared with single agent treatments. Previous work in our laboratory demonstrated E1B19K-deleted mutants were able to sensitise pancreatic and PCa cells to gemcitabine- and docetaxel-induced apoptosis (Leitner, Sweeney et al. 2009; Oberg, Yanover et al. 2010).

Based on results demonstrating that the removal of E1B19K in E1B55K- or E1ACR2-deleted mutants enhanced drug-induced cell killing, a double-deleted adenoviral mutant, AdΔΔ, deleted in the E1ACR2 and E1B19K region but retaining an intact E3 region was constructed (Oberg, Yanover et al. 2010). The genes encoding the E3 region are dispensable for virus replication *in vitro* however as discussed earlier in section 1.6.3.3.4, proteins expressed from this region modulate the host's immune response *in vivo.* Adenoviral mutants retaining the E3 region prevented premature elimination of infected cells by macrophages (Wang, Hallden et al. 2003). The E3B-deletion has been associated with high levels of macrophage infiltration at the injection site of glioblastoma patients (Fulci, Dmitrieva et al. 2007) indicating the reduced efficacy of ONYX-015 and other E3B-deleted viruses may be in part due to deletions of the E3 genes. This is supported by results from a murine immunocompetent model, where E3B-deletion mutants' demonstrated attenuated efficacy and greater virus clearance by macrophage infiltration compared with mutants with an intact E3 region (Hallden, Hill et al. 2003; Wang, Hallden et al. 2003). Furthermore, attenuated efficacy with E3-deleted mutants

could be rescued by combining adenoviral mutants with suboptimum doses of cytotoxic drugs (Cheong, Wang et al. 2008).

This suggested that retention of the E3 region in AdΔΔ could further improve viral efficacy. Potency of AdΔΔ as a single agent was ascertained to be greater or similar to wild-type virus *in vitro* in prostate, pancreatic and lung cancer cells while replication was attenuated more than single-deleted AdΔCR2 in normal cells (Oberg, Yanover et al. 2010). AdΔΔ and single-deleted mutants (AdΔCR2 and AdΔ19K) synergised with docetaxel and mitoxantrone in DU145 while in PC3 cells, synergistic cell death was greater for AdΔΔ + drug combinations compared with single-deleted mutants. In PC3 and DU145 prostate xenografts models, AdΔΔ in combination with docetaxel showed enhanced anti-tumour potency compared with respective single agent treatments. In addition, adenoviral mutants with intact E3B-genes (AdΔΔ or AdΔCR2) in immunocompetent murine mouse models were more efficacious compared with their corresponding E3B-deleted mutants with no increase in macrophage infiltration detected (Oberg, Yanover et al. 2010).

To date, a large proportion of oncolytic adenoviral mutants entering or already in human clinical trials lack the entire E3 region or the E3B gene. By retaining the E3 region AdΔΔ offers prolonged efficacy *in vivo* over current vectors while the removal of the E1B19K gene eliminates E1B19K-mediated inhibitory effects of drug-induced apoptosis resulting in enhanced cell killing. This therefore makes AdΔΔ an ideal candidate for further arming with therapeutic genes.

1.8. Research rationale

Treatment with ADT including medical castration and AR antagonists appears to be a major driving force in reactivating and deregulating the AR signalling pathway. Eventually a PCa phenotype resistant to hormonal deprivation therapy emerges and cytotoxic drug chemotherapy eventually becoming ineffective thus highlighting the urgent need to develop novel therapies for the treatment of CRPC. Crucially, knocking down AR expression in CRPC cells induced apoptosis *in vitro* and reduced tumour growth in xenografts models (Liao, Tang et al. 2005; Cheng, Snoek et al. 2006) providing evidence that targeting AR therapeutically is highly feasible. Since conventional antagonists such as bicalutamide bind AR with low affinity and either cannot supress AR activity in CRPC or act as a partial agonist, current strategies have focused on developing superior AR antagonists with higher AR binding affinity, reduced AR nuclear translocation and lower AR-mediated transactivation of target genes. It is however highly likely PCa tumours will develop resistance to these treatments as well. Therefore, other approaches aimed at inhibiting AR signalling are required.

Recently, a gene expression profiling study has shown that a transcription-based AR activity signature from androgen-dependent LNCaP cells was severely attenuated in CRPC cells (Mendiratta, Mostaghel et al. 2009). Genome-wide studies using ChIP-based analyses identified CRPC-specific AR binding events associated with a subset of genes that were not present in androgen-dependent LNCaP cells, suggesting ligand-free AR in CRPC cells regulates another group of genes which could contribute to the progression of CRPC (Wang, Li et al. 2009). This could potentially explain why current therapies, which block ligand-bound AR, cannot prevent ligand-free AR from driving cells through the cell cycle (Wang, Li et al. 2009). This underscores the significance of deregulated AR transcriptional activity in CRPC resulting in aberrant AR-mediated gene transcription. The identification of the Notch effector, Hey1 as a corepressor of AR signalling, presented a novel approach at inhibiting abnormal AR signalling. Since Hey1 has been found to be either downregulated or restricted to the cytoplasmic compartment in human primary PCa tumours, this could be functionally significant in PCa development, preventing Hey1-mediated modulation of androgen signalling in the prostate

(Belandia, Powell et al. 2005; Wang, Leow et al. 2006; Whelan, Kellogg et al. 2009). The ectopic expression of the transcriptional corepressor, Hey1 may therefore provide a means of targeting and blocking AR-dependent transcription thus circumventing the associated problems with other AR inhibitors such as antiandrogens. This strategy affords the advantage of enhanced specificity through interacting with other proteins unlike the small molecule approach, which cannot always guarantee specificity. Moreover Hey1 has been demonstrated to bind to the NTD region of AR and therefore has the potential of binding to and inhibiting not only ligand-bound AR but also constitutive AR splice variants that are deleted in the LBD region. This is the first study using a transcription factor corepressor to target AR activity.

We therefore hypothesised whether the introduction of Hey1 into AdΔΔ, an optimised replication selective adenovirus generated in our laboratory, may enhance viral efficacy in PCa cells. The relatively small size of Hey1 (897bp) permits its insertion into the adenoviral genome without compromising viral function. We proposed to replace the E3gp19K region of the viral genome with Hey1 since it was previously demonstrated deletion of E3gp19K enhanced viral gene expression and improved efficacy in an immunocompetent mouse model by increasing CTL infiltration (Wang, Hallden et al. 2003). To harness the highly temporal nature of viral gene expression Hey1 would be placed under the control of the early endogenous E3 promoter. This would be advantageous since E3 gene expression does not require virus DNA replication therefore allowing Hey1 expression during circumstances when virus replication may be attenuated.

A key feature of oncolytic adenovirus therapy is its enhanced efficacy in combination with other anticancer agents such as chemotherapy and radiotherapy (Hakkarainen, Rajecki et al. 2009; Oberg, Yanover et al. 2010; Radhakrishnan, Miranda et al. 2010). This trait has been attributed to E1A expression since E1A has been found to synergise with cytotoxic agents with distinct mechanisms of action. For example, E1A sensitised cells to DNA-damaging drugs gemcitabine or cytoskeleton-targeting drugs such as palitaxel (Lee, Tai et al. 2003; Liao, Zou et al. 2004; Leitner, Sweeney et al. 2009). The exact mechanisms involved in sensitisation are obscure since numerous cellular proteins can bind E1A thereby targeting a number of different cellular pathways (Frisch and Mymryk 2002; Berk 2005). Furthermore, the individual genetic

status present in cancer cells also controls the mechanism of E1A-dependent sensitisation. Our laboratory has previously ascertained the E1AΔCR2 deletion to be redundant for sensitisation in replication-selective adenoviruses rendering the AdΔΔ mutant suitable for further optimisation (Oberg, Yanover et al. 2010; Miranda, Maya Pineda et al. 2012). In addition to ascertaining the biological effects of Hey1 alone, we also sought to determine the activity of Hey1 in combination with chemotherapeutic drugs since the administration of these agents are likely to be required for optimum tumour efficacy of AdΔΔ-based mutants *in vivo*. Hey1 was initially inserted into a non-replicating adenoviral vector to establish proof-of-concept and to characterise the effects of Hey1 and putative mechanisms of action alone and in combination with cytotoxic drugs.

1.8.1. Previous work

Previous work in our laboratory investigated the effect of Hey1 in PCa cells by constructing a non-replicating recombinant adenovirus replacing the E1 gene with a CMV-Hey1 cassette and which was also deleted for the E3 gene (Ad5Hey1; ΔE1 and ΔE3) (Cheong *et al*, manuscript in preparation). Expression of Hey1 was verified in four PCa cell lines, AR-positive 22Rv1 and LNCaP cells and AR-negative DU145 and PC3 cells (Figure 12). Expression of Hey1 was observed in 22Rv1, LNCaP and DU145 cells from 24h post-infection. Hey1 expression in PC3 cells was delayed slightly but was evident from 48h post-infection (Cheong *et al*, manuscript in preparation). This difference is likely to be a reflection in decreased viral transduction in PC3 cells compared with the other cell types.

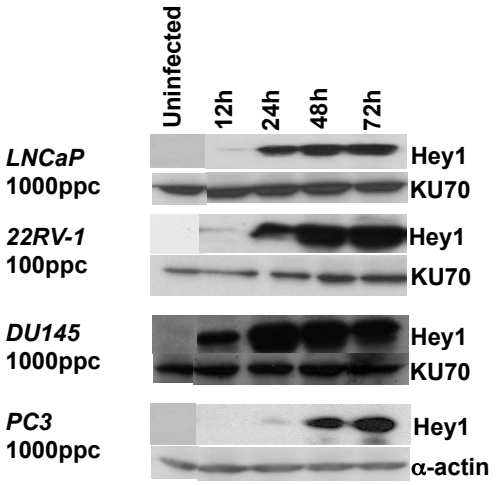

Figure 12. Western blot showing Hey1 expression over time in a panel of PCa cell lines

Cells were infected with Ad5Hey1#1 at 100ppc (22Rv1), and 1000ppc (LNCaP, DU145 and PC3) (section 2.7.1). After 2h infection medium was removed and replaced with 10% FBS-containing medium. Cell lysates were harvested at 12, 24, 48 and 72h post-infection and prepared for separation on polyacrylamide gels. 20μg of protein was loaded per lane and blotted for Hey1 using a rabbit anti-Hey1 antibody (Chemicon, Millipore, MA, USA) at a dilution of 1/300. KU70 or α-actin were used as loading controls (Cheong *et al*, manuscript in preparation)

To investigate whether Hey1 expressed from a non-replicating adenoviral vector was able to repress AR signalling, 22Rv1 cells were transfected with an AR-responsive luciferase reporter plasmid (MMTV-Luc) and the effect of Ad5Hey1 on AR transcriptional activity assessed (Figure 13). Addition of the synthetic androgen, mibolerone increased AR transcriptional activity compared with untreated cells and this was decreased when cells were infected with Ad5Hey1

(10-100ppc). The addition of the antiandrogen, bicalutamide partially inhibited mibolerone-induced AR activity and this was further decreased in the presence of Ad5Hey1 suggesting Hey1 and bicalutamide cooperate to decrease AR activity (Cheong *et al*, manuscript in preparation).

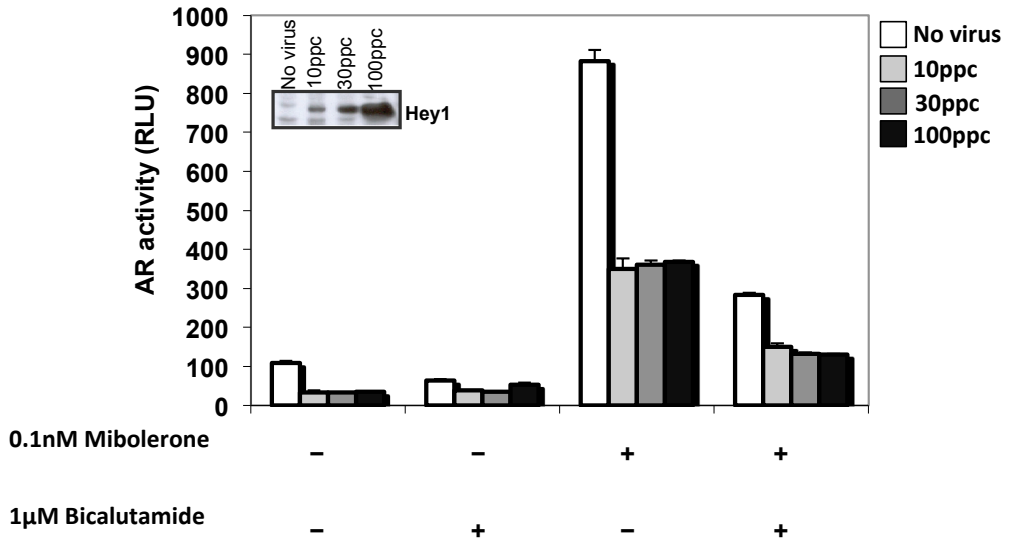

Figure 13. Ad5Hey1 represses AR transcriptional activity in 22Rv1 cells and cooperates with bicalutamide to further decrease AR activity

Cells were infected with 10, 30 and 100ppc Ad5Hey1#1. The following day cells were co-transfected with AR reporter plasmid MMTV-Luc and a renilla luciferase under the control of the SV40 promoter (pRL-SV40) for normalisation (section 2.5.1). The next day cells were treated with 0.1nM mibolerone and/or 1μM bicalutamide. Cells were lysed the following day and luciferase expression detected using a dual luciferase reporter assay system. Western blot analysis (insert) shows Hey1 expression at 72h post-infection. Data is mean of 3 independent experiments. (Cheong *et al*, manuscript in preparation).

Since Ad5Hey1 was able to decrease AR transcriptional activity in an AR-positive PCa cell line and AR signalling has been shown to be critical for the survival of PCa cells, the potency of Ad5Hey1 to inhibit cell growth was evaluated using the MTS cell viability assay. The dose required to kill 50% of cells (Effective Concentration; EC_{50}) was assessed. Ad5Hey1 was significantly more cytotoxic in the AR-positive cell lines 22Rv1 and LNCaP compared with the negative control virus, Ad5GFP (CMV-GFP replaces E1, intact E3) and was similar in potency to the apoptosis-inducing adenoviral E1A protein (AdE1A12S; CMV-E1A12S replaces E1, ΔE3) (Table 4). Surprisingly, Ad5Hey1 was also cytotoxic in AR-negative DU145 cells suggesting Ad5Hey1 is able to kill PCa cell via both AR-dependent and AR-independent mechanisms. In contrast, AR-negative PC3 cells, Ad5Hey1 was no longer as potent as AdE1A12S and activity was similar to Ad5GFP (Table 4) indicating Ad5Hey1-dependent

cytotoxicity is dependent on a variety of specific genetic alterations in PCa cells (Cheong *et al*, manuscript in preparation).

Table 4. EC_{50} values for Ad5Hey1, AdE1A12S and Ad5GFP in PCa cell lines

	Ad5Hey	AdE1A12S	Ad5GFP	p value
22Rv1	80±40	30±20	2200±600	p<0.05
LNCaP	17000±6600	13000±6400	65000±1200	p<0.01
DU145	12000±4400	5100±1700	191000±72000	p<0.05
PC3	>100000	13000±5300	>100000	ns

Dose response curves were constructed by treating cells with five-fold serially diluted Ad5Hey1#1, AdE1A12S and Ad5GFP and cell death determined by MTS viability assay 6 days post-infection to calculate EC_{50} (particles per cell; ppc). Results are average of 4 independent experiments ± SEM. Statistical analysis was carried out using an unpaired Student's t-test comparing Ad5Hey1 with Ad5GFP (Cheong *et al*, manuscript in preparation).

Many studies have shown enhanced efficacy of replication-selective adenoviruses in combination with chemotherapeutic drugs compared to single-agent treatments. Since the ultimate aim was to construct a Hey1-expressing oncolytic adenovirus, potency of Ad5Hey1 in combination with chemotherapeutic drugs currently used in the clinic for PCa was assessed. EC_{50} values for mitoxantrone and docetaxel with and without fixed virus doses were evaluated (Figure 14). After Ad5Hey1 infection, the EC_{50} values of both drugs were significantly decreased in 22Rv1, LNCaP and DU145 but not PC3 cells compared with an equal dose of Ad5GFP. As expected, AdE1A12S was even more potent at sensitising all cell lines to the chemodrugs, in agreement with published data of E1A proteins as a potent sensitising and apoptosis-inducing agents (Lowe, Ruley et al. 1993; Liao, Yu et al. 2007; Miranda, Maya Pineda et al. 2012). These results indicate that Ad5Hey1 not only sensitises AR-positive cells to chemodrugs but that it does so also through AR-independent mechanisms in DU145 cells (Cheong *et al*, manuscript in preparation).

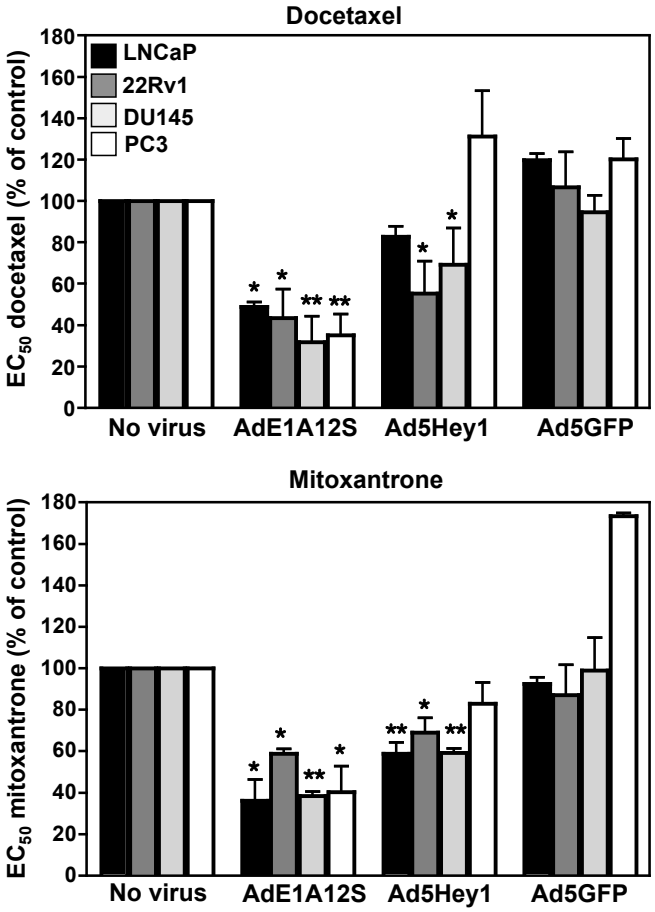

Figure 14. Ad5Hey1 sensitises 22Rv1, LNCaP and DU145 but not PC3 cells to docetaxel- and mitoxantrone-induced cell killing

Dose response curves to docetaxel or mitoxantrone with and without fixed dose of Ad5Hey#1, AdE1A12S or Ad5GFP (22Rv1, 30ppc, LNCaP, DU145 and PC3; 1000ppc) were generated and cell death determined 6 days post-treatment by MTS viability assay. Drug EC_{50} values were calculated for drug alone relative to untreated cells or in combination with each virus relative to the percentage of cell death induced by the virus alone. Histograms show relative EC_{50} values as a percentage of drug alone. Results are a mean of triplicate wells from 3 independent experiments ± SD. Statistical analysis was carried out using an unpaired Student's t-test comparing Ad5Hey1 with Ad5GFP, $p<0.05$ (*), $p<0.01$ (**) compared with drug alone (Cheong *et al*, manuscript in preparation).

As administration of non-replicating viruses as single-agents have little efficacy *in vivo* due to their limited viral spread, potency in combination with mitoxantrone and docetaxel was assessed to investigate whether the promising *in vitro* data could be translated to PCa xenograft models. In the LNCaP model, Ad5Hey1 ($5x10^9$vp; virus particles) significantly reduced tumour growth when administered as a single agent compared with Ad5GFP and also increased median survival from to 54 days (PBS or Ad5GFP) to 92 days (Ad5Hey1). Prolonged survival was also observed when Ad5Hey1 was combined with a non-efficacious dose of docetaxel (6mg/kg) with 75% of animals still alive after 110 days compared with 40% of animals after single-agent Ad5Hey1 treatment

and no animals alive with docetaxel alone or docetaxel with Ad5GFP (data not shown). In the DU145 model, Ad5Hey1 did not inhibit tumour growth when administered alone however in combination with a non-efficacious dose of docetaxel (10mg/kg), Ad5Hey1 ($1x10^{10}$vp) significantly reduced tumour growth and median survival was prolonged from 62 days for docetaxel or Ad5Hey1 alone to 96 days when combined (data not shown) (Cheong *et al*, manuscript in preparation).

In summary these results demonstrate that a non-replicating recombinant adenovirus construct is effective at expressing Hey1 in a panel of PCa cell lines over an extended period of time. In agreement with the literature, Hey1 expression results in repression of androgen-stimulated AR signalling in 22Rv1 cells and was also able to cooperate with bicalutamide to further repress AR activity. Furthermore, Ad5Hey1 was cytotoxic to 22Rv1, LNCaP and DU145 cells and sensitised these cells to chemotherapeutic drug-induced cell killing in a comparable manner to the positive-control virus, AdE1A12S. Most promisingly, Ad5Hey1 demonstrated efficacy in PCa xenograft mouse models as a single agent (LNCaP model) and in combination with docetaxel (DU145 and LNCaP models) demonstrating the potential use of Hey1 as a therapeutic transgene for the treatment of PCa when delivered by a replication-selective adenovirus.

1.9. Aims of this thesis

This research project was conducted with the aim to establish whether the AR-corepressor, Hey1 delivered from an adenoviral vector could reduce AR-driven PCa cell proliferation and be used as a potential novel therapeutic for PCa. Based on previously published findings and unpublished data generated in our team the following hypotheses for Hey-1-mediated mechanisms of action were investigated.

1. Ad5Hey-mediated cytotoxicity may function through inhibition of AR activity and activation of p53 signalling in AR and p53-positive 22Rv1 and LNCaP cells
2. Ad5Hey1-mediated cytotoxicity may function independently of the AR and p53 pathways by inhibiting constitutively active STAT3 to reduce cell viability in AR-negative and p53-mutant DU145 cells
3. In addition to reducing cell viability of 22Rv1, LNCaP and DU145 cells, Ad5Hey1 may synergise with chemotherapeutic drugs to enhance apoptotic cell death
4. Ad5Hey1 may cooperate with antiandrogens and remain efficacious in the presence of androgens
5. Ad5Hey1 may be effective in reducing the proliferation of castration-resistant PCa cells

Therefore, in this thesis I investigated the mechanism(s) of Ad5Hey1-mediated cytotoxicity and sensitisation to cytotoxic drugs in the PCa cell lines 22Rv1, LNCaP and DU145. To accomplish this, RNA interference, isogenic cell lines and selective small molecule inhibitors were used to identify possible targets involved in Ad5Hey1-mediated cytotoxicity. The role of Ad5Hey1 on cell cycle progression and cell cycle proteins was assessed and Ad5Hey1 evaluated for possible synergy with mitoxantrone and docetaxel. At doses, which resulted in synergistic cell death, cell death pathways were characterised and the molecular mechanisms underlying this sensitisation investigated. I also sought to assess efficacy of Ad5Hey1 in combination with androgens and bicalutamide and also assess the potency of Ad5Hey1 in AR-expressing castration resistant PCa cells.

2. Methods

2.1. Reagents

The synthetic androgen, mibolerone was acquired from Perkin Elmer (Seer Green, UK), dissolved in ethanol to give stock concentration of 1μM, aliquoted and stored at -20°C. The antiandrogen, bicalutamide was obtained from Sigma Aldrich (Dorset, UK) and was reconstituted in ethanol to give a stock concentration of 10mM, aliquoted and stored at -20°C. DHT (Sigma Aldrich) was made up to 10mM stock concentration dissolved in ethanol and stored at 20°C. Docetaxel was obtained from Fluka (Sigma Aldrich) and dissolved in dimethyl sulphoxide (DMSO) (Fisher Scientific, Loughborough, UK) at 6mM, aliquoted and stored at 20°C. A solution of mitoxantrone was provided at a 4.5mM stock by Onkoterene®, Baxter, Norfolk, UK and kept at 4°C. The small molecule JAK inhibitors AG490 and AZD1480 (Stratech Scientific Ltd, Newmarket, UK) were dissolved in DMSO to 20mM. Reagents used as positive controls for mitosis (nocodazole), apoptosis (staurosporine) and p53 activation (etoposide) (Sigma Aldrich) were reconstituted in DMSO to give stock concentrations of 500ug/ml, 1mM and 50mM respectively. Tetramethylrhodamine ethyl ester percholate (TMRE) (Invitrogen, Paisley, UK) was dissolved in DMSO to 1mg/ml.

2.2. Cell culture

The human PCa cell lines 22Rv1, LNCAP, VCaP, DU145 and PC3 were obtained from Cancer Research UK Cell Services (Clare Hall, Middlesex, UK originally purchased from American Type Culture Collection (ATCC) VA, USA). Characteristics of the PCa cell lines are shown in Table 5. Colorectal cell lines, HCT116wt and HCT116p53$^{-/-}$ were a kind gift obtained from Dr Spiros Linardopoulos, (The Institute of Cancer Research, London), originally from Dr. Bert Vogelstein (John Hopkins University Howard Hughes Medical Institute and Kimmel Cancer Center, Baltimore, MD, US). The LNCaP sublines 104-S (androgen-sensitive) and the androgen ablation-resistant and bicalutamide-resistant cells 104-R1 and CDXR3 respectively, were a generous gift from Dr

John M. Kokontis (University of Chicago, Chicago, USA). Both human embryonic kidney (HEK)293 cell line and its sub-clone, JH293s cells were obtained from Cancer Research UK Cell Services. HEK293s cells are transformed with the first 4344 nucleotides (E1 gene) of Ad5 and were used for primary viral expansions of non-replicating adenoviruses to provide the E1 gene in *trans* for virus production. JH293 cells were used for limiting dilution tissue culture infectious dose ($TCID_{50}$) assay. All cell lines with the exception of LNCaP cells and sub-lines 104-R1 and CDXR3 were cultured in Dulbecco's Modified Eagle medium (DMEM) supplemented with 10% fetal bovine serum (FBS), 100 units/ml penicillin, 100mg/L streptomycin and L-glutamine. The DMEM culture medium for the LNCaP 104-S, 104-R1 and CDXR3 cells were supplemented with 10% charcoal-stripped FBS (Sigma Aldrich) with 0.2nM DHT. Medium for 104-S, 104-R1 and CDXR3 cell was changed every 2-3 days if cells were not passaged. Regular LNCaP cells were cultured in Roswell Park Memorial Institute (RPMI) medium supplemented with 10% FBS, 100 units/ml penicillin and 100mg/L streptomycin and L-glutamine. Due to their poor adherence these cells were grown in CellBIND flasks (Corning, Amsterdam, The Netherlands) and seeded on CellBIND 6-well dishes for experiments. Cells were incubated at 37ºC in a humidified atmosphere with 5% CO_2. Experiments were carried out using cells between 5 and 30 passages and were sub-cultured every 3-4 days by washing the monolayer of cells with phosphate buffered saline (PBS) and trypsination. Aliquots of $1x10^6$ cells/ml were frozen in 10% DMSO, 20% FBS and 70% 10% FBS DMEM medium and stored in liquid nitrogen. All cell culture reagents were obtained from PAA Laboratories (Yeovil, UK).

Table 5. Characteristics and genetic status of PCa cell lines used in this project

	22Rv1	LNCaP	VCaP	DU145	PC3
Year established	1999	1980	2001	1978	1979
Reference	(Sramkoski, Pretlow et al. 1999)	(Horoszewicz, Leong et al. 1980)	(Korenchuk, Lehr et al. 2001)	(Stone, Mickey et al. 1978)	(Kaighn, Narayan et al. 1979)
Origin	1° tumour from CRW22Rv xenograft serially passaged in mice	Carcinoma supraclavicular lymph node metastasis	Vertebral metastatic lesion serially passaged in mice	Carcinoma brain metastasis	Grade IV adenocarcinoma bone metastasis
Androgen dependency	Androgen independent but responsive	Androgen sensitive	Androgen independent but responsive	Androgen independent	Androgen independent
AR	✓ Mutated (exon duplication and C-terminal truncation)	✓ Mutated (T877A) Promiscuous AR binding	✓ Wild-type (amplified gene locus)	✗ No mRNA or protein expressed	✗ No mRNA or protein expressed
PSA RNA	✓	✓	✓	✗	✗
PSA protein	✗	✓	✓	✗	✗
IL-6 receptor	✓	✓	mRNA	✓	✓
IL-6 secreted	✓	✗	✓	✓	✓
p53	Wild-type (Q331R heterozygous)	Wild-type	Mutated (A248W) homozygous	Mutated (P223L and V274F)	p53-deficient
p21	✓	✓	Unknown	✓	✓
pRb	✓	✓	Unknown	Mutated	✓
HDM2	✓	✓	Unknown	✓	✓
AKT	✓	✓	✓	✓	✓
PTEN	✓	✗	✓	✓	✗
STAT3	✓	✓	Unknown	✓	✗
Bcl-2	✓	✓	✓	✓	✓

✓ = expressed, ✗ = not expressed
(Bookstein, Shew et al. 1990; Isaacs, Carter et al. 1991; Ni, Lou et al. 2000; Tepper, Boucher et al. 2002; van Bokhoven, Varella-Garcia et al. 2003; Lu, Zhang et al. 2004; Loberg, St John et al. 2006; Skjoth and Issinger 2006; Hodgson, Shao et al. 2011; Fahrenholtz, Beltran et al. 2013)

2.3. Viruses

2.3.1. Adenoviral mutants

The experiments described in this thesis were carried out using replication-defective recombinant adenovirus based on type 5 (Ad5) and deleted for E1 and E3 genes (Table 6). For Ad5Hey1, the E1 gene was replaced with Flag-Hey1 under the control of the cytomegalovirus (CMV) promoter. Dr S.C. Cheong previously constructed Ad5Hey1 by PCR amplification of Flag-tagged-Hey1 from pSG5-Flag-Hey1 (a kind gift from Dr Charlotte Bevan, Imperial College London, London) and cloned into the multiple cloning site of the pShuttle-CMV vector (Stratagene, TX, USA). Homologous recombination with pAdEASY-1 vector (lacking E1 and E3 genes; Stratagene) generated Ad5Hey1. The cytotoxic gene E1A12S, a known inducer or apoptosis and sensitizer to chemotherapeutic drugs was inserted into the adenovirus replication-defective backbone pAdEASY-1 under the control of the CMV promoter as described for Ad5Hey1, and was used as a positive control (AdE1A12S). AdE1A12S was constructed by Dr Enrique Miranda wherein RNA was extracted from Ad5-infected A549 cells and cDNA synthesised by reverse transcriptase (RT)-polymerase chain reaction (PCR) (Dr Enrique Miranda, PhD Thesis, 2009). E1A cDNA was amplified by PCR using primers amplifying all E1A mRNAs and separated by gel electrophoresis. E1A12S cDNA was then extracted, purified and cloned into the pShuttle-CMV vector and recombined with the pAdEASY-1 vector. Ad5GFP was used as the negative control virus and was previously constructed at the Centre for Molecular Oncology (Prof. N. Lemoine, BCI, QMUL). Ad5GFP contains a CMV-GFP cassette replacing the E1 genes and contains an intact E3 region.

During the course of this research project I produced and used three batches of Ad5Hey1 (Ad5Hey1#1 - 3) and two/three batches of AdE1A12S (AdE1A12#1 - 3). I observed a degree of variation between the Ad5Hey1 virus batches in terms of potency and transgene expression. Previous work leading up to this research was undertaken with the original Ad5Hey1 batch (Ad5Hey1#1). Validation of each purified virus batch was carried out in terms of potency (virus dose response curves; section 2.4.1), transgene expression and viral activity (viral particle (vp)/plaque forming units (pfu); section 2.3.3 and 2.3.4) and these

values taken into consideration during experimental design. In this thesis, results were obtained using Ad5Hey1#1 and 2 for 22Rv1 cells and Ad5Hey1#2 and 3 for LNCaP and DU145 cells as indicated in the figure legends. Viral particle and pfu values for each batch are listed in Table 7.

Table 6. Adenoviral mutants with their respective transgene and deletions

Virus	Deletions	Insertions	Reference
Ad5	-	-	-
Ad5Hey1	ΔE1, ΔE3	CMV-FlagHey1	Dr S C Cheong (manuscript in preparation)
AdE1A12S	ΔE1, ΔE3	CMV-E1A12S	(Miranda, Maya Pineda et al. 2012)
Ad5noHey1	ΔE1, ΔE3	Defective CMV-FlagHey1	Dr S C Cheong (manuscript in preparation)
Ad5GFP	ΔE1	CMV-GFP	Prof N. Lemoine's laboratory

2.3.2. Large-scale virus production

Primary viral expansions were generated by infecting a sub-confluent T175 flask of HEK293 cells with 30µl of purified virus stock. Cells and medium were harvested between 48 and 72h after infection after the appearance of cytopathic effect (CPE) and stored at -80°C. HEK293 cells were grown to 80% confluence in 10% FBS DMEM in ten-layer cell factories (CF-10) (Fisher Scientific) and infected with 10ml of the primary expansion in 2% FBS DMEM. Cells and medium were harvested 72h after infection or when signs of CPE and detachment was observed. Cells and medium were collected and centrifuged for 10min at 2000rpm at 4°C in a Sigma 6K15 centrifuge (Sigma, Osterode am Harz, Germany). Cells were resuspended in 15ml cold PBS and centrifuged for 10min at 1000rpm and then resuspended in 12ml cold 10mM Tris-HCl (pH8). Viral suspensions were freeze-thawed three times to release intracellular viral particles and centrifuged at 6000rpm. The supernatants were layered onto caesium chloride (CsCl) gradients prepared in 3.5" ultracentrifuge tubes (Beckman Coulter, High Wycombe, UK) with 10ml 1.25g/ml CsCl under-layered with 7.6ml 1.4g/ml CsCl solution and were spun for 2h at 25000rpm at 15°C in a Beckman SW28 swing-out rotor in an Optima LE-80K ultracentrifuge. After centrifugation, a 19G needle was used to extract the bottom virus band containing encapsulated virus. The top band of cell debris and the second band

of empty viral particles were discarded. The virus suspension was layered onto 2.5ml 1.35g/ml CsCl solution in 2" ultracentrifuge tubes (Beckman) and centrifuged overnight at 40000rpm at 15°C in a Beckman SW55Ti swing-out rotor. The purified virus was collected using a 19G needle and the volume diluted 2-3 fold (up to a maximum of 12ml) with TSG buffer (96mM NaCl, 0.5mM Na2-HPO_4, 2.8mM KCl, 0.3mM $MgCl_2$, 0.5mM $CaCl_2$ and 30% (v/v) glycerol adjusted to pH7.5). The suspension was dialysed using a 3-12ml Slide-a-Lyser (Pierce Biotechnology, IL, USA) against a buffer containing 10mM Tris-HCl (pH7.5), 1mM $MgCl_2$, 150mM NaCl and 10% (v/v) glycerol for 24h at 4°C. The purified virus was then removed from the dialysis chamber, aliquoted and stored at -80°C.

2.3.3. Virus particle count determination

To determine the particle count of purified virus, DNA content was measured using the Quanti-iT PicoGreen dsDNA assay kit (Invitrogen) using a Tecan Infinite F200 plate reader (Tecan, Mannedorf, Switzerland) and Magellan software version 6.3 (Tecan). Viral stocks were diluted 1:2 in Tris-EDTA (TE) buffer (10mM Tris-HCl (pH8), 1mM EDTA) containing 0.5% SDS and heated at 56ºC for 10min. After heat inactivation virus was diluted to 1 in 120 and 1 in 200 in TE/0.5%SDS so concentrations could be assayed in triplicate. A standard curve of Lambda-phage DNA (provided in the kit) starting at 500ng/ml was prepared by 5-fold serial dilution using TE. 100µl of each virus or Lamda-phage DNA dilution in triplicate was transferred to a well of a 96-well black plate. PicoGreen reagent was diluted 200-fold in TE and 100µl added to each well. Emission was read at 535nm after excitation. Using the fluorescent measurements from the Lambda DNA linear regression curve using Graphpad Prism software was constructed by plotting DNA concentration vs. fluorescence (linear regression coefficient >0.98). The DNA concentration for each virus dilution was calculated using the standard curve taking into consideration the dilution factor for each sample. The number of viral particles per ml (vp/ml) for the purified virus was determined on the assumption that 1µg DNA is the equivalent of $2.7x10^{10}$ viral particles. As an internal control Ad5 of known particle count was included as a reference.

2.3.4. Infectious particle count determination

Viral activity for purified virus particles was determined by measuring viral replication using the limiting dilution tissue culture infectious dose ($TCID_{50}$) assay. JH293 cells were seeded in 96-well plates at a cell density of $1x10^4$cells/well in 200µl/well in 10% FBS in DMEM. The following day purified virus was diluted to $1x10^{-7}$ (Ad5) or $1x10^{-5}$ (non-replicating viruses) in serum free DMEM and used to infect the top row of duplicate or triplicate plates (20µl/well) and serially diluted down the plate by transferring 20µl/well from one row to the row below. The last rows of wells were left uninfected as controls. Plates were incubated for 7 to 10 days and each well was scored for signs of CPE. CPE was determined as the presence of plaques (indicated by holes in the monolayer) within the monolayer and/or when cell layer was rounded up. The titre of each plate was calculated in plaque-forming units (pfu)/ml as follows:

Wells exhibiting CPE were counted per dilution row and used in the following calculation to determine the $TCID_{50}$ value (O'Reilly. D 1994):

$TCID_{50} = 10^{A-D\,(S - 0.5)}$

$TCID_{50}/ml = TCID_{50} \times v$

A = Log of the highest dilution showing CPE in more than 50% of wells
D = Log of the dilution factor
S = summation of the proportion of CPE-positive wells in each row
V = infection volume = 0.02ml

pfu/ml = Log TCID50 x µ
where $\mu = -\ln p = 0.69$

According to the Poisson distribution:
µ is the mean concentration of infectious particles at a given dose
p is the proportion of cultures remaining uninfected, = 0.5

Virus particle/plaque forming units (vp/pfu) ratio was determined for each virus. Vp, pfu and vp/pfu values for each virus batch are listed in Table 7. All Ad5Hey1

and AdE1A12S batches used had a vp/pfu ratio <225. It was not possible to achieve this ratio for Ad5noHey1 or Ad5GFP batches.

Table 7. Particle count and viral titre and calculated vp/pfu ratio for virus batches

	Virus particle (vp) (vp/ml)	Viral Titre (pfu/ml)	Vp/pfu ratio
Ad5Hey1#1	5.20E+11	2.14E+10	24:1
Ad5Hey1#2	4.85E+11	2.21E+09	219:1
Ad5Hey1#3	1.78E+11	1.09E+09	163.3
AdE1A12S #1	1.91E+11	1.72E+09	111:1
AdE1A12S#2	1.10E+11	4.91E+08	224:1
AdE1A12S#3	7.72E+11	5.14E+09	150:1
Ad5noHey1	7.10E+11	1.33E+09	534:1
Ad5GFP	2.17E+11	1.53E+08	1418:1

2.3.5. Confirmation of E1 and E3 gene deletions

DNA from purified virus was extracted using the QIAmp DNA Blood Mini Kit (Qiagen, Manchester, UK). 20µl of proteinase K (Qiagen) was added to 200µl virus. Extraction buffer, buffer AL supplied with the extraction kit was then added at a 200µl volumes and incubated at 56°C for 10min. 200µl of ethanol was added and the sample mixed by pulse-vortexing for 15s and transferred to a QIAmp spin column in a 2ml collection tube. After centrifugation for 1min at 6000x g, the QIAmp spin column was transferred to a new collection tube and 500µl wash buffer, buffer AW1 (supplied) was added and the sample centrifuged for a further minute at 6000x g and the filtrate discarded. 500µl wash buffer, buffer AW2 (supplied) was added to the column and centrifuged at 20000x g for 3min. The spin column was placed in a sterile microcentrifuge tube and the DNA eluted in 70µl distilled H_2O at 6000x g for 1min.

Since the viruses used in this project were non-replicating, the absence of the E1 and E3 deletions were confirmed for all Ad5Hey1 and AdE1A12S batches produced. Polymerase chain reaction (PCR) primer sets identifying the adenoviral E1A, E1B and E3 regions were used with DNA extracted from adenoviral mutants. PCR products from these reactions were compared with PCR fragments generated from the amplification of Ad5 DNA and the

pAdEASY-1 backbone plasmid DNA. PCR were set up with 8 primer sets (Table 8) using the Advantage 2 PCR kit (Takara Bio Europe/Clontech, Saint-Germain-En-Laye, France). Each reaction contained 50ng purified viral DNA, 2.5µl each of forward and reverse primers (10µM), 1µl 50x dNTPS (10mM each), 3µl 10x PCR buffer and 1µl Taq polymerase made up to a final volume of 30µl with distilled H_2O. DNA was amplified by 35 cycles (94°C 40s, 62°C 60s, 72°C 90s) in a Gene Amp PCR system 9700 (Applied Biosystems; Thermo Scientific). Amplified PCR products were separated on a 1.5% agarose gel with a 100bp (New England BioLabs (NEB), Ipswich, UK) and 1kb+ DNA ladder (Invitrogen) to determine the size of the PCR products. The expected sizes for Ad5 were calculated from the known sizes of each sequence (Table 9). An example of a representative PCR gel for Ad5Hey1 and AdE1A12S is shown in Figure 15. Faint bands, which were of similar size to Ad5, were observed for Ad5Hey1 and AdE1A12S for primer sets 1, 2, 4, 5, 6 and 8. However these bands were also obtained when the empty pAdEASY-1 vector was amplified using the same primers. Primer set 7 resulted in a strong amplification of a band slightly smaller in size than the one generated from Ad5 DNA. This however was also observed from amplification from pAdEASY-1 plasmid DNA suggesting non-specific binding of primers and/or amplification. Other spurious bands were observed for the primer set corresponding to E1A12S from DNA extracted from Ad5Hey1 and pAdEASY-1 DNA. The non-specific products derived from these PCR reactions may be the result of using PCR primers that were specifically designed to amplify gene regions in replicating viruses and not recombinant adenoviral plasmids. Further verification by immunblotting for E1A expression verified that neither AdHey1 nor AdE1A12S nor AdGFP expressed the E1A proteins (section 3.2.1, Figure 35).

Table 8. PCR primers used to confirm virus deletion status

Primer set	Direction	Sequence
1	5' forward	CCCGGTGAGA TTCCTCAAGAGGCCAC
	3' reverse	CCGGACCCAAGGCTCTCTGCTCTCCGGCTGCTCGGGC
2	5' forward	GTAATGTTGGCGGTGCAGGAAGGGATTG
	3' reverse	GGGTCCCCCGTATTCCTCCGGTGATAATGAC
3	5' forward	GTGTTCGCTTTGCTATATGAGGACCTGTGGC
	3' reverse	CCTCGATACATTCCACAGCCTGGCGACGCCCACC
4	5' forward	CCTGTGATTGCGTGTGTGG
	3' reverse	GACAACAGTAGCAGGCGATTC
5	5' forward	GCATCTGTGGAGAGCGGTTGTGAGACAC
	3' reverse	GCGCCAGCAGATCAAGCTCATTAGCGC
6	5' forward	GCTTAATGACCAGACACCGTCCTGAGTG
	3' reverse	GCACCAAGTGA TCGGGCCTCAGCTCC
7	5' forward	CACCCTCACGCTCATCTGCAGCCTCATCACTGTGG
	3' reverse	CTTCAGACGGTCTTGCGCGCTTCA TCTGC
8	5' forward	CGCTGGGGTCGCCACCCAAGATGATTAGG
	3' reverse	GAGTAGGGTACAGACCAAAGCGAGCACTG
E1A12S	5' forward	GCGCGCACCATGAGACATATTATCTGCC
	3' reverse	CTCGAGTTATGGCCTGGGGCGTTTAC

Table 9. Regions of the Ad5 genome targeted by PCR primer sets and expected size of DNA fragments

Primer set	5' binding site	3' binding site	Target sequence	Expected Ad5 size (bp)
1	476	853	E1A start	377
2	767	1029	E1A-CR2	262
3	1069	1453	E1A end	384
4	1554	2086	E1B-19K	532
5	2073	2440	E1B-55K	367
6	2383	3434	E1B-55K	1051
7	29915	31038	E3B	1123
8	28715	29135	E3-gp19K	420
E1A12S	476	1453	E1A	800

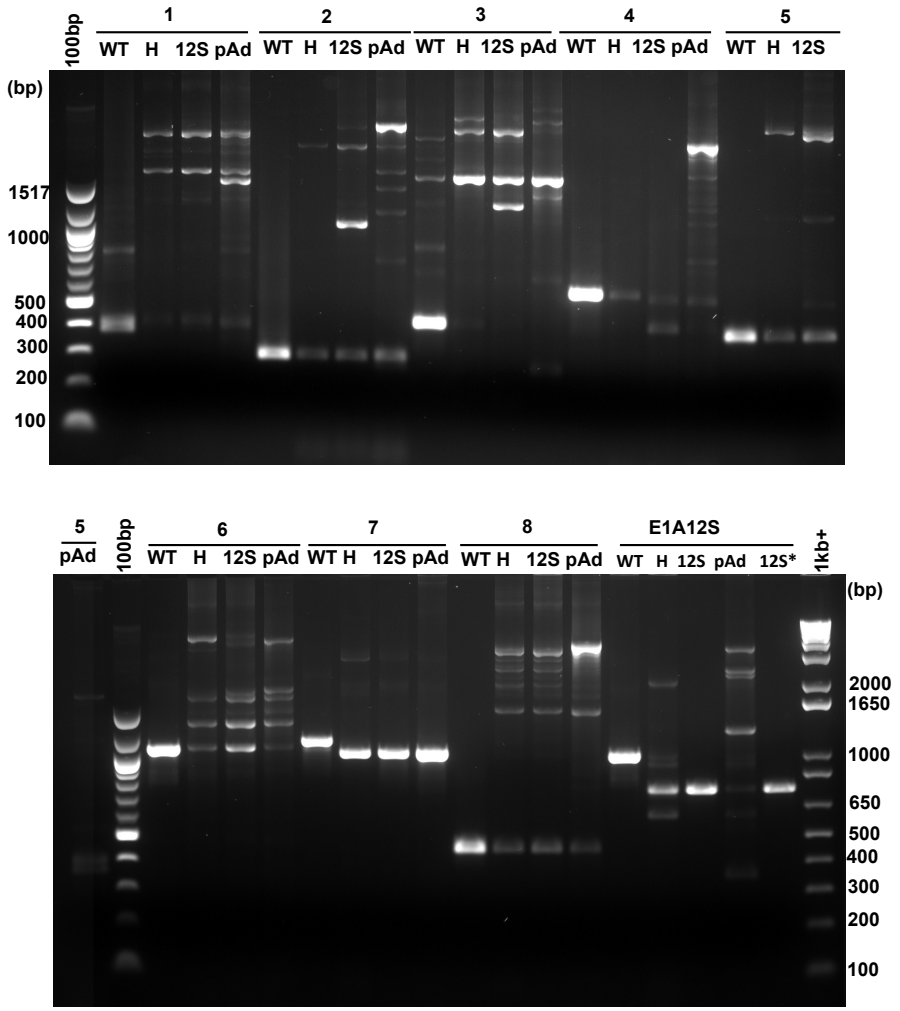

Figure 15. PCR verification of E1 and E3 deletions for representative batches of Ad5Hey1 and AdE1A12S

Amplification of Ad5 (WT), Ad5Hey1 (H), AdE1A12S (12S), pAdEasy-1 (pAd) and AdE1A12S original batch (12S*) DNA with primer sets 1-8 and primer set recognising E1A12S. Fragments sizes were estimated using DNA ladders (100bp and 1kb+) and for Ad5, compared to the expected sizes (Table 9) or analysed for the absence of E1 and E3 PCR products for non-replicating adenoviral mutants.

2.3.6. Virus replication

2.3.6.1. Burst assay

To assess the replication status of the non-replicating adenoviral mutants, burst assays were performed in 22Rv1 cells followed by the $TCID_{50}$ assay in JH293 cells as described in section 2.3.4. Cells were seeded at $3x10^5$ cells/well in 6-well plates. The next day, cells were infected with 10ppc of Ad5 and 10, 100 and 1000ppc of Ad5Hey1 or AdE1A12S in serum-free medium for 2h. The infection

medium was then removed and replaced with 10% FBS in DMEM, with each treatment in duplicate. At 48 and 72h post-infection cells were detached by scraping and collected together with the medium and stored at -80°C. Burst assay samples were freeze-thawed three times and centrifuged at 1200rpm for 5min and diluted $1x10^{-4}$ or $1x10^{-3}$ in serum-free medium for Ad5 and adenoviral mutants respectively and assayed by $TCID_{50}$.

2.3.6.2. Quantitative PCR

22Rv1 cells were seeded and treated as described in section 2.3.6.1 for the burst assay. At 24, 48 and 72h post-infection, medium was aspirated from the wells and the cells washed with PBS. Cells were scraped into a volume of 200µl of PBS per well and DNA immediately extracted using proteinase K and the DNA Blood Mini Kit as described in section 2.3.5.

Quantitative PCR (QPCR) quantified viral genome copy number as an indirect measurement of viral replication. Fold change of viral genome copies compared with Ad5 at 24h post-infection was carried out using the comparative quantification ($\Delta\Delta C_t$) method. Primers amplifying the E2A gene of the viral genome were used to determine the threshold cycle (C_t) values for E2A expression and normalised to an endogenous reference, glyceraldehyde-3-phosphate dehydrogenase (GAPDH). Another member of our research group had previously validated these primers to ensure amplification efficiencies of both primer sets were approximately equal.

C_t values for E2A and GAPDH expression were determined for each sample in duplicates using 0.6µl of each forward and reverse primer (10µM) (Table 10) with 10µl Power SYBR Green PCR MasterMix (Applied Biosystems) for 2µl (10ng/µl) DNA template in a total reaction volume of 20µl. The reactions were run on an ABI 7500 RealTime PCR System (Applied Biosystems). C_t values were determined using Sequence Detector Software version 1.9.1 (Applied Biosystems).

Fold change in viral copy numbers was then determined. The amount of E2A, normalised to GAPDH and relative to Ad5 at 24h is given by the following equation (Livak and Schmittgen 2001):

$$\textbf{Fold difference} = 2^{-\Delta\Delta Ct}$$

$$\Delta\Delta C_t = \Delta C_{t\ sample} - \Delta C_{t\ calibrator}$$

$\Delta C_{t\ sample}$ is the C_t value for a sample, normalised to the endogenous gene:

$C_{t\ E2A} - C_{t\ GAPDH} = C_{t\ sample}$

$\Delta C_{t\ calibrator}$ is the Ct value for the calibrator (Ad5 24h), normalised to the endogenous gene:

$C_{t\ E2A} - C_{t\ GAPDH} = \Delta C_{t\ calibrator}$

Table 10. Primer sequence of E2A and GAPDH used for QPCR

Primer	Sequence
E2A (5')	GGATACAGCGCCTGCATAAAAG
E2A (3')	CCAATCAGTTTTCCGGCAAGT
GAPDH (5')	TGGGCTACACTGAGCACCAG
GAPDH (3')	GGGTGTCGCTGTTGAAGTCA

2.4. Cell viability

2.4.1. Determining virus EC_{50} values

DU145 ($1x10^4$cells/well) or 22Rv1, HCT116wt and HCT116p53$^{-/-}$ cells ($2x10^4$cells/well) were seeded in 96-well plates in a volume of 200µl/well of 10% FBS DMEM. The next day the medium was decanted and replaced with 90µl/well 2% FBS in DMEM. Due to poor adherence of LNCaP cells, $1x10^4$cells/well were seeded in a volume of 90 µl/well of 2% FBS in RPMI and the medium was not removed before treatments. The LNCaP sub-lines, 104-S, 104-R1 and CDXR3 were also seeded in 90 µl/well of 2% charcoal-stripped FBS in DMEM and again the medium was not replaced. The next day, cells were infected with 5-fold serial dilutions of virus starting at a concentration of $1x10^5$ particles per cell (ppc). Viability was assessed 3 days post-treatment (4 days after seeding) using the MTS viability assay carried out according to the manufacturer's protocol (Promega, Southampton UK). When the tetrazolium salt MTS (3-(4,5-dimethylthiazol-2-yl)-5(3-carboxymethoxyphenyl)-2-(4-sulphophenyl)-2H-tetrazolium) is combined with phenazine methosulphate (PMS) it is reduced by mitchochondrial dehydrogenases, present in metabolically active cells to a soluble formazan compound. The soluble compound absorbs light at 490nm and the number of living cells is proportional to the concentration of formazan in the sample. After addition of the MTS reagent, cells were incubated at 37ºC for 6h (22Rv1), 4h (LNCaP and sub-lines), 2-3h (HCT116wt and HCT116p53$^{-/-}$) and 1-2h (DU145) and read using a microplate reader (Opsys MR, Dynex Technologies, VA, US) at a wavelength of 495nm. Values were corrected against background wells containing medium only and expressed as a percentage of cell death compared with untreated control cells.

$$\% \text{ Cell death} = 100 - \left\{ \frac{Abs_{sample} - Abs_{medium}}{Abs_{untreated} - Abs_{medium}} \right\}$$

Sigmoidal dose-response curves were generated by non-linear regression analysis using GraphPad Prism Version 6.0b for Macintosh (GraphPad

Software, San Diego, CA, USA) and used to determine the effective concentration $(EC)_{50}$ values (the dose required to kill 50% of cells) of each virus.

2.4.2. Determining drug and small molecule inhibitor EC_{50} values

DU145 and LNCaP ($1x10^4$cells/well) or 22Rv1, HCT116wt and HCT116p53$^{-/-}$ ($2x10^4$cells/well) were seeded in 96-well plates as described above. Cells were treated with 5-fold serial dilutions of the cytotoxic drugs mitoxantrone, docetaxel or 5-FU at a starting dose of 400μM, 80μM and 10μg/ml respectively. The starting dose of small molecule JAK inhibitors, AG490 and AZD1480 was 1mM. Agents were diluted in serum-free medium and were made up at a 10-fold higher concentration. 10μl of each dilution was added to 90μl medium in the well in duplicates or triplicates. Medium alone and untreated cells served as controls. Cell viability was determined by MTS assay 3 days after treatment as described in section 2.4.1

2.4.3. Combination assays

2.4.3.1. Synergy: Fixed dose of virus and drug

PCa cell lines were treated with a combination of either mitoxantrone or docetaxel and non-replicating viruses at fixed concentrations. Mitoxantrone and docetaxel were used at sub-optimum doses at 25nM and 5nM respectively (22Rv1), 50nM and 5nM (DU145) and 25nM and 2.5nM (LNCaP) determined to kill <20% of cells. Mitoxantrone and docetaxel were combined with either Ad5Hey1 or AdE1A12S at a dose that resulted in approximately 30% cell death (EC_{30}). These viral doses were selected for each cell line based on the dose response studies for each virus. The concentrations of drugs and viruses used are shown in Table 11. Ad5GFP was used as a negative control at the same dose used for Ad5Hey1.

Table 11. Adenoviral mutant and drug doses used in PCa cell lines in combination studies

Treatment	22Rv1	DU145	LNCaP
Ad5Hey1	480ppc	1800ppc	360ppc
AdE1A12S	120ppc	900ppc	240ppc
Ad5GFP	480ppc	1800ppc	360ppc
Mitoxantrone	25nM	50nM	25nM
Docetaxel	5nM	5nM	2.5nM

DU145 cells were seeded in 96-well plates at $1x10^4$cells/well, 22Rv1 cells at $2x10^4$cells/well in 200µl 10% FBS in DMEM and LNCaP cells at $1x10^4$cells/well in 90µl 2% FBS in RPMI. The following day medium was decanted in the case of DU145 and 22Rv1 cells and replaced with either 80 or 90µl 2% FBS DMEM depending on the addition of single or combination treatment to a total volume of 100µl. The volume of medium for LNCaP cells was adjusted so that after the addition of virus and/or dug, the total volume was 100µl. Cells were treated with virus and/or drugs in 6 replicate wells per condition. Cell viability was assessed by MTS assay 3 days after treatment as described in section 2.4.1. Values were corrected against background wells containing medium only and expressed as a percentage of cell death compared with untreated control cells.

To determine whether the interaction between Ad5Hey1 and either drug was synergistic (i.e. produced supra-additive cell death) the summation method was applied wherein the sum of the percentage of cell death for each agent alone (theoretical additive effect) was compared with the observed effect. If the observed effect was greater than the sum of the effects of each agent alone the agents were considered to act synergistically.

The theoretical additive effect was calculated as follows:

$E(d_a d_b) = E(d_a) + E(d_b)$

$E(d_a)$ = effect of agent a alone at dose d
$E(d_b)$ = effect of agent b alone at dose d
$E(d_a d_b)$ = effect of the combination of agents a and b

Due to the variable nature of the cell viability assay, it was not possible to combine the results from more than one experiment and therefore data from representative experiments is shown. To obtain the mean theoretical additive

effect for one experiment, the lowest percentage of cell death obtained from the 6 replicates wells for virus single-agent treatment was combined with the lowest percentage of cell death for the drug single-agent treatment. This value represented the minimum theoretical additive effect between the two agents. The maximum theoretical additive effect was calculated by combining the highest percentage of cell death for virus and drug single-agent treatments. The mean of the minimum and maximum theoretical additive effects was calculated and compared with the observed effect.

2.4.3.1.1. PicoGreen cell viability assay

Cell viability was also determined using PicoGreen, which specifically binds to double-stranded DNA to determine cell number. Cells were seeded and treated as described in section 2.4.3.1 and cell viability measured 3 days after treatment. Medium was decanted and cells washed twice with 200µl/well PBS. PBS was removed and plates left at -80°C for 30min and which they were removed and allowed to return to RT. CyQuant lysis buffer (Invitrogen) and PicoGreen was diluted 1/20 and 1/200 respectively with distilled water and 100µl added to each well. Emission was read at 535nm after excitation at 485nm on a Fluostar Optima (BMG Biotech, MA, USA) microplate reader. Values were corrected against background wells containing medium only and expressed as a percentage of cell death compared with untreated control cells.

2.4.3.1.2. Sulforhodamine B cell viability assay

Cell viability was assessed by sulforhodamine B (Acid red 52) (Sigma) which measures total biomass of cellular proteins by binding basic amino acid residues on trichloroacetic-fixed cells. Medium was decanted and cell washed with PBS (200µl/well) and then fixed with 100µl/well trichloroacetic (TCA) and incubated at 4°C for 30min. TCA was then removed and cells washed three times with distilled water (100µl/well). Plates were left to air dry at RT and when dry 100µl of sulforhodamine B (0.4%) added to each well and left to stain for 20min. Sulforhodamine B was discarded and cells washed in 1% acetic acid (100µl/well) until the dye was removed. Plates were left to air dry and 100µl 10mM Tris-HCL (pH9.0) was added to each well and incubated for 5min at RT. Absorbance was measured at 560nm using a Wallac 1420 Multilabel counter

plate reader (PerkinElmer). Values were corrected against background wells and cell survival expressed as a percentage of cell death compared with untreated control cells.

2.4.3.2. Sensitisation: Dose response to virus in the presence of fixed dose of drug

DU145 and HCT116 cell lines were seeded and infected with a dose response of virus as described in section 2.4.1 and treated simultaneously with either mitoxantrone, 5-FU, AG490 or AZD1480 at sub-optimum doses wherein they induced <30% cell death. This assessed changes in cell sensitivity to virus when combined with drugs.

2.4.3.3. Fixed doses of virus in combination with mibolerone ± bicalutamide

One day before seeding, cell culture medium was changed to 10% charcoal-stripped FBS-containing growth medium to remove residual hormones that are present in standard FBS. DU145 at $1x10^4$cells/well or 22Rv1 at $2x10^4$cells/well were seeded in 96-well plates in 10% charcoal-stripped FBS in DMEM. The LNCaP cells and the AR-positive VCaP cells were seeded at $1x10^4$ and $2x10^4$cells/well respectively in 90µl 2% charcoal stripped FBS in DMEM (VCaP) or in RPMI (LNCaP). The following day medium was decanted from 22Rv1 and DU145 cells and replaced with 2% charcoal-stripped FBS DMEM. Cells were infected with a fixed dose of Ad5Hey1 that would kill approximately 50% of cells (EC_{50}) or Ad5GFP (at the same ppc) and combined with 1nM mibolerone ± 5, 10 or 20µM of bicalutamide. Uninfected and untreated cells were treated with 0.2% ethanol as a vehicle control and all other treatments combinations were adjusted to contain the same percentage of ethanol. Cell viability was assessed 3 days post-treatment by MTS.

2.5. Luciferase reporter assay

2.5.1. Measuring AR transcriptional activity in 22Rv1 cells in response to Ad5Hey1 infection

22Rv1 cells were seeded in 24-well plates at a density of $2x10^5$ cells/well in 1ml 10% FBS in DMEM. The following day (day 2) medium was removed and cells were infected with Ad5Hey1 or Ad5GFP at 0.1, 0.3, 1, 3 and 10ppc in serum-free medium for 2h after which infection medium was removed and replaced with 1ml/well of 10% charcoal stripped FBS in DMEM. The next day (day 3) cells were transfected with 0.75µg of the androgen receptor activity reporter plasmid MMTV-Luc (kindly provided by Dr Charlotte Bevan) and 0.25µg pRL-SV40 (generously provided by Dr Spiros Linardopoulos) to normalise for transfection efficiency. Transfection was carried out using JetPEI-RGD transfection reagent (PeqLab Ltd, Sarisbury Green, UK) according to the manufacturer's protocol. 24h later (day 5), medium was removed and cells treated with either 0.1nM mibolerone or 0.1% ethanol in 1ml/well in 10% charcoal-stripped FBS in DMEM. On the final day (day 6) cells were lysed with passive lysis buffer (Promega) and firefly and renilla luciferase activities measured using the Dual-Luciferase reporter assay system (Promega) according to the manufacturer's instructions.

2.6. RNA interference

2.6.1. siRNA selection

Short interfering RNA (siRNA) was used to silence AR and p53 expression in 22Rv1 cells. One particular sequence out of four available by Dharmacon (Thermo Scientific) was found to knockdown AR more successfully and was previously confirmed by Dr S.C. Cheong. To increase the possibility of successful knockdown without testing individual sequences we selected the SMARTpool On-Target plus siRNA (Thermo Scientific) to specifically silence p53. A non-targeting siRNA sequence (Thermo Scientific) was used as a non-

silencing control. Details of the siRNAs used in this study are summarised in Table 12.

Table 12. Sequence of AR, p53 and non-targeting control siRNA

	Catalog number
On-Target plus AR siRNA	J-003400-08
SMARTpool On-Target plus p53 siRNA	L-003329-00
SiGenome Non-targeting siRNA pool	D-001206-14

On-Target plus AR siRNA, SMARTpool On-Target plus p53 siRNA and siGenome Non-targeting siRNA pool were reconstituted in RNAse-free 1x siRNA buffer (Thermo Scientific) according to the manufacturer's protocol to obtain a concentration of 20μM. Aliquots were stored at -20°C.

2.6.2. Transient transfection of siRNA to monitor protein knockdown

22Rv1 cells were seeded in 6-well plates at $3x10^5$ cells/well in 2ml/well 10% FBS in DMEM without antibiotics. This seeding density resulted in approximately 30-40% confluency the following day. Transfection of siRNA was performed 24h later using Dharmafect 1 transfection reagent (Thermo Scientific) according to the manufacturer's instructions. The final concentration of siRNA per well was 100nM. Cells were incubated at 37°C and were harvested 24, 48 and 120h post-transfection and monitored for knockdown efficiency by western blotting (described in section 2.7).

2.6.3. Determining virus EC_{50} values after siRNA-mediated AR knockdown

22Rv1 cells were seeded in a 10cm diameter dish at a density of $3x10^6$ cells in 10% FBS in DMEM without antibiotics. The following day cells were transfected with AR or control siRNA (100nM each) as described in section 2.6.2. 24h later cells were trypsinised and reseeded into 96-well plates at $2x10^4$ cells/well in a volume of 200μl 10% FBS DMEM. The next day, 48h after the initial transfection, medium was decanted and replaced with 2% FBS DMEM and cells

infected with 5-fold serial dilutions of Ad5Hey1, AdE1A12S or Ad5noHey1. Three days after infection, 120h after initial transfection cell viability was determined by MTS.

2.6.4. Determining the percentage of cell death after siRNA-mediated p53 knockdown

22Rv1 cells were seeded in 6-well plate at $3x10^5$ cells/well in 2ml/well 10% FBS in DMEM without antibiotics. The format for siRNA transfection was changed to a 6-well format after being advised this may increase knockdown efficiency. The next day 6 wells were transfected with either p53 or control siRNA (100nM each) as described in section 2.6.2. The following day cells from each siRNA transfection were trypsinised and pooled. Cells were reseeded into 96-well plates at a density of $2x10^4$ cells/well in a volume of 200µl 10% FBS in DMEM. The next day, cells were infected with a fixed dose of Ad5Hey1, AdE1A12S or Ad5noHey1 that would kill approximately 50% of cells. These doses were selected for each virus based on the dose response studies in 22Rv1 cells.

2.7. Protein expression levels

2.7.1. Whole cell extract preparation

DU14, LNCaP, 22Rv1, HCT116wt and HCT116p53$^{-/-}$ cell lines were seeded in 6-well plates at 1.5x10^5 (DU145 and LNCaP) and 3.0x10^5 cells/well (22Rv1, HCT116wt and HCT116p53$^{-/-}$) in 2ml/well 10% FBS supplemented medium. The following day, cells were infected for 2h with virus doses shown in Table 13. These doses were selected based on the results of the virus dose-response studies of Ad5Hey1 and AdE1A-12S. Three fixed doses were chosen so as to produce a low, medium or high-degree of cell death by Ad5Hey1. After 2h infection medium was removed and replaced with 10% FBS supplemented medium and incubated at 37°C. For detection of protein expression levels during combination treatment with mitoxantrone or docetaxel, cells were infected and treated with virus and drug at doses shown in Table 11. Whole cell lysates were collected at 48 and 72h post-infection.

Table 13. Virus doses used for Ad5Hey1 (22Rv1; Ad5Hey1#2, LNCaP, DU145, HCT116wt and HCT116p53$^{-/-}$; Ad5Hey1#3), AdE1A12S#2, Ad5noHey1 and Ad5GFP in virus only studies

	Dose	22Rv1 (ppc used)	LNCaP (ppc used)	DU145 (ppc used)		HCT116wt	HCT115p53$^{-/-}$
Ad5Hey1	1	10	300	500	1500	1500	1500
	2	100	500	250	3000	4500	4500
	3	1000	1000	4500	4500	7500	7500
AdE1A12S	1	10	300	500	1500	1500	1500
	2	100	500	2500	3000	4500	4500
	3	1000	1000	4500	4500	7500	7500
Ad5noHey1	1	10					
	2	100	N/A	N/A	N/A	N/A	N/A
	3	1000					
Ad5GFP	1	10	300	500	1500	1500	1500
	2	100	500	2500	3000	4500	4500
	3	1000	1000	4500	4500	7500	7500

Floating and attached cells were collected; medium containing floating cells was collected in 15ml tubes and attached cells washed twice with ice-cold PBS and trypsinised and collected with 10% FBS supplemented medium. Cells were centrifuged at 1200rpm for 5 min in an Allegra X-22 centrifuge (Beckman

Coulter), and medium aspirated. Cells were resuspended in 1ml ice-cold PBS and transferred to 1.5ml micocentrifuge tubes and spun down at 1200rpm for 5min in a benchtop microcentrifuge (5415C, Eppendorf, Stevenage, UK). PBS was removed and cells were lysed with 1x Radio Immuno Precipitation Assay (RIPA) buffer (25mM Tris-HCL pH8, 150mM NaCl, 1% NP-40, 1% sodium deoxycholate, 0.1% SDS) containing a protease inhibitor cocktail tablet and a PhosSTOP phosphatase inhibitor tablet (Roche, Diagnostics, Burgess Hill, UK). Lysates were incubated on ice for 30min and centrifuged at 13000rpm at 4°C for 10min and the supernatant transferred to new microcentrifuge tubes and stored at -80°C.

2.7.2. Determining protein concentrations

Protein concentrations for each sample were determined using the Bradford assay (Bio-Rad, Hemel Hempstead, UK) and using Bovine Serum Albumin (BSA) (Sigma Aldrich) at a stock of 1mg/ml. Bradford assay 5x reagent buffer was diluted with distilled water to obtain a 1x concentration and 200µl added to wells of a 96-well plate. One µl per sample was added to duplicate wells. Protein standards were prepared by adding 0, 1, 2, 2.5, 3, 3.5 and 4µl BSA into duplicate wells. Protein concentrations were determined by absorbance at 595nm using a microplate reader (Opsys MR). Cell lysates were diluted to 1µg/µl in protein sample buffer, heated to 95°C for 5min and stored at -20°C. Sample buffer was made at 5x with 2% sodium dodecyl sulfate (SDS), 250mM Tris-HCl pH7.5, 5mM EDTA, 50% glycerol and bromophenol blue (0.25% w/v). β-mercaptoethanol was added fresh (2% v/v) before diluting the samples.

2.7.3. SDS polyacrylamide gel electrophoresis and western blotting

Total protein (typically 20µg) from cell lysates was loaded onto 10-12% SDS reducing polyacrylamide gels using the Bio-Rad system (Bio-Rad). A PageRuler Prestained protein ladder (Fermentas; Thermo Scientific) was used to determine protein size. The samples and ladder were separated by electrophoresis at 120V for 90min in a running buffer containing 25mM Tris pH 7.4, 250mM glycine and 0.1% SDS. Proteins were transferred to polyvinylidene fluoride membranes (PVDF) (GE Healthcare, Amersham, UK) using the Trans Blot SD semi-dry transfer Cell (Bio-Rad) method according to the manufacturers' instructions. Membranes were blocked with either 5% (w/v) dry milk (Marvel, Morrison's, London) or 5% BSA in Tris-buffered saline Tween-20 buffer (TBS-T) containing 20mM Tris-HCl pH 7.4, 500mM NaCl and 0.05% Tween-20. The membranes were incubated overnight at 4°C with primary antibodies (Table 14) in 1.5% BSA in TBS-T, washed and incubated with secondary antibodies conjugated to horseradish peroxidase (Dako, Stockport, UK) in TBS-T for 1h at room temperature. The membranes were washed six times for 5min with TBS-T after antibody incubation. Protein bands were visualised on X-ray film (FujiFilm, Bedford, UK) using Western Lightening ECL or ECL *plus* reagent (Perkin Elmer) or visualised using G:Box iChemi-XT, Gel Doumentation System (Syngene, Cambridge, UK). Images were acquired with GeneSys v.1.2.0.5 software and protein bands quantified with GeneTools 4.03(a). Protein bands detected on X-ray film were scanned and quantified using Image J 1.47.

Table 14. Primary antibodies used for western blotting and flow cytometry

Protein	Species and Clone	Clone	Catalogue Number	Company	Dilution
β-Actin	Goat	C-11	sc-1615	Santa Cruz	1/1000
AR	Rabbit	N-20	sc-816	Santa Cruz	1/300
β-tubulin	Mouse monoclonal	SAP.4G5	ab11312	Abcam	1/20000
Bax	Rabbit polyclonal	N-20	sc-493	Santa Cruz	1/1000
Cleaved caspase-7	Rabbit polyclonal	-	9491	Cell Signaling	1/1000
Cyclin-B1	Mouse monoclonal	V152	4135	Cell Signaling	1/1000
Cyclin D1	Rabbit polyclonal	M-20	sc-718	Santa Cruz	1/500
E1A	Mouse monoclonal	M58	MS-587-P0	Thermo Scientific	1/1000
Flag	Mouse monoclonal	M2	F3165	Sigma	1/2000
GFP	Mouse monoclonal	B2	Sc-9996	Santa Cruz	1/1000
KU70	Goat polyclonal	C-19	sc-1486	Santa Cruz	1/1000
p53	Mouse monoclonal	DO-1	sc-126	Santa Cruz	1/1000
phospho p53 (ser15)	Rabbit polyclonal	-	9284	Cell Signaling	1/1000
phospho (ser10)-histone 3	Rabbit polyclonal	-	ab5176	Abcam	1/1000
PARP (full length and cleaved forms)	Rabbit polyclonal	-	9542	Cell Signaling	1/1000
PARP (cleaved form)	Rabbit polyclonal	-	9541	Cell Signaling	1/1000
PCNA	Mouse monoclonal	PC10	sc-56	Santa Cruz	1/1000
STAT3	Rabbit monoclonal	79D7	4904	Cell Signaling	1/2000
STAT3 (Y705)	Rabbit monoclonal	D3A7	9145	Cell Signaling	1/1500

2.8. Flow cytometry

2.8.1. Infectability

Cells were seeded in 24-well plates at a density of $2x10^5$ cells (22Rv1) and $1x10^5$ cells/well (DU145 and LNCaP) in 1ml volume of 10% FBS supplemented medium. The following day cells were infected for 2h with 500ppc Ad5GFP in serum-free medium (500µl/well). After infection, medium was removed and replaced with 1ml/well 10% FBS supplemented medium. Uninfected cells served as controls. Cells were incubated at 37ºC for 48h. Cells were collected by trypsinisation and washed twice with 3ml/sample of ice-cold PBS and resuspended in 500µl PBS. Cells were kept on ice until analysis by flow cytometry. Ten thousand events were acquired by flow cytometry on a FACScalibur cytometer (Becton, Dickinson, NJ, USA) with CellQuest Pro v5 Software (BD Biosciences). The events were analysed by gating forward side scatter (FSC) versus right angle side scatter (SSC) and quantifying GFP-positive cells on a plot of green fluorescence (FL-1) versus FSC and setting the marker to encompass <1% of the uninfected control. Post acquisition, data was analysed using FlowJo v7 software (Tree Star Inc., OR, USA) and gates set as described for acquisition.

2.8.2. Cell cycle analysis

2.8.2.1. Cell cycle changes in response to Ad5Hey1 in 22Rv1 and DU145 cells

DU145 and 22Rv1 cells were seeded in 6-well plates at a density of $1.5x10^5$cells/well and $3x10^5$cells/well respectively. Cells were infected with virus using doses shown in Table 15. After 2h, the infection medium was removed and replaced with 2ml/well 10% FBS supplemented medium. At 24, 48 and 72h post-infection cells were harvested by trypsinisation, washed in PBS and fixed in 1ml 70% ethanol (Fisher Scientific) at stored at -20ºC overnight. DNA content of cells was analysed by washing samples twice with PBS (3ml/sample) and then stained with 25µg propidium iodide (PI) and 5µg RNase (Sigma Aldrich) per

sample in a final volume of 500µl PBS. Flow cytometry acquisition was carried out as follows: Cells were gated on FSC vs. SSC dot blot to exclude cell debris. Live cells were gated by pulse-area (FL2-A) vs. pulse-width (FL2-W) to exclude doublets. PI fluorescence (FL3-H) was plotted against cell counts on a linear scale to differentiate between the different phases of the cell cycle. G_1 was set to the first peak to define 2N DNA content. The S phase marker included the cells between 2N and 4N DNA content. The G2/M marker included cells with 4N content and delimited the >4N DNA content. The sub-G_1 marker counted cells with <2N DNA. Post acquisition, data was analysed using FlowJo software and cell cycle markers defined as when acquisition was carried out.

Table 15. Doses of Ad5Hey1#2, AdE1A12S#2 and Ad5noHey1 used for cell cycle analysis

	Dose	22Rv1 (ppc used)	DU145 (ppc used)
Ad5Hey1	1	N/A	2000
	2	100	5000
	3	1000	8000
AdE1A12S	1	N/A	2000
	2	100	5000
	3	1000	8000
Ad5noHey1	1	N/A	2000
	2	100	5000
	3	1000	8000

2.8.2.2. Cell cycle changes in response to Ad5Hey1 in 104-S, 104-R1 and CDXR3 cells

The LNCaP sub-lines 104-S, 104-R1 and CDXR3 cells were seeded in 6-well plates at $3.0x10^5$ cells/well in 2ml/well 10% charcoal-stripped FBS in DMEM. The following day cells were infected with a fixed dose of Ad5Hey1 that could kill approximately 30% of cells (EC_{30}). After 2h infection, medium was removed and replaced with 10% charcoal-stripped medium supplemented with ethanol or 0.1nM mibolerone ± 5µM bicalutamide. All treatments contained 0.05% ethanol and were treated in duplicates. At 72h cells were collected and treated as described in 2.8.2.1. Cell cycle analysis was analysed on a BD LSRFortessa Analyzer (Becton, Dickinson) with BD FACS DIVA software (Becton, Dickinson). Live cells were gated on FSC vs. SSC dot blot to exclude cell debris and single cells discriminated from doublets by gating 560nm yellow green laser (610/20

collection filter) pulse-height (YG-610/20-H) vs. YG-610/20 pulse-area (YG-610/20-A). Cell cycle data was acquired by plotting PI fluorescence (YG-610/20-A) vs. cell counts on a linear scale. Post acquisition, data was analysed using FlowJo software and cell cycle markers defined as described in section 2.8.2.1.

2.8.3. Intracellular cyclin B1 and pH3 expression

22Rv1 cells were seeded in 6-well plates at a density of $3x10^5$cells/well. The following day cells were infected with viruses at 100 or 1000ppc Ad5Hey1, AdE1A12S or Ad5noHey1. After 2h, infection medium was removed and replaced with 2ml/well 10% FBS supplemented medium. Cells were treated overnight with 100ng/ml nocodazole so as to arrest cell in mitosis. At 48h post-infection, medium and cells were harvested by trypsinisation, washed in PBS (3ml/sample), permeabilised and fixed with 500µl 100% methanol (Fisher Scientific) and stored overnight at -20ºC. The next day cells were washed with 1.0% BSA-containing PBS and stained with either cyclin B1 antibody (1/400) or phospho-histone 3 (pH3) antibody (1/1000) (Table 14) diluted in 1% BSA-PBS for 1h at RT. Cells were then washed with BSA-PBS and FITC-conjugated anti-mouse or anti-rabbit secondary FITC-conjugated antibody added at a dilution of 1/250 for cyclin B1 or pH3 antibodies respectively. Cells were incubated in the dark at RT for 30min after which the cells were washed twice with BSA-PBS. Cells were resuspended in 500µl PBS containing 25µg PI and 5µg RNase per sample. Events were acquired with FACScalibur cytometer. Cells were gated on FSC vs. SSC dot blot to exclude cell debris and live cells were gated by pulse-area (FL2-A) vs. pulse-width (FL2-W) to exclude doublets. Bivariate analysis of cyclin B1 or pH3 expression was carried out by plotting FITC fluorescence (Fl-1) on a log scale vs PI fluorescence (FL3-H) on a linear scale so as to discriminate between DNA content and intracellular protein expression. 10000 single cell events were acquired. Post acquisition, data was analysed using FlowJo software.

2.8.4. Mitochondrial membrane potential depolarization

DU145, LNCaP and 22Rv1 cell lines were seeded in 6-well plates at $1.0x10^5$, $1.5x10^5$ and $3.0x10^5$ cells/well respectively in 2ml/well 10% FBS supplemented medium. The following day, cells were infected as single replicates (time-course experiment) or in triplicates (96h stand-alone experiments) with an EC_{30} dose of virus. Two hours later cells were incubated with either normal 10% FBS medium or drug-containing medium using the doses that resulted in synergistic cell death (Table 11). Treatment overnight with the apoptosis-inducer staurosporine at 1μM (DU145 and LNCaP) or 0.5μM (22Rv1) served as a positive control. Cells and medium were harvested between 24-120h by trypsinisation. Samples were washed once with PBS (3ml/sample) and stained with TMRE by adding 5μl (22Rv1) or 40 μl (22Rv1 and LNCaP) of 1μg/ml TMRE working stock to cells resuspended in 500μl PBS. Sample was mixed thoroughly with TMRE by inverting tube 2-3times. Cells were incubated for 30min at 37°C in the dark, washed with PBS, resuspended with 500μl PBS and 50μl 1mg/ml 4',6-diamidino-2-phenylindole (DAPI) (Invitrogen) was added to exclude necrotic cells (disrupted cellular membrane). Cells were analysed by flow cytometry using the BD LSRFortessa Cell Analyzer (Becton, Dickinson). Cells were analysed by flow cytometry using the BD LSRFortessa Cell Analyzer (Becton, Dickinson). Cell debris was excluded by gating on the FSC vs. SSC bivariate scatterplot (Figure 16). A 560nm yellow-green laser with a 585/15-bandpass filter was used to detect TMRE fluorescence and a 405nm violet laser with a 450/50-bandpass filter for DAPI fluorescence. A bivariate scatterplot of TMRE fluorescence vs. DAPI fluorescence (both on a logarithmic scale) allowed for the separation of cells according to live cells (TMRE+/DAPI-), apoptotic cells (TMRE-/DAPI-) and necrotic cells (TMRE-/DAPI+) using BD FACS Diva software (BD Biosciences). Post acquisition, data was analysed using FlowJo software. The percentage of apoptotic cells was plotted as a function of time. 10000 events were collected when possible on the FSC/SSC gated population.

As cells infected with Ad5GFP were also subject to staining with TMRE, the laser and filter for TMRE event collection was selected to ensure minimal spectral overlap between the emission wavelength of GFP and TMRE. A 560nm excitation laser was selected with a bandpass filter of 585/15 for TMRE

(excitation/emission; 549/574nm). To verify that the distribution of TMRE- and DAPI-stained cells was not altered when cells were infected with Ad5GFP, GFP was excited using a 488nm excitation laser with a bandpass filter of 530/30. GFP-negative and GFP-positive cells were gated according to GFP fluorescence and bivariate scatterplots of TMRE fluorescence vs. DAPI fluorescence constructed for each sub-population of cells (Figure 16B,C). The distribution of the each cell population differentially stained by TMRE and DAPI was comparable in the GFP-positive population as it was in the GFP-negative population (Figure 16C). In addition, similar percentages of cells were found in each quadrant of either sub-population indicating GFP did not interfere with the behaviour of the mitochondrial probe.

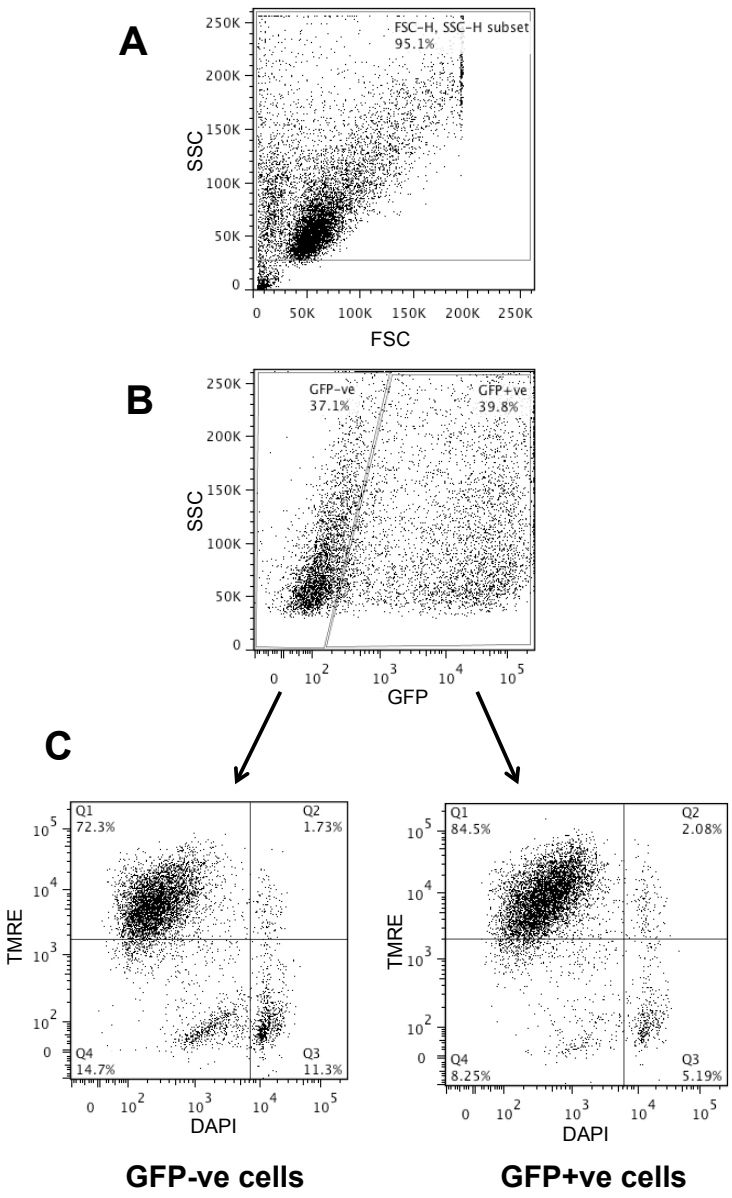

Figure 16. GFP fluorescence of Ad5GFP-infected cells does not interfere with TMRE emission

22Rv1 cells were infected with 1000ppc Ad5GFP and 2h later infection medium removed and replaced with 10% DMEM. 48h post-infection cells were harvested and stained with TMRE and DAPI according to the protocol above. (A) Cells were gated using SSC vs FSC to gate out cell debris. (B) the gated cells were further divided according to GFP fluorescence, GFP-negative or GFP-positive. (C) sub-populations were analysed according to TMRE vs. DAPI staining and quadrants established to distinguish cells according to mitochondrial $\Delta_{\psi m}$ (TMRE) and cell membrane integrity (DAPI). (Q1; Live, Q2; Necrotic, Q3; Necrotic, Q4; Apoptotic).

2.8.5. Active caspase-3 detection

Cells were seeded and treated as described section 2.8.4. Cells were treated overnight in 0.5μM staurosporine. At 72h post-infection cells and medium were collected by trypsinisation and washed with PBS (3ml/sample) and labelled with a FITC-conjugated anti-active caspase-3 antibody according to the manufacturers' instructions (Active caspase-3 FITC Mab apoptosis kit 1, BD Pharmingen, Becton, Dickinson). Cells were analysed by flow cytometry on a FACScalibur cytometer with CellQuest Pro software. Data was analysed by gating FSC vs. SSC for live cells and then quantifying GFP-positive cells on a plot of green fluorescence (FL-1) versus FSC, setting the marker to encompass <1% of the uninfected, untreated control. Post acquisition, data was analysed using FlowJo software.

2.9. Constructing a replication-selective AdΔΔHey1

The design of a replicating Hey1 adenovirus (AdΔΔHey1) was based on the cancer-selective AdΔΔ backbone described previously (Oberg, Yanover et al. 2010). For the description of the cloning strategy for AdΔΔHey1 see section 3.5.1.

2.9.1. Construction of pSuperShuttle LARAHey1

2.9.1.1. PCR amplification of inserts

750bp PCR fragments flanking the E3gp19k region termed the Right Arm (RA) and Left Arm (LA) were amplified from Ad5 DNA and the Hey1 from pSG5-Flag-Hey1 (a kind gift from Dr Charlotte Bevan) using the primer sequences in Table 16. For RA and LA amplification each reaction contained 10ng purified viral DNA, 2.5µl each of forward and reverse primers (10µM), 1µl dNTPs (10mM each), 10µl 5x Phusion HF buffer (part of Phusion High-Fidelity DNA polymerase kit; Finnzymes, Thermo Scientific) and 0.5µl Phusion DNA polymerase made up to a final volume of 50µl with distilled H_2O. For amplification of Hey1 the pSG5-Flag-Hey1 plasmid (10ng) was used. DNA was amplified by 30 cycles (98°C 10s, 58°C 30s, 72°C 30s) in a Gene Amp PCR system 9700. Buffers and contaminants in the PCR products were removed using QIAquick PCR Purification kit (Qiagen). The PCR products were then digested with EcoRV to generate phosphorylated ends (see section 2.9.1.2). The EcoRV-digested PCR fragments were run out on a 0.8% agarose gel for subsequent gel extraction using the QIAquick Gel Electrophoresis kit (Qiagen) and DNA eluted in 30µl distilled H_2O.

Table 16. Primers used to generate RA and LAHey1 inserts for pSSLARAHey1 construction

Primer Name	Sequence (5' – 3')
E3gp19K RA forward	GTACGATATCTTTACTAAGTTACAAAGCTAATGTC
E3gp19K RA Reverse	GTACGATATCCTGGATAAAGGCGATGACCAC
E3gp19K LA Forward	GTACGATATCCCCCCTGCTAGTTGAGCG
E3gp19K LA Hey1 Reverse	GTCATCGTCGTCCTTGTAGTCCATGGTGGCCTTGGGTGGCGACCCCAG
Hey1 fusion Forward	GGACTACAAGGACGACGATGACAAGAAGCGAGCTCACCCCGACTAC
Hey1 Reverse	GTACGATATCTTAAAAAGCTCCGATCTCCGTCCC
RAseq Reverse	GATTCTGTGGATAACCGTATTAC

2.9.1.2. Digestion of pSS and pSSRA by restriction enzymes

2µg pSS or pSSRA were linearised with either EcoRV or SnaB1 (NEB) respectively. Restriction digests were carried out in a 50µl reaction volume containing 5µl 10x NEBuffer 3 (EcoRV) or NEBuffer 4 (SnaBI), 5µl 10x BSA and 1µl of either EcoRV or SnaBI made up to 50µl with distilled H_2O. The reaction was incubated at 37°C.

2.9.1.3. Dephosphorylation of linearised pSS or pSSRA

After enzyme digestion, linearised pSS or pSSRA was subjected to dephosphorylation using Antarctic Phosphatase (NEB). 5µl 10x Antarctic Phosphatase Reaction Buffer and 1µl Antarctic Phosphatase was added to the linearised and gel extracted plasmid preparation and incubated at 37°C for 15min. The linearised and dephosphorylated pSS or pSSRA was run on a 0.8% agarose gel and the band gel extracted and DNA eluted in 30µl distilled H_2O.

2.9.1.4. Generation of LA-Hey1 insert by PCR SOEing

Seamless fusion of LA and Hey1 was carried out using SOEing PCR before it was cloned into pSSRA. After gel extraction, LA and Hey1 PCR products were annealed in a 1:1 molar ratio in the presence of DNA polymerase with no primers. Annealing conditions were 95°C 4min, 55°C 3min and 72°C 5min. Primers E3gp19K LA Forward and Hey1 Reverse were added to the annealed

LA–Hey1 and PCR conditions in 2.9.1.1 extended and amplified the fusion product.

2.9.1.5. Ligation of insert into pSS or pSSRA

Ligations were carried out using the Rapid Ligation Kit (Roche) according to the manufacture's instructions. The volumes of linearised and dephosphorylated vector DNA and insert were calculated using the equation below:

$$\frac{\text{Insert size (bp)}}{\text{Vector size (bp)}} \times \frac{\text{insert intensity}}{\text{vector intensity}} \times \text{volume of vector for ligation} \times 3$$

Ligations were incubated at RT for 30min and ligation reactions transformed into TOP10 chemically competent *E.coli* (Invitrogen).

2.9.1.6. Transformation of pSS or pSSRA into competent *E.coli*

1µl of ligation reactions of pSS or pSSRA were added to thawed chemically competent TOP10 bacteria and incubated on ice for 30min after which they were transferred to 42°C water bath for 30s. 250µl of pre-warmed S.O.C. medium was added to each transformation and the vials incubated at 37°C with agitation for 1h and the bacterial culture plated onto agar plates containing 20µg/ml of chloramphenicol (Sigma-Aldrich). Plates were inverted and incubated overnight at 37°C

2.9.1.7. Screening recombinant clones

Initial screening to assess presence of insert was by crude extraction of DNA from the overnight bacterial culture with phenol-chloroform (USB Corporations, OH, US). In the case of identifying pSSRA, DNA was run on a 0.8% agarose gel along with undigested pSS for size comparison. Orientation was determined by carrying out PCR on the culture medium of selected clones. The primers set used for RA were E3gp19K RA forward and RAseq reverse primer (recognising a sequence outside the EcoRV cloning site in the pSS vector) (Table 16). Successful PCR amplification would only result if the RA were in the correct

orientation. Successful insertion of LA-Hey1 into pSSRA was initially screened with PmeI and SwaI digestion. At each cloning step (pSSRA or pSSLARAHey1), sequencing was performed to determine 100% homology and confirm correct orientation of RA and LARAHey1 DNA sequences in the shuttle vector. All sequence analyses was performed by the Genome Centre at Barts Cancer Institute (London).

2.9.1.8. Homologous recombination

pSSLARAHey1 was digested with PmeI using NEBuffer 4 and incubated at 37ºC for 1h to remove the Origin of Replication (OriR). Digested pSSLARAHey1 was purified by phenol chloroform extraction and then precipitated with ethanol. Digested pSSLARAHey1 and AdΔΔ plasmid were electroporated into BJ5183 *E.coli* at 50 and 100ng respectively. 250µl of pre-warmed S.O.C. medium was then added to the bacteria and incubated with agitation for 1h at 37°C. Bacterial culture was plated onto agar plates containing 25µg/ml chloramphenicol and kanamycin each and incubated overnight at 37°C.

3. Results

3.1. Investigating the intrinsic cytotoxicity of Ad5Hey1-mediated cell death in PCa cells

3.1.1. Ad5Hey1 is cytotoxic to 22Rv1, LNCaP and DU145 cells

To verify the potency of Ad5Hey1 and relative toxicity between cell lines, cell viability assays were performed in the panel of prostate cancer cells previously used. Dose-response curves to replication defective adenoviral mutants were generated and cell death assessed three days post-infection to determine the dose required to kill 50% of cells (Effective Concentration, EC_{50}) for Ad5Hey1, the positive control virus AdE1A12S expressing E1A12S, a recognised inducer of apoptosis and the negative control virus, Ad5GFP expressing the non-toxic transgene, GFP (Figure 17). Ad5Hey1 showed similar potency to the control virus AdE1A12S in all cell lines as determined previously (Cheong *et al*, manuscript in preparation). Furthermore, the AR-positive 22Rv1 and LNCaP were more susceptible than the AR-negative DU145 cells to both Ad5Hey1- and AdE1A12S-induced cytotoxicity. The EC_{50} values of Ad5Hey1 and AdE1A12S varied between cell lines (Figure 17 and Table 17). One contributing factor is the variability in the infectability of the cell lines; a more potent triggering of cell death mechanisms occurs in the sensitive 22Rv1 cells compared with the less infectable DU145 cells (Figure 18). Furthermore, each PCa cell line has a distinctive set of genetic alterations in cell cycle and cell death pathways (Table 5), which will influence the sensitivity of the cell to a specific transgene. Interestingly, in AR-negative PC3 cells only AdE1A12S was able to induce cell death whereas Ad5Hey1 did not (section 1.8.1; Table 4, S.C. Cheong *et al*, manuscript in preparation).

The potency of Ad5Hey1 varied between the two main virus batches used in this thesis (Batches 2 and 3; Table 17; section 2.3.4; Table 7). Ad5Hey1#3 was more cytotoxic compared with Ad5Hey1#2 in all tested cell lines while the comparative order of sensitivity between the cell lines were the same for both Ad5Hey1 batches as well as the relative potency between AdE1A12S and Ad5GFP. The sensitivity of 22Rv1 cells and LNCaP cells to Ad5Hey1 was similar whereas DU145 cells were the least sensitive (Figure 17). While AdE1A12S had lower EC_{50} values than Ad5Hey1, the relative sensitivity of cells to AdE1A12S was the same as to Ad5Hey1; 22Rv1 and LNCaP cells the most sensitive and DU145 the least. The negative control mutants AdFlagHey1 or Ad5GFP were approximately between 10 to 20-times less potent than Ad5Hey1 in these cells.

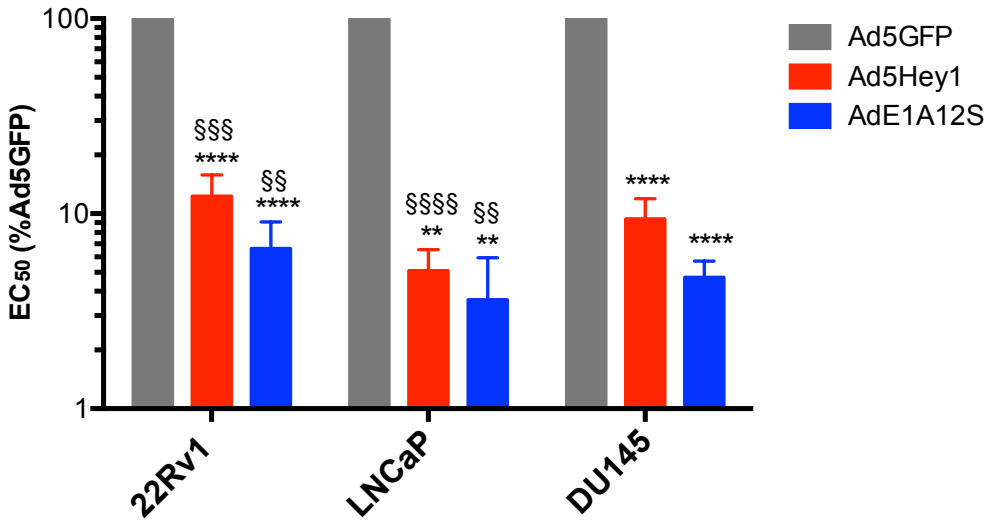

Figure 17. Ad5Hey1 possesses intrinsic cytotoxicity in 22RV1, LNCaP and DU145 cells.

Cells were seeded in 96-well plates and the following day infected in duplicate or triplicate with five-fold serially diluted Ad5Hey1#3, AdE1A12S#3 or Ad5GFP. EC_{50} values are expressed as a percentage of Ad5GFP to determine relative potency of Ad5Hey1 and AdE1A12S in each cell line. Results were obtained three days post-infection by MTS cell viability assay. Results are mean from ≥3 experiments ± SEM. Statistical analysis on raw EC_{50} values (Table 17) with one-way ANOVA using a Dunnet's post-test $p<0.01$ (**) and $p<0.001$ (****) comparing Ad5Hey1 or AdE1A12S with Ad5GFP within each cell line. One-way ANOVA using multiple comparisons with a Tukey post-test, $p<0.01$ (§§), $p<0.001$ (§§§/§§§§) comparing raw Ad5Hey1 or AdE1A12S EC_{50} values in 22Rv1 or LNCaP cells with corresponding viruses infected in DU145 cells.

Table 17. EC_{50} values for Ad5Hey1, AdE1A12S, AdFlagHey1 and Ad5GFP in PCa cell lines

	22Rv1			LNCaP			DU145		
	Mean	SEM	N	Mean	SEM	N	Mean	SEM	N
Ad5Hey1#2	776	± 56	7	1988	± 219	4	7225	± 640	3
Ad5Hey1#3	569	± 94	3	613	± 86	4	2829	± 267	8
AdE1A12S#1	73	± 19	3	Not performed			Not performed		
AdE1A12S#2	Fixed doses used			Not performed			Fixed doses used		
AdE1A12S#3	307	± 65	3	428	± 114	4	1417	± 135	5
Ad5noHey1	2594	± 753	4	>20000		3	29108	± 4327	3
Ad5GFP	4633	± 121	3	14136	± 2400	4	30056	± 6553	3

Dose response curves were constructed by treating cells in duplicate or triplicate with five-fold serially diluted Ad5Hey1#2-3, AdE1A12S#1-3, Ad5noHey1 or Ad5GFP and cell death assessed by MTS 3 days post-infection. Results are mean of 3-8 independent experiments ± SEM.

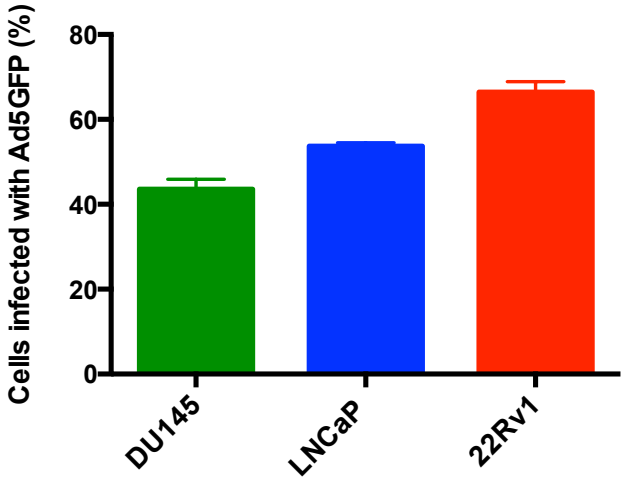

Figure 18. Infectability of PCa cells

Cells were seeded in 24-well plates and the following day infected with non-replicating Ad5GFP at 500ppc. After 2h, medium was removed and replaced with either 10% DMEM (DU145 and 22Rv1) or 10% RPMI (LNCaP). At 48h post-infection, cells were harvested for flow cytometry analysis as described in section 2.8.1. Results shown are mean of duplicates from one experiment ± SEM.

3.1.2. Hey1 expressed from a non-replicating adenovirus acts as an AR corepressor

Ad5Hey1 was previously demonstrated to repress AR signalling of an MMTV reporter construct (MMTV-Luc) in mibolerone-stimulated 22Rv1 cells and cooperate with bicalutamide to further decrease AR signalling (section 1.8.1; Figure 13).

The response to Ad5Hey1 was not dose dependent at the previously tested concentrations of 10-100ppc and as maximal inhibition was already reached at 10ppc, lower doses of Ad5Hey1 were assessed (Figure 19). A dose dependent decrease in AR transcriptional activity was observed with escalating doses between 0.1 and 10ppc. Ad5GFP was found to decrease AR activity in one of the two experiments presumably through non-specific toxic effects of GFP. This, together with the previous findings demonstrates that Hey1 represses AR transcriptional activity in a dose-dependent fashion (0.1–10ppc) when expressed from a non-replicating adenovirus mutant similar to previous reports of Hey1 and HeyL expressed from other vectors in *in vitro* systems and MCF7 cells (Belandia, Powell et al. 2005; Villaronga, Lavery et al. 2009).

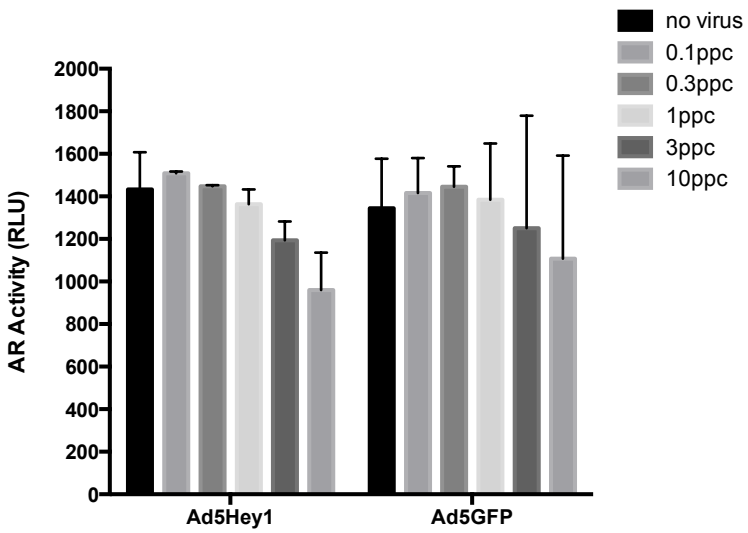

Figure 19. Ad5Hey1 repression of AR transcriptional activity is dose-dependent in 22Rv1 cells

Cells were seeded and the following day infected at escalating doses of Ad5Hey1#1 or Ad5GFP (0.1, 0.3, 1.0, 3.0 and 10ppc). 24h later cells were co-transfected with AR reporter plasmid MMTV-Luc and a plasmid expressing renilla luciferase under the control of a SV40 promoter (pRL-SV40) for normalisation. 48h after virus infection cells were treated with 0.1nM mibolerone and the following day, 72h post virus infection, cells were lysed and luciferase expression detected using a dual luciferase reporter assay system. Data shows mean of single replicates from 2 independent experiments ± SEM.

3.1.3. Ad5Hey1-dependent cytotoxicity is only partially mediated by repression of AR-activity

Following verification of Ad5Hey1 as a corepressor to AR, we sought to determine to what extent Ad5Hey1-induced cell death was dependent on AR-expression considering that Ad5Hey1 also induces cell killing in AR-negative DU145 cells. To determine the role of AR for Ad5Hey1-mediated cytotoxicity, siRNA (previously identified to be specific for AR by Dr S.C. Cheong) was used to knockdown AR and cell viability was assessed with and without Ad5Hey1 infection. Western blotting (Figure 20) confirmed that AR knockdown was successful and stable up to 120h (5 days) post-transfection while a non-targeting control siRNA sequence did not affect AR expression. Knockdown of AR in 22Rv1 cells under these conditions resulted in only modest cell death (10.0±4.78%) (Figure 21C). A low level of AR expression was still detectable after AR knockdown and may have been sufficient to stimulate AR signalling and cell growth.

After AR knockdown, a dose response curve to Ad5Hey1 was generated to determine EC_{50} values in cells treated with AR siRNA or control siRNA. Ad5noHey1 (not expressing Hey1) was used as a negative control instead of Ad5GFP due to a problem in Ad5GFP production. The knockdown of AR resulted in desensitisation of 22Rv1 cells to Ad5Hey1 **(**Figure 21A). The extent of the desensitisation was observed as a two-fold increase in EC_{50} value compared with cells transfected with control siRNA (Figure 21B). The EC_{50} values of AdE1A12S and Ad5noHey1 did not significantly alter when AR was knocked down. These data demonstrate that inhibition of the AR only partially mediates the potency of Ad5Hey1 in 22Rv1 cells and suggest that additional mechanisms are involved.

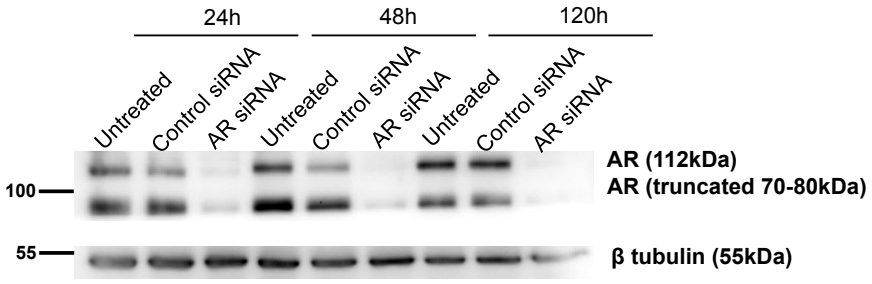

Figure 20. Knockdown of AR by siRNA in 22Rv1 cells

Cells were seeded and the following day transfected with 100nM AR siRNA. Cell lysates were harvested 24h, 48h and 120h post-transfection and prepared for separation on polyacrylamide gels. 20µg protein was loaded per lane and immunoblotted for AR and β tubulin as a loading control.

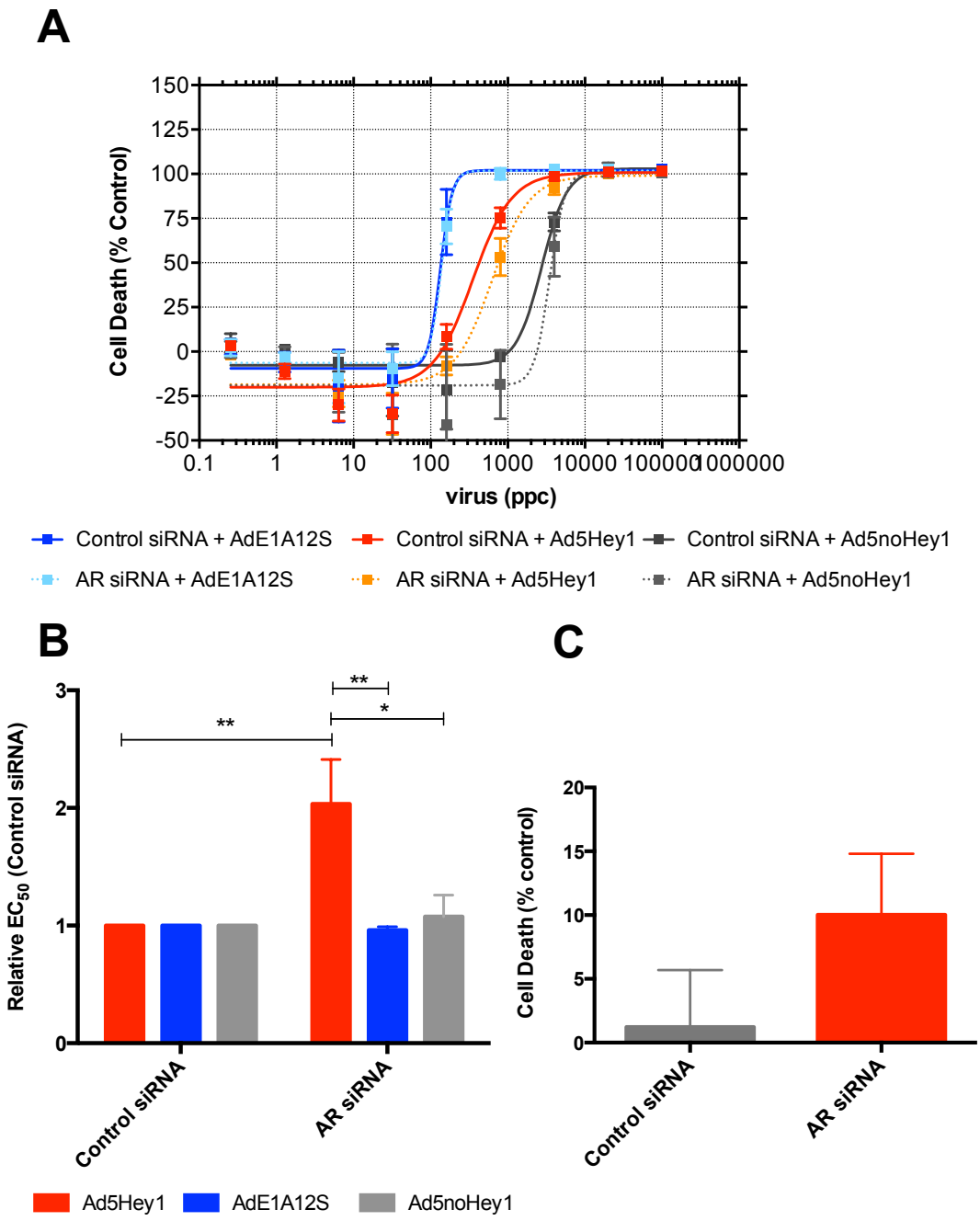

Figure 21. The sensitivity to Ad5Hey1 decreases when AR is knocked down in 22Rv1 cells

A) Dose response curves in cells infected with five-fold serially diluted Ad5Hey1#2, AdE1A12S#1 or Ad5noHey1 48h after transfection with AR or Control siRNA. Cell death was assayed 3 days post-infection/5 days post-transfection by MTS assay and expressed as a percentage relative to AR siRNA or Control siRNA-treated cells. Results are shown as means of duplicates wells from 2-3 independent experiments ± SEM. B) Histogram showing relative EC_{50} values of data from (A) compared to control siRNA. Results are means of 2-3 independent experiments ± SEM with two-way ANOVA statistical analysis using multiple comparisons with a Tukey post-test, $p<0.05$ (*) and $p<0.01$ (**). C) Percentage of cell death (relative to transfection reagent alone) after treatment with siRNA 120h post-infection. Results shown as mean of duplicate wells from 3 independent experiments.

3.1.4. The significance of p53 signalling for Ad5Hey1-dependent cytotoxicity in 22Rv1 and LNCaP cells

3.1.4.1. Ad5Hey1 stabilises and activates p53 in 22Rv1 and LNCaP cells

As suggested in section 3.1.3, repression of AR activity by Ad5Hey1 is likely not the sole mechanism for Ad5Hey1-induced cell death in 22Rv1 cells. Previous reports have demonstrated overexpression of Hey1 induces inhibition of cell proliferation or apoptosis as a consequence of p53 stabilisation through the inhibition of HDM2 at the transcriptional level (Huang, Raya et al. 2004; Villaronga, Lavery et al. 2009).

Based on these findings I assessed whether overexpression of Hey1 resulted in p53 stabilisation in 22Rv1 and LNCaP cells which both express functional p53. The doses were selected based on the EC_{50} values obtained from three-day cell viability MTS assays. In 22Rv1 cells, Ad5Hey1 and AdE1A12S resulted in dose-dependent increases in total p53 expression at 48 and 72h post-infection (Figure 22) while Ad5GFP resulted in only a small increase in p53 expression. An identical trend in p53 induction was obtained for a further two independent experiments at 48h post-infection and one further experiment at 72h post-infection (Appendix ; Figure_Apx 1 and Figure_Apx 2). The fold-change of p53 expression varied considerably between experiments, owing to different detection systems, different virus batches and western blotting being undertaken on different days. Consequently it was not possible to combine results. Activation of p53 was confirmed by detection of phosphorylated serine 15 (Ser15) (Figure 22). Etoposide, a topoisomerase inhibitor was used as a positive control as it is a well-known inducer of p53 expression via inhibition of HDM2 synthesis (Arriola, Lopez et al. 1999).

Although a direct comparison was not made, basal levels of total p53 were higher in LNCaP cells compared with 22Rv1 cells. In LNCaP cells, infection of Ad5Hey1 or AdE1A12S induced stabilised p53 expression (Figure 23) while p53 expression in Ad5GFP-infected cells was reduced below basal levels. A similar

trend at different virus doses was also observed (Appendix ; Figure_Apx 3). Phospho (ser15) p53 expression after Ad5Hey1 or AdE1A12S infection was not detected (data not shown).

Upregulation of p53 expression and activation of this pathway in these cells supported previous findings that Hey1 and Hey1-related, Hes1 inhibit HDM2 transcription thereby stabilising p53 (Huang, Raya et al. 2004). Several studies have confirmed the presence of HDM2 in both 22Rv1 and LNCaP cells and the small- molecule HDM2-inhibitor nutlin-3 has been shown to inhibit HDM2 activity and stabilise p53 indicating this pathway is functional in these cell lines (Logan, McNeill et al. 2007; Udayakumar, Hachem et al. 2008; Tovar, Higgins et al. 2011). Upregulation of p53 expression by AdE1A12S has been found to occur through multiple cellular targets that converge to activate p53 signalling. These include sequestration of pRb by E1A (E1ACR1 and/or E1ACR2-dependent) which releases E2F and in turn leads to the induction of $p14^{ARF}$, a mediator of HDM2 inhibition (de Stanchina, McCurrach et al. 1998; Deng, Kloosterbooer et al. 2002) as well as interacting with p300/CBP thereby facilitating disruption of HDM2-p53 complexes and contributing to p53 stabilisation (Grossman, Perez et al. 1998). Additionally, E1A may stabilise p53 through direct binding to the 26S proteasome (Turnell, Grand et al. 2000).

Taken together, these findings suggest that stabilisation of p53 could also contribute to Ad5Hey1-dependent cytotoxicity in addition to AR inhibition and may explain previous findings that p53-null and AR-negative PC3 cells were insensitive to Ad5Hey1 (Cheong S.C. *et al* manuscript in preparation).

A 22Rv1 48hpi

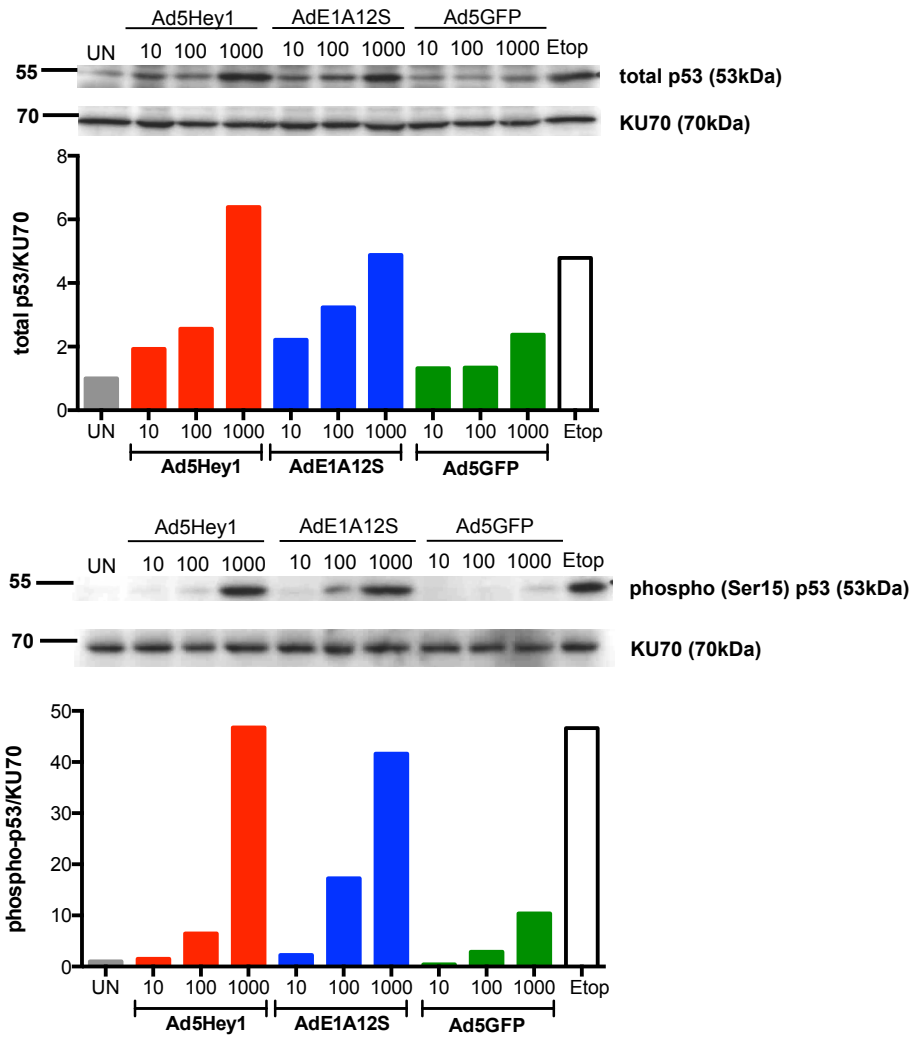

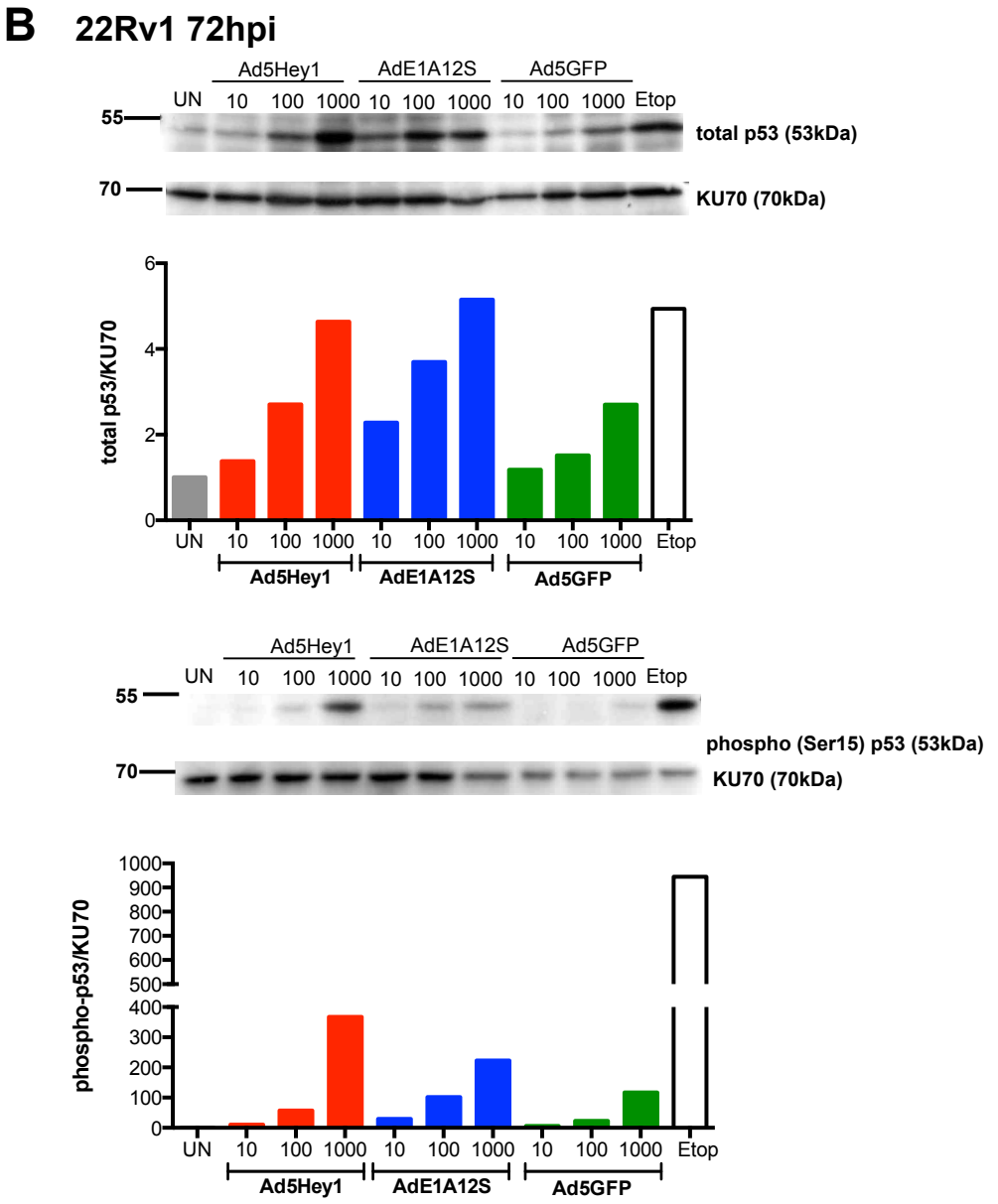

Figure 22. Ad5Hey1-infection causes stabilisation and activation of p53 in 22Rv1 cells

Cells were infected with Ad5Hey1#2, AdE1A12S#2 and Ad5GFP at 10, 100 and 1000ppc. After 2h, infection medium was removed and replaced with 10% FBS DMEM. Cells were treated overnight with 10μM etoposide to serve as a positive control. Cell lysates were harvested at 48hpi (A) and 72hpi (B) and prepared for separation on polyacrylamide gels. 20μg protein was loaded per lane and total p53 and phospho (ser15) p53 blotted for on separate gels. KU70 was used as a loading control. Histograms showing total p53 and phospho (ser15) p53 protein expression normalised to KU70 and expressed relative to uninfected (UN) cells. A) For total p53. results show one blot, representative of 3 independent experiments and for phospho (ser15) p53, one experiment. B) For total p53, results show one blot, representative of 2 independent experiments and for phospho (ser15) p53, one experiment.

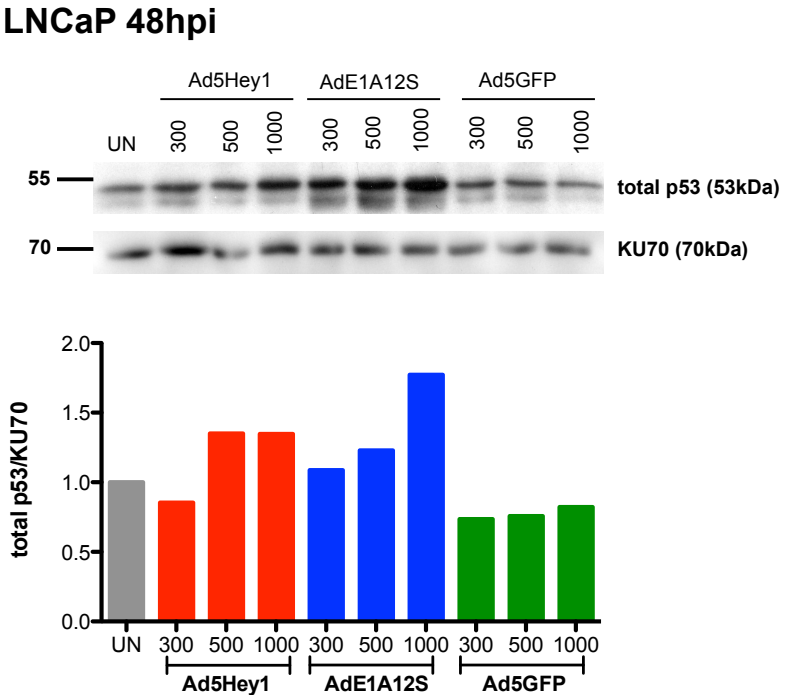

Figure 23. Ad5Hey1-infection stabilises p53 in LNCaP cells

Cells were infected with Ad5Hey1#3, AdEA12S#3 and Ad5GFP at 300, 500 and 1000ppc. After 2h, infection medium was removed and replaced with 10% FBS RPMI. Cell lysates were harvested at 48h post-infection and prepared for separation on polyacrylamide gels. 25µg protein was loaded per lane and total p53 blotted with KU70 as loading control. Histogram showing p53 protein expression normalised to KU70 and expressed relative to uninfected (UN) cells. Results show one blot from 2 independent experiments.

3.1.4.2. Ad5Hey1-induced cell killing is also mediated through p53-dependent pathway in 22Rv1 cells

The observation that Ad5Hey1 infection resulted in p53 activation in 22Rv1 cells led us to investigate whether p53 expression is a requirement for mediating Ad5Hey1-induced cytotoxicity. A SMARTpool On-Target siRNA specific to p53 was employed to deplete 22Rv1 cells and assess cell viability after Ad5Hey1 infection. To preserve viral stocks, fixed doses at EC_{50} for adenoviral mutants were used rather than constructing dose response curves. The use of fixed virus doses was also easier and faster to perform with the aim of obtaining more reproducible data in less time. Knock down of p53 was confirmed by western blotting (Figure 24) and was stable up to 120h post-transfection. Knockdown of p53 did not induce significant cell death compared with control siRNA presumably due to the activity of other cell survival mechanisms.

Ad5Hey1 infection of p53 knockdown cells resulted in a statistically significant decrease in cell death compared with cells transfected with control siRNA: 24.5% and 53.2% cell death respectively (Figure 25). Knockdown of p53 also resulted in a 20.7% reduction of AdE1A12S-induced cell death compared with AdE1A12S-mediated cell death in control siRNA-transfected cells (54.8% and 75.6% cell death respectively), although this was not statistically significant. Induction of cell death by Ad5noHey1 (deemed to be non-specific due to the high dose of virus used) was not affected by p53 status. These results indicate the activation of the p53-pathway in these cells is important for mediating Ad5Hey1-dependent cytotoxicity and concurs with similar studies where p53 was knocked down in U2OS-HEY1 cells preventing Hey1-induced cell growth arrest (Villaronga, Lavery et al. 2009).

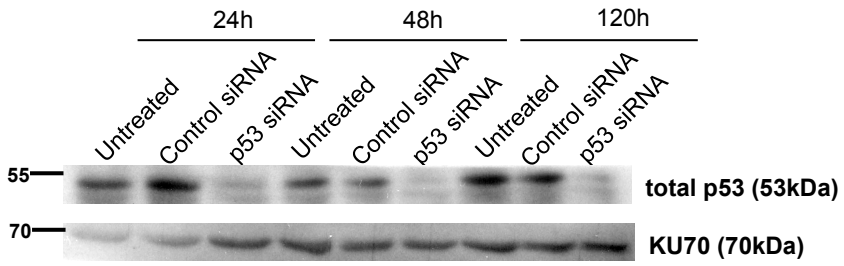

Figure 24. Knockdown of p53 by siRNA in 22Rv1 cells

Cells were seeded and the following day transfected with 100nM p53 siRNA or Control siRNA. Cell lysates were harvested 24h, 48h and 120h post-transfection and prepared for separation on

polyacrylamide gels. 20μg protein was loaded per lane and blotted for p53 and β-actin as a loading control.

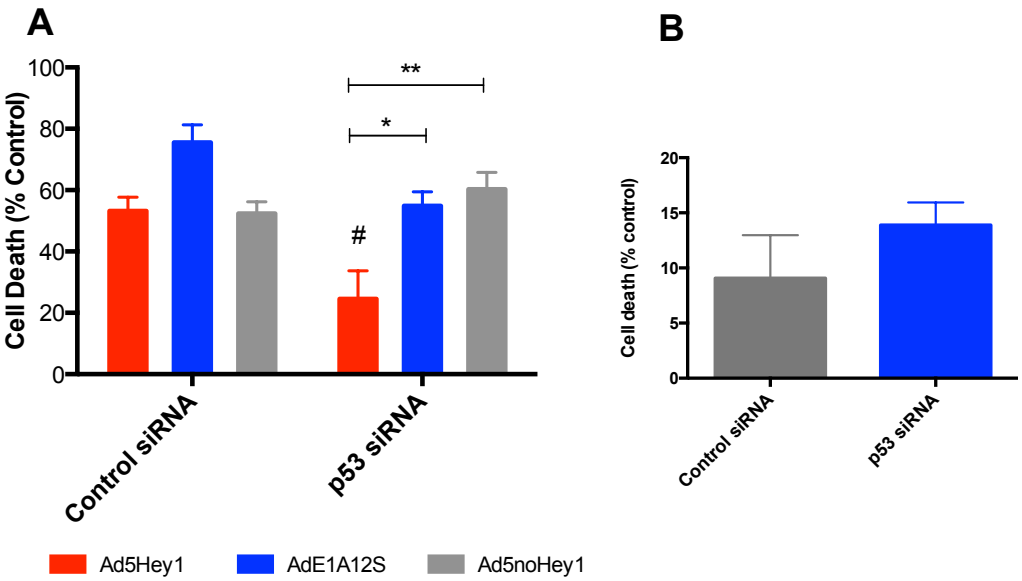

Figure 25. Sensitivity to Ad5Hey1 decreases when p53 is knocked down in 22Rv1 cells

A) Cells were transfected with either p53 siRNA or Control siRNA (100nM) and 48h after transfection cells infected with a fixed dose (EC_{50}) of Ad5Hey1#2 (800ppc), AdE1A12S#2 (150ppc) or Ad5noHey1 (2500ppc). Cell death was assayed 3 days post-infection/5 days post-transfection by MTS assay and expressed as a percentage relative to p53 siRNA or Control siRNA-treated cells. Results are shown are means of 6 replicate wells from 4 independent experiments ± SEM with two-way ANOVA statistical analysis using multiple comparisons with a Tukey post-test, $p<0.05$ (*) and $p<0.01$ (**) compared to p53 siRNA-treated cells infected with Ad5Hey1. $p<0.05$ (#) compared with control siRNA-treated cells infected with Ad5Hey1. B) Percentage of cell death (relative to untreated cells) after treatment with siRNA 120h post-infection. Results shown as the mean of 4 replicate wells from 4 independent experiments ± SEM.

3.1.4.3. Contribution of AR-and p53-signalling to Ad5Hey1-mediated cytotoxicity in 22Rv1 cells

In summary, AR knockdown resulted in a 2-fold increase in the EC_{50} of Ad5Hey1. On the other hand knockdown of p53 desensitised cells to a fixed dose of Ad5Hey1 resulting in >50% reduction in Ad5Hey1-dependent cell death than when p53 was expressed. Since these two studies were not equivalent, parallel with the p53 knockdown studies, AR was knocked down in 22Rv1 cells and infected with an identical fixed dose of Ad5Hey1, AdE1A12S and Ad5noHey1. To permit a comparison to be made, Ad5Hey1-mediated cell killing after AR or p53 knockdown was expressed relative to Ad5noHey1 (Table 18). In agreement with results shown in section 3.1.3, knockdown of AR resulted in a decrease in Ad5Hey1-mediated cell death relative to Ad5noHey1 (0.69±0.13) whereas the absence of AR did not affect AdE1A12S-dependent cell killing

(0.99±0.5). Unlike the previous study described section 3.1.3, the reduction of Ad5Hey1-mediated cytotoxicity after knockdown of the AR was not statistically significant compared with Ad5noHey1. Analysis of the data as shown in Table 18 showed knockdown of p53 resulted in a statistically significant decrease in both Ad5Hey1- and AdE1A12S-induced cell death (0.78±0.04 and 0.64±0.04 respectively).

Table 18. Relative % cell death with EC_{50} fixed dose of either Ad5Hey1 or AdE1A12S after AR or p53 knockdown

	AR siRNA			p53 siRNA		
	Mean	**SEM**	**p value**	**Mean**	**SEM**	**p value**
Ad5noHey1	1.00	0.00	-	1.00	0.00	-
Ad5Hey1	0.69	0.13	ns	0.78	0.04	p<0.01
AdE1A12S	0.99	0.50	ns	0.64	0.04	p<0.001

22Rv1 cells were infected with a fixed dose (EC_{50}) of Ad5Hey1#2 (800ppc), AdE1A12S#2 (150ppc) or Ad5noHey1 (2500ppc) 48h after transfection with either AR, p53 or control siRNA (100nM). Cell death was assayed 3 days post-infection/5 days post-transfection by MTS assay. Percentage cell death values resulting from Ad5Hey1 or AdE1A12S in AR or p53 siRNA transfected cells was normalised to percentage cell death of similarly virus-infected cells transfected with control siRNA. Normalised data was then expressed relative to Ad5noHey1 as a mean of 4 independent experiments ± SEM. Statistical significance was assessed with a one-way ANOVA comparing values with Ad5noHey1 for either AR or p53 knockdown.

In conclusion, the potency of Ad5Hey1-mediated cytotoxicity in 22Rv1 cells is significantly decreased when p53 is removed suggesting that in these cells, Ad5Hey1-dependent cytotoxicity functions by a p53-mediated mechanism in addition to inhibiting AR signalling. I have endeavoured to assess the relative significance of each pathway in Ad5Hey1-mediated cytotoxicity and have determined both AR and p53 play a role in facilitating cell killing by Ad5Hey1.

3.1.5. Ad5Hey1-infected 22Rv1 cells but not DU145 cells accumulate in G2/M phase

As discussed in section 3.1.1, Ad5Hey1 possesses intrinsic cytotoxicity in cells expressing AR and wild-type p53 (22Rv1 and LNCaP) as well as AR-negative DU145 cells which express a non-functional form of p53. This suggests Ad5Hey1 has a mechanism of action that does not always require the presence of either functional AR or p53. This is of significance since 50% of most human cancer possess mutations in p53 rendering cells either devoid of p53 expression or harbouring non-functioning p53 (Vogelstein, Lane et al. 2000). In PCa, p53 mutations occur more frequently in advanced PCa including CRPC (Shen and Abate-Shen 2010). Commonly cancer cells with mutated p53 are more resistant to cytotoxic agents (Velculescu and El-Deiry 1996).

Ad5Hey1-mediated upregulation/stabilisation and activation of p53 in 22Rv1 and LNCaP cells suggest cells are driven towards cell cycle arrest or cell death. Therefore, cell cycle changes in response to Ad5Hey1 infection were assessed in 22Rv1 and compared with DU145 cells to establish whether Ad5Hey1 had a role in abrogating the cell cycle in cells of contrasting genetic background.

Cell cycle progression was examined by flow cytometry using propidium iodide (PI) between 24 and 72h post-infection using increasing doses of virus (Figure 26). The range of doses selected for each cell line were based on the EC_{50} values obtained for Ad5Hey1 after 3 days of infection. Cells were infected with Ad5noHey1 at the same doses as Ad5Hey1 to control for the presence of the virus particles.

At 24h, infection with Ad5Hey1, AdE1A12S or Ad5noHey1 resulted in decreased proportions of 22Rv1 cells in G1 and an increase in the fraction of cells in S and G2/M phases suggesting that the presence of a virus particle alone has an effect on the cell cycle (Figure 26). At 48h more discernable changes in the cell cycle of Ad5Hey1- and AdE1A12S-infected cells were observed (Figure 27). Significant increases in the fraction of cells in G2/M were observed for Ad5Hey1-infected cells compared with uninfected cells (a two-fold difference in Ad5Hey1-infected cells, a smaller increase for AdE1A12S-infected cells) (Figure 27). The Ad5Hey1-induced G2/M population was also significantly higher than

for cells infected with Ad5noHey1 (Figure 27). Another distinct feature was the accumulation of AdE1A12S-infected cells with a >4N DNA content compared with cells infected with Ad5Hey1. At 72h, Ad5Hey1-infected cells resulted in an increase in the proportion of cells with >4N content and sub-G1 fraction (Figure 26) suggesting apoptosis was occurring.

I have shown that Ad5Hey1 causes p53-dependent stress, which may result in cells accumulating in G2/M. Since EC_{50} values indicate AdE1A12S is a more potent inducer of cell death compared with Ad5Hey1 (307.4±65.6 and 776.1±56.2 respectively) it is interesting to note that at 1000ppc of Ad5Hey1 a larger fraction of cells in G2/M accumulated at all time points and was more prominent at 48h, compared to an equal dose of AdE1A12S (Figure 26 and Figure 27). p53 expression is induced at 48h to a similar extent by both viruses at the higher dose (1000ppc) and knockdown of p53 by siRNA resulted in significant attenuation for Ad5Hey1- and AdE1A12S-mediated cytotoxicity (Table 18). In view of the fact AdE1A12S has been reported to induce cell death through p53-independent mechanisms in addition to p53-dependent processes we cannot exclude the possibility that AdE1A12S-dependent cell cycle changes are as a result of functional alterations to non-p53 targets by AdE1A12S leading to an increase of cell cycle progression to >4N and sub-G1 in these cells.

In contrast, Ad5Hey1 produced no discernable changes in the cell cycle of DU145 cells compared with Ad5noHey1 (Figure 26). As DU145 harbour mutations in pRb and p53, both the G1 and G2/M checkpoints are defective. At 48h (Figure 28), only AdE1A12S infection resulted in statistically significant dose-dependent decreases in cells in G1 and subsequent increases of cells entering S phase, indicative of cell cycle progression (Berk 2005). Changes resulting by Ad5Hey1 in terms of G1, S and G2/M-phase cell fractions also occurred after infection with Ad5noHey1. The dose equivalent to the EC_{50} of AdE1A12S, 2000ppc, resulted in a significant increase in the proportion of cells in G2/M and this was enhanced further at supra-optimal doses. However, doses approximately equivalent to the EC_{50} of Ad5Hey1 and AdE1A12S (8000 and 2000ppc respectively) induced a similar degree of changes in the population of cells with >4N resulting in a significant increase in cells with a >4N DNA content compared with uninfected and Ad5noHey1-infected cells. Higher doses of AdE1A12S further increased the proportion of cells with this phenotype.

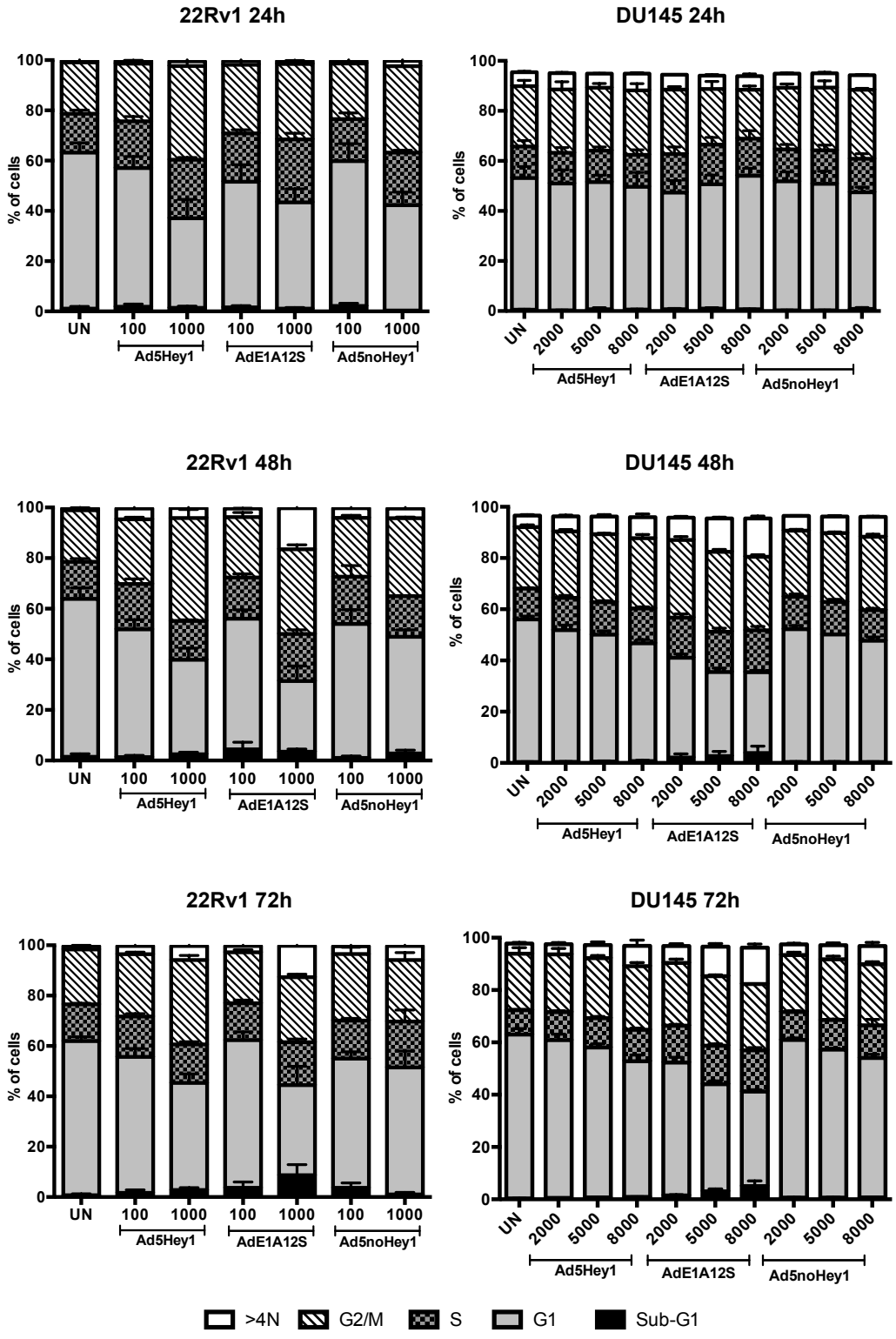

Figure 26. Time-dependent effects of Ad5Hey1 on cell cycle progression in 22Rv1 and DU145 cells

Cells were infected with escalating doses of Ad5Hey1#2, AdE1A12S#2 and Ad5noHey1. A) 22Rv1; 100 and 1000ppc B) DU145; 2000, 5000 and 8000ppc. After 2h infection, medium was removed and replaced with 10% FBS DMEM. Cell cycle analysis was performed at 24, 48 and 72h post-infection by flow cytometry. Results are shown as the mean of single replicates from 3 independent experiments ± SEM

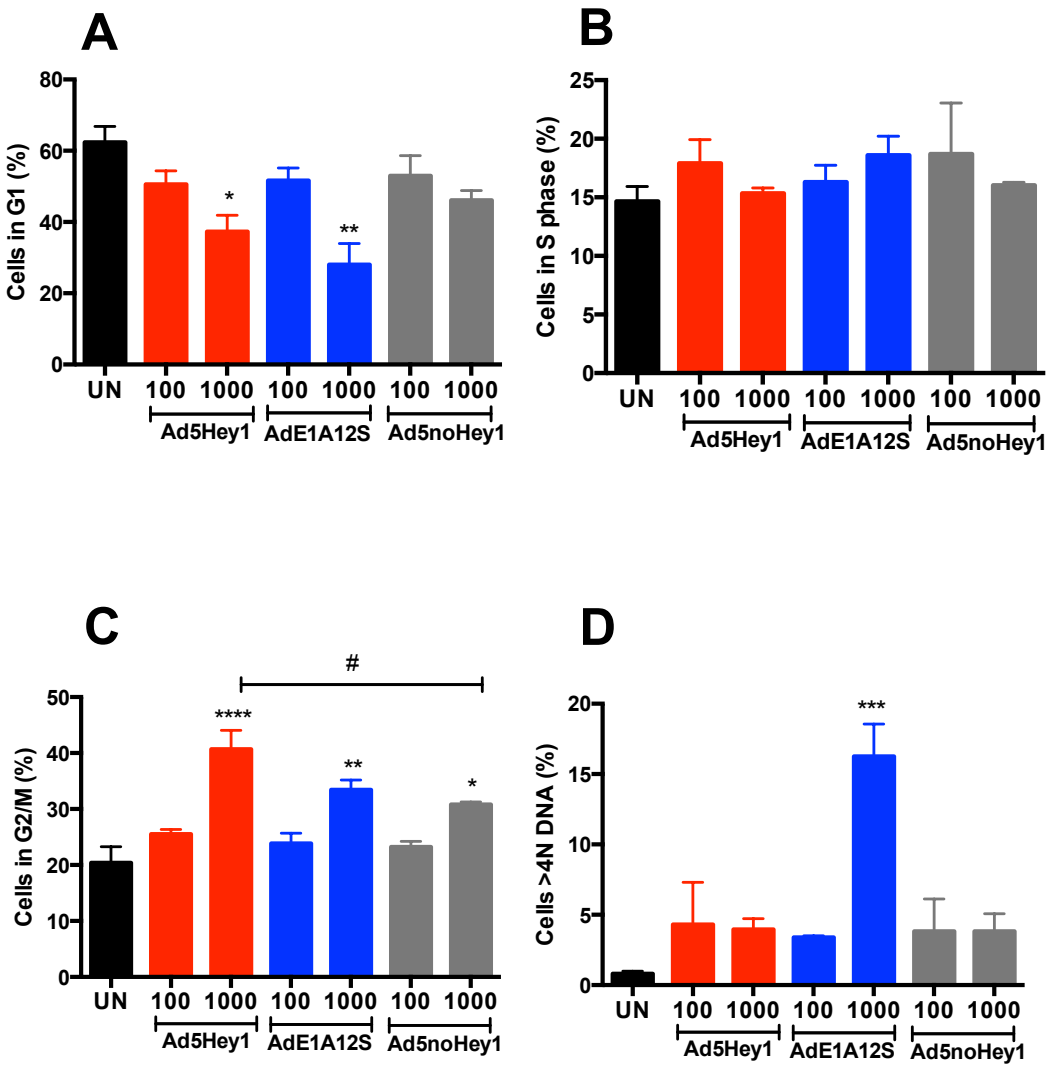

Figure 27. Dose-dependent effects of Ad5Hey1 on G1, S, G2/M and >4N cell populations at 48h after infection in 22Rv1 cells

22Rv1 cells were infected with Ad5Hey1#2, AdE1A12S#2 and Ad5noHey1 at 100 and 1000ppc. After 2h, infection medium was removed and replaced with 10% FBS DMEM. Cell cycle analysis was performed at 48h post-infection by flow cytometry. Results were extracted from Figure 26 and separated into phases of the cell cycle G1 (A), S (B), G2/M (C) and >4N DNA content (D). One-way ANOVA statistical analysis was performed using multiple comparisons with a Tukey post-test, $p<0.05$ (*), $p<0.01$ (**), $p<0.001$ (****) compared to uninfected cells (UN), $p<0.05$(#) compared with 1000ppc Ad5noHey1.

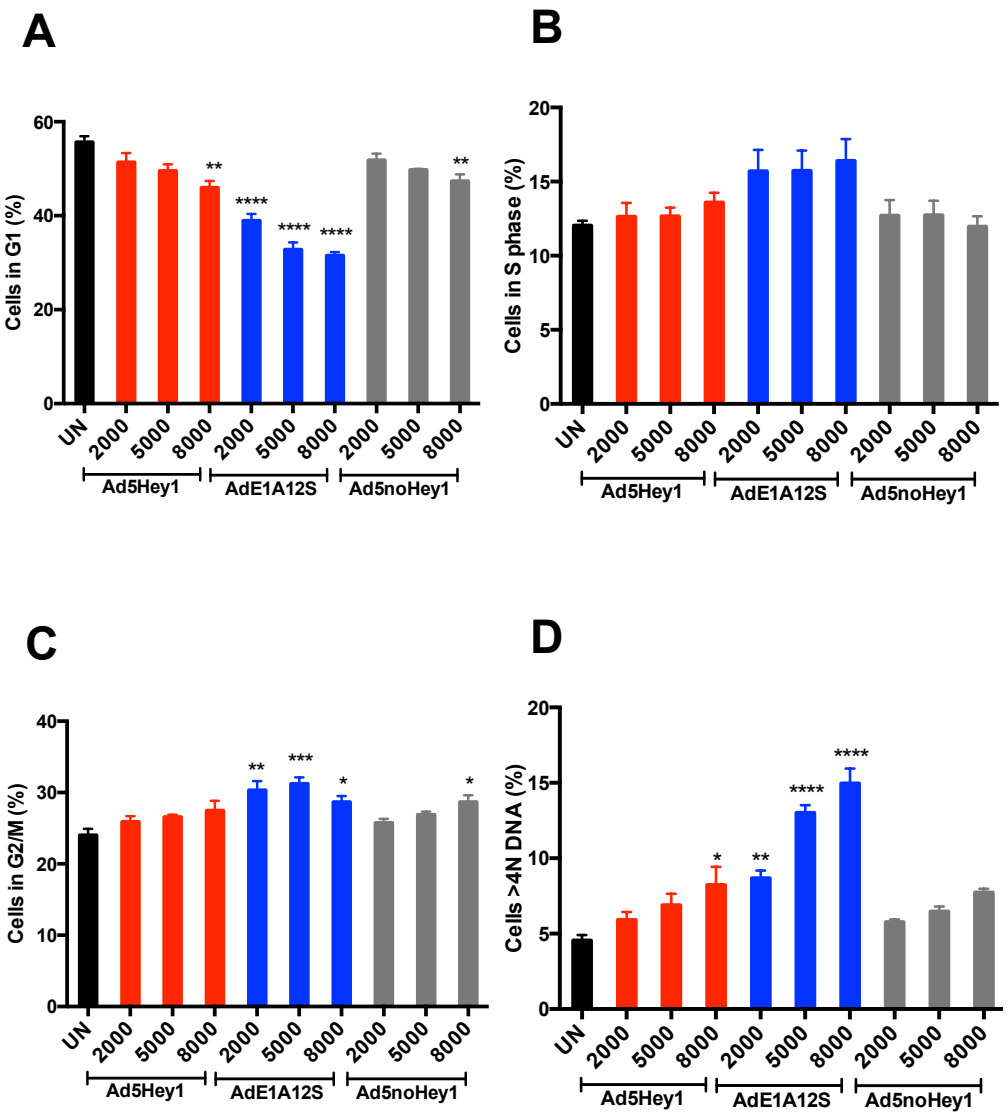

Figure 28. Dose-dependent effects of Ad5Hey1 on G1, S, G2/M and >4N cell populations at 48h after infection in DU145 cells

DU145 were cells infected with Ad5Hey1#2, AdE1A12S#2 and Ad5noHey1 at 2000, 5000 and 8000ppc. After 2h infection, medium was removed and replaced with 10% FBS DMEM. Cell cycle was performed at 48h post-infection by flow cytometry. Results were extracted from Figure 26 and separated into phases of the cell cycle G1 (A), S (B), G2/M (C) and >4N DNA content (D). One-way ANOVA statistical analysis was performed using multiple comparisons with a Tukey post-test, $p<0.05$ (*), $p<0.01$ (**), $p<0.001$ (***/****) compared to uninfected cells (UN).

3.1.6. Ad5Hey1 accumulates cells in G2 phase and delays mitotic entry

Numerous studies have implicated the importance of G2/M checkpoint abrogation or arrest in enhancing the effect of DNA damaging agents or that enhanced cytotoxicity is associated with cell cycle arrest (DiPaola 2002; Bucher and Britten 2008). I therefore sought to elucidate the mechanism by which Ad5Hey1 kills prostate cancer cells. Since Ad5Hey1 infection in DU145 cells did not exhibit any appreciable differences in cell cycle progression I did not examine the proteins involved in the cell cycle in this cell line.

As discussed in section 3.1.5, Ad5Hey1 demonstrated a dose-dependent increase in the proportion of cells in G2/M in 22Rv1 cells. To verify this observation cell cycle proteins involved in this phase of the cell cycle were assessed after Ad5Hey1 infection. Cyclin B1 levels are tightly regulated by transcription and degradation. Cyclin B1 accumulates during S and G2 phases due to transcriptional activation (Pines and Hunter 1991) and inactivation of the ubiquitin-mediated degradation pathway (Peters 2002). Levels decrease at the beginning of the metaphase-anaphase transition during mitosis and continue decreasing until G1 (Pines and Hunter 1991; Peters 2002).

Cyclin B1 expression was assessed at 48 and 72h post-infection by western blotting at 100 and 1000ppc of Ad5Hey1 or AdE1A12S in 22Rv1 cells (Figure 29). A dose dependent increase in cyclin B1 expression was observed in response to Ad5Hey1 infection at both time points confirming our cell cycle data. Upregulation of cyclin B1 expression in AdE1A12S –infected cells was more prominent at 48h and decreased slightly to that above basal levels by 72h suggesting these cells may have progressed through the G2/M checkpoint as suggested by the cell cycle analysis (Figure 26). Together with Ad5Hey1-dependent increases of total and activated p53, accumulation of cyclin B1 suggests Hey1 activates the p53 checkpoint in 22Rv1 cells resulting in cell cycle arrest. Therefore I endeavoured to establish whether Ad5Hey1 infection resulted in a G2 block thereby preventing cells from entering mitosis or if Ad5Hey1 could halt cells during mitosis resulting in a mitotic catastrophe-like cell death.

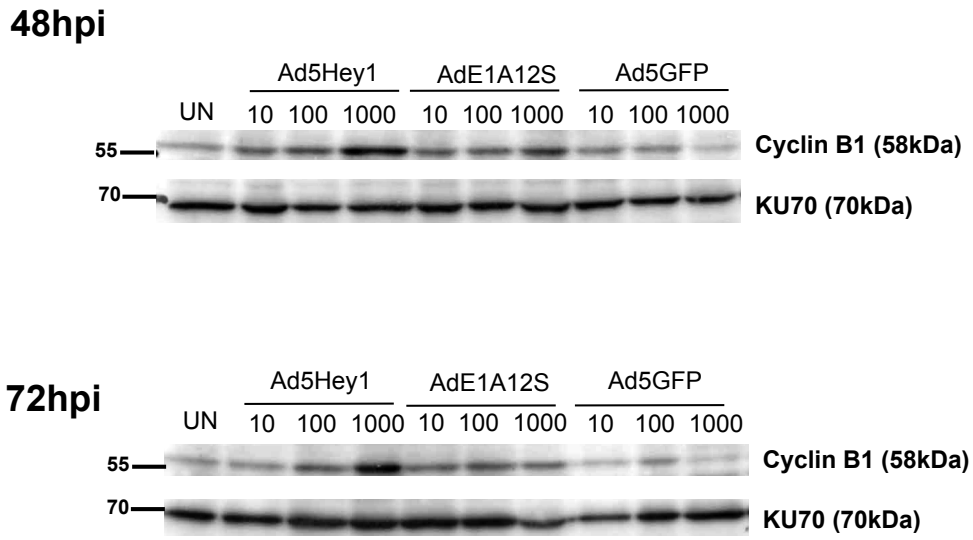

Figure 29. Dose-dependent induction of cyclin B1 protein expression at 48h and 72h in 22Rv1 cells

Cells were infected at 10, 100 and 1000ppc Ad5Hey1#2, AdE1A12S#2 and Ad5GFP. After 2h infection, medium was removed and replaced with 10% FBS DMEM. Cell lysates were harvested at 48 and 72h post-infection and prepared for separation on polyacrylamide gels. 20µg protein was loaded per lane and cyclin B1 was blotted for KU70 used as a loading control. Results show one blot, representative of 3 independent experiments.

Since cyclin expression detected by western blotting cannot be correlated to a specific cell cycle phase, intracellular cyclin B expression was assessed by flow cytometry to exclude the possibility of an “unscheduled” mode of expression. Cells were permeabilised, stained with an anti-cyclin B1 antibody and then stained with a FITC-labelled secondary antibody. Finally, cells were treated with PI so as to simultaneously monitor cell cycle changes. At 48h, Ad5Hey1 induced a dose- dependent increase in cyclin B1 expression at G2/M (Figure 30) with an accumulation of 52.1±2.5% at 1000ppc compared with 25.7±2.2% for uninfected control cells and 37.8±3.4% for Ad5noHey1-infected cells. AdE1A12S infection resulted in a smaller accumulation of cyclin B1 expression of 45.4±3.7% probably reflecting the lesser extent to which AdE1A12S mediated p53-dependent cell cycle changes.

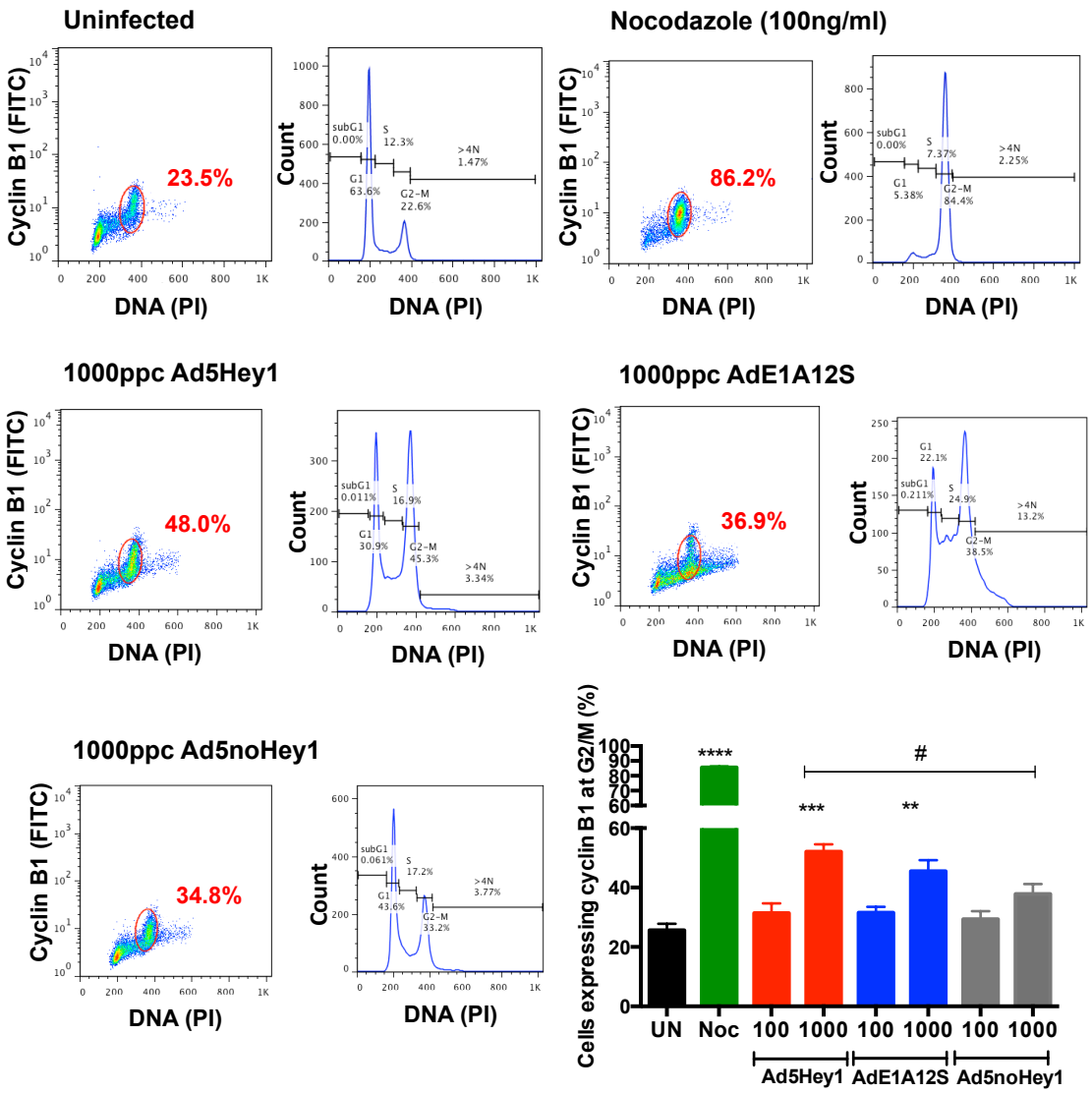

Figure 30. Ad5Hey1 results in a dose-dependent increase in cyclin B1 expression at G2/M in 22Rv1 cells

Cells were infected with 100 or 1000ppc Ad5Hey1#2, AdE1A12S#2 or Ad5noHey1. After 2h infection, medium were replaced with 10% FBS DMEM. Cells were treated overnight with nocodazole (100ng/ml) to arrest cells in mitosis. At 48h post-infection cells were harvested and analysed by flow cytometry. Cells were first stained with anti-cyclin B1 primary antibody and then FITC-conjugated anti-mouse secondary antibody. Prior to analysis, cells were treated with PI and RNase for simultaneous detection of the cell cycle in addition to cyclin B1 expression. Cyclin B1 was plotted relative to DNA content (PI). Cyclin B1-positive cells were gated at G2/M (red oval) and the percentage of cyclin B1 calculated (shown in red adjacent to the gate). Alongside each sample are histograms for their respective cell cycle profiles. Bivariate dot blot diagrams and cell cycle profiles are representative of 3 independent experiments. Histogram shows mean of single replicates from 3 independent experiments ± SEM. One-way ANOVA statistical analysis was performed using multiple comparisons with a Tukey post-test, $p<0.05$ (*), $p < 0.001$ (***/****) compared to uninfected cells. $p<0.05$(#) compared with 1000ppc Ad5noHey1.

Western blotting confirmed cyclin B1 expression was maintained at the later time point of 72h (Figure 29) suggesting a mitotic arrest had occurred; cyclin B1 degradation would be expected if cells had overcome this arrest. For this reason expression of the mitotic marker, phospho-serine 10-histone H3 (pH3) was

assessed since phosphorylation of histone 3 accompanies chromosome condensation and the onset of mitosis (Hans and Dimitrov 2001). Expression of pH3 after infection with 100-1000ppc of virus was assessed at 48h concurrent with detection of the phases of the cell (Figure 31). Nocodazole-treated cells stained with pH3 functioned as a positive control for mitotic cells. Determining the proportion of cells expressing pH3 and calculating this as a total number of cells in G2/M generated a mitotic index. Uninfected control cells had a mitotic index of 15.1±1.9% and nocodazole-treated cells an index of 65.9±6.7%. Infection of 22Rv1 cells with 1000ppc Ad5Hey1 or AdE1A12S increased the mitotic index to 28.9±0.8% and 23.1±3.1% respectively. A mitotic index of 15.6±2.5% for Ad5noHey1-infected cells was similar to control cells. The population of cells with a high fluorescence of pH3 staining located at the top of the gate in uninfected and virus-infected cells are most likely to be cells undergoing mitosis. The trail of pH3-positive cells observed in Ad5Hey1- and AdE1A12S-infected cells that enter into the bottom half of the gate are perhaps cells about to enter mitosis and since phosphorylation of histone 3 is first detected at late G2 in pericentrometric heterochromatin (Hans and Dimitrov 2001), this population of cells may be indicative of cells undergoing a delay in G2. This is in contrast to the location of exclusively mitotic pH3-positive cells in nocodazole-treated cells, which are all found within the gate.

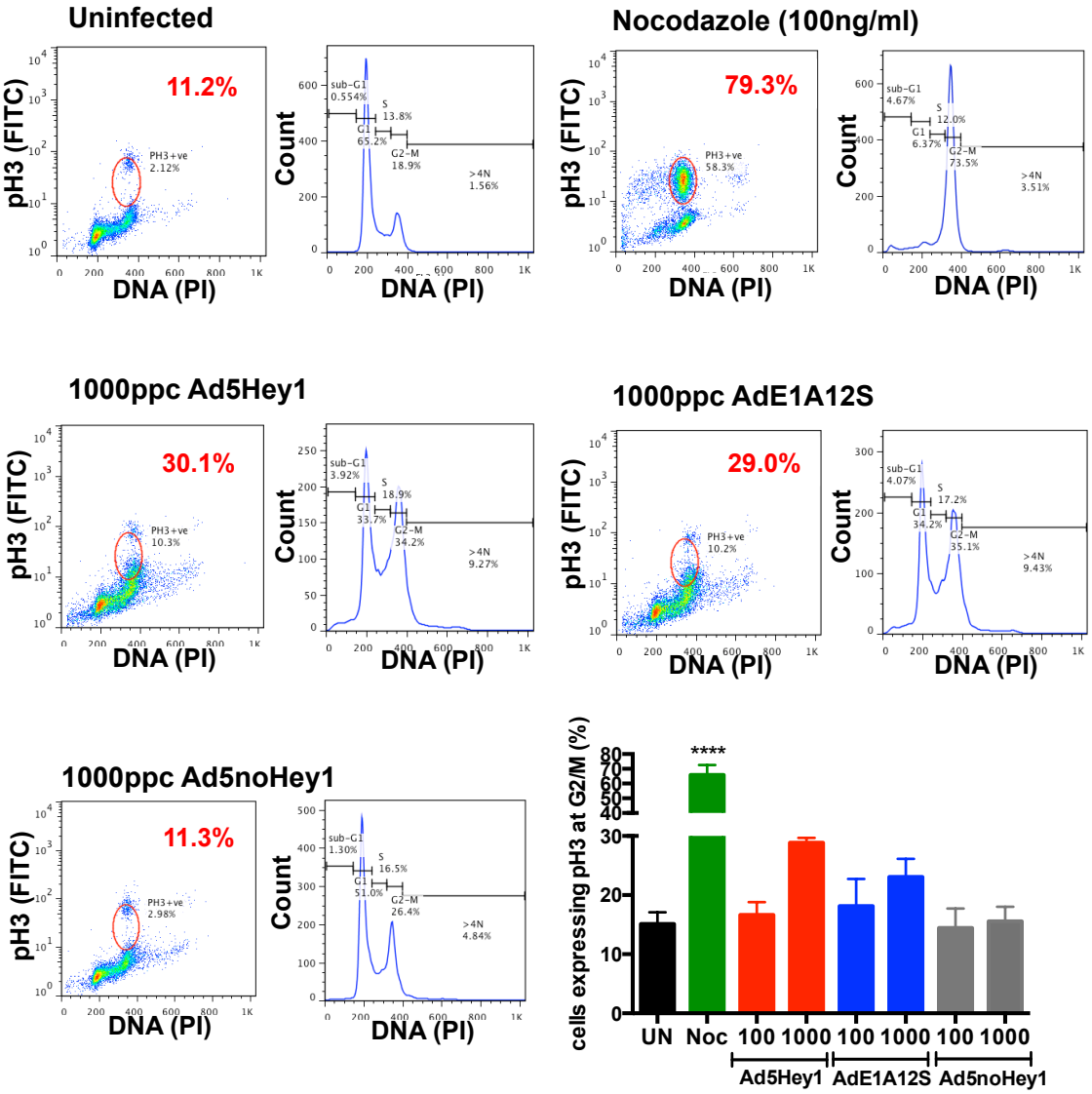

Figure 31. Dose dependent increase in phospho-histone H3 levels in Ad5Hey1-infected 22Rv1 cells at 48h

Cells were infected with 1000ppc Ad5Hey1#2, AdE1A12S#2 or Ad5noHey1 for 2h after which infection medium was removed and replaced with 10% FBS DMEM. Cells were treated overnight with nocodazole (100ng/ml) to arrest cells in mitosis. Cells were harvested at 48h post-infection and analysed for the mitotic marker, pH3 by staining cells with anti-pH3 primary antibody and then a FITC-conjugated anti-mouse secondary antibody. Cells were treated with PI and RNase and analysed by flow cytometry and pH3 plotted relative to DNA content (PI). A mitotic index (values in red) was calculated by gating the pH3-positive cells (red oval) as a percentage of the cells in G2/M phase. Alongside each sample are histograms for their respective cell cycle profiles. Bivariate dot blot diagrams and cell cycle profiles are representative of 3 independent experiments. Histogram shows mean of single replicates from 3 independent experiments ± SEM. One-way ANOVA statistical analysis was performed using multiple comparisons with a Tukey post-test, p <0.001 (****) compared with uninfected cells.

3.1.7. Ad5Hey1 does not replicate in 22Rv1 cells

It has been previously reported that high loads of E1A-deleted adenoviral mutants can replicate in certain cell lines through complementation of transcription factors (Shenk 2001). To verify that the Ad5Hey1-mediated cytotoxicity and cell cycle changes were caused solely by Hey1 expression I investigated whether Ad5Hey1 could replicate in 22Rv1 cells. To this end 22Rv1 cells were infected with 100 or 1000ppc Ad5Hey1 or AdE1A12S or 10ppc Ad5. After 24-72h of infection, medium and cells were collected and replication determined by the limiting dilution $TCID_{50}$ assay measuring intracellular and released viral particles. Replication was not detected after 48 or 72h post-infection for either Ad5Hey1 or AdE1A12S (Figure 32). AdE1A12S had previously been confirmed replication-defective in 22Rv1 and DU145 cells in our laboratory (Miranda, Maya Pineda et al. 2012).

Further verification was undertaken using quantitative PCR (QPCR) to assess amplification of the viral genome by detection of the E2A product (Figure 33), an early gene encoding a DNA-binding protein that activates early and late viral promoters and also essential for viral DNA replication (Shenk 2001). DNA isolation from 22Rv1 cells infected with 1000ppc Ad5Hey1 or AdE1A12S yielded minimal DNA amplification for Ad5Hey1 and a small degree of amplification for AdE1A12S. This may be explained by the presence of E2 in the pAdEASY-1 backbone from which the non-replicating viruses were constructed. It is known that E1A is able to activate the E2A promoter through its TATA binding motif (Shenk 2001). Additionally, cellular transcription factor E2F can also bind the E2 promoter via two inverted E2F-binding sites upstream of the TATA binding (Kovesdi, Reichel et al. 1986; Yee, Reichel et al. 1987). Binding of E2F and E1A to the E2 promoter is likely to have resulted in a cooperative effect on its transactivation leading to enhanced E2A gene amplification but not viral replication or propagation of the AdE1A12S mutant. PCR characterisation of the Ad5Hey1 genome confirmed the absence of E1 in Ad5Hey1 viral stocks (section 2.3.5; Figure 15) and transactivation of E2A does not occur, reflected in absence of viral DNA amplification and viral replication.

It can therefore be concluded that Hey1 and E1A12S expression cause the observed delay in the G2/M phase in 22Rv1 cells. Furthermore, the increase in G2/M is greater with Ad5Hey1 (48-72h post-infection). AdE1A12S-mediated abrogation of cell cycle checkpoints with formation of a >4N population may therefore account for this difference.

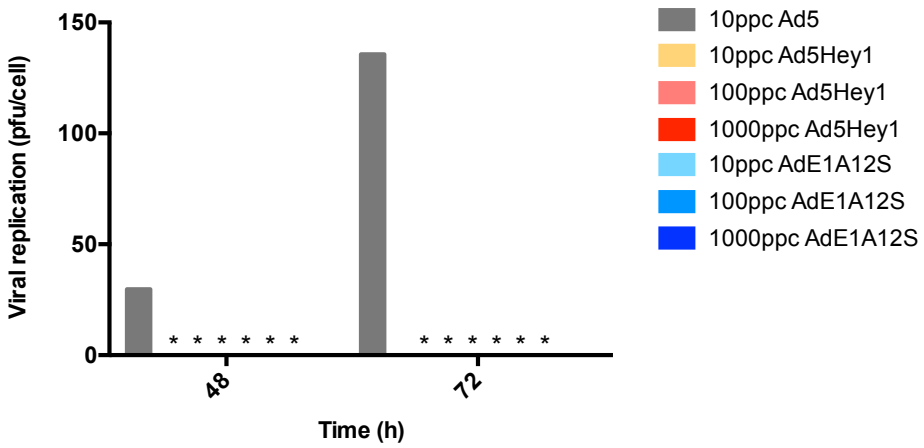

Figure 32. Ad5Hey1 and AdE1A12S do not replicate in 22RV1 cells

Cells were infected with 10ppc Ad5 and 10, 100 and 1000ppc Ad5Hey1#1 or AdE1A12S#1. Two hours after infection, medium was removed and replaced with 10% FBS DMEM. Cells and medium were harvested at 48 and 72h post-infection and lysates frozen at -80°C. Before viral titres were determined by $TCID_{50}$ assay, cell lysates were freeze-thawed twice to lyse cells and release viral particles. Cell lysates were spun down and the supernatant diluted 1:10000 and 1:1000 for Ad5 and adenoviral mutants respectively and used to serially infect JH293 cells seeded in 96-well plates. Results show mean of duplicate 96-well plates per condition for one experiment. * indicates replication was below the detection limit for this assay of <1pfu/cell.

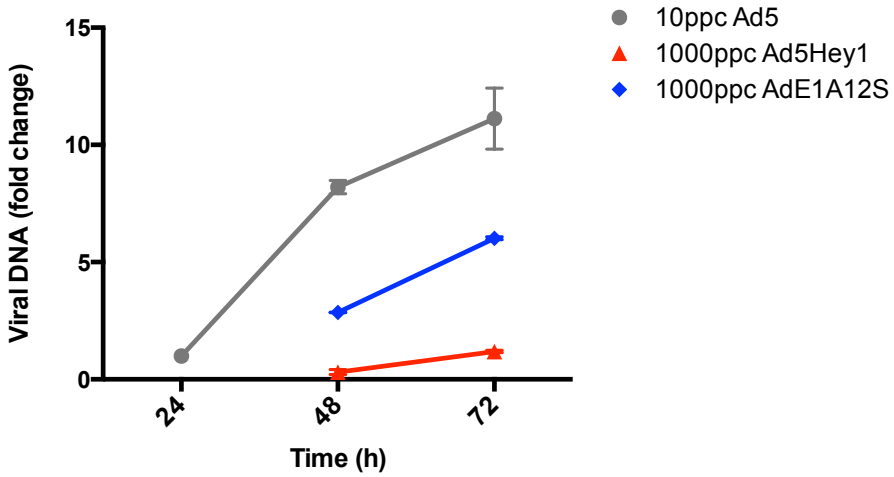

Figure 33. Viral genome amplification does not occur during Ad5Hey1 infection in 22Rv1 cells

Cells were infected at 10ppc of Ad5 or 1000ppc of Ad5Hey1#1 or AdE1A12S#1. Two hours after infection, medium was removed and replaced with 10% FBS DMEM. Cells were harvested at the indicated time points. DNA was extracted, quantified and analysed by quantitative PCR for viral genome amplification (E2A) relative to cellular GAPDH. Results are expressed as a fold change relative to Ad5 at 10ppc at 24h post-infection. Results are mean ± SEM of duplicates for one experiment.

3.2. Ad5Hey1 enhances cell killing in prostate and colorectal cancer cells in combination with chemotherapeutic agents

3.2.1. At fixed concentrations Ad5Hey1 and cytotoxic drugs produce synergistic cell death in 22Rv1 and DU145 cells

Previous experiments in 22RV1, DU145 and LNCaP cells demonstrated Ad5Hey1 sensitised these cells to mitoxantrone- and docetaxel-mediated cell death suggesting Ad5Hey1 and chemotherapeutic drugs, indicated for the treatment of PCa, could work in a synergistic manner (Figure 14 in section 1.8.1 and S.C. Cheong *et al*, manuscript in preparation).

To enable investigation of the cellular mechanisms involved in the sensitisation, I opted to use fixed doses of virus and drug combinations rather than complete synergy assays employing isobole analysis from which combination index values can be calculated. The latter approach is performed by combining 5-fold serially diluted drug and viruses at a range of fixed ratios and cell viability determined usually at 6 day post-infection (previously ascertained in our group to produce optimum synergy). This method, although quantitative and stringent, does not allow tangible treatment doses to be determined that allow for mechanistic studies. Therefore combination treatments that produced synergy at fixed concentrations at 72h as assessed by the MTS assay were selected as the experimental setup.

Fixed-dose combination studies to evaluate Ad5Hey1 in combination with mitoxantrone and docetaxel were carried out in 22Rv1, LNCaP and DU145 cells. Sub-optimum doses of drugs which induced <20% cell death were selected and combined with fixed doses of Ad5Hey1 or AdE1A12S that killed <30% of cells (Figure 34). Virus doses were selected based on EC_{50} values calculated from dose response curves of Ad5Hey1 and AdE1A12S (Table 17).

Sub-optimal doses of mitoxantrone and docetaxel were derived from EC_{50} values generated from dose response curves after 3 days of treatment (Table 19). All cell lines were more sensitive to docetaxel compared with mitoxantrone. The cells most sensitive to mitoxantrone were DU145 and LNCaP (no difference between these) and the least sensitive, 22Rv1. LNCaP cells were the most sensitive to docetaxel and DU145 and 22Rv1 cells the least sensitive. The fixed doses of mitoxantrone used for 22Rv1 and DU145 cells (25nM and 50nM respectively) did not reflect the EC_{50} order of sensitivity but where chosen based also on observations from my assessment of drug-induced mitochondrial membrane potential ($\Delta\psi_m$) (discussed in section 3.3.1). Preliminary experiments indicated $\Delta\psi_m$ in 22Rv1 cells was extremely sensitive to mitoxantrone at 50nM and I therefore decided to lower the dose to 25nM. Infected 22Rv1 and DU145 cells expressed high levels of Hey1 or E1A12S (Figure 35). To control for the effect of foreign transgene expression, Ad5GFP was used at the same doses as Ad5Hey1.

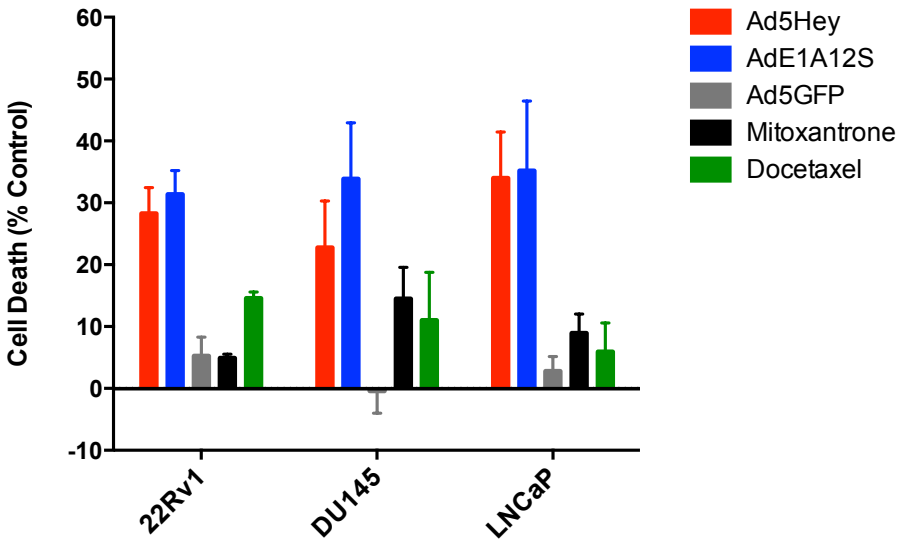

Figure 34. The effects of cell viability at fixed doses of adenoviral mutants and drugs used for combination studies

22Rv1, DU145 and LNCaP cells were infected with Ad5Hey1#2 (22Rv1) or Ad5Hey1#3 (DU145 and LNCaP), AdE1A12S#3 and Ad5GFP using doses in Table 11. Cell viability was assessed at 3 days post-infection by MTS assay. Results are the mean of 6 replicate wells from 3-4 independent experiments ± SEM.

Table 19. EC_{50} values for mitoxantrone and docetaxel in PCa cell lines

Drug	22Rv1			DU145			LNCaP		
	Mean	SEM	N	Mean	SEM	N	Mean	SEM	N
Mitoxantrone	293.0	± 17.3	3	184.0	± 21.7	2	197.2	± 36.9	3
Docetaxel	42.3	± 8.0	3	55.1	± 10.6	2	17.1	± 0.34	3

Dose response curves were constructed by treating cells in triplicate with five-fold serially diluted mitoxantrone or docetaxel and cell death assessed by MTS 3 days post-infection. Results are mean of 2-3 independent experiments ± SEM.

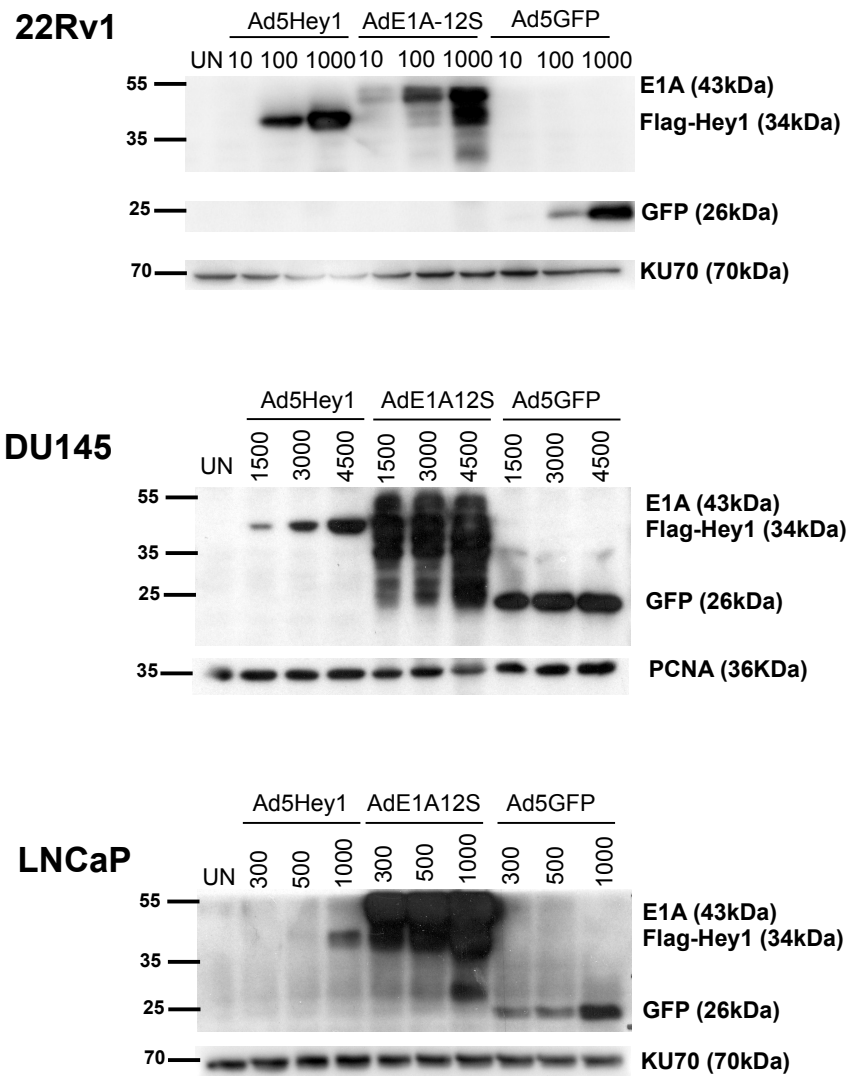

Figure 35. Western blots showing Hey1, E1A12S and GFP expression in 22Rv1, DU145 and LNCaP cells at 48h

Cells were infected with Ad5Hey1#2, AdE1A12S#3 and Ad5GFP at 10, 100 and 1000ppc (22Rv1) and Ad5Hey1#3, AdE1A-2S#3 and Ad5GFP (DU145; 1500, 3000 and 4500ppc and LNCaP, 300, 500 and 1000ppc). After 2h infection, medium was removed and replaced with 10% FBS DMEM. Cells lysates were harvested at 48h post-infection and prepared for separation on polyacrylamide gels. 20µg protein (22Rv1 and DU145) or 25µg (LNCaP) was loaded per lane and blotted for Flag, E1A, GFP expression and KU70 or PCNA as a loading control.

In 22Rv1 and DU145 cells, supra-additive (synergistic) effects were observed when Ad5Hey1 was combined with either mitoxantrone or docetaxel at the selected doses (section 2.4.3.1; Table 11) improving cell-killing efficacy (Figure 36). Synergistic cell death was also observed for AdE1A12S with both drugs as previously observed (Miranda, Maya Pineda et al. 2012). No supra-additive effect was detected with Ad5GFP demonstrating Hey1 or E1A12S expression is required for chemosensitisation. Due to the variable nature of the cell viability assay, the percentage of cell death induced by Ad5Hey1 and AdE1A12S varied between experiments, however the extent of cell death induced by combination treatments was consistently greater than the theoretical additive effect over >3 independent experiments in 22Rv1 cells and for two independent experiments in DU145 cells.

Although previous work suggested that Ad5Hey1 could sensitise LNCaP cells to mitoxantrone and docetaxel-induced cell killing (Figure 14), no synergistic cell death with the selected doses was observed (Figure 36). When Ad5Hey1 was combined with mitoxantrone or docetaxel slightly more or less cell death for each drug respectively was induced compared with virus alone. However in the presence of AdE1A12S, less cell death was induced with either drug-combination compared with virus alone. These observations suggest the selected doses of mitoxantrone or docetaxel with Ad5Hey1 have negligible effects on cell death enhancement when combined or an antagonistic effect when AdE1A12S is present. This irregularity was puzzling considering previous sensitisation experiments suggested greater cell death would occur when Ad5Hey1 or AdE1A12S was combined with cytotoxic drugs (Figure 14 and Cheong *et al*, manuscript in preparation). Studies have demonstrated significant inconsistencies when using MTS- or MTT-based assays when determining anti-proliferative activity of agents compared with ATP and DNA-based methods in LNCaP cells. MTS and MTT-assays are a measure of mitochondrial activity and some chemicals and plant-based agents have been found to alter mitochondria dehydrogenase activity (Lee, Zhan et al. 2003; Wang, Henning et al. 2010). For this reason I measured cell viability in LNCaP cells after combination treatment using either picogreen, a DNA-based method or sulforhodamine B, a measure of cellular protein mass. However under the selected conditions in LNCaP cells using the alternative viability assays, similar trends in cell killing as described above were observed (data not shown). In conclusion, the chosen fixed doses in LNCaP cells did not cause synergistic cell death while the drug EC_{50} values

were clearly lower in the presence of either Ad5Hey1 or AdE1A12S (Figure 14). Extensive further testing at various dose-combinations would be necessary to establish synergy at one fixed dose combination.

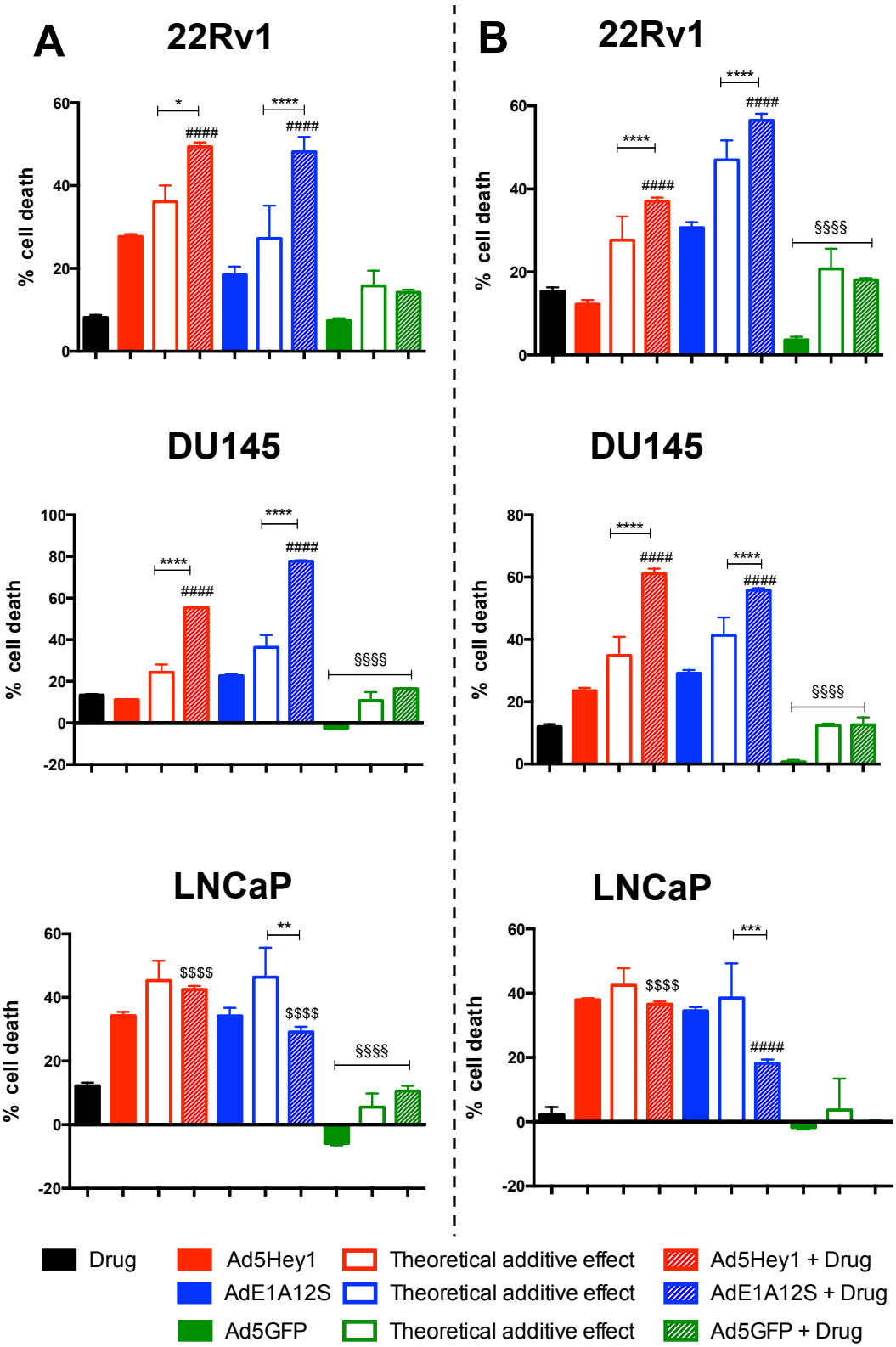

Figure 36. The effect on cell viability by mitoxantrone (A) or docetaxel (B), viral mutants or a combination of both in 22Rv1, DU145 and LNCaP cells

Cells were infected with Ad5Hey1#2 (22Rv1) or Ad5Hey1#3 (DU145 and LNCaP), AdE1A12S#3 or Ad5GFP and/or treated with drug and at the doses shown in Table 11. Black bars indicate the percentage of cell death caused by the drug alone. Red, blue and green bars indicate the percentage of cell death by Ad5Hey1, AdE1A12S or Ad5GFP respectively as single agents. White and hatched bars in respective colours for each virus represent the theoretical additive cell death and the observed cell death when virus and drug were combined respectively. Virus and drug

were added simultaneously and cell viability assayed 3 days post-infection and the percentage of death calculated relative to untreated cells. Results shown are means of 6 replicate wells ± SEM from one experiment with one-way ANOVA statistical analysis using multiple comparisons with a Tukey post-test, $p<0.05$ (*), $p<0.01$ (**) and $p<0.001$ (***/****) compared with theoretical additive effect. $p<0.001$(####) combination treatments compared with its respective virus and drug. $p<0.001$(§§§§) compared with Ad5GFP alone. $p<0.001$($$$$) compared with drug alone. Results are representative of >3 independent experiments (22Rv1), 2 experiments (DU145) and >3 experiments (LNCaP).

3.2.2. Investigating the intrinsic cytotoxicity and sensitising role of Ad5Hey1 in colorectal p53 isogenic HCT116 cell lines

3.2.2.1. Ad5Hey1 possess intrinsic cytotoxicity in p53-deficient HCT116 cells as well as HCT116wt cells

In chapter 3.1 I concluded Ad5Hey1-dependent cytotoxicity was mediated in part, through the AR-inhibition (22Rv1 cells) and activation of p53 signalling in wild-type p53 expressing cells (22Rv1 and LNCaP). However, Ad5Hey1 was also able to kill DU145 cells known to harbour mutant non-functional p53 (Isaacs, Carter et al. 1991). Since the PCa cell lines in this study vary widely in terms of their genetic alterations we sought to establish the absolute requirement of the HDM2-p53 feedback loop in Ad5Hey1-dependent sensitisation and toxicity. To this end I employed the isogenic colorectal cancer cell lines, HCT116wt ($p53^{+/+}$) and the knockout, $HCT116p53^{-/-}$. These cells are devoid of AR expression (Figure 37) allowing us to assess the p53-dependence of Ad5Hey1-mediated cytotoxicity without AR-mediated effects on cell growth.

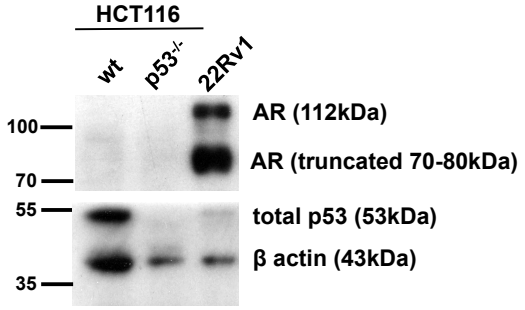

Figure 37. The p53 and AR status of HCT116wt and $HCT116p53^{-/-}$ cells

HCT116wt, $HCT116p53^{-/-}$ and 22Rv1 cells were seeded and left untreated. Cell lysates were harvested 48h later and prepared for separation on polyacrylamide gels. 20µg protein was loaded per lane and blotted for AR, total p53 and β-actin as a loading control. n=1

Dose-response curves of Ad5Hey1, AdE1A12S and Ad5 were generated and cell death was assessed three days post-infection to determine EC_{50} values. Ad5 virus was used as an internal control since it kills cells independently of p53 status (Shiina, Lacher et al. 2009) resulting in similar EC_{50} values for both cell

lines (Figure 38). Ad5Hey1 and AdE1A12S EC_{50} values were normalized against EC_{50} values obtained for the reference virus, Ad5 and expressed as ratios (Figure 39A). Transgene expression for Ad5Hey1 and AdE1A12S was similar in both cell lines (Figure 39C). Stabilisation of p53 by Ad5Hey1 was induced at the lowest dose of 1500ppc and near maximum expression of p53 was attained at this dose. In agreement with the comparative levels of p53 stabilisation between Ad5Hey1 and AdE1A12S in 22Rv1 cells, infection by AdE1A12S was not as potent as Ad5Hey1 in stimulating p53 expression since a dose of 4500ppc was required for AdE1A12S-induced p53 stabilisation (Figure 39C).

Interestingly, in contrast to the reduction in cell death by Ad5Hey1 when p53 was knocked down in 22Rv1 cells, Ad5Hey1 was as potent in HCT116$p53^{-/-}$ cells as in HCT116wt cells agreeing with our earlier results of a Ad5Hey1-mediated p53-independent mechanism of cell death observed in DU145 cells. Potency of AdE1A12S increased in cells devoid of p53 (Figure 39B) suggesting optimal potency of AdE1A12S is via a p53-independent mechanism in HCT116 cells in contrast to desensitisation to AdE1A12S-mediated cytotoxicity in 22Rv1 cells when p53 was absent. These results therefore suggest that Ad5Hey1 can regulate factor(s) other than p53 and AR not present in DU145 cells.

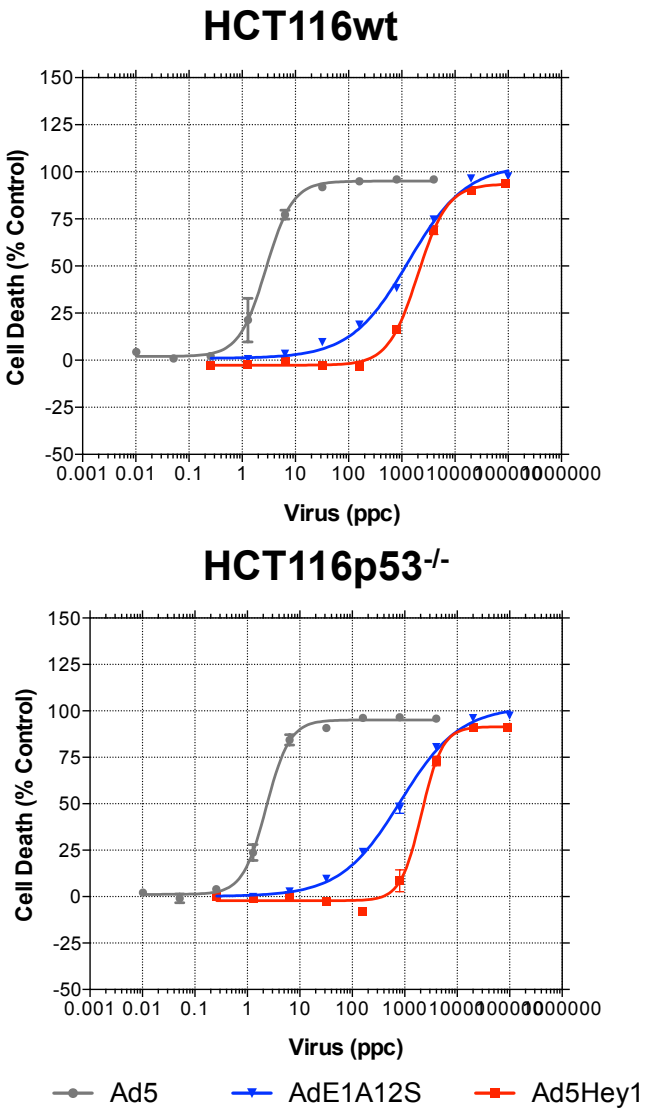

	HCT116wt	HCT116p53$^{-/-}$
Ad5	2.8	2.3
Ad5Hey1	2006	2091
AdE1A12S	1331	826

Figure 38. Ad5Hey1 is cytotoxic in HCT116wt and HCT116p53$^{-/-}$ cells

Representative virus dose-response assays in HCT116wt and HCT116p53$^{-/-}$ cells of triplicate samples ± SEM. Cells were infected with serial dilutions of Ad5 (grey), Ad5Hey1#3 (red) and AdE1A12S#3 (blue). Cell death was determined by MTS 3 days post-infection and EC_{50} values (ppc) were calculated (table inset). Graph and table shows mean of triplicates from one experiment, representative of six.

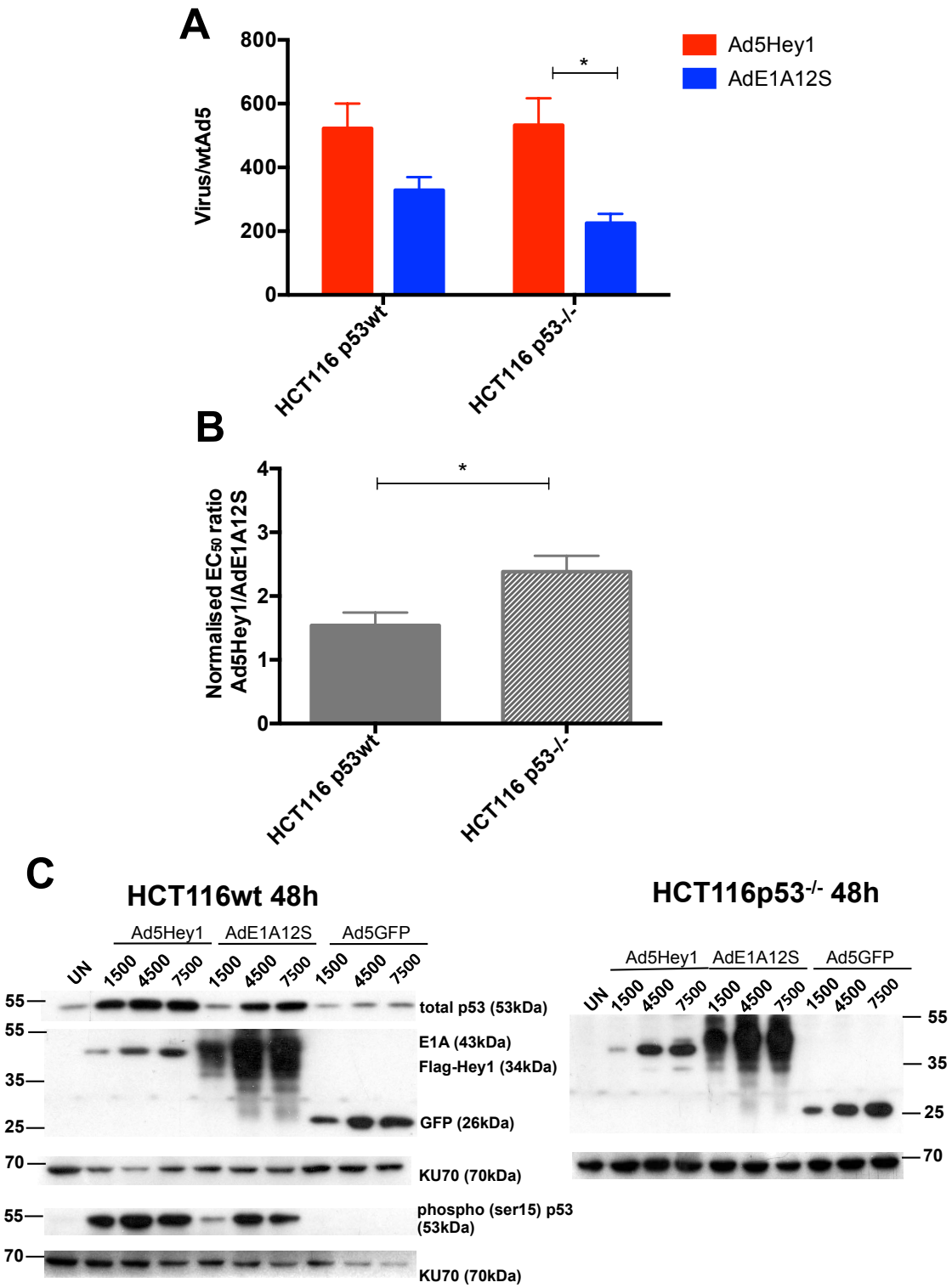

Figure 39. Ad5Hey1 is as potent as AdE1A12S in HCT116wt cells. Absence of p53 sensitises cells to AdE1A12S while potency of Ad5Hey1 is similar to HCT116wt cells

Histogram showing EC_{50} values of Ad5Hey1#3 and AdE1A12S#3 expressed as a ratio of Ad5 in HCT116wt and HCT116p53$^{-/-}$ cells. Results are the mean of six independent experiments ± SEM. Statistical analysis was carried out with two-way ANOVA using multiple comparisons with a Tukey post-test $p<0.05$ (*). (B) Ad5Hey1 and AdE1A12S EC_{50} values were normalised to the EC_{50} value of Ad5 and the normalised EC_{50} values of Ad5Hey1/AdE1A12S expressed as a ratio for each cell line. Results shown are mean of six independent experiments ± SEM with statistical analysis using two-tailed, unpaired Student t-test, $p<0.05$ (*). (C) Western blots showing Flag, E1A12S and GFP expression in HCT116wt and HCT116p53$^{-/-}$ cells at 48h post-infection. Cells were infected with virus at 1500, 4500 and 7500ppc for 2h. After infection, medium was removed and replaced

with 10% FBS DMEM. Cell lysates were collected at 48h post-infection and prepared for separation on polyacrylamide gels. 20µg protein was loaded per lane and blotted for Flag, E1A and GFP expression and in the case of HCT116wt cells, total p53 and phospho (ser15) p53 blotted on separate gels. KU70 expression was used as a loading control. UN = uninfected.

3.2.2.2. Ad5Hey1 sensitises HCT116 cells to 5-FU and mitoxantrone by p53-dependent and –independent mechanisms

We and others have shown that overexpression of Hey1 in wild-type p53-expressing tumour cells has a sensitising effect to a range of chemotherapeutic agents, namely mitoxantrone and docetaxel (Cheong *et al*, manuscript in preparation and section 3.2.1) as well as platinum-based cisplatin and anthracycline derivative doxorubicin (Villaronga, Lavery et al. 2009). Furthermore, I provide evidence that Ad5Hey1 sensitises mutant p53 DU145 cells to mitoxantrone and docetaxel leading to synergistic cell death (section 3.2.1). To investigate the requirement of p53 in Ad5Hey1-mediated sensitisation to cytotoxic drugs, HCT116wt and HCT116p53$^{-/-}$ cells were infected with Ad5Hey1 to generate dose-response curves and treated with sub-optimal fixed concentrations of 5-FU or mitoxantrone that induced <30% cell death alone. Cell viability was assessed after 3 days post-treatment and EC_{50} values for the viruses were calculated with and without the drugs and expressed as a percentage of the EC_{50} of virus alone (Figure 40).

At the selected doses, 5-FU and mitoxantrone produced similar toxicity in both cell lines. HCT116p53$^{-/-}$ cells were slightly more resistant to drug treatment although not statistically significant at these concentrations (Figure 40A). Loss of p53 conferred resistance to mitoxantrone and 5-FU as indicated by increased EC_{50} values for drugs in HCT116p53$^{-/-}$ compared with HCT116wt cells (data not shown) confirming previous reports (Bunz, Hwang et al. 1999). Sensitisation by mitoxantrone and 5-FU to Ad5Hey1-mediated cell killing in HCT116wt cells was extensive reducing the EC_{50} value of Ad5Hey1 by 59 and 49% respectively (Figure 40B). Sensitisation of HCT116wt cells by mitoxantrone to AdE1A12S-induced cell death was comparable to combination treatment with Ad5Hey1. Interestingly, sensitisation by 5-FU resulted in a smaller decrease in the EC_{50} value (24%) compared with Ad5Hey1 (49%).

As anticipated and in agreement with our findings in DU145 cells, sensitisation by mitoxantrone and 5-FU to Ad5Hey1 was also observed in HCT116p53$^{-/-}$ cells resulting in 25 and 39% reductions in the EC_{50} value of Ad5Hey1 respectively (Figure 40C). The extent of sensitisation was less than with HCT116wt cells indicative of enhanced sensitivity to the Ad5Hey1 when p53 is expressed. 5-FU sensitised both HCT116wt and HCT116 p53$^{-/-}$ similarly to Ad5Hey1 whereas sensitisation by mitoxantrone was significantly less in HCT116 p53$^{-/-}$ compared with HCT116wt cells (Table 20). Notably, the absence of p53 did not impact on the extent of sensitisation when AdE1A12S was combined with mitoxantrone (a 68 and 67% reduction in the EC_{50} value of AdE1A12S in HCT116wt and HCT116p53$^{-/-}$ respectively) but 5-FU had a significantly greater sensitising effect on HCT116p53$^{-/-}$ cells when combined with AdE1A12S (Table 20). This suggests optimum AdE1A12S-mediated cell killing in a p53-deficient background is dependent on the type of chemotherapeutic used and its mechanisms of action whereas Ad5Hey1-mediated cell killing was optimal when p53 was expressed. In the case of Ad5Hey1, 5-FU was also better in HCT116p53$^{-/-}$ cells at sensitising cells to Ad5Hey1 compared with mitoxantrone.

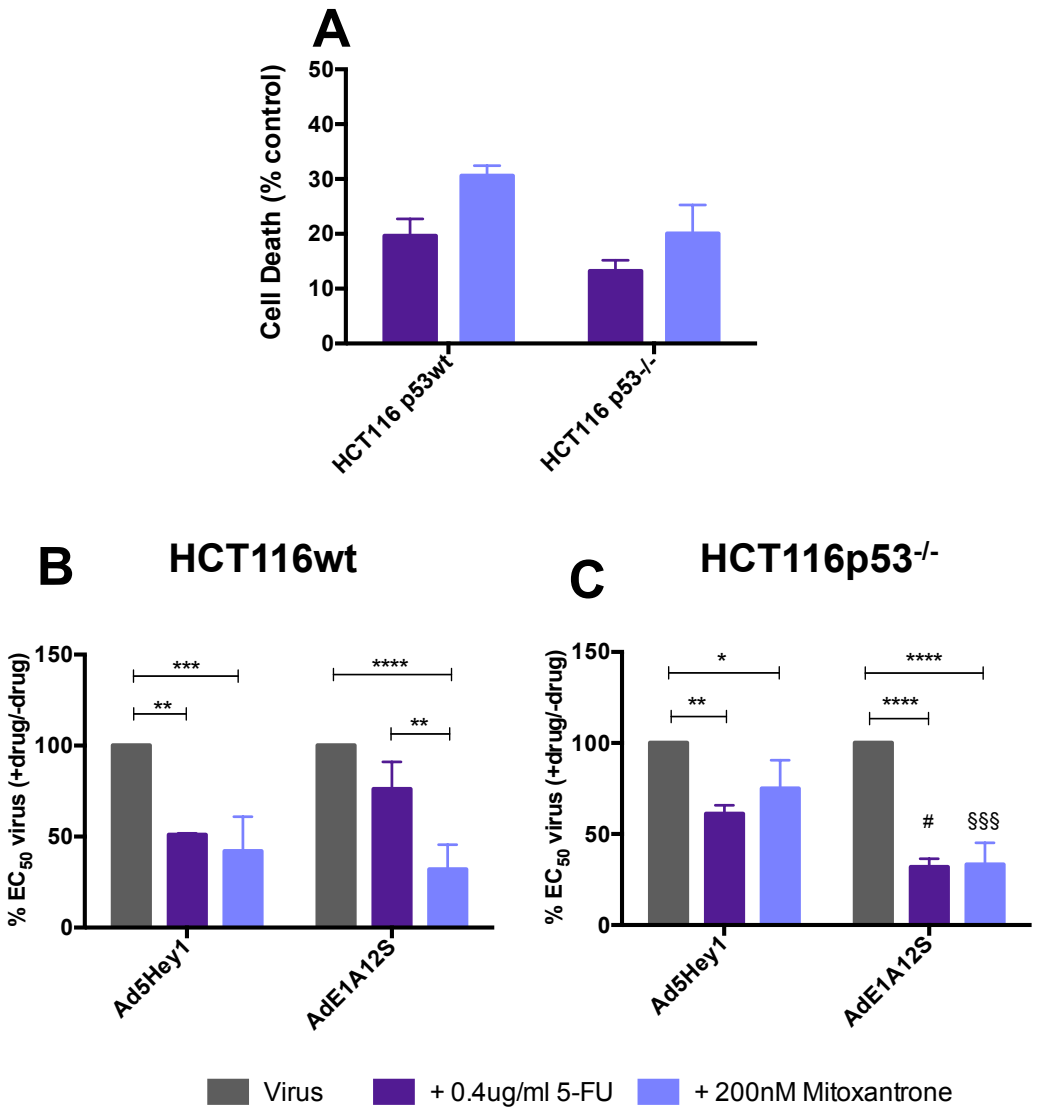

Figure 40. Ad5Hey1 sensitises HCT116wt and HCT116p53$^{-/-}$ cells to 5-FU and mitoxantrone

(A) Histogram showing percentage of cell death at fixed concentrations of 5-FU or mitoxantrone 72h after treatment relative to untreated cells. Results show mean for 3 independent experiments ± SEM. (B) & (C) Dose response curves to Ad5Hey1#3 or AdE1A12S#3 with and without 5-FU or mitoxantrone were generated and cell death determined 3 days post-infection by MTS viability assay. Virus EC_{50} values were calculated for virus alone relative to uninfected cells or in combination with each agent relative to the percentage of cell death induced by the drug alone. Histograms show relative EC_{50} values as a percentage of virus alone in (B) HCT116wt cells and (C) HCT116p53$^{-/-}$ cells. Results are a mean of duplicate wells from 3 independent experiments ± SD. All histograms were analysed by two-way ANOVA statistical analysis using multiple comparisons with a Tukey post-test, $p<0.05$ (*), $p<0.01$ (**) $p<0.001$ (***/****). $p<0.05$ (#) was compared with Ad5Hey1 + 0.4ug/ml 5-FU. $p<0.001$ (§§§) was compared with Ad5Hey1 + 200nM mitoxantrone.

Table 20. Comparing %EC_{50} values of Ad5Hey1 or AdE1A12S treated with fixed doses of 5-FU or mitoxantrone between HCT116p53wt and HCT116p53$^{-/-}$ cells

Treatment	Ad5Hey1			AdE1A12S		
	p53$^{+/+}$ mean±SD	p53$^{-/-}$ mean±SD	p value	p53$^{+/+}$ mean±SD	p53$^{-/-}$ mean±SD	p value
Virus only	100±0.00	100±0.00	ns	100±0.0	100±0.0	ns
+ 0.4µg/ml 5-FU	51.0±0.75	61.2±4.56	ns	76.2±14.8	32.1±13.5	p<0.01
+ 200nM Mitox	42.05±18.8	75.1±14.4	p<0.01	32.0±4.43	33.3±11.8	ns

Results extracted from Figure 40A and C and analysed using a two-way ANOVA statistical analysis comparing %EC_{50} values obtained in HCT116p53wt cells with those in HCT116p53$^{-/-}$ cells using a bonferroni post-test, p<0.01 (**), p<0.001 (***). Results shown are mean of 3 independent experiments ± SD.

To summarise, cytotoxic drugs sensitised both HCT116wt and HCT116p53$^{-/-}$ cells to Ad5Hey1-mediated cell killing and the extent of sensitisation was similar to that of AdE1A12S in HCT116wt cells. In the absence of p53, significantly more cell killing by AdE1A12S occurred in combination with drugs than with Ad5Hey1+drug combinations suggesting optimum AdE1A12S-mediated cell killing occurs in a p53-deficient background. Interestingly sensitisation to Ad5Hey1 or AdEA12S was independent of p53 status when cells were treated with 5-FU and mitoxantrone respectively highlighting the importance of the specific interactions between toxic transgene- and drug-activated cell signalling pathways.

Thus far I have determined that Ad5Hey1-dependent cell death in AR-positive and p53 wild-type, 22Rv1 cells requires the presence of both AR and p53 for effective cytotoxicity. However, in AR-negative p53 isogenic HCT116 cells, Ad5Hey1 kills these cells to a similarly extent irrespective of p53 status. Ad5Hey1 effectively stimulated the stabilisation of p53 in HCT116wt cells in agreement with Huang *et al* however since Ad5Hey1 was cytotoxic in HCT116p53$^{-/-}$ cells this suggests activation of p53 signalling is not the sole mechanism by which Ad5Hey1 kills. Therefore Ad5Hey1 must function through other pathways in AR-negative and p53-deficient DU145 and HCT116p53-/- cells to induce cell death and sensitisation to chemotherapeutic drugs.

3.2.3. Ad5Hey1-mediated targeting of constitutively active STAT3 in DU145 cells

3.2.3.1. Ad5Hey1 decreases levels of phospho-STAT3 and levels of STAT3-target, cyclin D1

In light of the results obtained in the p53 isogenic HCT116 cell lines I sought to investigate the mechanism of Ad5Hey1 action in DU145 cells. As discussed in the Introduction (section 1.5.1), Notch signalling is a central regulator of gene expression. Crosstalk between Notch signalling and other pathways such as the BMP/TGF-β, JAK/STAT, Ras and hypoxia induced factor (HIF) signalling have been found to enhance activation and expression of hairy and Enhancer of split bHLH protein subfamilies, Hes and Hey (Fischer and Gessler 2007). These and other reports suggest that exogenous expression of Hey1 could transduce and participate in signalling from numerous pathways. Hairy-related proteins interact with a wide range of other binding partners including bHLH proteins, histone deacetylases and also form complexes with transcription factors thus turning these into transcriptional co-repressors (Fischer and Gessler 2007).

A common feature of prostate cancer is the dependence on STAT3 for survival. Activation of the transcription factor has been demonstrated to be involved in malignant progression of prostate cancer cells (Ni, Lou et al. 2000; Barton, Murphy et al. 2001). Hes1 and Hes5 were found to mediate Notch-induced activation of STAT3 signalling by forming a complex with JAK2 and STAT3. Maximum binding to STAT3 and activation was mapped to the bHLH and Orange domain (Figure 5) resulting in STAT3 phosphorylation and activation (Kamakura, Oishi et al. 2004). Overexpression of Hey1 and Hey2 in COS-1 cells in the same study induced phosphorylation of STAT3 and activated STAT3-dependent transcriptional activity (Kamakura, Oishi et al. 2004).

Since the related Hes1 protein was found to regulate STAT3 activity and is structurally conserved with Hey1, I hypothesised whether Ad5Hey1 may regulate constitutively active STAT3 signalling in DU145 cells (Ni, Lou et al. 2000; Barton, Murphy et al. 2001). I also postulated whether the reason for the lack of Ad5Hey1-mediated cytotoxicity and sensitisation in PC3 cells was due to the absence of STAT3 expression in these cells (Clark, Edwards et al. 2003;

Yuan, Guan et al. 2005). Western blotting for phosphorylation of STAT3 on conserved tyrosine residue 705 (a measure of STAT3 dimerization; an indirect measure of STAT3 activity) and total STAT3 confirmed the absence of STAT3 expression in PC3 cells used in our laboratory, in agreement with the literature reports (Figure 41).

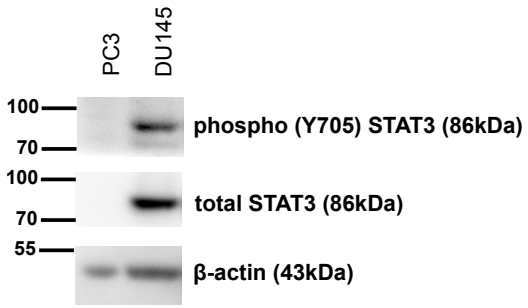

Figure 41. Differential expression of STAT3 between PC3 and DU145 cells

PC3 and DU145 cells were seeded and left untreated. Cell lysates were harvested 48h later and prepared for separation on polyacrylamide gels. 20μg protein was loaded per lane and blotted for phospho (Y705) STAT3 and β-actin as a loading control. The membrane was later stripped and probed for total STAT3 expression. n=1

I analysed phospho-STAT3 in response to increasing doses of Ad5Hey1 in DU145 cells at 48h post-infection. Treatment with resveratrol, an established inhibitor of STAT3 signalling in DU145 cells through inhibition of Src tyrosine kinase activity was used as a control (Kotha, Sekharam et al. 2006). I found Ad5Hey1 decreased phospho-STAT3 in a dose-dependent fashion (Figure 42A) compared with Ad5GFP where no change in phospho-STAT3 levels was observed. Western blotting membranes in Figure 42A were stripped to remove phospho-STAT3 antibody and reprobed with an antibody recognising total STAT3. No changes in total STAT3 levels were observed for cells infected with Ad5Hey1- and Ad5GFP. A decrease in the STAT3-target gene, cyclin D1 (Figure 42B) indicated that Ad5Hey1 also reduced expression of a downstream STAT3 target gene. Total STAT3 levels shown in Figure 42B were reduced for both Ad5Hey1 and Ad5GFP-infected cells compared with uninfected cells. This is puzzling as this trend was not observed in Figure 42A and the untreated control sample may have been incorrect or mislabelled. Additional experiments are required to establish the effect of Ad5Hey1 on STAT3 target gene expression. In summary, my data suggests Ad5Hey1 might regulate STAT3 activity by either direct binding to STAT3 thus preventing phosphorylation of

STAT3 and downstream activation of STAT3 target genes or indirectly inhibiting STAT3 signalling.

Cells treated with escalating doses of AdE1A12S similarly exhibited a dose-dependent decline in phospho-STAT3 expression as well as a decrease in total STAT3 levels and cyclin D1 expression (Figure 42). This reduction agrees with current knowledge of E1A-mediated inhibition of STAT protein activity. E1A circumvents the host defence mechanisms by blocking the JAK/STAT pathway by either indirectly interfering with the transcriptional activity of STAT proteins (Takeda, Nakajima et al. 1994; Paulson, Pisharody et al. 1999) or by direct binding to STAT proteins disrupting their interaction with other cofactors (Look, Roswit et al. 1998; Chatterjee-Kishore, van Den Akker et al. 2000). AdE1A12S-mediated inhibition of STAT3 signalling could be one mechanism by which AdE1A12S induced cell killing and sensitisation to cytotoxic drugs in DU145 cells.

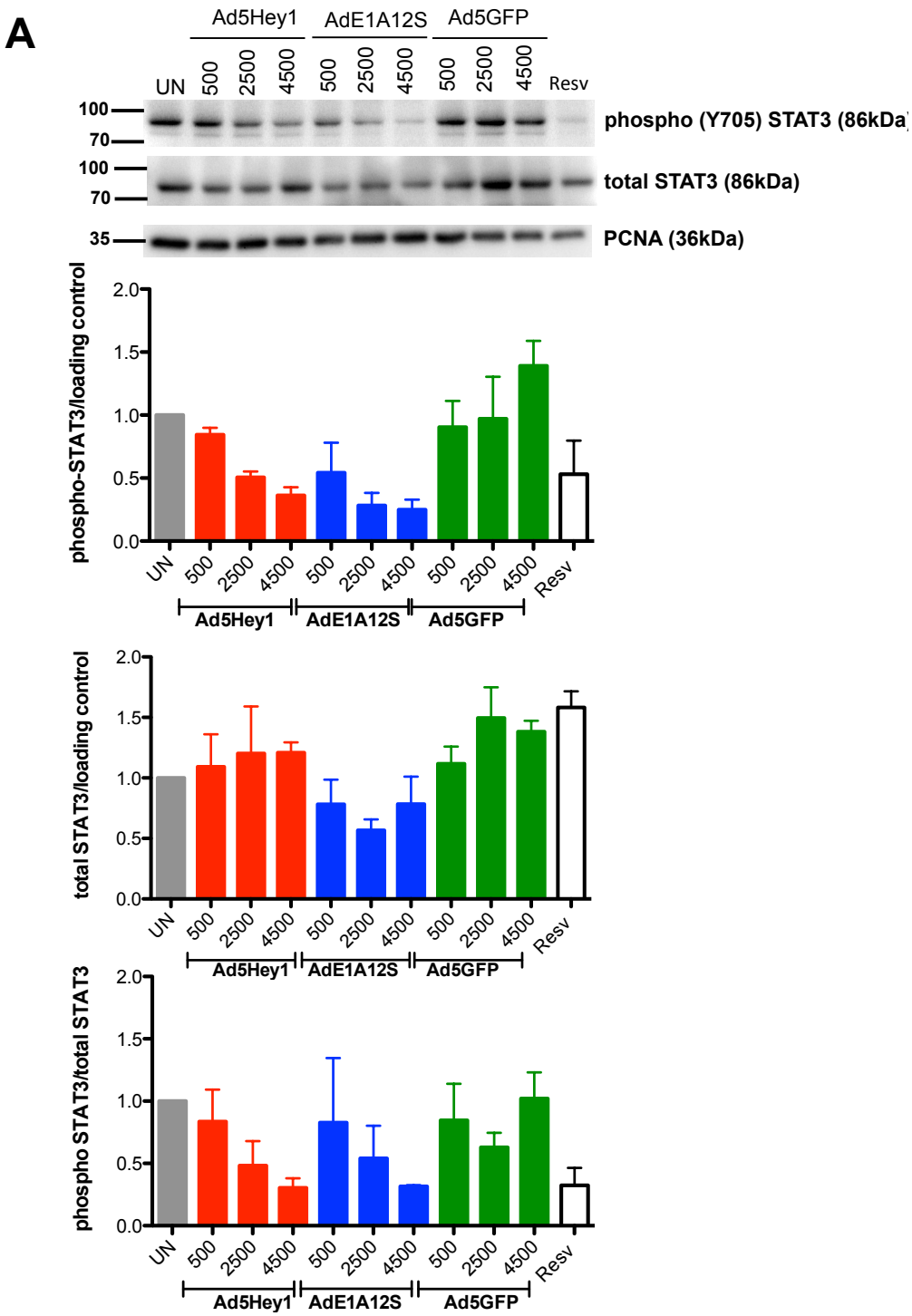
A
Ad5Hey1
AdE1A12S
Ad5GFP
UN
500
2500
4500
Resv
100
70
phospho (Y705) STAT3 (86kDa)
total STAT3 (86kDa)
35
PCNA (36kDa)
phospho-STAT3/loading control
total STAT3/loading control
phospho STAT3/total STAT3
2.0
1.5
1.0
0.5
0.0

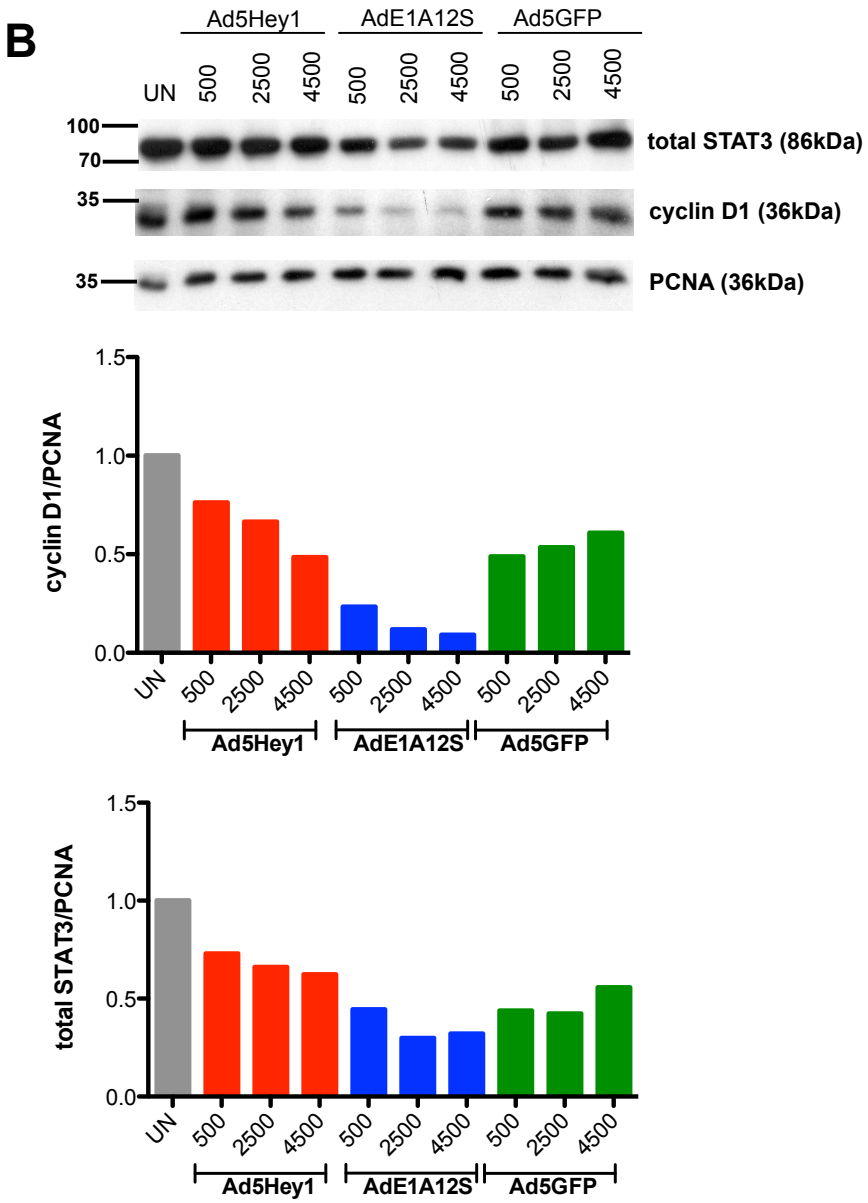

Figure 42. Ad5Hey1 decreases phospho (Y705) STAT3 and cyclin D1 at 48h in DU145 cells

A) Cells were infected with 500-4500ppc Ad5Hey1#3, AdE1A12S#3 or Ad5GFP. Two hours after infection, medium was replaced with 10% FBS DMEM. Cells were treated overnight with 50μM resveratrol overnight as a positive control for STAT3 dephosphorylation. At 48h post-infection, cell lysates were harvested and prepared for separation on polyacrylamide gels. 20μg protein was loaded per lane and blotted for phospho (Y705) STAT3 and PCNA as a loading control. The membrane was later stripped and probed for total STAT3 expression. Results show one blot, representative of 2 independent experiments. Histograms showing expression levels of phospho (Y705) STAT3 (top graph) and total STAT3 (middle graph) normalised to loading control and expressed relative to uninfected (UN) cells. Phospho (Y705) STAT3 expression levels were then normalised to total STAT3 and expressed relative to uninfected cells (bottom graph). Results show mean of 2 independent experiments ± SEM. B). Cells were treated as describe in A). Cell lysates harvested at 48h post-infection were prepared for separation on polyacrylamide gels. 20μg protein was loaded per lane and blotted for total STAT 3 and cyclin D1. Histograms showing total cyclin D1 (top graph) and STAT3 (bottom graph) protein expression normalised to PCNA and expressed relative to uninfected (UN) cells. Results are of one experiment.

3.2.3.2. Ad5Hey1 targets the JAK/STAT pathway in DU145 cells

To determine whether a decrease in STAT3 activity by Ad5Hey1 may play a role in Ad5Hey1-mediated cytotoxicity and sensitisation, two JAK inhibitors were used to determine whether there was any affect on Ad5Hey1-induced cell killing when STAT3 was inhibited. Impeding upstream tyrosine kinases such as (JAK1 and JAK2) is an efficient method to prevent STAT3 activation. Since constitutive STAT3 activity in DU145 cells may also occur as a result of upstream signalling pathways activating JAK proteins (e.g. EGFR) (Russell, Bennett et al. 1998), inhibition of JAK1 or JAK2 was approached at two levels; firstly using the small molecule inhibitor AG490, a selective inhibitor of EGFR, HER2/neu as well as JAK2 (Gazit, Osherov et al. 1991; Meydan, Grunberger et al. 1996) and secondly with AZD1480, an ATP-competitive inhibitor which targets JAK1/2 (Hedvat, Huszar et al. 2009).

DU145 cells were treated with Ad5Hey1 or AdE1A12S to generate dose response curves and treated with and without fixed concentrations of AG490 or AZD1480 that induced <30% cell death alone. Cell death after combination treatments was evaluated 3 days post-infection. Interestingly I observed clear sensitisation for both Ad5Hey1 and AdE1A12S in the presence of AG490 (Figure 43) whereas treatment with AZD1480 did not sensitise cells to Ad5Hey1 and AdE1A12S-mediated cell killing (Figure 44). A dose-dependent decrease in Ad5Hey1 EC_{50} was observed when cells were treated with 10 and 25μM AG490 with a reduction of 47 and 73% respectively Similarly the EC_{50} of AdE1A12S decreased by 46 and 81% respectively (Figure 43D). In contrast, AZD1480 increased the EC_{50} value of Ad5Hey1 by 28% (Figure 44D) while increasing doses of the inhibitor restored cell killing by Ad5Hey1 to similar levels to that induced by the virus alone (no significant differences). Likewise, cells treated with increasing doses of AZD1480 were desensitised to AdE1A12S-mediated cell killing with 1μM and 25μM resulting in the greatest desensitising effect.

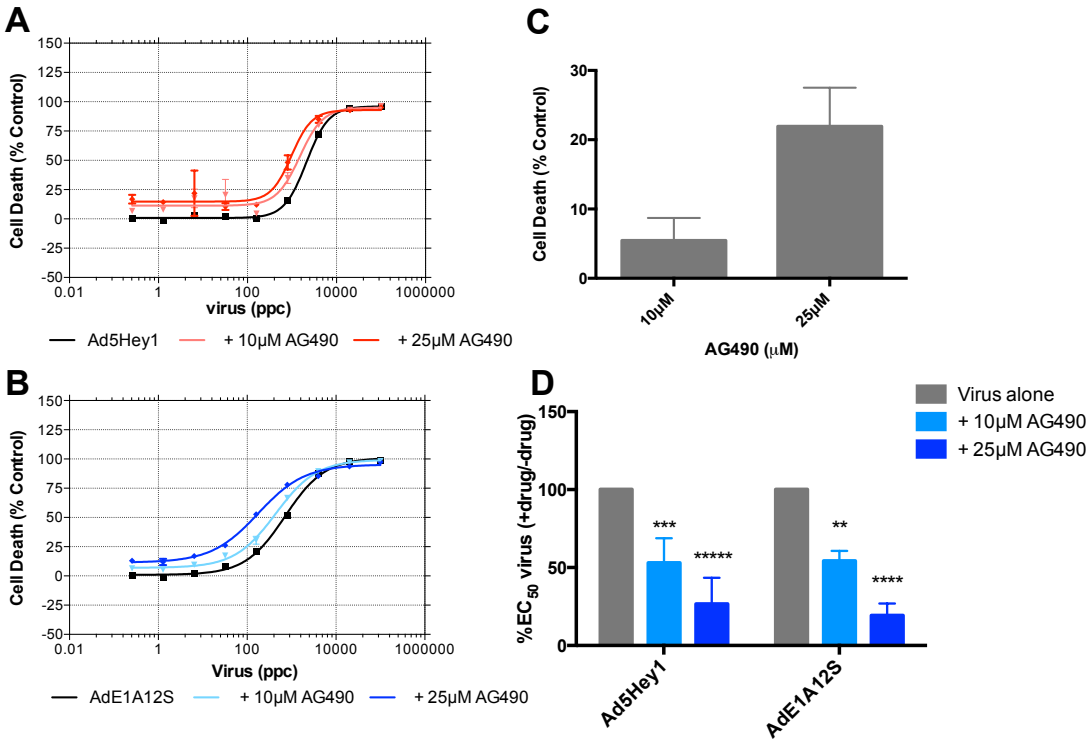

Figure 43. The EGFR/HER2/JAK2 inhibitor, AG490 sensitises Ad5Hey1-infected DU145 cells to enhanced cell death

Representative virus dose response curves in DU145 cells for Ad5Hey1#3 (A) and AdE1A12S#3 (B). Cells were infected with serial dilutions of virus with and without AZDG490 (10 and 25μM). Cell death was assayed by MTS viability assay 3 days post-infection and data shown is mean of duplicates ± SEM from one experiment representative of 2-4. (C) Percentage of cell death (relative to untreated cells) after treatment with 10 and 25μM AG490 after 3 days of treatment. Results show mean of duplicate wells for 3 independent experiments ± SEM. (D) Histogram showing relative EC_{50} values as a percentage of virus alone. Virus EC_{50} values were calculated for virus alone relative to uninfected cells or in combination with each agent relative to the percentage of cell death induced by the drug alone. Results show mean of duplicate wells for 2-4 independent experiments ± SEM. Statistical analysis was carried out using two-way ANOVA using multiple comparison with a Tukey post test. $p<0.01$ (**) and $p<0.001$ (***/****) compared with each respective virus alone.

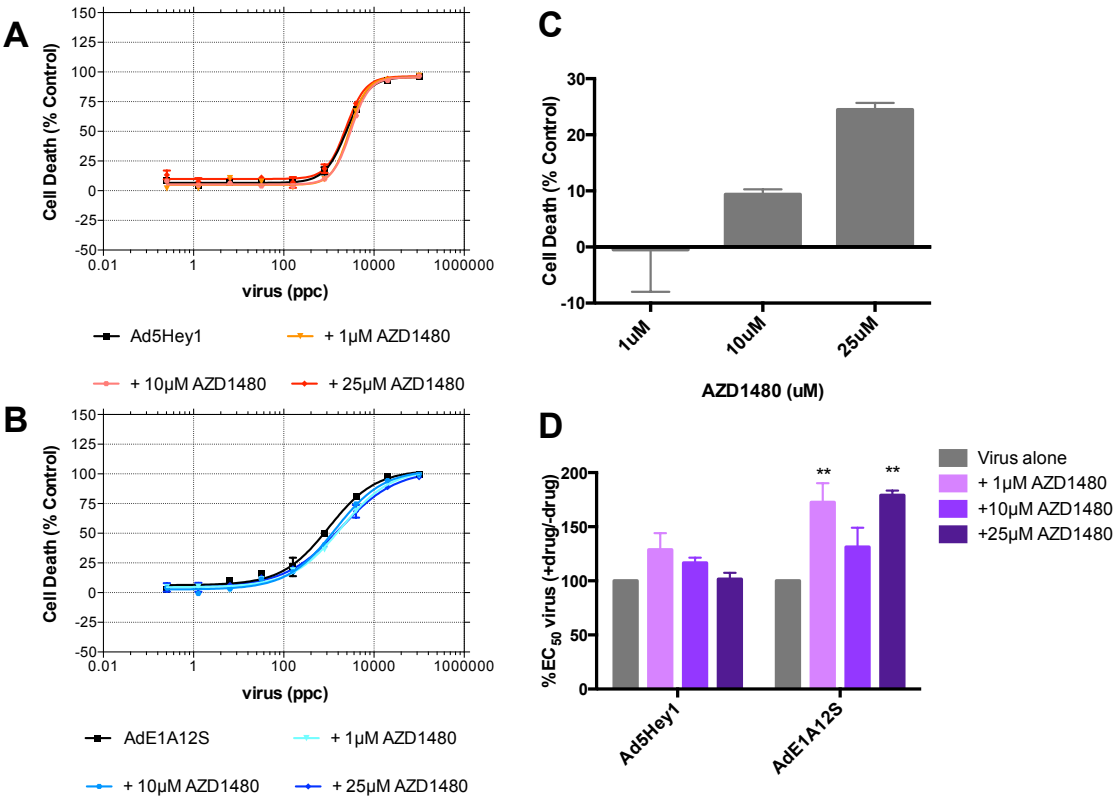

Figure 44. The JAK1/2 inhibitor, AZD1480 does not sensitise Ad5Hey1-infected DU145 cells to further cell death

Representative virus dose response curves in DU145 cells for Ad5Hey1#3 (A) and AdE1A12S#3 (B). Cells were infected with serial dilutions of virus with and without AZD1480 (1, 10 and 25μM). Cell death was assayed by MTS viability assay 3 days post-infection and data shown is mean of duplicates ± SEM from one experiment representative of 2-3. (C) Percentage of cell death (relative to untreated cells) after treatment with 1, 10 and 25μM AZD1480 after 3 days of treatment. Results show mean of duplicate wells for 2-3 independent experiments ± SEM. (D) Histogram showing relative EC_{50} values as a percentage of virus alone. Virus EC_{50} values were calculated for virus alone relative to uninfected cells or in combination with each agent relative to the percentage of cell death induced by the drug alone. Results show mean of duplicate wells for 2-3 independent experiments ± SEM. Statistical analysis was carried out using two-way ANOVA using multiple comparison with a Tukey post test. $p<0.01$ (**) compared with each respective virus alone.

Following the results described in Figure 43, I acknowledged that although the combination of AG490 with Ad5Hey1 generated interesting results suggesting a possible synergistic interaction, inhibition of EGFR and HER2/neu signalling was likely to have an effect on other survival pathways in DU145 cells such as the PI3K/AKT signalling (Zheng, Ren et al. 2009). Therefore, AG490 would not be a suitable tool from which to determine Ad5Hey1-specific effects on the JAK/STAT pathway. I therefore focused on AZD1480 due to its greater selectivity for the JAK/STAT signalling pathway. In addition, I recognized small molecule inhibitors commonly have a short half-life such that it was likely AZD1480 had degraded by the end of the time course. For this reason phospho-STAT3 expression was monitored over 12h (Figure 45) with phospho-STAT3 expression levels being restored by 12h.

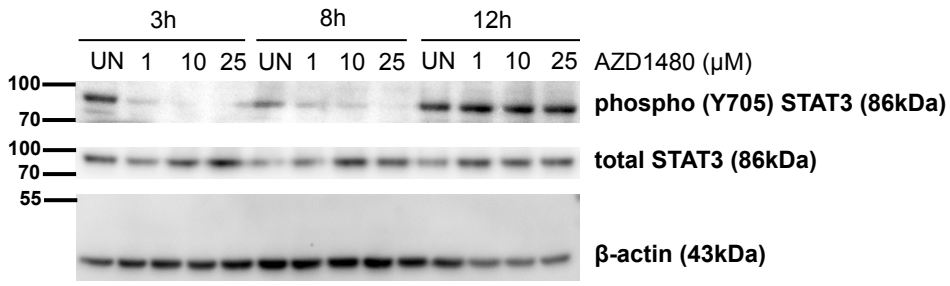

Figure 45. Dose- and time-dependent effects of AZD1480 treatment levels of phospho-STAT3 in DU145 cells

Cells were treated with AZD1480 at the indicated doses in 10% FBS DMEM and cell lysates harvested at 3, 8 and 12h post treatment and prepared for separation on polyacrylamide gels. 20μg of protein was loaded per lane and blotted for phospho-STAT3 expression and actin as a loading control. The membrane was later stripped and reprobed for total STAT3 expression. UN = untreated. Results of one experiment.

Considering the short inhibitory effect of phospho-STAT3 in response to AZD1480, probably due to a short half-life of the inhibitor, I changed the treatment schedule. AZD1480 was added simultaneously to virus infection on day 1 with further additions every 24h and cell viability was assessed 72h after initial treatment (Figure 46). Despite increasing the level of active AZD1480 in the culture medium for the duration of the experiment, the presence of AZD1480 did not sensitise cells to Ad5Hey1 and AdE1A12S-mediated cell death as before (Figure 44). From these preliminary experiments, it was possible to hypothesise further inhibition of STAT3 by AZD1480 does not occur since Ad5Hey1 or AdE1A12S are already targeting the JAK/STAT signalling pathway.

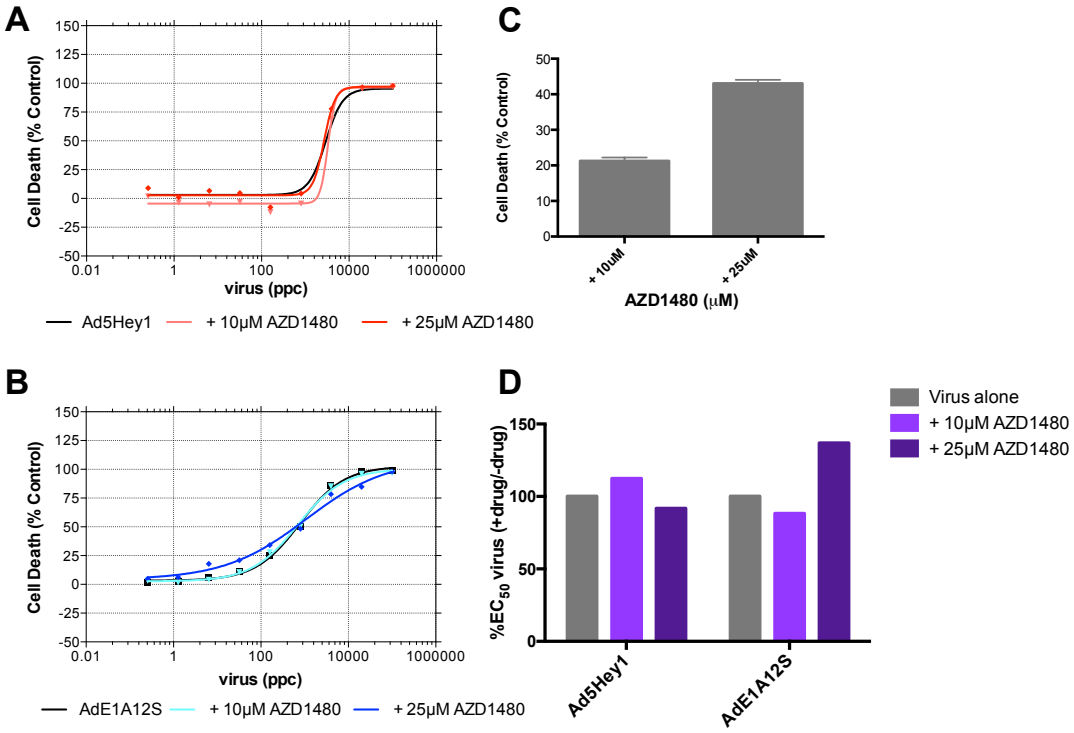

Figure 46. Continuous inhibition of STAT3 activity by AZD1480 desensitises DU145 cells to Ad5Hey1-mediated cell death

Virus dose response curves in DU145 cells for Ad5Hey1#3 (A) and AdE1A12S#3 (B). Cells were infected with serial dilutions of virus with and without AZD1480 (10 and 25μM) the following day (day 1). Further additions of inhibitor were added on days 2 and 3. Cell death was measured by MTS assay 3 days post-infection and data shown is mean of duplicates ± SEM from one experiment. (C) Percentage of cell death (relative to untreated cells) after treatment with 10 and 25μM AZD1480 after 3 days of treatment with drug added on days 1, 2 and 3. Results show mean of duplicate wells over 2 plates for one experiment. (D) Histogram showing relative EC_{50} values as a percentage of virus alone. Virus EC_{50} values were calculated for virus alone relative to uninfected cells or in combination with each agent relative to the percentage of cell death induced by the drug alone. Results show mean of duplicate wells from one experiment.

To further clarify the significance of our initial findings, Ad5Hey1 at a dose which resulted in reduced levels of phospho-STAT3, was combined with AZD1480 (10 or 25μM) and levels of phospho-STAT3 assessed by western blotting. This was carried out 24h post-treatment with cells treated every 12h to maintain levels of active AZD1480.

At 24h, both doses of AZD1480 completely ablated phospho-STAT3 levels in DU145 cells (Figure 47). However all viruses including Ad5GFP result in a decrease in phospho-STAT3 levels compared with untreated cells suggesting that that this is a non-specific effect of virus infection. We have shown Hey1 is expressed at this time point (section 1.8.1; Figure 12), however presumably 24h may be too early for a Hey1-mediated effect on STAT3 activity as was shown in Figure 42. Surprisingly, combining 10μM AZD1480 with Ad5Hey1 resulted in

higher phospho-STAT3 levels suggesting Ad5Hey1 was increasing STAT3 activity. This is in contrast to combination treatment with AdE1A12S, which maintained phospho-STAT3 to similar levels compared to drug alone. Ad5GFP infection with AZD1480 resulted in an intermediate level of phospho-STAT3 suggesting the presence of viral particles may have a positive correlation with STAT3 activity. Combining Ad5Hey1 or AdE1A12S with 25μM AZD1480 resulted in contrasting effects; the higher more toxic dose of AZD1480 (Figure 46C) counteracted the effect of Ad5Hey1 on phospho-STAT3 resulting in lower phospho-STAT3 expression whereas AdE1A12S seemed to increase phospho-STAT3 activity. Since STAT3 activity is associated with survival in DU145 cells the levels of phospho-STAT3 observed for combination treatment with Ad5Hey1 and AdE1A12S at the selected doses of AZD1480 correlate with the increase in cell viability with Ad5Hey1 and AdE1A12S when combined with AZD1480 (Figure 46D).

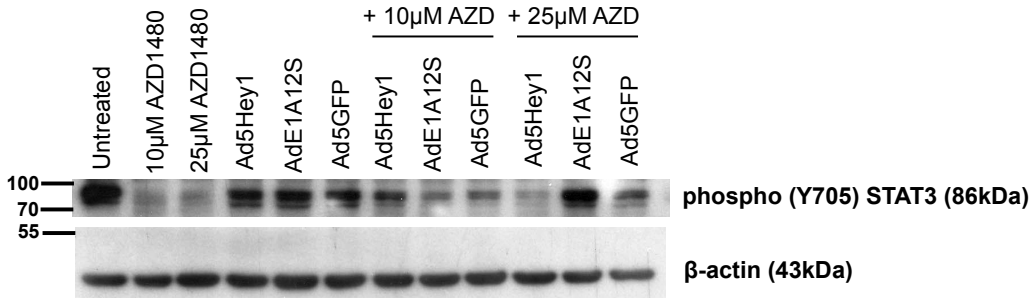

Figure 47. Ad5Hey1 and AdE1A12S upregulate phospho-STAT3 levels in DU145 cells in the presence of JAK1/2 inhibitor, AZD1480

Cells were infected with Ad5Hey1#3 (4500ppc), AdE1A12S#3 (500ppc) or Ad5GFP (4500ppc). Two hours later infection medium was replaced with 10% FBS DMEM or medium containing 10 or 25μM AZD1480. At 12h post-infection medium was replaced with fresh medium containing AZD1480. At 24h post-infection cell lysates were harvested and prepared for separation on polyacrylamide gels. 20μg protein was loaded per lane and blotted for phospho (Y705) STAT3 and β-actin as a loading control. Results for one experiment.

In summary, I have determined Ad5Hey1 dose–dependently reduced phospho-STAT3 expression in DU145 cells and that the JAK1/2 small molecule inhibitor, AZD1480 did not sensitise cells to Ad5Hey1 or the positive control virus, AdE1A12S. Assessment of phospho-STAT3 expression during concurrent treatment with Ad5Hey1 and AZD1480 suggested upregulation of phospho-STAT3 in the presence of the inhibitor. Therefore inhibition of JAK1/2 by AZD1480 disrupts the effect Ad5Hey1 or AdE1A12S has on STAT3 signalling suggesting that Hey1 or E1A12S works through the same pathway as the small molecule inhibitor and could be inhibiting JAK/STAT signalling in DU145 cells.

3.3. Characterisation of cell death mechanisms under synergistic conditions

The chemotherapeutic drugs mitoxantrone and docetaxel cause toxicity in most cell types by inducing apoptosis (Bellosillo, Colomer et al. 1998; Mhaidat, Zhang et al. 2007; Fabbri, Amadori et al. 2008; Symes, Kurin et al. 2008). E1A12S is a potent inducer of apoptosis and sensitiser to chemotherapeutic drugs (Debbas and White 1993; Lowe and Ruley 1993; Lowe, Ruley et al. 1993; Grand, Grant et al. 1994; Sabbatini, Lin et al. 1995) and in combination with mitoxantrone and docetaxel cause synergistic cell killing (Miranda, Maya Pineda et al. 2012). Considering that AdHey1 could stabilise p53 and inhibit AR-activity I speculated whether the synergistic cell death of Ad5Hey1 when combined with mitoxantrone and docetaxel (section 3.2.1) occurred as a result of an augmented apoptotic process induced by these drugs.

3.3.1. Ad5Hey1-mediated enhancement of drug-induced apoptosis is drug- and cell line-dependent

3.3.1.1. Mitochondrial membrane depolarisation

The intrinsic apoptotic pathway is stimulated by a range of non-receptor-mediated pro-apoptotic signals resulting in intracellular signalling and destabilization of the mitochondrial outer membranes. The formation of the pores, including the permeability transition pore (PTP) leads to dissipation of the mitochondrial membrane potential ($\Delta_{\psi m}$) and subsequent release of intermembrane space apoptogenic factors such as cytochrome C, Smac/DIABLO and apoptosis-inducing factor (AIF) (Kroemer, Galluzzi et al. 2007). Depolarisation of the $\Delta_{\psi m}$ is characteristically deemed an early stage in apoptosis preceding DNA degradation, reactive oxygen species (ROS) production and membrane permeability (Darzynkiewicz, Juan et al. 1997).

Respiring mitochondria generate a proton gradient (Δp) across the inner mitochondrial membrane via the electron transport chain (ETC) resulting in a pH (ΔpH_m) and electrochemical gradient ($\Delta_{\psi m}$) (Cottet-Rousselle, Ronot et al. 2011). Cationic dyes used as mitochondrial probes preferentially localise in the mitochondrial matrix according to the electrochemical gradient established by the Nernst equation (Ehrenberg, Montana et al. 1988).

$$V = -\frac{RT}{ZF} \ln \frac{C_i}{C_o}$$

V = membrane potential
Z = ion charge
R = ideal gas constant
T = absolute temperature
F = Faraday constant
C_i = concentration inside cell
C_o = concentration outside cell

Physiological values for $\Delta_{\psi m}$ range from 120 to 180mV (mitochondrial matrix being electronegative) result in the concentration of cations in the mitochondrial matrix being 2-3 logs higher compared with the cytosol (Kroemer, Galluzzi et al. 2007). Tetramethylrhodamine ethyl ester (TMRE) was employed in these studies to measure $\Delta_{\psi m}$ as it accumulates rapidly in living cells due to its lipophilic nature; it is highly fluorescent and has low toxicity. It is highly specific to mitochondria and does not form aggregates nor display binding-dependent changes in fluorescence efficiency as well as having the lowest ETC inhibition of all the $\Delta_{\psi m}$-sensitive probes (Ehrenberg, Montana et al. 1988; Cottet-Rousselle, Ronot et al. 2011; Perry, Norman et al. 2011).

Cells were treated with Ad5Hey1 or AdE1A12S in combination with either mitoxantrone or docetaxel at the doses determined to have produced synergistic cell killing in 22Rv1 and DU145 cells (Section 3.2.1, Table 11). Since Ad5Hey1 was previously shown to sensitise LNCaP cells to cytotoxic drug-induced cell death (section 1.8.1), this cell line was also included using fixed doses (Table 11). Cells were collected between 24 and 120h and analysed by flow cytometry for $\Delta_{\psi m}$ using TMRE and the exclusion dye, DAPI. Viable cells were defined as the highly fluorescent population (Figure 28; I, high TMRE and low DAPI) whereas apoptotic cells with depolarised $\Delta_{\psi m}$ were identified as the population with lower fluorescence (Figure 48; III, low TMRE and low DAPI). Cells were treated with staurosporine to serve as positive controls for apoptosis and to

distinguish the live and apoptotic populations (Figure 48). Since transient loss of $\Delta_{\psi m}$ may occur under certain physiological circumstances, a static comparison between relative $\Delta_{\psi m}$ of untreated and treated cells was assessed and plotted as a function of treatment duration (Figure 49 and Figure 50).

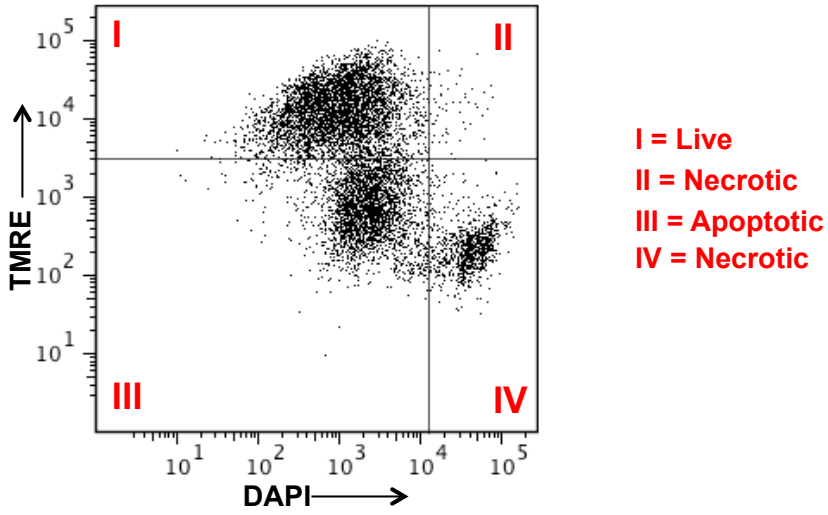

Figure 48. Assessment of $\Delta_{\psi m}$ depolarisation by TMRE flow cytometry

Flow cytometry analysis of DU145 cells treated with 0.5μM staurosporine overnight. Cell populations were classified according to TMRE and DAPI staining. Quadrant I represents live cells (TMRE+ve/DAP-ve) and III apoptotic cells (TMRE-ve/DAPI-ve). Necrotic cells (DAPI+) are gated in quadrants II and IV.

The tendency of $\Delta_{\psi m}$ to depolarise in PCa cells varied between cell types (Figure 49). In 22Rv1 cells, 8.3% of cells were without an intact $\Delta_{\psi m}$ at the start of the time course whereas in LNCaP and DU145 cells <1% of cells had lost $\Delta_{\psi m}$ reflective of the different properties and genetic backgrounds of the cell lines.

3.3.1.2. Mitochondrial depolarisation in cells treated with docetaxel and infected with viruses

In 22Rv1 cells, Ad5Hey1 and AdE1A12S alone were able to induce changes to the $\Delta_{\psi m}$ (Figure 49). By 96h, the percentage of cells that had lost $\Delta_{\psi m}$ increased to 33% and 25.1% for Ad5Hey1 and AdE1A12S respectively compared with 11.6% of untreated cells. At 48h, 17.8% of cells treated with docetaxel had lost their $\Delta_{\psi m}$ and this was increased to 41.6% by 96h. The effect of combining Ad5Hey1 with docetaxel increased the proportion of cells that had lost $\Delta_{\psi m}$; 96h; 55.7% compared with 41.6% and 33% for docetaxel and Ad5Hey1, respectively.

A similar trend was observed for the combination treatment with AdE1A12S although the percentage of cells with depolarised $\Delta_{\psi m}$ was slightly lower than the Ad5Hey1 combination treatment at 52.8%. No augmentation of $\Delta_{\psi m}$ was observed when Ad5GFP was combined with the drug.

In LNCaP cells, none of the viruses significantly depolarised $\Delta_{\psi m}$ at any time point. Treatment with docetaxel enhanced $\Delta_{\psi m}$ depolarisation and by 120h, 30.8% of cells were without an intact $\Delta_{\psi m.}$ Surprisingly, in contrast to the results obtained in the cell viability studies, Ad5Hey1 in combination with docetaxel increased the number of cells with depolarised $\Delta_{\psi m}$ (96-120h). At 120h, 57.5% of cells had lost $\Delta_{\psi m}$ when treated with Ad5Hey1 and docetaxel compared with 30.8% for cells treated with docetaxel alone. A similar trend was observed for AdE1A12S in combination with docetaxel. A small increase in $\Delta_{\psi m}$ depolarisation was also seen when Ad5GFP was combined with docetaxel indicating that the expression of a non-toxic transgene in this cell line had an impact on cell survival, resulting in partial augmentation of $\Delta_{\psi m}$ depolarisation.

In DU145 cells, neither Ad5Hey1 nor AdEA12S affected $\Delta_{\psi m}$ depolarisation. Treatment with docetaxel resulted in 21.7% of cells with no $\Delta_{\psi m}$ compared with 6.3% of untreated cells by 96h. When Ad5Hey1 was combined with docetaxel, the proportion of cells at 96h undergoing $\Delta_{\psi m}$ depolarisation increased by a third and more than doubled when AdE1A12S was present. $\Delta_{\psi m}$ in response to Ad5GFP with docetaxel did not increase compared with drug alone.

In conclusion, Ad5Hey1 was able to enhance docetaxel-induced $\Delta_{\psi m}$ depolarisation in all three PCa cell lines examined. The extent of augmentation appeared to be dependent on cell type. Ad5Hey1-mediated enhancement was similar to that of AdE1A12S in 22Rv1 and LNCaP. The differences between Ad5Hey1 and AdE1A12S were more apparent in DU145 cells, presumably due to mechanism-based variations in these cells.

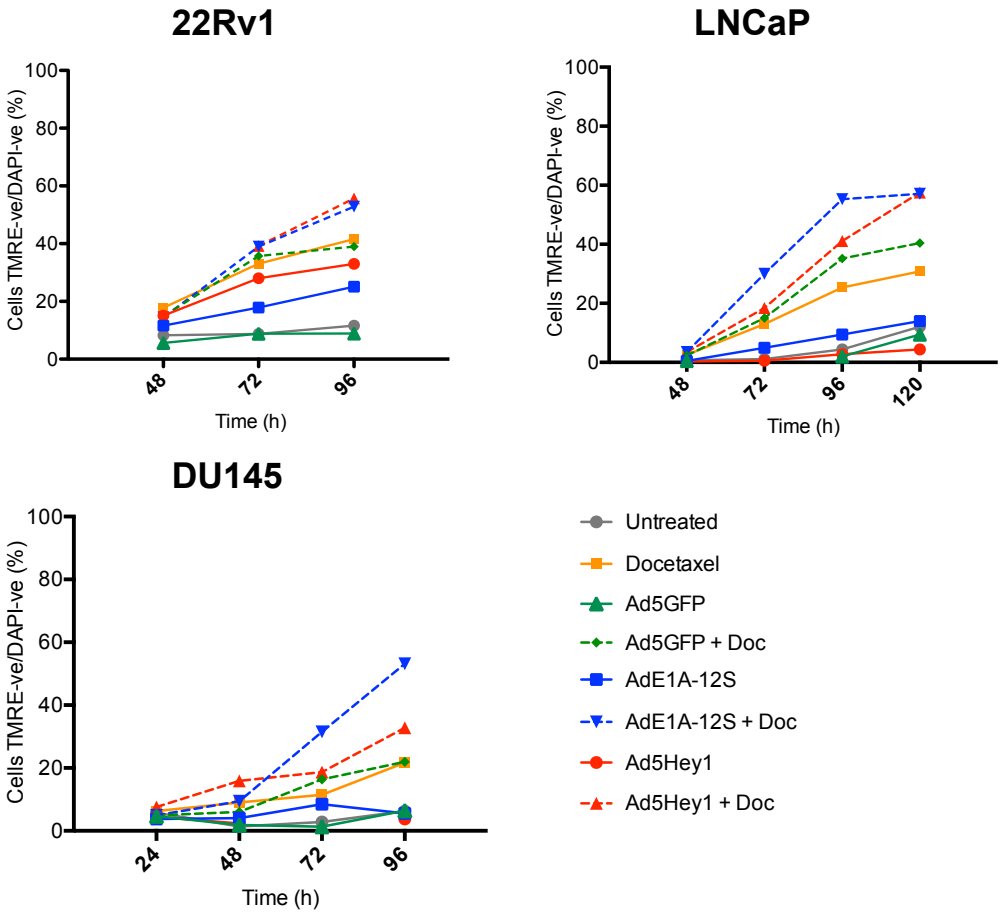

Figure 49. Ad5Hey1 augments docetaxel-dependent $\Delta_{\psi m}$ depolarisation in 22Rv1, LNCaP and DU145 cells

Cells were infected with Ad5Hey1#2 (22Rv1) or Ad5Hey1#3 (DU145 and LNCaP), AdE1A12S#3 or Ad5GFP and/or treated with docetaxel in 10% FBS medium at the doses shown in Table 11. At the indicated times, cells were harvested for flow cytometry analysis as described in the Materials and Methods and stained with TMRE and DAPI. Cells that lost TMRE staining (inactive mitochondria) and remained negative for DAPI (intact cellular membrane) were considered "apoptotic." Results shown are single replicates for each condition, representative of 2-3 independent experiments showing a similar trend.

3.3.1.3. Mitochondrial depolarisation in cells treated with mitoxantrone and infected with viruses

In 22Rv1 cells, mitoxantrone alone induced loss of $\Delta_{\psi m}$ (50.2%) at 96h compared with 11.6% of untreated cells (Figure 50) and the presence of Ad5Hey1 augmented drug-induced $\Delta_{\psi m}$ depolarisation resulting in 72.3% of cell at 96h without an intact $\Delta_{\psi m}$. AdE1A12S enhanced the drug-induced $\Delta_{\psi m}$ depolarisation, in agreement with previous findings (Miranda, Maya Pineda et al. 2012). Surprisingly, the mitoxantrone-induced augmentation of mitochondrial depolarisation was greater with Ad5Hey1. Again, Ad5GFP did not augment the loss of $\Delta_{\psi m}$ in combination with mitoxantrone.

In LNCaP cells, mitoxantrone was not a strong inducer of $\Delta_{\psi m}$ dissipation in contrast with the docetaxel data. The proportion of cells with $\Delta_{\psi m}$ depolarisation was less than basal levels. Visual assessment indicated that cells were growth arrested in response to mitoxantrone-treatment at this low dose (25nM); cells were sparser in comparison with untreated cells and were not rounded as is typical of dying cells. This suggests that mitoxantrone at this dose had a cytostatic effect on cell viability. Nevertheless, combination of mitoxantrone with AdHey1 resulted in a distinct increase in $\Delta_{\psi m}$ depolarisation from 72h onwards; 26.3% of cells had lost $\Delta_{\psi m}$ compared with 3.0% when treated with mitoxantrone alone after 120h. Combination treatment with AdE1A12S resulted in an even greater enhancement in $\Delta_{\psi m}$ depolarisation (52.2%). Ad5GFP in combination with mitoxantrone did not augment $\Delta_{\psi m}$ in contrast to the docetaxel–combination (Figure 49).

In DU145 cells, mitoxantrone induced $\Delta_{\psi m}$ depolarisation in 45.0% of cells after 96h. Intriguingly, Ad5Hey1 combined with mitoxantrone reduced the proportion of depolarised cells ($\Delta_{\psi m}$=32.6%; 96h) indicating that expression of Hey1 had a protective effect. In agreement with published results, AdE1A12S enhanced $\Delta_{\psi m}$ depolarisation compared with drug alone (Miranda, Maya Pineda et al. 2012). The presence of Ad5GFP slightly increased the drug-induced $\Delta_{\psi m}$ changes suggesting that the observed Ad5Hey1-mediated inhibition of drug-induced depolarisation is specific.

In summary, Ad5Hey1 augmented mitoxantrone-induced $\Delta_{\psi m}$ depolarisation in 22Rv1 and LNCaP cell but not DU145. The sensitising function of Ad5Hey1 in

mitoxantrone-combinations was greater than AdE1A12S in 22Rv1 cells but not in LNCaP. In DU145 cells, Ad5Hey1 protected cells from mitoxantrone-mediated $\Delta_{\psi m}$ depolarisation an effect that suggests synergistic cell death with this combination treatment is a result of alternative modes of cell death.

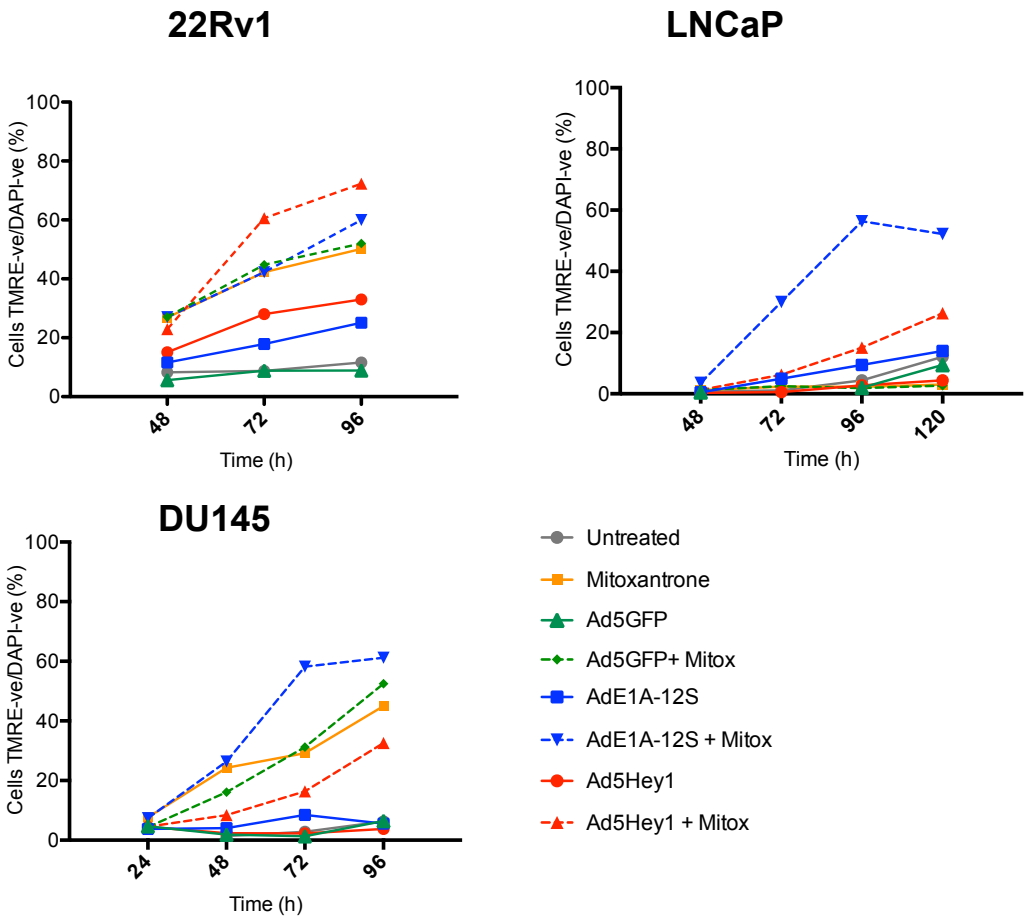

Figure 50. Ad5Hey1 enhances mitoxantrone-induced $\Delta_{\psi m}$ depolarisation in 22Rv1 and LNCaP but not DU145 cells.

Cells were infected with Ad5Hey1#2 (22Rv1) or Ad5Hey1#3 (DU145 and LNCaP), AdE1A12S#3 or Ad5GFP and/or treated with mitoxantrone in 10% FBS medium at the doses shown in Table 11. At the indicated times, cells were harvested for flow cytometry analysis as described in the Materials and Methods and stained with TMRE and DAPI. Cells that lost TMRE staining (inactive mitochondria) and remained negative for DAPI (intact cellular membrane) were considered "apoptotic." Results shown are single replicates for each condition, representative of 3 independent experiments showing a similar trend.

3.3.1.4. Apoptosis and necrosis contribute to the enhanced cell death in combination-treated cells

The relative proportion of live, apoptotic and necrotic cells were assessed at 96h post treatment when the greatest distinction between single agent and combination treatment was detected. This was undertaken to gain further insight into the comparative differences by which the cytotoxic drugs killed cells in the presence or absence of Hey1 or E1A12S expression.

The effects of mitoxantrone and docetaxel on $\Delta_{\psi m}$ were dependent on cell type (Figure 51). Mitoxantrone induced greater cytotoxic effects in DU145 than LNCaP cells; stimulating a greater proportion of cells to undergo $\Delta_{\psi m}$ depolarisation and accumulation of necrotic cells. Whereas docetaxel-induced cell death was largely via $\Delta_{\psi m}$ depolarisation in LNCaP cells, in DU145 cells more necrotic cells accumulated. Both drugs had similar effects in 22Rv1 cells in terms of accumulation of necrotic cells although mitoxantrone was more potent in enhancing $\Delta_{\psi m}$ depolarisation.

In 22Rv1 cells, both apoptotic and necrotic cells accumulated in response to Ad5Hey1 or AdE1A12S infection alone. The effect was greatest with Ad5Hey1 with less live cells than with AdE1A12S, however this study does not take into account the differences in cell death kinetics by the viruses. The proportion of cells undergoing $\Delta_{\psi m}$ depolarisation after combination treatment with both drugs corresponded to our observations from the time course experiments (Figure 49 and Figure 50). Ad5Hey1 caused a greater increase of apoptotic cells whereas AdE1A12S-infection resulted in accumulation of more necrotic cells in mitoxantrone-combinations possibly as a result of variations in mechanisms of sensitisation of Ad5Hey1 or AdE1A12S when mitoxantrone was present. In contrast, the proportion of necrotic cells in docetaxel-combinations was similar for both viral mutants indicating that the mechanism of drug action has an impact on mode of cell death in 22Rv1 cells.

In LNCaP cells, toxicity resulting from combination treatments resulted in an increase in both apoptotic and necrotic cells with either drug. However, in combination with Ad5Hey1 or AdE1A12S a greater increase in apoptotic and necrotic cells was noted in the presence of mitoxantrone than docetaxel.

In DU145 cells, depending on drug context, the effect of Hey1 expression resulted in different effects on the extent of $\Delta_{\psi m}$ depolarisation and the proportion of necrotic cells (Figure 51). When combined with mitoxantrone, the protective effect of Ad5Hey1 on $\Delta_{\psi m}$ was accompanied by an increase in the percentage of necrotic cells (41.2%) compared with drug alone (34.4%). Synergistic cell death in combination with Ad5Hey1 and mitoxantrone could therefore not be attributed to an enhanced drug-induced apoptosis suggesting alternative non-apoptotic cell death mechanisms may be occurring. However, combination with AdE1A12S showed a clear increase in apoptotic cells. In combination with docetaxel, Ad5Hey1 resulted in an increase in cells with depolarised $\Delta_{\psi m}$ and necrotic cells compared with drug alone. However, although statistically significant, this trend was also observed when the drug was combined with Ad5GFP. This is inconsistent with the results obtained for the time course experiment (Figure 49) where no difference in $\Delta_{\psi m}$ depolarisation was observed between Ad5GFP and docetaxel and drug alone.

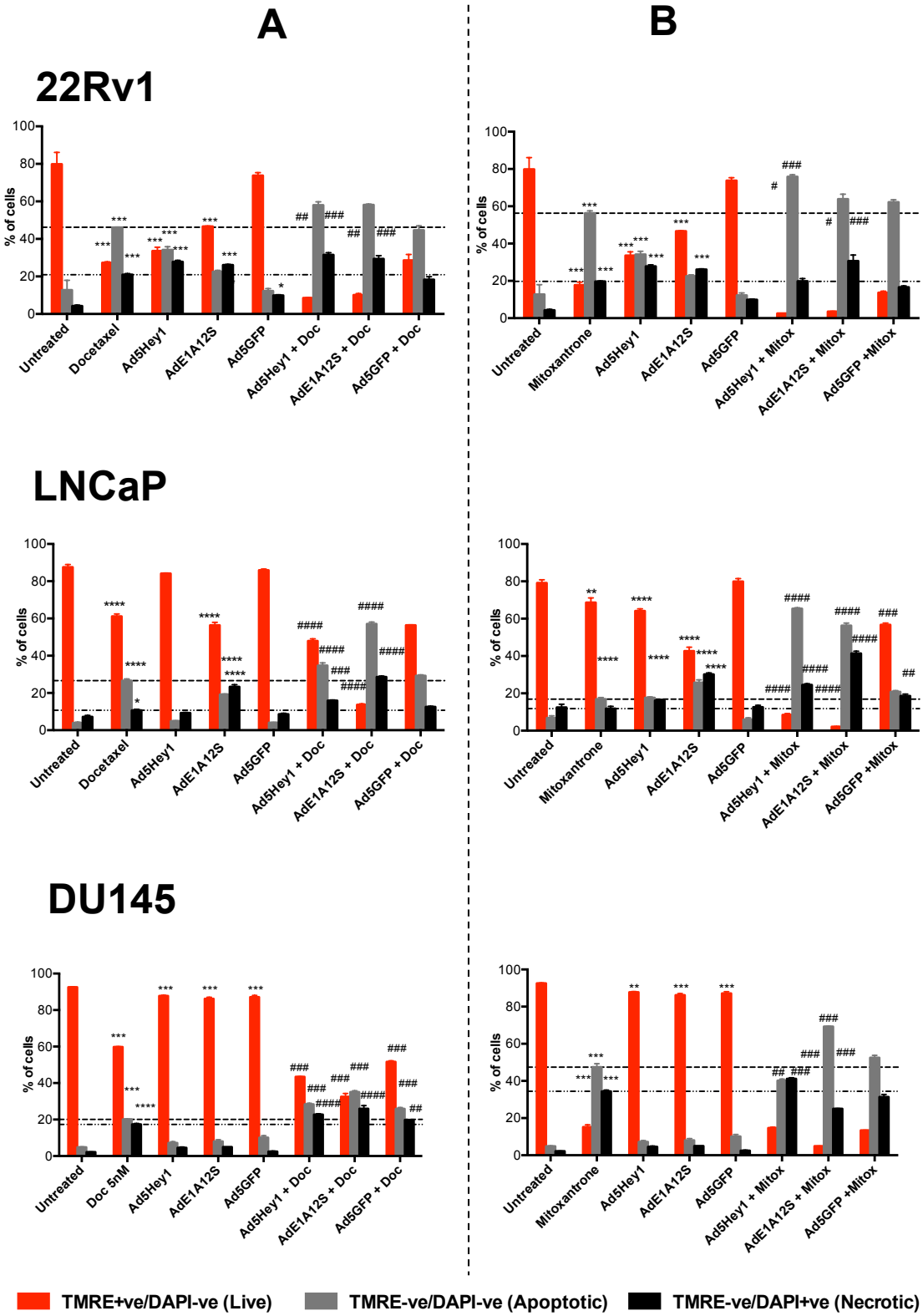

Figure 51. Changes in the live, apoptotic or necrotic cells 96h after treatment with docetaxel or mitoxantrone, viral mutants or combination treatments

Cells were infected with Ad5Hey1#2 (22Rv1) or Ad5Hey1#3 (DU145 and LNCaP), AdE1A12S#3 or Ad5GFP and/or treated with either docetaxel (A) or mitoxantrone (B) in 10% FBS medium at the doses listed in Table 11. At 96h post-treatment cells were harvested and stained with TMRE and DAPI and analysed by flow cytometry. Results shown are for triplicate wells for each condition, representative for 1-2 independent experiments. Statistical analysis was carried out

using a one-way ANOVA statistical analysis using multiple comparisons with a Tukey post-test for either “live”, “apoptotic” or “necrotic” populations. $p<0.05$ (*), $p<0.01$ (**) $p<0.001$ (***/****) compared with untreated cells $p<0.05$ (#), $p<0.01$ (##) $p<0.001$ (###/####) was compared with respective single drug treatment. Dashed line refers to the percentage of apoptotic cells resulting from drug only treatment and dashed/dotted line the percentage of necrotic cells.

3.3.1.5. Hyperpolarisation of $\Delta_{\psi m}$ by drug treatment is drug- and cell-line dependent

During the course of the $\Delta_{\psi m}$ studies, I observed an increase in TMRE fluorescence under certain conditions, revealing additional effects on the membrane potential. Either drug- or virus-treatment revealed an increase in TMRE fluorescence compared with untreated cells. As well as detecting depolarisation of $\Delta_{\psi m}$, TMRE is also sensitive to an increase in negative charge within the mitochondrial matrix resulting in a hyperpolarised $\Delta_{\psi m}$ (McGowan, Alling et al. 2011; Perry, Norman et al. 2011).

In response to Ad5Hey1 and AdE1A12S (but not Ad5GFP), TMRE fluorescence intensity increased in LNCaP cells compared with untreated cells but not in 22Rv1 or DU145 cells (Figure 52, Table 21). In line with AdE1A12S as a potent inducer of apoptosis, a second lower peak was also detected for LNCaP cells corresponding to a proportion of cells exhibiting no TMRE fluorescence. This was also observed in 22Rv1 cells in response to Ad5Hey1- or AdE1A12S-infection but not in DU145 cells

When LNCaP or DU145 cells were treated with docetaxel, 2 peaks were noted, one corresponding to cells with enhanced TMRE fluorescence compared with untreated cells and the other consistent with cells with depolarised $\Delta_{\psi m}$. This was reflected in an increase in relative mean fluorescence intensity (MFI) of TMRE in LNCaP cells but not in DU145 (Table 21). A decrease in the proportion of cells with enhanced TMRE fluorescence was observed in both cell lines when treated with docetaxel-combinations (Figure 52, Table 21). In contrast, 22Rv1 cells treated with docetaxel did not exhibit an increase in TMRE fluorescence.

As with docetaxel, mitoxantrone treatment in LNCaP cells resulted in a proportion of cells displaying enhanced TMRE fluorescence compared with untreated cells (Figure 52, Table 21) while the addition of Ad5Hey1 or AdE1A12S increased the proportion of cells with depolarised $\Delta_{\psi m}$. Unlike with

docetaxel-combinations, this did not result in a concomitant decrease in the proportion of cells with enhanced TMRE fluorescence and mitoxantrone-induced hyperpolarisation was maintained during Ad5Hey1- or AdE1A12S-mediated augmentation of apoptosis. Conversely, in DU145 cells only a small increase of TMRE fluorescence by mitoxantrone was noted, the majority of cells undergoing $\Delta_{\psi m}$ depolarisation after single or combination treatment. As before, 22Rv1 cells displayed only decreases in $\Delta_{\psi m}$ in response to mitoxantrone-combination treatments.

In conclusion, drug- and virus-induced $\Delta_{\psi m}$ hyperpolarisation in PCa cells appears to be cell-line dependent. Both drugs resulted in $\Delta_{\psi m}$ hyperpolarisation in LNCaP and DU145 but only LNCaP cells were sensitive to Ad5Hey1 or AdE1A12S-mediated $\Delta_{\psi m}$ hyperpolarisation. 22Rv1 cells did not exhibit $\Delta_{\psi m}$ hyperpolarisation in response to either virus or drug and as discussed in section 3.3.1.1 a greater proportion of untreated cells exhibited $\Delta_{\psi m}$ depolarisation compared with the other two cells lines.

The implication of drug-induced enhancement of TMRE fluorescence and mitochondrial hyperpolarisation (Maldonado, Patnaik et al. 2010) was beyond the scope of this research project but does allow us to postulate the potential modes of action these drugs have on mitochondrial dysfunction and hypothesise by what cell-type specific mechanisms of cell death are enhanced when a cellular or viral gene is overexpressed. It is not possible to make direct inferences on respiratory status or ΔpH_m solely by measuring $\Delta_{\psi m}$. Other measurements on mitochondrial function are necessary to ascertain the reasons behind drug-induced $\Delta_{\psi m}$ hyperpolarisation. This may be due to enhanced Δp, resulting in a greater ATP generating capacity or instead, rising cytosolic $[Ca^{2+}]$ as a consequence of Ca^{2+} release from endoplasmic reticulum (ER) or mitochondrial stores (Perry, Norman et al. 2011).

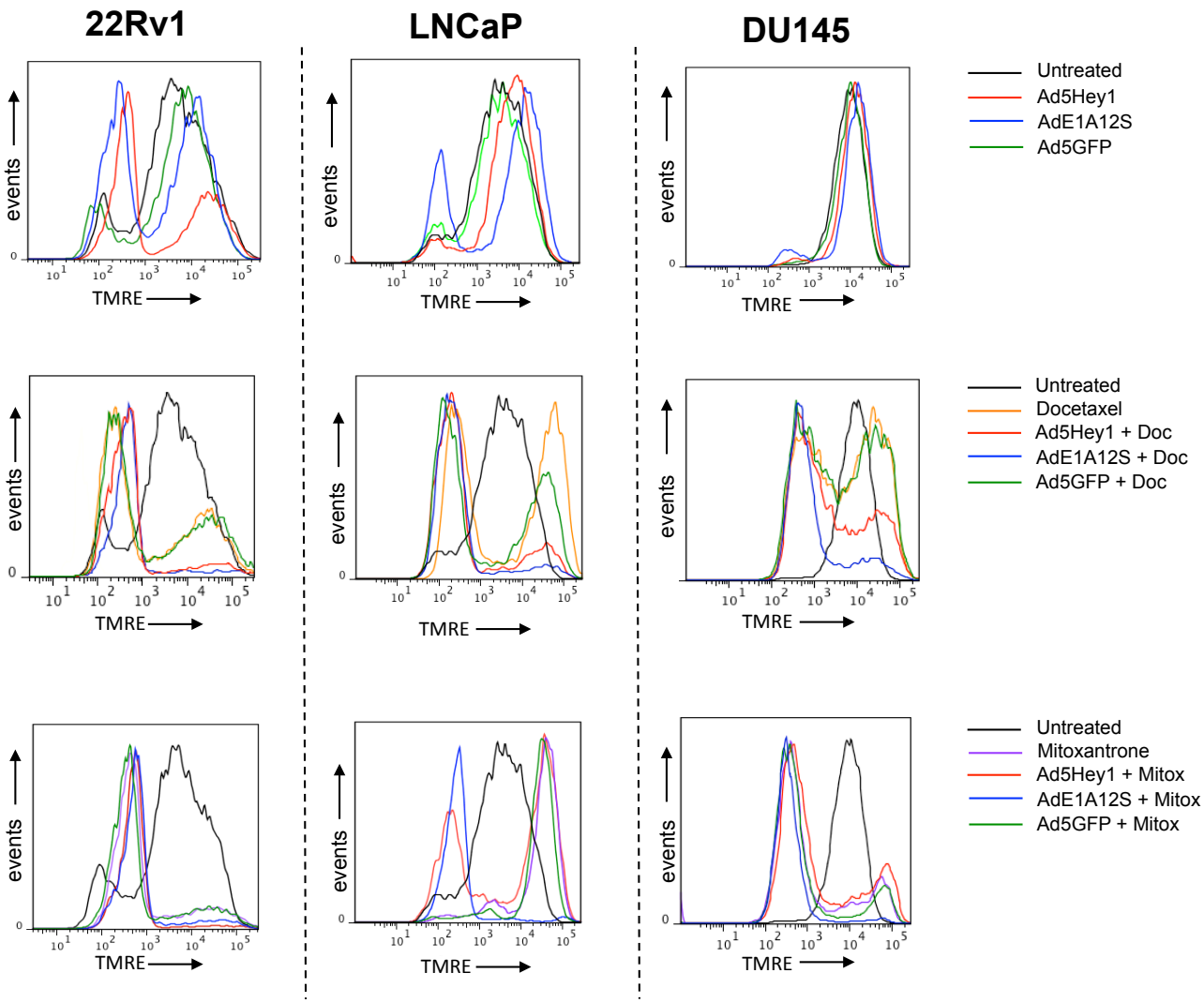

Figure 52. Drug treatment of PCa cells result in differential effects on $\Delta_{\psi m}$ polarisation

Data shown in Figure 49 and Figure 50 for 22Rv1 and DU145 (96h) and LNCaP (120h) displayed as a histogram of TMRE fluorescence vs. number of events

Table 21. Table showing relative geometric mean of TMRE fluorescence intensity after treatment with virus, drug or a combination at 96h (22Rv1 and DU145) or 120h (LNCaP)

	22Rv1	LNCaP	DU145
Untreated	1.0 ± 0.0	1.0 ± 0.0	1.0 ± 0.0
Ad5Hey1	0.51 ± 0.02	1.63 ± 0.06	1.07 ± 0.10
AdE1A12S	0.51 ± 0.00	1.40 ± 0.11	1.12 ± 0.18
Ad5GFP	0.89 ± 0.07	1.09 ± 0.19	1.02 ± 0.00

	22Rv1	LNCaP	DU145
Docetaxel	0.35 ± 0.03	1.98 ± 0.45	0.46 ± 0.04
Ad5Hey1 + Doc	0.20 ± 0.05	0.30 ± 0.13	0.33 ± 0.03
AdE1A12S+Doc	0.22 ± 0.04	0.16 ± 0.05	0.20 ± 0.07
Ad5GFP+ Doc	0.45 ± 0.01	0.51	0.47 ± 0.01

	22Rv1	LNCaP	DU145
Mitoxantrone	0.25 ± 0.02	7.73 ± 0.22	0.21 ± 0.09
Ad5Hey1 + Mitox	0.14 ± 0.02	1.59 ± 0.26	0.23 ± 0.03
AdE1A12S + Mitox	0.17 ± 0.02	0.18 ± 0.05	0.11 ± 0.06
Ad5GFP + Mitox	0.21	7.68 ± 0.59	0.10 ± 0.00

The relative mean fluorescence intensity (MFI) of TMRE fluorescence was determined by flow cytometry and expressed relative to untreated cells. Results show average relative geometric mean values for 2-3 independent experiments ± SEM. When no SEM value is given, n=1

3.3.2. Caspase-3 activation

Reduction of $\Delta_{\psi m}$ on its own is not an absolute indicator of apoptosis as dissipation of $\Delta_{\psi m}$ may also occur as a result of stress-induced inhibition of mitochondrial respiration. Further confirmation of apoptosis was undertaken by detection of activated caspases. The extrinsic and intrinsic apoptotic pathways culminate with activation of the execution caspases and mark the final stage of apoptosis. I investigated levels of active caspase-3, a central executioner caspase activated by the initiator caspases, caspase-8 or -10 (extrinsic pathway) or caspases-9 (intrinsic pathway).

Cells were treated with Ad5Hey1 or AdE1A12S with and without chemotherapy as before and cells harvested and stained for active caspase-3 and examined by cytometric analysis at 72h post treatment. Ad5GFP was not included in this study since the active caspase-3 antibody was labelled with a fluorescein (FITC) tag. Induction of caspase activation was also examined by western blot (section 3.3.3).

Treatment with staurosporine indicated relative activation levels of caspase-3 varied between cell lines with 22Rv1 cells the least resistant (66.6% of cells) and DU145 cells the most resistant (45.6% of cells) (Figure 53). In agreement with the $\Delta_{\psi m}$ studies, induction of active caspase-3 by adenoviral mutants or drugs alone varied between cell

lines and the extent of relative caspase-3 activation mirrored the degree of $\Delta_{\psi m}$ depolarisation for each agent. In 22Rv1 and LNCaP cells, adenoviral mutants significantly induced active caspase-3 over that of untreated cells whereas in DU145 cells they did not.

The differences between combination treatments and single drug treatment reflected the results obtained in the $\Delta_{\psi m}$ studies. In 22Rv1 cells, Ad5Hey1 significantly enhanced docetaxel and mitoxantrone-induced activation of caspase-3 compared with drug treatment alone. However Ad5Hey1 alone was also able to stimulate active caspase-3 in 55.6% of cells and was more potent than AdE1A12S (28.8%). Although high levels of active capase-3 was generated by the adenoviral mutants, combination with cytotoxic drugs did not produce an additive effect with respect to active caspase-3 levels rather the presence of Ad5Hey1 augmented drug-induced capase-3 activation.

Although treatment with mitoxantrone did not result in $\Delta_{\psi m}$ depolarisation in LNCaP cells, a small but significant proportion of cells expressed active caspase-3 (9.0%) compared with 2.7% in untreated cells suggesting mitoxantrone may be activating the extrinsic apoptotic pathway. Ad5Hey1 and AdE1A12S induced similar levels of active caspase-3 to mitoxantrone (10.4 and 15.8% respectively). Docetaxel, the more potent of the two drugs in stimulating $\Delta_{\psi m}$ depolarisation, induced activate caspase-3 in 20.8% of cells. The expression of Hey1 in combination with either drug significantly increased levels of active caspase-3 compared with drug alone (mitoxantrone; 22.7% of cells and docetaxel; 36.5%). AdE1A12S in combination with either drug also increased the proportion of cells with active caspase-3, 39.2% when combined with mitoxantrone and 53.7% with docetaxel.

DU145 cells were resistant to adenoviral-mediated caspase-3 activation (<5% of cells) but were sensitive to cytotoxic drug treatment with 29.8% or 73.4% of cells with active caspase-3 after treatment with docetaxel and mitoxantrone respectively. Ad5Hey1 in combination with mitoxantrone resulted in a significant decrease in the proportion of cells with activated caspase-3 (50.4%) in agreement with the time course data, compared with drug alone and corresponded with the decrease in $\Delta_{\psi m}$ depolarisation. Conversely, Hey1 expression with docetaxel treatment resulted in a small increase in the percentage of cells with active caspase-3 (36.0%) compared with drug alone. In line with results obtained in 22Rv1 and LNCaP cells, AdE1A12S was able to enhance both mitoxantrone and docetaxel-mediated accumulation of cells with active caspase-3.

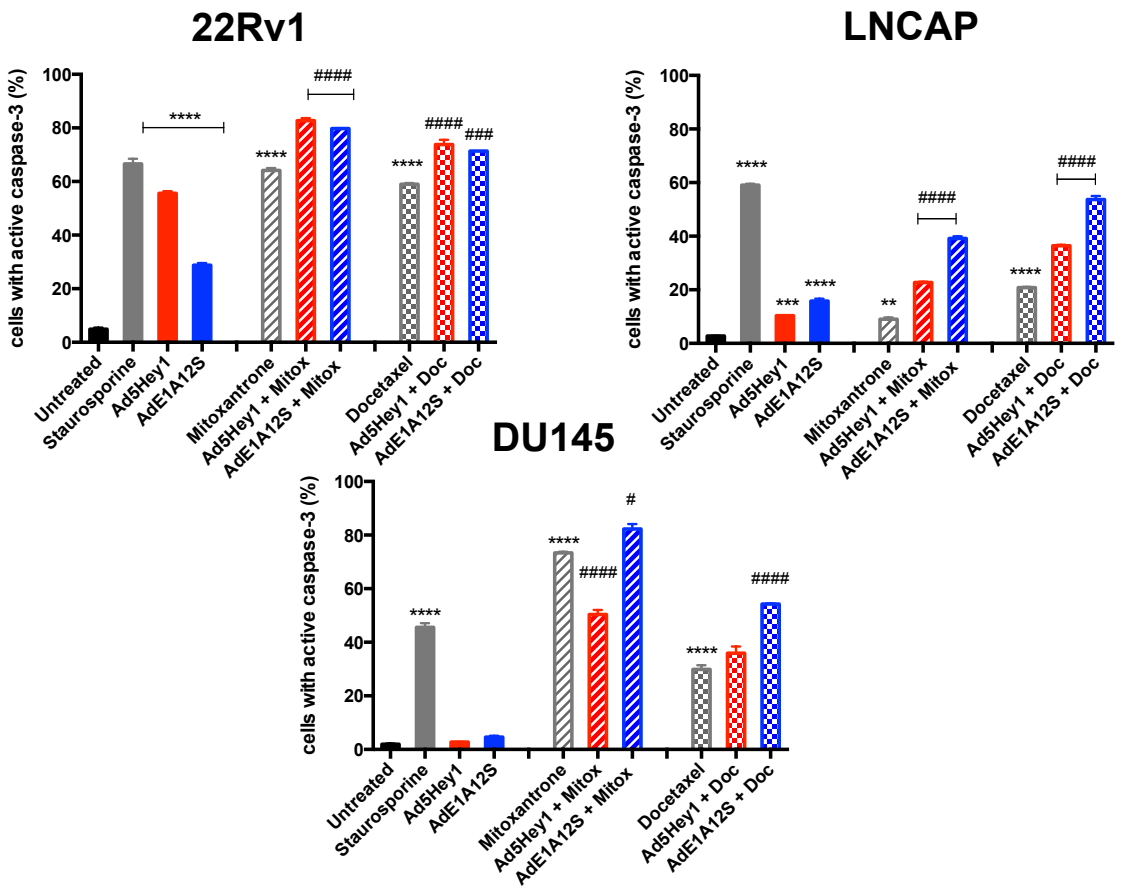

Figure 53. Ad5Hey1 enhances mitoxantrone and docetaxel-induced active caspase-3 in 22Rv1 and LNCaP cells but only docetaxel-induced active caspase-3 in DU145 cells

Cells were infected with Ad5Hey1#2 (22Rv1) or Ad5Hey1#3 (DU145 and LNCaP) or AdE1A12S#3 and/or treated with either mitoxantrone or docetaxel in 10% FBS medium at the doses listed in Table 11. Cells were treated with 0.5μM staurosporine overnight as a positive control for apoptosis. At 72h cells were harvested, permeabilised and stained with a FITC-labelled specific for active caspase-3 antibody and analysed by flow cytometry. Results are shown for duplicate wells ± SEM for one experiment, representative of two independent experiments. Statistical analysis was carried out using one-way ANOVA with multiple comparisons Tukey post-test.p<0.01 (**) p<0.001 (***/****) compared with untreated cells p<0.05 (#), p<0.01 (##) p<0.001 (###/####) compared with respective single drug treatment.

3.3.3. Expression levels of proteins involved in apoptosis increase during combination treatment

Expression levels of proteins involved in synergistic cell death were investigated to verify whether Ad5Hey1 sensitised PCa cells to drug-induced apoptosis. Cells were treated with the same doses of virus and drugs as used in the $\Delta_{\psi m}$ and active capsase-3 studies and lysates harvested 48h post-treatment and prepared for western blot analysis. In 22Rv1 cells, increased expression of total p53 and phospho-p53 was detected in Ad5Hey1-infected combination treatments compared with single agent

treatments (Figure 54). Synergy between Ad5Hey1 and drugs resulted in enhanced p53 activation compared with AdE1A12S-infected combinations supporting the theory that Ad5Hey1-mediated mechanisms of sensitisation is facilitated through increased p53 signalling compared with AdE1A12S. Confirmation of increased cell death by combination treatment with Ad5Hey1 in 22Rv1 cells was indicated by a decrease in expression levels in full-length poly ADP ribose polymerase (PARP) and an increase in levels of cleaved PARP compared with drug or virus alone treatments (Figure 54). Enhancement of apoptotic cell death in combination treatments was corroborated by increased expression of cleaved caspase-7. No cleaved PARP and low levels of cleaved caspase-7 was observed in the Ad5GFP-infected treatments confirming sensitising effect of Hey1 or E1A12S was specific (Figure 54). To characterise the apoptotic mechanism of cell death further, protein expression of Bax, a pro-apoptotic protein associated with the mitochondria was analysed. Bax, functions with Bak or tBid to form channels in the outer mitochondrial membrane to facilitate mitochondrial membrane permeabilisation (Taylor, Cullen et al. 2008). A trend towards an increase in Bax expression at approximately 23kDa was observed after treatment with either drug, Ad5Hey1 or AdE1A12S alone. Interestingly, a small faint band (~15KDa) was also detected with these treatments, which was not present in untreated cells or the Ad5GFP-infected sample. Combination treatment with mitoxantrone or docetaxel increased expression of the lower band and more expression was observed in the Ad5Hey1 or AdE1A12S-infected samples compared with Ad5GFP combinations. It is not possible to confirm whether the smaller band represents a smaller isoform or a cleaved form of Bax although expression patterns seem to correlate with enhanced apoptosis in these samples. This was observed in only one experiment and therefore further experiments would be necessary to confirm this trend. A stauroporine-treated control would indicate whether this is a product of apoptosis.

22Rv1 48hpi

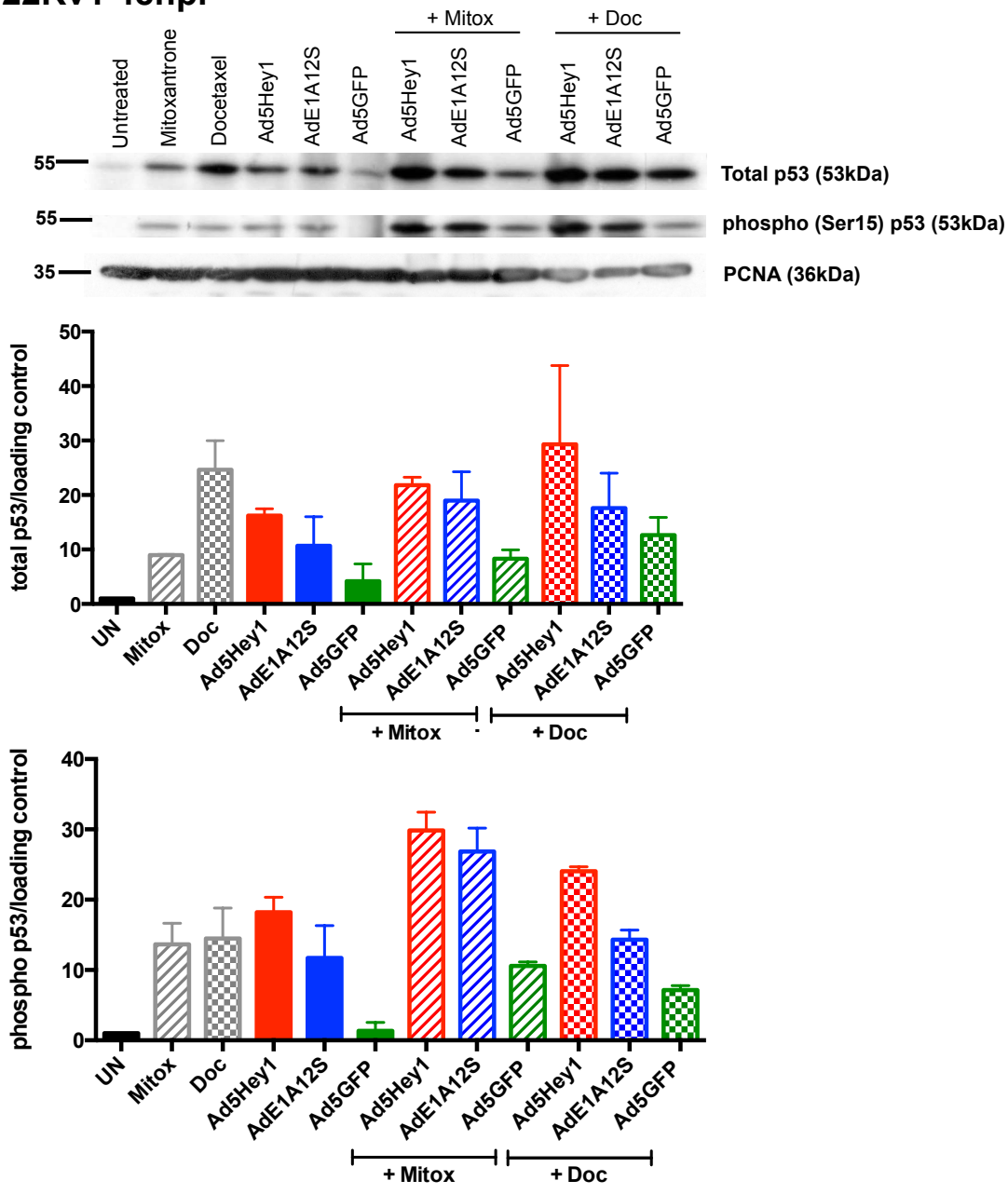
+ Mitox
+ Doc
Untreated
Mitoxantrone
Docetaxel
Ad5Hey1
AdE1A12S
Ad5GFP
Ad5Hey1
AdE1A12S
Ad5GFP
Ad5Hey1
AdE1A12S
Ad5GFP
55
55
35
Total p53 (53kDa)
phospho (Ser15) p53 (53kDa)
PCNA (36kDa)
total p53/loading control
50
40
30
20
10
0
UN
Mitox
Doc
Ad5Hey1
AdE1A12S
Ad5GFP
Ad5Hey1
AdE1A12S
Ad5GFP
Ad5Hey1
AdE1A12S
Ad5GFP
+ Mitox
+ Doc
phospho p53/loading control
40
30
20
10
0
UN
Mitox
Doc
Ad5Hey1
AdE1A12S
Ad5GFP
Ad5Hey1
AdE1A12S
Ad5GFP
Ad5Hey1
AdE1A12S
Ad5GFP
+ Mitox
+ Doc

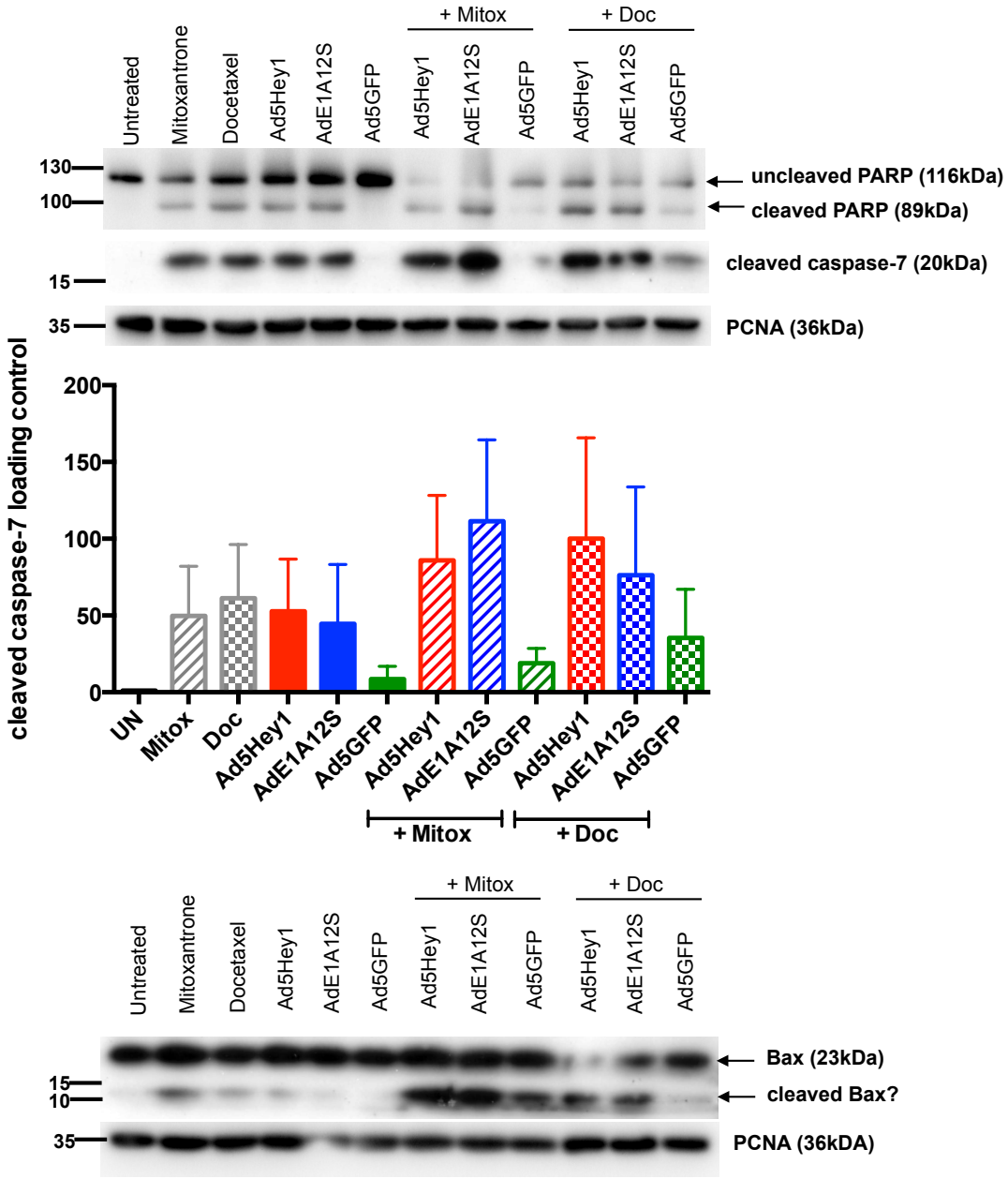

Figure 54. Ad5Hey1 enhances drug-induced p53 signalling resulting in increased expression of proteins involved in apoptosis in 22Rv1 cells

22Rv1 cells were infected with Ad5Hey1#2 (480ppc), AdE1A12S#3 (120ppc) and Ad5GFP (480ppc). After 2h, medium was removed and replaced with either standard 10% FBS DMEM or medium containing 25nM mitoxantrone or 5nM docetaxel. Lysates were harvested 48h post-treatment and prepared for separation on polyacrylamide gels. 20μg of protein was loaded per lane and probed for PARP, cleaved caspase-7 or Bax expression. Membranes were blotted for phospho (ser15) p53 first and then stripped before being probed for total p53. PCNA was used as a loading control. Histograms showing mean total p53, phospho (ser15) p53 and cleaved caspase-7 protein expression normalised to PCNA and expressed relative to untreated (UN) cells of two independent experiments ± SEM. Blots showing total, phospho (ser15) p53 and cleaved caspase-7 expression are representative of 2 independent experiments. Blots showing PARP cleavage and Bax expression are from one experiment.

From the results of one experiment in DU145 cells, docetaxel-induced apoptosis was enhanced in Ad5Hey1-infected cells as detected by increased levels of cleaved PARP and caspase-7 levels (Figure 55). In agreement with the caspase-3 studies, levels of cleaved PARP and caspase-7 were increased when Ad5Hey1 was combined with mitoxantrone compared with single drug treatment. PARP cleavage occurs by caspase-dependent and –independent means (other proteases include calpains, cathespins, granzymes and matrix metalloproteinases) and the resulting PARP fragments mediate diverse mechanisms of cell death (Chaitanya, Steven et al. 2010). The modes of PARP-mediated cell death in DU145 cells are unknown, it is conceivable that in this cell line the main mechanism of PARP cleavage is caspase-dependent and therefore it would not be surprising to detect a reduction in PARP fragmentation under these circumstances. Consequently alternative mechanisms of cell death when Ad5Hey1 is combined with mitoxantrone should be considered.

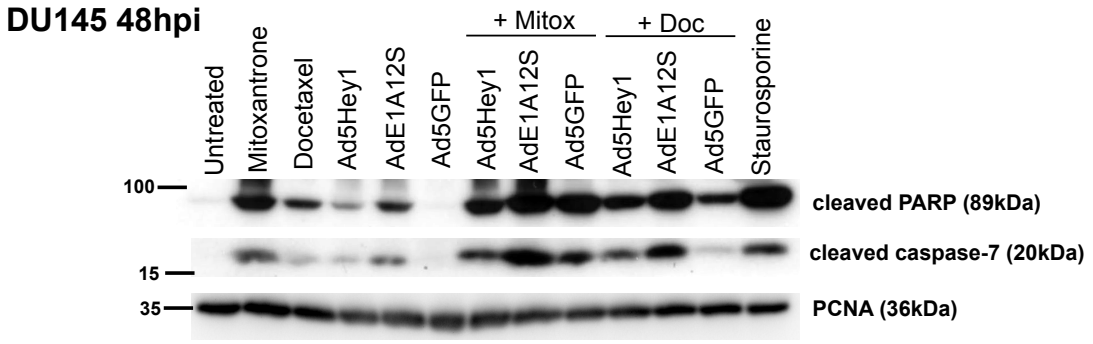

Figure 55. Ad5Hey1 enhances docetaxel- but not mitoxantrone-induced apoptosis in DU145 cells

DU145 cells were infected with Ad5Hey1#3 (1800ppc), AdE1A12S#3 (900ppc) and Ad5GFP (1800ppc). After 2h, medium was removed and cells treated with standard 10% FBS DMEM or medium containing 50nM mitoxantrone or 5nM docetaxel. Lysates were harvested 48h post-treatment and prepared for separation on polyacrylamide gels. 20μg of protein was loaded per lane and blotted for PARP or cleaved caspase-7. PCNA was used as a loading control.

Observations from one experiment in LNCaP cells demonstrated Ad5Hey1 or AdE1A12S in combination with either mitoxantrone or docetaxel increased phospho-p53 levels compared with respective drug treatments alone (Figure 56). At the doses of Ad5Hey1 and AdE1A12S used as single agent treatments, phosphorylation of p53 was not significantly induced and was similar to Ad5GFP. Enhancement of apoptosis when Ad5GFP was combined with docetaxel (Figure 49) was also reflected in phospho-p53 levels indicating the presence of GFP might enhance p53 signalling in these cells and could also account for the small increase of apoptotic cells observed in the TMRE time course study. An increase in phospho-p53 was also observed for Ad5GFP combined with mitoxantrone. However from the loading control this might be due to more protein

being present in this lane. Increased cell death when Ad5Hey1 was combined with drugs was observed through increased expression of cleaved caspase-7 in the presence of mitoxantrone (but no PARP cleavage) and both increased cleaved caspase-7 (multiple forms) and PARP cleavage in the presence of docetaxel.

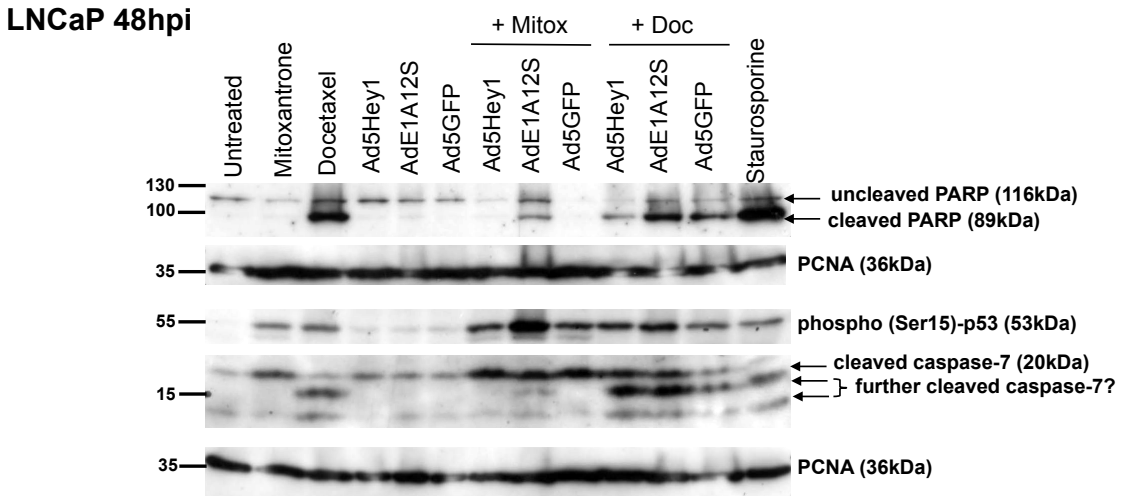

Figure 56. Ad5Hey1 augments drug-induced p53 signalling resulting in increased apoptosis in LNCaP cells

LNCaP cells were infected with Ad5Hey1#3 (360ppc), AdE1A12S#3 (240ppc) and Ad5GFP (360ppc). After 2h, medium was removed and cells treated with standard 10% FBS RPMI or medium containing 25nM mitoxantrone or 5nM docetaxel. Lysates were harvested 48h post-treatment and prepared for separation on polyacrylamide gels. 20μg of protein was loaded per lane and blotted for phospho (ser15) p53, PARP or cleaved caspase-7. PCNA was used as a loading control.

3.3.4. Summary of apoptotic cell death studies

The results obtained from the $\Delta_{\psi m}$ depolarisation and active caspase-3 studies indicate the level of apoptosis induced by chemotherapeutic drugs or adenoviral mutants was cell line-dependent. In terms of virus-induced apoptosis, 22Rv1 cells were the most sensitive stimulating both $\Delta_{\psi m}$ depolarisation and caspase-3 activation to similar degrees. In LNCaP cells, neither virus induced $\Delta_{\psi m}$ depolarisation while both activated caspase-3 similarly. In DU145 cells, neither virus mutant stimulated $\Delta_{\psi m}$ depolarisation or caspase-3 activation above basal levels. Sensitivity of cells to drugs appeared to be dependent on the mechanism of action employed by the drug. 22Rv1 cells were the most sensitive to drug-induced apoptosis and both drugs depolarised $\Delta_{\psi m}$ and activated caspase-3 to a similar degree. LNCaP and DU145 cells were less sensitive to docetaxel-induced $\Delta_{\psi m}$ depolarisation than 22Rv1 cells whereas mitoxantrone-induced $\Delta_{\psi m}$ depolarisation in DU145 cells was similar to 22Rv1 cell and no mitoxantrone-induced $\Delta_{\psi m}$ depolarisation was observed in LNCAP cells. Levels of activated caspase-

3 paralleled this cell line-dependent relationship for docetaxel in both LNCaP and DU145 cells and only in DU145 for mitoxantrone. Mitoxantrone treatment induced a small increase in caspase-3 activation in LNCaP cells indicating activation of apoptosis via non-mitochondrial pathways.

Combining Ad5Hey1 with docetaxel or mitoxantrone in 22Rv1 and docetaxel in LNCaP cells resulted in augmentation of drug-induced $\Delta_{\psi m}$ depolarisation and activation of caspase-3. Combining Ad5Hey1 with mitoxantrone in LNCaP cells resulted in significant $\Delta_{\psi m}$ depolarisation not seen with either virus or drug alone. This suggests cooperation between Ad5Hey1- and mitoxantrone-induced modes of cell death. These differences were accurately reflected on the protein level in 22Rv1 cells 48h post-treatment; enhanced PARP cleavage and cleaved caspase-7 in combination with Ad5Hey1 with either docetaxel or mitoxantrone. In LNCaP cells, cleaved caspase-7 protein levels were increased in either drug combination treatment, in agreement with the active caspase-3 studies. Curiously, no PARP cleavage was observed when Ad5Hey1 was present although this was detected for the AdE1A12S combination.

In DU145 cells, Ad5Hey1-mediated enhancement of drug-induced apoptosis was not as well defined as with cells expressing functional p53. Ad5Hey1 enhanced docetaxel-induced $\Delta_{\psi m}$ depolarisation and increased PARP and caspase-7 cleavage above levels induced by docetaxel alone. On the other hand, combination treatment with Ad5Hey1 and mitoxantrone in DU145 cells resulted in a decrease in $\Delta_{\psi m}$ depolarisation and active caspase-3 compared to cells treated with mitoxantrone alone despite synergistic cell death demonstrated at these doses of virus and drug (section 3.2.1). Apoptotic protein expression levels were in agreement with these findings; reduced levels of PARP and caspase-7 cleavage. Ad5Hey1 seemed to have a protective effect on apoptosis with this treatment combination as significantly more necrotic cells were detected than drug alone indicating cells were dying by a non-apoptotic process. As expected, AdE1A12S enhanced both docetaxel and mitoxantrone-induced apoptosis in line with previous findings (Miranda, Maya Pineda et al. 2012).

In conclusion, Ad5Hey1 enhanced docetaxel-induced apoptosis in all cell lines but augmented mitoxantrone-induced apoptosis only in 22Rv1 and LNCaP cells. In DU145 cells, Ad5Hey1 sensitised cells to mitoxantrone-induced cell killing through non-apoptotic cell death mechanisms. Docetaxel and mitoxantrone have differential effects on cell growth inhibition; a cytotoxic effect in 22rv1 and DU145 cells and at the low dose in these experiments, a cytostatic effect in LNCaP cells. Since the cytostatic

effect was observed visually, examination of the cell cycle in response to mitoxantrone in these cells is required. These contrasting drug-induced effects on cell viability may influence the mode of cell death during sensitisation with Ad5Hey1. The analysis of drug-induced $\Delta_{\psi m}$ hyperpolarisation in LNCaP and DU145 cells may pertain to possible action on mitochondrial function

3.4. Efficacy of Ad5Hey1 in androgen-responsive and androgen-ablation resistant PCa cells

3.4.1. Ad5Hey1 attenuates mibolerone-stimulated cell growth and cooperates with bicalutamide to reduce growth of AR-positive cells

I have demonstrated (section 3.1.2) that Ad5Hey1 decreased AR transcriptional activity in a dose-dependent manner in 22Rv1 cells, specifically in response to Hey1 expression. In addition, Ad5Hey1 cooperated with bicalutamide to further decrease AR signalling in this cell line. Ad5Hey1-mediated cytotoxicity was partially dependent on the expression of AR and knockdown of AR resulted in a reduction of Ad5Hey1-dependent cell death (section 3.1.3). Considering most PCa evolve into antiandrogen resistance phenotypes (CRPC), I hypothesised that Ad5Hey1 could sensitise AR-expressing and hormone ablation-resistant PCa to drugs such as bicalutamide.

Ad5Hey1-mediated reduction in cell viability was assessed in three AR-positive cell lines, LNCaP, 22Rv1 and VCaP cells each reflecting a different point of AR re-activation in the transition of androgen-dependent PCa to CRPC. LNCaP and 22Rv1 both possess mutations in their AR whereas VCaP cells contain an amplified AR gene locus that encodes wild-type AR protein (section 2.2; Table 5). As well as studying the effect of Ad5Hey1 in combination with bicalutamide, I also stimulated cells with mibolerone to assess the efficacy of Ad5Hey1 under conditions that induced cell growth. This aspect of the experimental setup was to re-establish a more physiological setting since CRPC tumours have been found to be receptive to very low levels of androgens allowing them to grow during ADT.

Cells were infected with a fixed dose of Ad5Hey1 (EC_{50}) or an equal dose of Ad5GFP (negative control) in the presence of 1nM mibolerone ± 5, 10 or 20μM bicalutamide and cell viability measured 3 days post treatment. The doses of bicalutamide selected have

previously been used by others (Cai, He et al. 2011; De Leon, Iwai et al. 2011) and in this study were shown not to cause significant cell killing alone.

In agreement with the literature, mibolerone stimulated growth of androgen-sensitive LNCaP cells (146.7±7.1% relative to vehicle-treated; 100%) (Figure 57). Bicalutamide reduced both mibolerone-stimulated and basal growth in a dose-dependent manner. All conditions with bicalutamide reduced growth below basal levels except for 1nM mibolerone+5μM bicalutamide. Infection with Ad5Hey1 inhibited mibolerone-induced cell growth by 60% (to 86.2±9.6%) below levels of mibolerone-treated cells whereas infection with Ad5GFP remained similar (146.2±11.4%). Higher doses of bicalutamide (10 and 20μM) cooperated with Ad5Hey1 to further decrease mibolerone-stimulated cell growth (10μM; 66.9±4.0% and 20μM; 54.2±0.75%) and resulted in less cell growth compared with the corresponding conditions without AdHey1. Interestingly, no additional growth inhibition was observed with 5μM bicalutamide in the presence of AdHey1 and mibolerone. In the absence of mibolerone, 5μM bicalutamide further repressed Ad5Hey1-mediated growth inhibition from 42.8±4.5% to 33.8±5.0%; no further improvement was observed with higher doses of bicalutamide. This reduction was significant compared with uninfected cells treated with 5μM bicalutamide (79.7±3.9%). A small degree of non-specific toxic effects occurred as a result of infection with Ad5GFP alone (75.4±2.6%), however no statistical difference was observed between Ad5GFP combination treatments and uninfected cells treated with bicalutamide at any dose.

The 22Rv1 cells, androgen-responsive but independent, were less sensitive to the effects of mibolerone than LNCaP cells resulting in 120.5±2.6% cell growth (Figure 57). Increasing doses of bicalutamide inhibited mibolerone-stimulated growth in a dose dependent fashion (5μM; 107.8±3.7%, 10μM; 104.6±3.2%, 20μM; 97.6±3.3%). However, in the absence of mibolerone growth was not affected by bicalutamide at any dose. Surprisingly, stimulating 22Rv1 cells with mibolerone resulted in a sensitising effect to Ad5Hey1-dependent cell growth inhibition (Ad5Hey1; 43.2±3.7%, AdHey1 with mibolerone; 31.8±3.8%) not observed with Ad5GFP (Ad5GFP; 93.2±0.5%, with mibolerone; 108.4±3.2%). Interestingly, the addition of bicalutamide to mibolerone and Ad5Hey1 treatment did not contribute any further benefit to cell growth inhibition. This was unexpected based on the cooperative effects Ad5Hey1 and bicalutamide had on AR transcriptional activity (section 1.8.1, Figure 13). In contrast, bicalutamide slightly prevented androgen-dependent growth stimulation in Ad5GFP-infected cells. In the absence of mibolerone, Ad5Hey1 in combination with bicalutamide resulted in further

decreases in cell growth compared with the virus alone however a trend towards biphasic growth (peaking at 10μM) was observed with bicalutamide, which was not observed in uninfected or Ad5GFP-infected cells.

The VCaP cells were introduced into this study as an additional AR-positive cell line. These cells are more responsive to mibolerone stimulation than LNCaP cells (160.4±2.3%) (Figure 57). However addition of 5 or 10μM bicalutamide did not result in cell growth inhibition. Only the highest dose of 20μM partially reversed the growth effect of mibolerone (141.95%). Basal growth was also unaffected by bicalutamide treatment. Infection of Ad5Hey1 efficiently killed cells as a single agent. However, in the presence of mibolerone Ad5Hey1 did not significantly reduce androgen-stimulated cell growth (129.3±14.3%; compared to mibolerone alone, 160.4±2.3%) in contrast to the decrease observed in LNCaP cells. Encouragingly however, additional treatment with bicalutamide cooperated with Ad5Hey1 to further reduce cell growth (5μM; 96.1±11.9%, 10μM; 79.3±8.8% and 20μM; 72.3%). As with LNCaP, VCaP cells were more sensitive to growth inhibitory effects of Ad5GFP (73.2±1.6%). Nevertheless, combination treatment with mibolerone and bicalutamide in the presence of Ad5GFP resulted in effects that were more similar to those noted for uninfected cells.

As anticipated, AR-negative and androgen independent DU145 cells were not responsive to either mibolerone or bicalutamide although were efficiently killed by Ad5Hey1 (Figure 57). These findings suggest that, cell growth-inhibition in AR-positive cell lines in response to Ad5Hey1 in combination with mibolerone and/or bicalutamide are caused by AdHey1-mediated effects on the AR proliferation pathway.

In summary, the effectiveness of Ad5Hey1 in the presence of growth stimulating conditions appeared to be cell-line dependent and may be reliant on factors such as the AR mutation status and/or AR copy number of the particular cell line. From the point of view of a therapeutic application, Ad5Hey1 was able to cooperate with bicalutamide in the presence of mibolerone to inhibit growth or when mibolerone was absent, Ad5Hey1 did not counteract the effects of bicalutamide which would be relevant in the context of castrate serum levels of testosterone when levels of circulating androgens are very low (<50ng/dL/1.7nmol/L) (Heidenreich 2012).

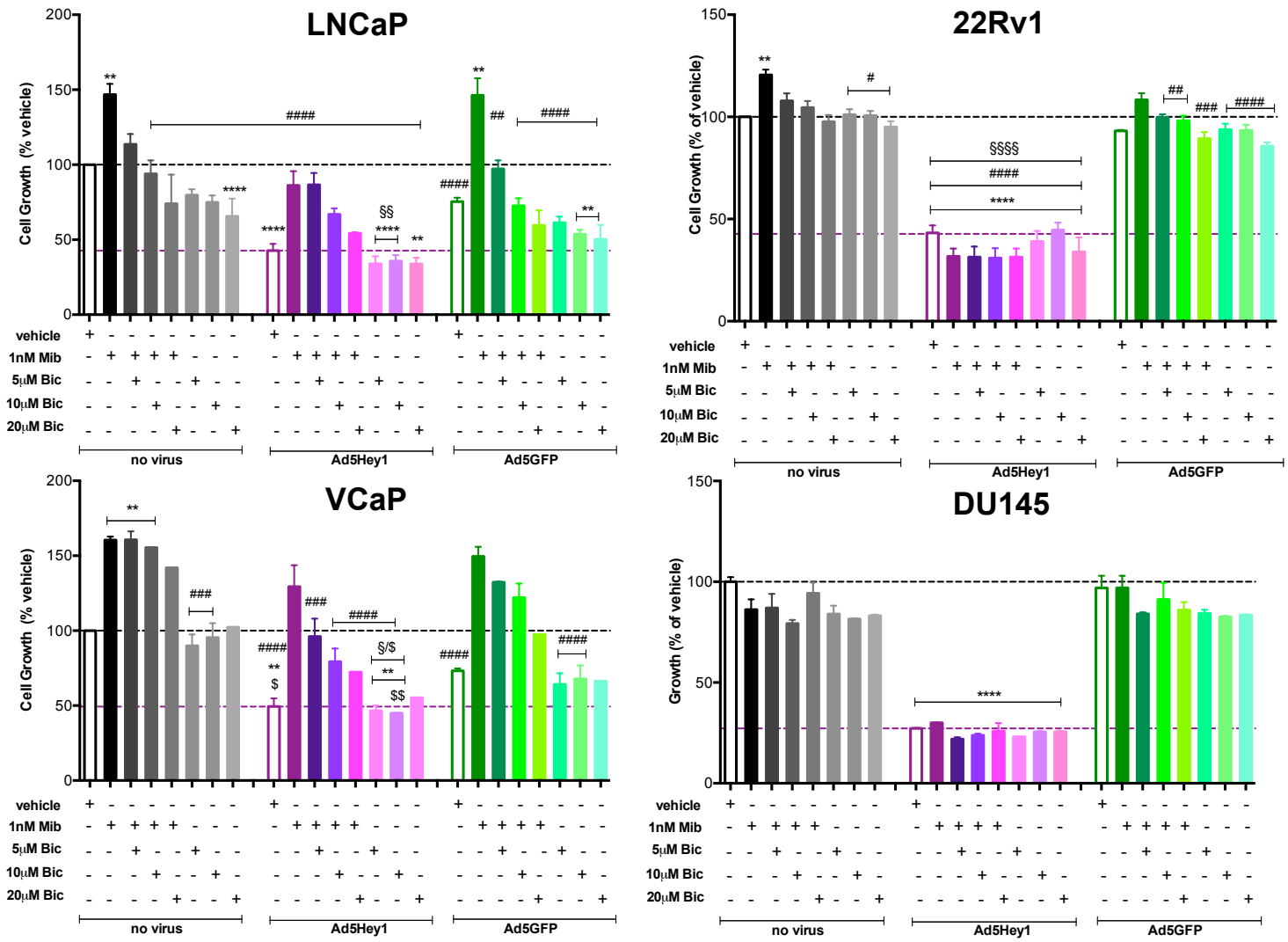

Figure 57. Ad5Hey1 in combination with mibolerone and bicalutamide has differential effects on cell growth inhibition in AR-positive LNCaP, 22Rv1 and VCaP cells

Cells were infected with a fixed dose (EC_{50}) of Ad5Hey1#2 (22Rv1; 800ppc) or Ad5Hey1#3 (LNCaP; 600ppc, VCaP; 6000ppc and DU145; 1800ppc) and treated with either vehicle (0.2% ethanol) or 1nM mibolerone (Mib) ± 5, 10 or 20μM bicalutamide (Bic) in 0.2% ethanol. Cell viability was assessed 3 days post-treatment by MTS assay and cell growth expressed as a percentage relative to vehicle control. Results shown are means of duplicate wells from 6 independent experiments (22Rv1 and LNCaP 1nM mibolerone ± 5-10μM bicalutamide), 2 independent experiments (22Rv1 and LNCaP 1nM Mib ± 20μM Bic and VCaP, except 20μM Bic conditions, n=1) ± SEM and duplicate wells of one experiment ± SEM (DU145). One way ANOVA statistical analysis was carried out using multiple comparisons with a Tukey post-test, p<0.01 (**) and p<0.001 (***/****) compared to vehicle. p<0.05 (#), p<0.01 (##) and p<0.001 (###/####) compared with mibolerone-treated cells. p<0.01 (§§) compared with 5μM Bic (LNCaP), p<0.001 (§§§§) compared with 5,10 and 20μM Bic (22Rv1), p<0.05 (§) compared with 5μMBic, p<0.05 ($), p<0.01 ($$) compared with 10μM Bic (VCaP).

3.4.2. Androgen-independent and androgen ablation-resistant PCa cells, 104-R1 and CDXR3 are more sensitive to Ad5Hey1 than parental 104-S

I demonstrated in the studies above, that Ad5Hey1 could cooperate with bicalutamide to enhance growth inhibition in androgen-sensitive LNCaP and androgen-responsive VCaP cells. I therefore sought to explore the effect of Ad5Hey1 in androgen-independent, bicalutamide-insensitive cell lines. LNCaP cells were chosen since historically androgen-independent sub-clones of this cell line have been well characterised. We obtained three LNCaP cell lines designated 104-S, 104-R1 and CDXR3. The parental cell line, androgen-sensitive LNCaP 104-S is stimulated and repressed by androgen and bicalutamide, respectively, while the sub-clones 104-R1 and CDXR3 are paradoxically repressed by androgen and unresponsive to bicalutamide (Kokontis, Takakura et al. 1994; Kokontis, Hay et al. 1998; Kokontis, Hsu et al. 2005). 104-R1 cells were established by long-term culturing of 104-S cells in androgen-depleted conditions. To more closely mimic the clinical situation, 104-S were cultured in androgen-deficient medium supplemented with 5μM bicalutamide to derive CDXR3 cells (Kokontis, Hsu et al. 2005). Both 104-R1 and CDXR3 cells have been reported to express elevated AR protein levels and exhibit increased AR transcriptional activity however selection of CDXR3 cells by antiandrogen treatment is thought to bypass the intermediary 104-R1 stage and are considered more advanced in terms of disease progression (Kokontis, Takakura et al. 1994; Kokontis, Hsu et al. 2005; Chuu, Kokontis et al. 2011).

Virus dose response curves were generated for Ad5Hey1 and the percentage of cell death assessed three days post-infection to determine EC_{50} values. In this study Ad5GFP was not included as incomplete dose response curves (not shown) made it impossible to accurately calculate EC_{50} values. For this reason I used Ad5 as a suitable reference and comparable cell killing was induced by Ad5 infection in all cell lines (Figure 58A). Interestingly, I found the androgen ablation-resistant and antiandrogen-resistant sub-lines were more sensitive to Ad5Hey1-mediated cytotoxicity compared with the parental 104-S cells (Figure 58B).

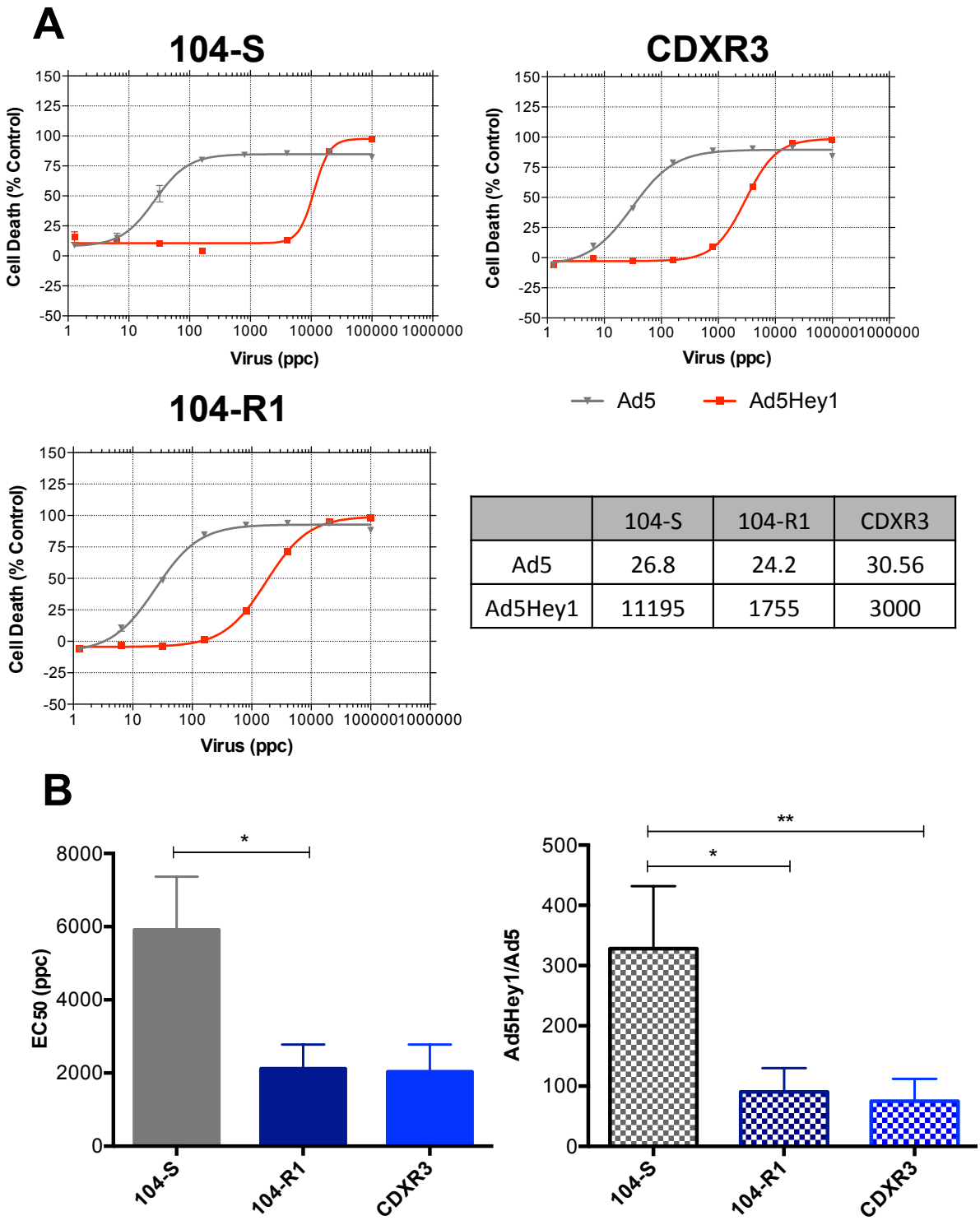

	104-S	104-R1	CDXR3
Ad5	26.8	24.2	30.56
Ad5Hey1	11195	1755	3000

Figure 58. Sensitivity to Ad5Hey1 is enhanced in androgen ablation-resistant LNCaP sublines compared with parental 104-S cells

A) Representative virus dose response curves for Ad5 and Ad5Hey1 in 104-S, 104-R1 and CDXR3 cells. Cells were infected with serial dilutions of Ad5 (grey) and Ad5Hey1 (red) and cell death assayed by MTS 3 days post-infection. EC_{50} values (ppc) calculated (table inset). Data shown is mean of duplicate wells from one experiment representative of 5-6. (B) Histogram on the left shows mean EC_{50} values of Ad5Hey1 in 104-S, 104-R1 and CDXR3 cells from 5-6 independent experiments ± SEM. Histogram on the right shows EC_{50} values of Ad5Hey1 expressed as a ratio of Ad5 for 3 independent experiments ± SEM. Statistical analysis was carried out using the one-way ANOVA with multiple comparisons with a Tukey post test, $p<0.05$ (*) and $p<0.01$ (**).

3.4.3. Proliferation of 104-R1 and CDXR3 cells are repressed by mibolerone and insensitive to bicalutamide treatment

It was encouraging to detect enhanced sensitivity to Ad5Hey1-mediated cytotoxicity in 104-R1 and CDXR3 cells. Since I observed a cooperative effect between Ad5Hey1 and bicalutamide in LNCaP and VCaP cells I investigated whether Ad5Hey1 could also sensitise ablation-resistant and antiandrogen insensitive cells to bicalutamide. As the design of the study required treating cells with mibolerone and bicalutamide it was essential to confirm the response of the 104-S sub-lines to these agents before investigating the effect of Ad5Hey1 in combination.

To verify that the response of these cells to androgen and bicalutamide corresponded to the published literature I used the same doses of androgen and bicalutamide (0.1nM mibolerone and 5μM bicalutamide) and measured cell proliferation by the percentage of cells in S phase. In agreement with previous studies by Kokontis *et al*, 0.1nM mibolerone stimulated cell cycle progression in androgen-sensitive 104-S cells measured by an increase in cells in S phase (12.5%) compared with control (5.6%) (Figure 59) (Kokontis, Hay et al. 1998; Kokontis, Hsu et al. 2005). A higher dose of 10nM resulted in a decrease in the proportion of cells in S phase compared with control cells indicative of an antiproliferative effect owing to the biphasic nature of androgens on LNCaP cell growth (de Launoit, Veilleux et al. 1991). The proportion of cells in S phase was noticeably higher in 104-R1 and CDXR3 cells compared with 104-S cells reflecting the high proliferative index of these cells. In agreement with the published literature (Kokontis, Hay et al. 1998; Kokontis, Hsu et al. 2005), the proportion of 104-R1 cells in S phase was repressed by 0.1nM mibolerone to 20.6 compared with control (25.8%) and was similarly repressed in CDXR3 cells to 17.6% compared with control (22.9%) (Figure 59). The higher dose of mibolerone at 10nM also repressed cell growth in agreement with previous reports (Kokontis, Hay et al. 1998). Treatment with 5μM bicalutamide repressed mibolerone-stimulated growth and basal growth of 104-S cells whereas it had no effect on the proliferation index of 104-R1 and CDXR3 cells. Conversely bicalutamide was able to reverse the repressive effect when treated with 0.1nM mibolerone in agreement with previous reports suggesting androgen-mediated repression of proliferation of 104-R1 and CDXR3 cells is mediated through the AR (Kokontis, Hay et al. 1998; Kokontis, Hsu et al. 2005). The dose of bicalutamide in this study was not sufficient to over come the inhibitory effects of 10nM mibolerone in the

104-R1 and CDXR3 cells indicating bicalutamide-mediated release of mibolerone-induced repression was dose-dependent.

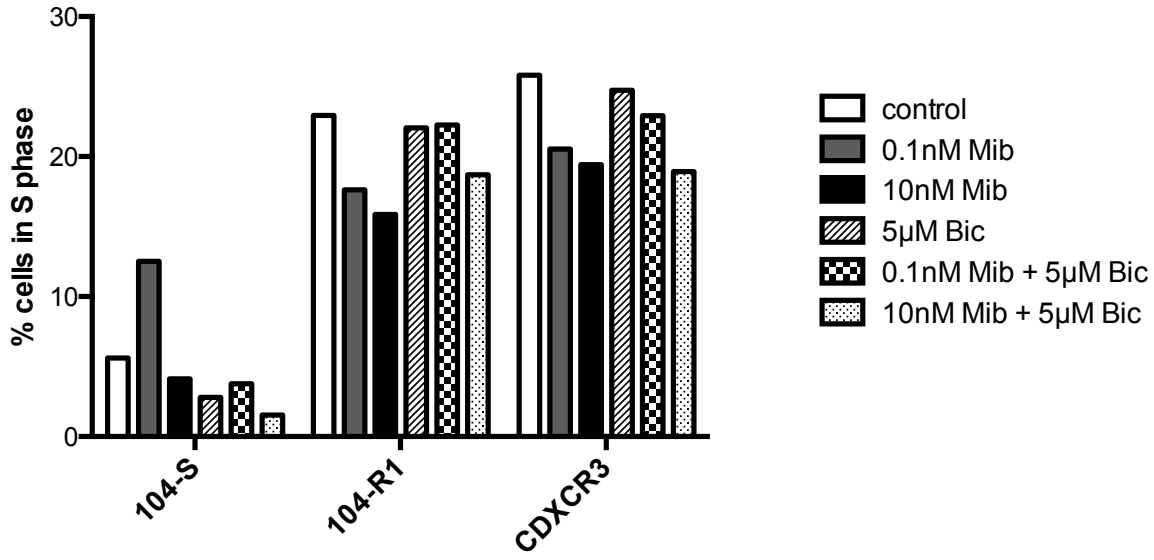

Figure 59. The effect of mibolerone ± bicalutamide on the percentage of cells in S phase in 104-S, 104-R1 and CDXR3 cells

Cells were seeded and the next day incubated in medium containing ethanol vehicle (control; 0.05% ethanol), 0.1nM and 10nM mibolerone ± 5μM bicalutamide for 96h. Cells were harvested and analysed by cell cycle analysis. Data shows single replicates representative of two independent experiments.

3.4.4. Ad5Hey1 infection induces an accumulation of cells in G1 in 104-R1 and CDXR3 cells

The effect of Ad5Hey1 on cell cycle distribution was assessed in the 104-S sub-lines. Doses of Ad5Hey1 determined to kill <30% of cells were selected based on EC_{50} values calculated from dose-response curves. Cells were infected with 3000ppc (104-S) or 1200ppc (104-R1 and CDXR3) of Ad5Hey1 or Ad5GFP and then treated with 0.1nM mibolerone with and without 5μM bicalutamide. Cell cycle progression was assessed 72h after infection/treatment.

At the doses selected, Ad5Hey1 infection of 104-R1 and CDXR3 cells resulted in a striking decrease in the percentages of cells in S phase with a corresponding increase of the proportion of cells in G1 (Figure 60). As expected, uninfected 104-S cells were responsive to mibolerone-induced S phase accumulation however in this particular experiment, the growth-inhibitory affects of bicalutamide were not apparent. However

in cells infected with Ad5Hey1 or Ad5GFP the stimulatory and repressive effects of mibolerone and bicalutamide respectively were more noticeable. In Ad5Hey1-infected cells an increase in the sub-G1 fraction was observed compared with uninfected or Ad5GFP-infected cells for all treatment combinations indicating the dose was effective at killing cells. In cells infected with Ad5Hey1 and treated with mibolerone a larger sub-G1 fraction was observed compared with other Ad5Hey1 combination treatments (Ad5Hey1 with mibolerone; 4.7%, Ad5Hey1 alone; 1.7%). Cells were still receptive to mibolerone stimulation as demonstrated by the larger S and G2/M phases compared with Ad5Hey1 alone. The addition of bicalutamide decreased the proportion of cells in the S and G2/M fractions indicating cells remain responsive to bicalutamide treatment.

On the other hand, Ad5Hey1 induced 104-R1 and CDXR3 cells to accumulate in G1. In Ad5Hey1-infected 104-R1 cells, 65.5% of cells accumulated in G1 phase compared with 49.6% of uninfected cells and 55.0% of GFP-infected cells. In CDXR3 cells, the difference was even more pronounced, 92.1% of cells were in G1 following Ad5Hey1-infection compared with 58.7% of uninfected cells and 74.7% for Ad5GFP-infected cells. The expression of GFP has a modest non-specific effect on cell cycle progression compared with uninfected cells that will require further investigation. A small increase in sub-G1 fraction also accompanied Ad5Hey1 infection in both cell lines that was not present in uninfected of Ad5GFP-infected cells. In this study, the androgen-mediated suppression of S phase was only observed for 104-R1 cells and not CDXR3. I cannot account for the anomaly in CDXR3 cells. However, in 104-R1 cells, androgen-mediated suppression of S phase was no longer apparent when cells were infected with Ad5Hey1, possibly due to the over-riding effects on cell cycle-dependent proteins mediated by Ad5Hey1.

To conclude, I have demonstrated Ad5Hey1 to have advantageous effects in an androgen-independent LNCaP cancer progression model as proved by enhanced sensitivity to Ad5Hey1-mediated cytotoxicity in 104-R1 and CDXR3 cells compared with parental 104-S cells. Mechanisms contributing to this effect have been explored and may be as a result of Ad5Hey1-mediated reduction on proliferative index as consequence of cells accumulating in G1. These initial promising results will require further investigation including studies assessing the temporal and dose-dependent effects of Ad5Hey1 infection on cell cycle distribution, TUNEL assay to determine in which phase the cells may be dying and confirmation of apoptotic cell death by caspase cleavage.

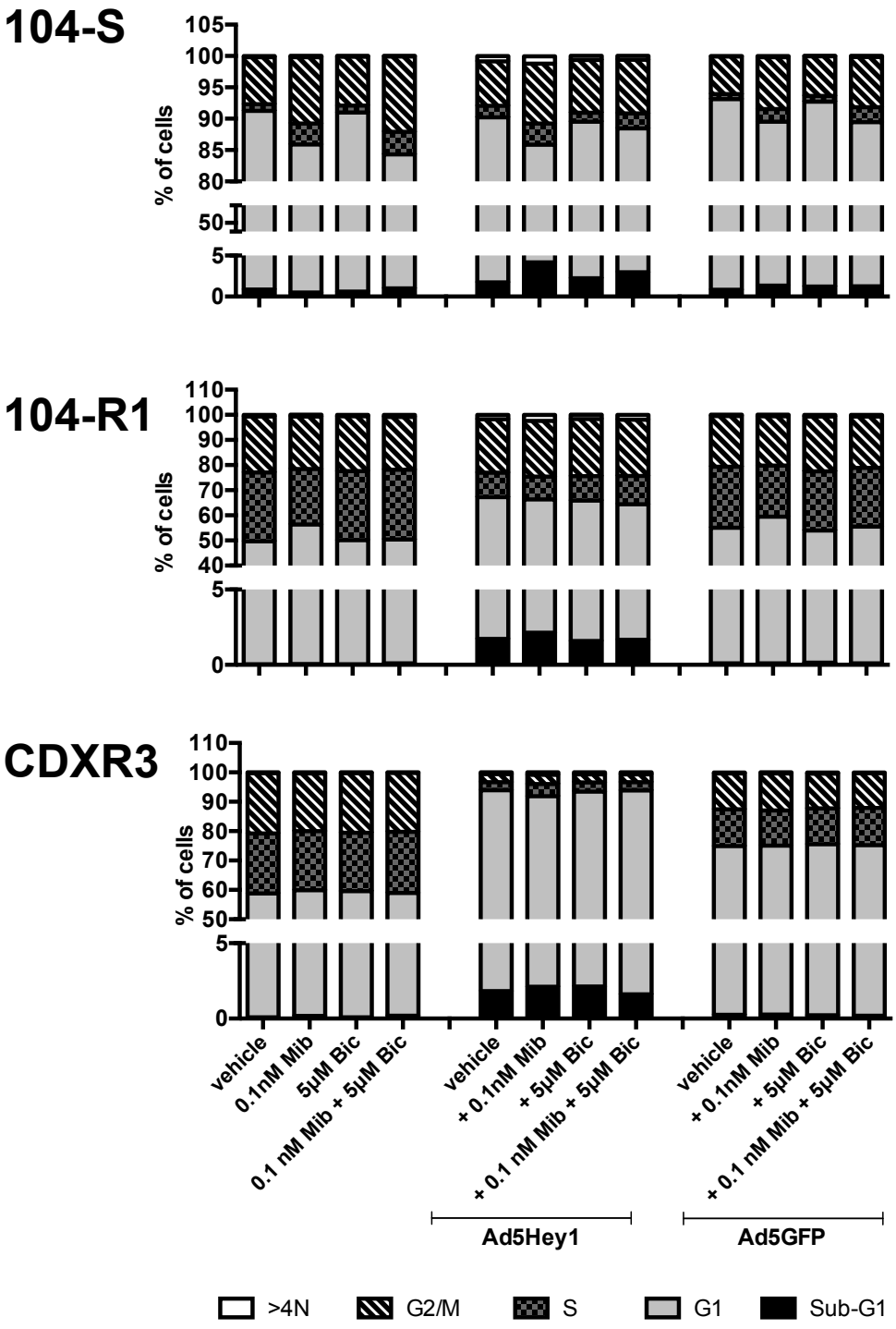

Figure 60. Androgen ablation-resistant 104-R1 and CDXR3 cells are more susceptible than parental 104-S cells to Ad5Hey1-mediated growth arrest

Cells were infected with either 3000ppc Ad5Hey1#3 or Ad5GFP (104-S) or 1200ppc Ad5Hey1#3 or Ad5GFP (104-R1 and CDXR3). After 2h, infection medium was removed and replaced with 10% FBS DMEM containing either vehicle (0.05% ethanol) or 0.1nM mibolerone and/or 5μM bicalutamide (total ethanol, 0.05%). Cells were harvested at 72h by trypsination and fixed in 70% ethanol. Cell cycle analysis was performed with PI staining. Results shown are single replicates representative of 2 independent experiments

3.5. Construction of a replication-selective oncolytic virus expressing Hey1 (AdΔΔHey1)

The replication-selective double-deleted Ad5 mutant (AdΔΔ) has recently been characterised in our research laboratory (Oberg, Yanover et al. 2010). AdΔΔ is deleted in the E1ACR2-region for selective replication in cancer cells with deregulated cell cycle control (e.g. pRb and p16 alterations) and is also deleted for E1B19K, an anti-apoptotic Bcl-2-homologue which is commonly deregulated in tumour cells (Leitner, Sweeney et al. 2009; Oberg, Yanover et al. 2010). As discussed (section 1.7.1.4), it is advantageous to preserve the E3B genes in oncolytic adenoviruses to prevent premature elimination of infected cells by macrophages and thus maintaining anti-tumour efficacy.

Two main strategies are used for engineering transgene-expressing oncolytic adenoviruses: either the insertion of a transgene cassette with a promoter and polyadenylation signal or insertion as part of a viral transcription unit. We selected the latter method since this exploits endogenous viral gene expression for transgene expression (nuclear export and translation of capped cellular mRNA are supressed during late adenovirus replication) and allow the highly regulated nature of the lytic life cycle to be harnessed for temporal specific expression of the transgene. This approach removes the requirement of exogenous regulatory sequences since the adenovirus genome can only stably package an additional 5% of the genome (approximately 1.8kb) (Heise, Hermiston et al. 2000). However, placement of the therapeutic transgene is restricted since early genes E1, E2 and E4 are required for viral replication and late structural genes are essential for viral assembly.

Previously it was demonstrated that adenoviruses deleted for the E3A gene product E3gp19K (*dl*704) demonstrated enhanced viral gene expression and increased CTL infiltration in an immunocompetent mouse model and resulted in improved efficacy (Wang, Hallden et al. 2003). Based on these findings, we hypothesized that replacing E3gp19K with the Flag-Hey1 (Hey1) transgene in the AdΔΔ backbone would improve selectivity and potency for the treatment of PCa on a number of levels. Firstly, the E1ACR2 and E1B19K deletions ensure viral replication only occurs within tumour cells. Secondly, the majority of the E3 region remains intact thereby improving viral potency

in the presence of an immune response with the E3gp19K gene deletion enhancing the CTL response. Thirdly, the expression of a transcriptional corepressor such as Hey1 may provide additional specificity to oncolytic adenovirus-induced cell killing in PCa cells, which often have deregulated Notch signalling pathways. By modulating the crosstalk between Notch signalling and other aberrant signalling pathways in PCa such as p53, AR and JAK/STAT, Hey1 may be able to therapeutically rewire PCa cells to inhibit cell proliferation and also sensitise cells to established chemotherapeutic drugs. Expression of Hey1 from the E3 promoter would be advantageous from the point of view of ensuring early expression of the cytotoxic transgene in the event of abortive viral replication.

3.5.1. Cloning strategy

The generation of Ad5 mutants by homologous recombination was previously established and described (Chartier, Degryse et al. 1996). Construction of AdΔΔHey1 was based on a cloning strategy developed by Dr Daniel Öberg, Barts Cancer Institute, London. A shuttle vector, pSuperShuttle (pSS), designed and constructed by Dr Daniel Öberg (manuscript in preparation) to facilitate gene-deletions and insertions was used to transfer the cDNA sequence of Hey1 into the AdΔΔ backbone. To facilitate homologous recombination, sequences flanking the E3gp19K region in the Ad5 genome (termed left arm (LA) and right arm (RA)) were placed either side of Hey1 to produce pSSLARAHey1. Co-transfection of pSSLARAHey1 and plasmid AdΔΔ genome would generate the recombinant AdΔΔHey1 plasmid (Figure 61). Subsequent linearization of AdΔΔHey1 and transfection into A549 cells would result in virion particles of AdΔΔHey1 that could then be expanded and produced in bulk (section 2.3.2).

Due to unforeseen technical issues during the construction of AdΔΔHey1 and time constraints, only the pSSLARAHey1 was constructed and the homologous recombination stage attempted. The implications of the use of a replication selective oncolytic virus armed with Hey1 for the treatment of CRPC will be considered within the discussion.

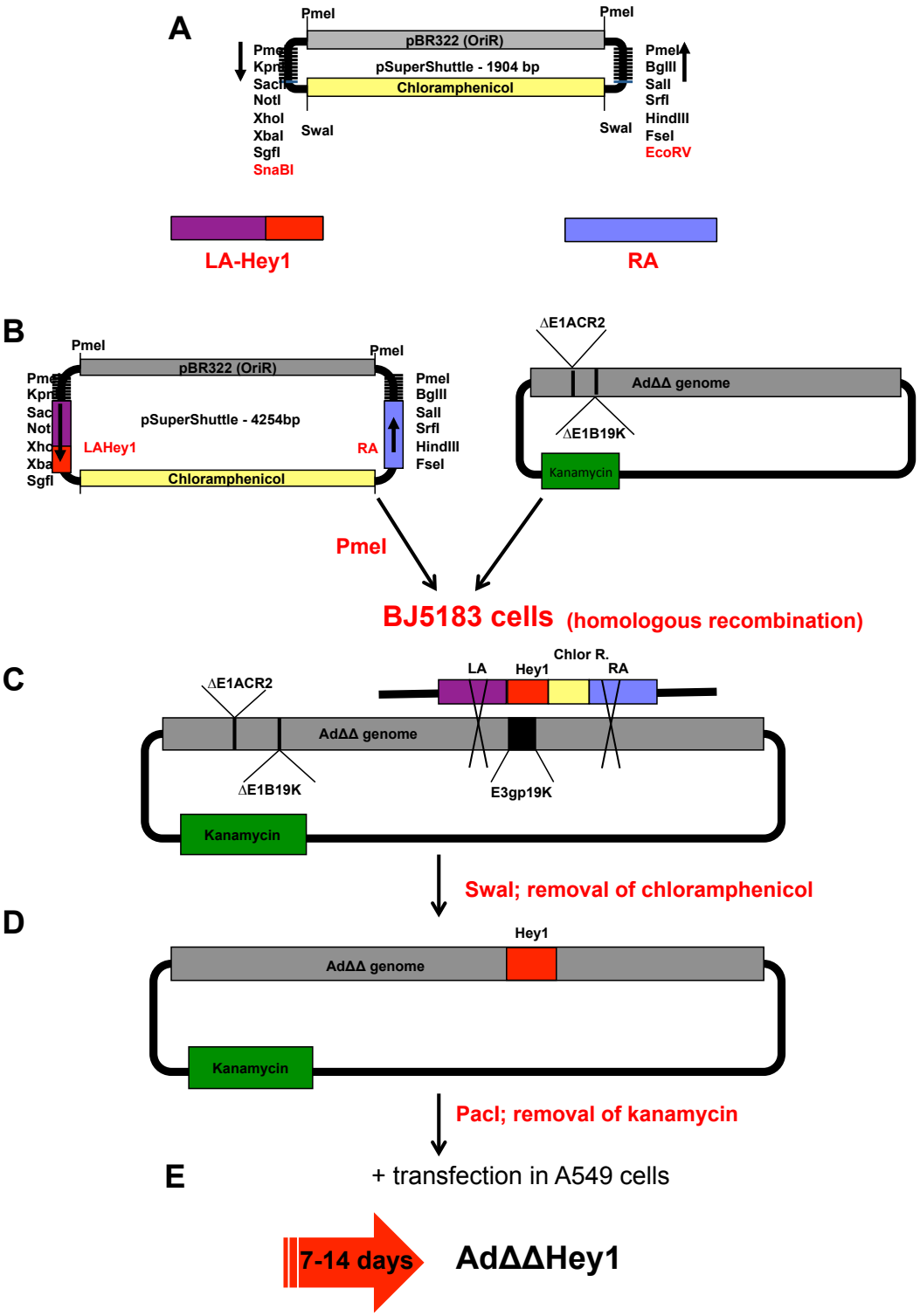

Figure 61. Cloning strategy for generating AdΔΔHey1

A) pSuperShuttle (pSS) with multiple cloning sites. Right arm (RA), left arm (RA) and Hey1 products were PCR amplified. Insertion of RA was via EcoRV digestion. LA and Hey1 fused by PCR SOEing and then inserted into pSS via SnaBI digestion. (B) pSSLARAHey1 was digested with PmeI to remove the origin of replication (OriR) (C) Linearised pSSLARAHey1 and plasmid DNA of AdΔΔ were co-transfected into BJ5183 to undergo homologous recombination (D) Recombinant plasmid AdΔΔHey1 can be identified with double chloramphenicol and kanamycin selection. Extracted DNA from overnight cultures of plasmid AdΔΔHey1 is digested with SwaI to remove chloramphenicol selection and the plasmid can be retransformed into electrocompetent bacteria and selected using kanamycin. Sequencing of the E3 region will confirm the presence of the Flag-Hey1 sequence (E) AdΔΔHey1 is transfected into A549 cells to produce virion particles. Supernatant is collected 7-14 days post-transfection after CPE is observed.

4. Discussion

The rationale behind this research was to introduce Hey1 into PCa cells through adenoviral-mediated delivery as a means of readdressing the balance between deregulated Notch and AR signalling. Belandia *et al* showed Hey1 to be excluded from the nucleus in PCa tumours and localised to the cytoplasm, mislocalisation of Hey1 thus possibly contributing to the development of CRPC (Belandia, Powell et al. 2005). Other studies demonstrated Hey1 was downregulated in PCa specimens further strengthening the concept that deregulated Hey1 might be important in PCa tumourigenesis (Wang, Leow et al. 2006; Whelan, Kellogg et al. 2009). In this study, we postulated whether the action of Hey1 as an AR corepressor might inhibit cell growth and proliferation of PCa cells.

The data presented in this thesis demonstrates that a non-replicating adenovirus expressing Hey1 is cytotoxic to the PCa cell lines 22Rv1, LNCaP and DU145 cells. RNA interference targeting AR or p53 determined Ad5Hey1-mediated cytotoxicity required the expression of both these proteins for optimum efficacy in 22Rv1 cells. Experiments performed with the p53 isogenic HCT116wt and HCT116p53$^{-/-}$ cells revealed neither AR nor p53 expression were essential for Ad5Hey1-mediated cytotoxicity or sensitisation to cytotoxic drugs, verifying our observations of Ad5Hey1-induced cell killing in AR-negative and p53-mutant DU145 cells. In DU145 cells, Ad5Hey1 decreased the levels of phosphorylated STAT3 and cyclin D1 and when the JAK1/2 inhibitor AZD1480 was added, no sensitisation was observed, implying Ad5Hey1 may interfere with JAK/STAT signalling.

In view of the fact that combination therapy approaches are likely to be the most feasible treatment option for oncolytic adenoviral therapy, I also investigated whether Ad5Hey1 could enhance drug-induced cell death. In 22Rv1, LNCaP and DU145 cells, synergistic cell killing was demonstrated when Ad5Hey1 was combined with sub-optimal doses of docetaxel or mitoxantrone. Enhanced cell killing was attributed to Ad5Hey1-mediated enhancement of drug-induced apoptosis in combination with either drugs in 22RV1 and LNCaP cell lines but

only with docetaxel in DU145 cells. Interestingly, in DU145 cells, I observed a reduction in apoptotic cell death when Ad5Hey1 and mitoxantrone were combined suggesting synergistic cell death was as a consequence of other non-apoptotic cell death mechanisms.

Since adrenal derived androgen synthesis and *de novo* androgen synthesis in CRPC maintains AR signalling despite castrate serum levels of testosterone, second-line bicalutamide treatment remains a therapy option for these patients. The degree of Ad5Hey1 potency when AR-positive cells were stimulated with androgen was cell-line dependent, however in the presence of bicalutamide, greater inhibition of cell growth was observed in LNCaP and VCaP cells compared with Ad5GFP-infected or non-infected cells suggesting Ad5Hey1 cooperated with bicalutamide. I further clarified the potential of Ad5Hey1 in an androgen-independent LNCaP cancer progression model. These cells were found to be more sensitive to Ad5Hey1-induced cell killing compared with the androgen-dependent cell line resulting in an accumulation of cells in G1 phase of the cell cycle. This evidence suggests that Ad5Hey1 is a potent cytotoxic agent for androgen-independent and castration-resistant PCa cell lines. From this data, I propose that the expression of Hey1 from a replication-selective adenoviral vector remains a promising treatment for CRPC.

4.1. Ad5Hey1 represses androgen-dependent and -independent AR activity in 22Rv1 cells

An AR-responsive luciferase reporter assay system previously determined Ad5Hey1 repressed androgen-dependent AR transcriptional activity in 22Rv1 cells (Cheong *et al*, manuscript in preparation). No dose response was observed between 10 and 100ppc since maximum repression was observed at 10ppc. Evaluating lower doses confirmed Ad5Hey1 repressed AR activity in a dose-dependent manner. Identical doses of Ad5GFP resulted in a limited decrease in AR activity as well. Non-replicating adenoviruses such as Ad5GFP and the E1A-deleted *dl312* virus result in non-specific effect on cell viability as a result of the presence of the virus particle, which in turn may affect AR transcriptional activity

to a certain extent. However the current data suggests the response of Ad5GFP is not dose-dependent and consequently non-specific in contrast to Ad5Hey1-mediated repression. This study is the first demonstration that Hey1 expressed from an adenoviral vector is able to represses the activity of endogenous AR in PCa cells and is in concordance with published literature of Hey1 repressing transcriptional activity of the AR using *in vitro* systems and repression of endogenous AR in breast cancer MCF7 cells (Belandia, Powell et al. 2005). I did not assess the levels of SRC1 in these cells but it is presumed Hey1 binds to the bHLH-PAS domain of SRC1 and either inhibits recruitment of this coactivator to the AF-1 domain in the AR or competes with SRC1 for AF-1 binding (Belandia, Powell et al. 2005) thus regulating the activity of AR through recruitment of additional corepressor proteins to the transcriptional complex.

Androgen-independent 22Rv1 cells express three AR variants: one full length and two alternatively spliced, constitutively active, AR ΔLBD species (Dehm, Regan et al. 2007) . It was previously demonstrated by Belandia *et al* that Hey1 was able to repress SRC1-mediated activation of an AR ΔLBD mutant (Belandia, Powell et al. 2005). This suggests that Hey1 may interact and repress transcriptional activity of all three isoforms in 22Rv1 cells. It was previously demonstrated in the absence of mibolerone, Ad5Hey1 at doses >10ppc decreased androgen-independent AR transcriptional activity (Cheong et al, manuscript in preparation). Overall, it can be concluded from this study that Ad5Hey1 is able to repress AR transcriptional activity of both androgen-dependent and –independent AR isoforms in 22Rv1 cells. Encouragingly, we also observed further suppression of AR activity in the presence of bicalutamide suggesting possible cooperation between these agents. On this basis, growth inhibition was assessed in combination treatments with bicalutamide in AR-positive PCa cell lines. The results will be discussed later in this chapter.

The effect of Hey1 as an AR corepressor in LNCaP cells was not assessed, however it might be expected that Hey1 could also function as an AR corepressor in these cells. Hey1 targeted repression of the AF-1 region for AR transactivation may be of benefit for eliminating PCa tumours which harbour a mutated AR-LBD and provides a promising tool for targeting AR-positive PCa tumours in circumstances of promiscuous ligand-dependent activation of the AR.

4.2. AR and p53 are required for Ad5Hey1-mediated cytotoxicity in 22Rv1 cells

4.2.1. The intrinsic cytotoxicity of Ad5Hey1 is partially mediated by AR in 22Rv1 cells

As maximum repression of androgen-dependent AR activity was achieved at a low dose, I hypothesised whether the corepressor action of Hey1 could also affect constitutively active AR splice variants. AR was knocked down to assess the absolute requirement of AR for Ad5Hey1-mediated cytotoxicity. RNA interference directed towards the N-terminal region of AR was employed to knockdown all AR splice variants in 22Rv1 cells. I found that knockdown of AR desensitised cells to Ad5Hey1-dependent cytotoxicity and resulted in a significant two-fold increase in Ad5Hey1 EC_{50} value compared with control siRNA-treated cells. In addition, non-specific cell death induced by the negative control virus, Ad5noHey1 at high viral doses was not affected by the knockdown of AR. As concluded above, Ad5Hey1 is able to repress androgen-dependent and –independent AR transcriptional activity. Therefore knockdown of all AR isoforms and the resulting desensitisation to Ad5Hey1-induced cytotoxicity suggests Ad5Hey1-mediated repression of full-length AR and AR splice variants in 22Rv1 cells may partially account for Ad5Hey1-mediated cytotoxicity in these cells. Since cell death was not completely inhibited this suggested the AR repressor function of Hey1 and inhibition of AR signalling was not entirely responsible for the intrinsic cytotoxicity of Ad5Hey1. It is highly likely that unidentified targets, amenable to Hey1 repression, are also regulated. This is evident since Ad5Hey1 is cytotoxic in AR-negative DU145 cells.. Despite western blotting demonstrating good knockdown, a small subpopulation of cells expressing AR still remain and these cells would be sensitive to Ad5Hey1-dependent cytotoxicity and affect the final EC_{50} value. In addition, although adenovirus efficiently transduces 22Rv1 cells (~65% infected), some cells will not be infected also influencing the final EC_{50} value.

binding and sequestration of p300/CBP (Aarnisalo, Santti et al. 1999; Debes, Schmidt et al. 2002). Interestingly, the potency of the positive control virus, AdE1A12S was not affected by the absence of AR demonstrating that AR is not important for AdE1A12S-dependent cell death in 22Rv1 cells. It has previously been shown in our laboratory that AdE1A12S was able to decrease AR expression in 22Rv1 cells (Dr Enrique Miranda, PhD Thesis, 2009). It is speculated that this may be as a consequence of E1A opposing the activity of AR regulators, p300, HDAC and HDM2 resulting in HDM2-mediated AR degradation. However, AdE1A12S-dependent effect on AR levels did not correlate with enhanced potency since non-replicating AdE1A12S mutants with N-terminal regions deleted, did not downregulate AR protein levels, demonstrating comparable cytotoxicity with that of AdE1A12S (Dr Enrique Miranda, PhD Thesis, 2009). Taken together, other E1A12S-dependent mechanism are likely to play a part in mediating cell killing and in contrast to Ad5Hey1, AR was not required for AdE1A12S-mediated cell death.

Numerous studies have shown that knockdown of AR through transient and stable knockdown methods have resulted in significant cell death indicating inhibition of AR is sufficient to induce cell death in AR-positive cells (Liao, Tang et al. 2005; Cheng, Snoek et al. 2006). I did not observe this in my studies with 22Rv1 cells. One obvious reason for the differences are the use of different cell lines - the majority of studies previously reported were in the LNCaP cell line, which are more dependent on AR for cell proliferation than the 22Rv cells. Under our conditions, knockdown of AR resulted in approximately 10% cell death. This is in contrast to a recent study, which demonstrated AR knockdown could inhibit growth of 22Rv1 cells by up to 50% (Azuma, Nakashiro et al. 2010). This disparity is probably because of different cell culture conditions, cell line passages and degree of knockdown between the two studies. I found that the 22Rv1 cells were highly sensitive to cytotoxic agents for several passages after recovery from liquid nitrogen and therefore our AR knockdown studies were carried out after 4-5 passages. It is now realised that AR signalling crosstalks with a number of different other signalling pathways. A recent study identified reciprocal regulation between AR and the PI3K/AKT pathway where RNA interference of AR or treatment with antiandrogen, MDV3100 enhanced AKT activity in PTEN-negative LNCaP cells and the $PTEN^{-/-}$ PCa mouse model through the downregulation of the androgen-regulated FKBP5 protein which itself is a negative regulator of AKT activity (Carver, Chapinski et al. 2011).

Depletion of AR in LNCaP cells can also result in PI3K-independent activation of AKT through elevated levels of calcium/calmodulin-dependent kinase II (CaMKII) (which is usually repressed by AR signalling) (Rokhlin, Taghiyev et al. 2007). Another factor to consider are growth factors in the cell culture medium. 22Rv1 cells express both EGFR and HER2/neu receptors in complete medium (Pignon, Koopmansch et al. 2009). Interestingly in this study, siRNA targeting the N-terminal of AR resulted in reduction of EGFR but an increase in HER2/neu expression. This was found to correlate with a reduction in cell growth compared with untreated or siRNA specific to the full-length AR isoform in steroid-depleted medium (Pignon, Koopmansch et al. 2009). However, as I carried out the experiments in complete medium, stimulation of HER2/neu receptor might be occurring resulting in enhanced cell growth. In light of these results, we should be mindful that deregulated AR signalling by RNA interference could influence other signalling pathways, which might affect the outcome of Ad5Hey1-mediated cytotoxicity.

4.2.2. Ad5Hey1 induction of p53 contributes to Ad5Hey1-dependent cytotoxicity in cells expressing functional p53

In view of the partial desensitisation of 22Rv1 cells to Ad5Hey1-mediated cytotoxicity after AR knockdown, I reasoned additional Hey1-mediated regulatory mechanisms must contribute to Ad5Hey1-dependent cell killing in this cell line. As discussed in section 1.5.3.3, genome-wide functional analysis identified Hey1 as a p53 regulator and Hey1-mediated inhibition of HDM2 expression was credited as the mechanism by which Hey1 indirectly regulated p53 stabilisation and activation (Figure 62) (Huang, Raya et al. 2004; Villaronga, Lavery et al. 2009). Furthermore, upregulation of p53 by Hey1 was correlated to induction of apoptosis *in vivo* in a zebrafish and an avian developmental model (Huang, Raya et al. 2004) or inhibited growth of U2OS cells when Hey1 expression was induced (Villaronga, Lavery et al. 2009). On this basis, I found Ad5Hey1 dose-dependently increased levels of total p53 in 22Rv1, LNCaP and HCT116wt cells in agreement with Hey1-dependent upregulation of p53 in U2OS-HEY1 (Villaronga, Lavery et al. 2009). In addition, HDM2 levels where

previously found to decrease modestly after Ad5Hey1 infection in 22Rv1 cells (Cheong *et al*, manuscript in preparation) in accordance with the results demonstrated in the U2OS-HEY1 cells (Villaronga, Lavery et al. 2009). As a consequence of our adenoviral-mediated expression system, Hey1 expression is prolonged compared with other *in vitro* systems and will lead to further HDM2 expression due to the auto-regulatory feedback loop (Chène 2003). This might explain the more modest decrease in HDM2 expression after prolonged activation of p53.

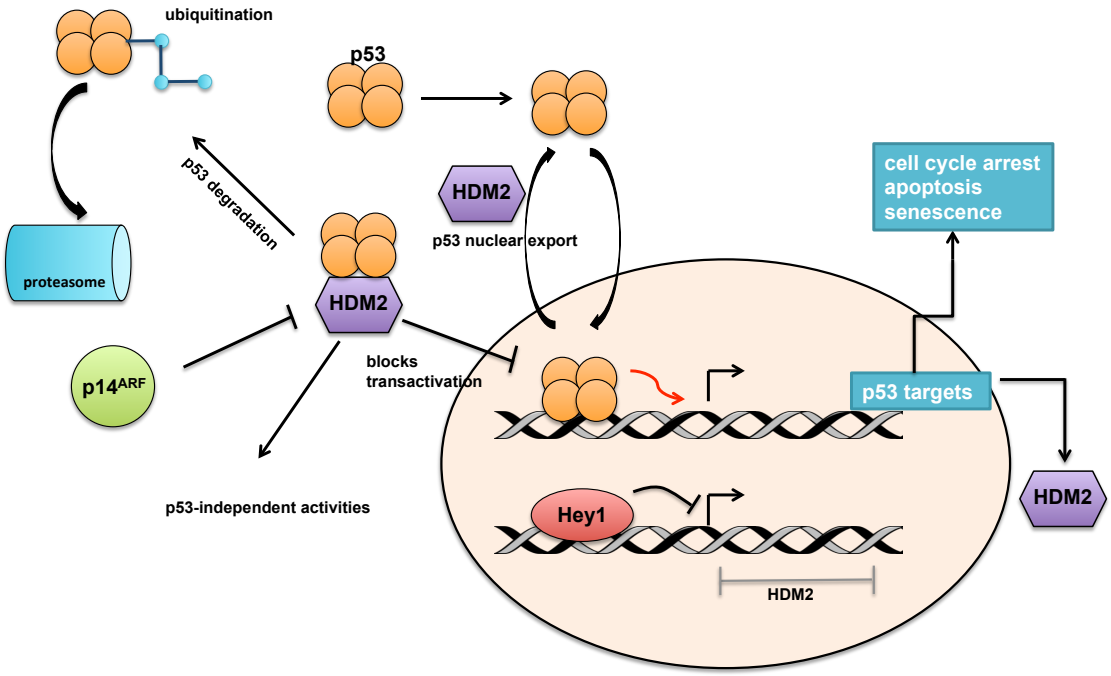

Figure 62. Regulation of p53 stabilisation by HDM2 and Hey1

Hey1 induces p53 stabilisation by inhibiting HDM2 expression though transcriptional repression of the HDM2 promoter. Hey1 binding to the promoter is indirect and facilitated by as yet unidentified protein binding partners (Huang, Raya et al. 2004). p53 and HDM2 form an auto-regulatory feedback loop wherein HDM2 expression is regulated by p53 Various signals including DNA damage and oncogenic activation of $p14^{ARF}$ induce p53. HDM2 blocks p53 activity through a number of mechanisms: 1) stimulation of p53 degradation by ubiquitination, 2) promoting nuclear export of p53 and 3) inhibiting p53 transactivation. Figure adapted from (Chène 2003).

Since p53 activity is regulated by a series of posttranslational modifications, the phosphorylation status of p53 on ser15 was also assessed. Phosphorylation at this residue has been demonstrated to enhance the interaction of p53 with transcriptional coactivators such as p300/CBP and PCAF for subsequent acetylation and stabilisation of the protein (Dumaz and Meek 1999). In response to increasing doses of Ad5Hey1, expression of phospho-ser15-p53 was enhanced in 22Rv1 and HCT116wt cells. The transcriptional activity of p53 was not assessed since it is well established that phospho-ser15-p53 is an adequate

marker for p53 activation (Dumaz and Meek 1999). Furthermore other laboratories have shown Hey1-induced p53 expression is transcriptionally active (Villaronga, Lavery et al. 2009).

The results obtained in my study in relation to p53 phosphorylation status are in contrast to those demonstrated after ectopic expression of Hey1 in Ewing's sarcoma TC252 cells which did not result in phosphorylation of ser15-p53 (Ban, Bennani-Baiti et al. 2008). Inhibiton of HDM2 by mechanisms other than transcriptional repression have yielded similar results. For example, depletion of HDM2 by RNA interference caused induction of p53 transcriptional activity in the absence of p53 phosphorylation or acetylation (Giono and Manfredi 2007) while the small molecule inhibitor of HDM2, Nutlin-3, also stimulated p53 activity in the absence of phosphorylation at specific residue sites associated with stress-induced p53 activation (Thompson, Tovar et al. 2004). Phosphorylation of p53 at ser15 is as a result of phosphorylation by checkpoint protein, ataxia telangiectasia mutated (ATM), a serine/theronine kinase activated as consequence of the DNA-damage response (DDR) pathway. I did not characterise the activation status of this pathway, however it is conceivable that DDR is triggered through Hey1 and E1A-specific mechanisms which are not activated in response to Ad5GFP-infection since no phospho-ser15-p53 was detected in these samples.

As discussed in section 1.6.3.3.2, E1A stabilises p53 levels through a variety of mechanisms through p300/CBP and pRb-dependent binding as well as direct interaction with regulators of p53. In both 22Rv1 and HCT116wt cells, AdE1A12S did not stabilise p53 as effectively as Ad5Hey1 – higher doses of AdE1A12S were required to stabilise p53 to a similar degree suggesting the main mechanism of AdE1A12S-induced cell death in not p53-mediated. In contrast, AdE1A12S-mediated upregulation of p53 expression in LNCaP cells was greater than for Ad5Hey1-infected cells highlighting that the extent to which Hey1 and AdE1A12S stabilise p53 in cells with functional p53 differ between cell lines. It is possible that constitutive activation of the PI3K/AKT pathway in LNCaP cells might result in upregulation of HDM2 activity through AKT-mediated phosphorylation preventing more complete stabilisation of p53.

Previous studies have determined phosphorylation and activation of p53 is linked to the loss of pRB or overexpression of E2F1 (Pan, Yin et al. 1998).

Infection of an adenoviral vector expressing E1A resulted in the formation of γH2AX foci, a marker of DNA double-stranded breaks. This observation was consistent with E1A-mediated accumulation of E2F3 resulting in autophosphorylation and activation of ATM, through the DDR pathway and subsequent phosphorylation of p53 (Hong, Paulson et al. 2008). Therefore the ability of E1A to override the cellular control of pRb-E2F is one possible mechanism that could account for AdE1A12S-mediated activation of p53 in 22Rv1 and HCT116wt cells. In a different study, knockdown of both pRb alleles in mouse adult fibroblasts resulted in E2F1 accumulation, ATM activation and subsequent phosphorylation of p53 and apoptosis. However this occurred in the absence of ATM autophosphorylation and without formation of γH2AX foci. This indicated E2F1 was able to activate ATM through a mechanism distinct from agents that induce double-stranded DNA breaks and DDR factors can also contribute to oncogenic stress-induced signalling to p53 (Powers, Hong et al. 2004). Since ATM is known to be activated through pathways other than DNA damage (Bakkenist and Kastan 2003), it would be of interest to assess the activation status of ATR, ATM and γH2AX in response to Ad5Hey1 infection.

In view of the fact that Ad5Hey1-dependent cytotoxicity was accompanied by the activation of the p53 pathway over an extended time period, this suggested Ad5Hey1 might mediate p53-dependent apoptosis. To assess whether p53 was important for Ad5Hey1-dependent cytotoxicity, 22Rv1 cells were transfected with siRNA directed towards p53 and cell viability determined. We observed a 50% decrease in the percentage of cell death stimulated by a fixed dose of Ad5Hey1 after cells were depleted of p53. This is in agreement with an earlier study which observed a reduction in Hey1-mediated cell growth inhibition in siRNA-p53-transfected U2OS-HEY1 cells (Villaronga, Lavery et al. 2009). This laboratory later extended their studies to the involvement of the ATF/CREB transcription factor, CREBZF in Hey1-mediated growth inhibition. siRNA directed towards CREBZF partially rescued the proliferation arrest caused by Hey1 expression (López-Mateo, Villaronga et al. 2012). CREBZF levels were not assessed in my study however this may be of interest in the future since CREBZF was found to interact with both Hey1 and p53 *in vitro* and cooperated with Hey1 to activate and stabilise p53 (López-Mateo, Villaronga et al. 2012). This and other unidentified Hey1-interacting proteins, which bridge p53 with Hey1, may provide an alternative explanation for the observed Ad5Hey1-induced phosphorylation of p53.

The purpose of reanalysing the data produced from this study was to assess the importance of p53 and AR in Ad5Hey1-mediated cell killing in 22Rv1 cells. Overall it was demonstrated that knockdown of either protein abrogated Ad5Hey1-dependent cell death. A dual knockdown approach was not carried out in this study however it may substantiate the requirement of both proteins in Ad5Hey1-mediated cytotoxicity. Recent studies have shown that crosstalk exists between the AR and p53 signalling pathways. In both 22Rv1 and LNCaP cells, it was previously shown that both induction of p53 expression or inhibition of p53 activity resulted in a decrease in AR-mediated transactivation suggesting physiological levels of p53 are required to stabilise AR signalling (Cronauer, Schulz et al. 2004). Conversely, treatment with DHT was shown to decrease p53 protein levels in LNCaP cells and inhibit apoptosis in a dose-dependent manner while serum starvation also resulted in decrease in p53 protein expression (Rokhlin, Taghiyev et al. 2005). In light of this, it should be taken into account that my data, which demonstrated Ad5Hey1-dependent decrease in AR transcriptional activity in 22Rv1 cells may partly be a consequence of Ad5Hey1-induced p53 activation. In a study by Alimirah *et al*, p53 was found to associate with a 5' regulatory region of the AR gene when LNCaP cells were stimulated with etoposide suggesting p53 negatively regulates AR expression in these cells (Alimirah, Panchanathan et al. 2007). It is also hypothesised that depletion of p53 by siRNA described in this thesis could, analogously to the results reported by Cronauer *et al*, inhibit AR signalling in 22Rv1 cells. If this is the case, indirect downregulation of AR may have resulted in desensitisation to Ad5Hey1-induced cytotoxicity. Alternatively in another study, knockdown of p53 in LNCaP cells resulted in enhanced AR expression compared with mock-treated cells (Rokhlin, Taghiyev et al. 2005). Therefore, complex context-specific mutual regulation of expression occurs between AR and p53. In this thesis I have presented evidence that in 22Rv1 cells, which express endogenous AR and functional p53, both must be functional for optimal Ad5Hey1 potency. The proposed mechanisms of Ad5Hey1-mediated cytotoxicity in these cells are presented in Figure 63.

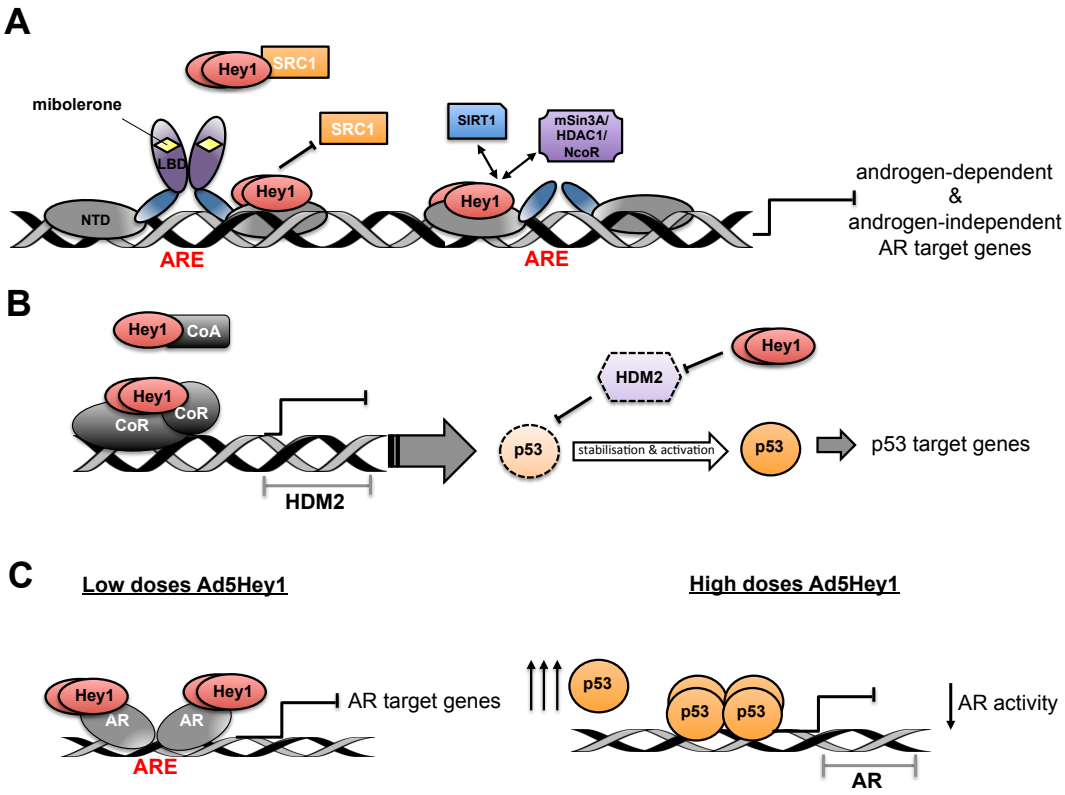

Figure 63. A schematic diagram illustrating the mechanisms of Ad5Hey1-mediated cytotoxicity in 22Rv1 cells.

A). Hey1 expressed from an adenoviral vector functions as a corepressor of full length AR and ΔLBD splice variants by interacting with the NTD region and modulating the levels of corepressor and coactivators at androgen-dependent and-independent AR transcription complexes thus downregulating AR-dependent growth. Repressive activity of Hey1 occurs through HDAC-dependent mechanisms interacting with mSin3A and NCoR and recruitment of HDACs (Iso, Sartorelli, 2001) as well as HDACI/II-independent mechanisms (Nakagawa, McFadden et al. 2000; Takata and Ishikawa 2003). Binding of Hey1 to coactivator SRC1 also regulates SRC1 binding to AR and/or sequesters SRC1 from the AR transcription complex (Belandia, Powell et al. 2005). B) Hey1 can inhibit HDM2 transcription independent of DNA-binding by recruitment of other corepressors and/or sequestering coactivator proteins by forming non-functional complexes resulting in inhibition of HDM2-mediated negative regulation of p53 and induction of apoptosis (Huang, Raya et al. 2004). C) Crosstalk between AR and p53 signalling pathways exist in PCa cells (Cronauer, Schultz et al. 2004). I hypothesise that at doses of Ad5Hey1, which do not result in stabilisation of p53, Hey1 functions as a corepressor of AR. However at doses sufficient to result in p53 transactivation, downregulation of AR signalling possibly through the association of p53 with a regulatory region of the AR gene (Alimirah, Panchanathan et al. 2007) occurs in addition to p53-dependent apoptotic responses.

I also demonstrated that AdE1A12S-dependent cytotoxicity in 22Rv1 cells was partly mediated through p53-dependent activation of cell death pathways since AdE1A12S-induced cell death decreased after depletion of p53. In agreement with our results, a similar study also found E1A-induced cytotoxicity of ovarian clear cell carcinoma (CCC) cells was partly dependent on p53 after siRNA targeted to p53 resulted in a decrease in E1A-mediated cell death (Itamochi, Kigawa et al. 2007). Further evidence to support a p53-dependent mechanism of cytotoxicity, was a modest increase in the expression of Bax, a target gene of

p53 transactivation. Expression levels of p53-independent cellular targets induced by AdE1A12S were not assessed. E1A has been implicated in downregulating EGFR expression through binding to p400 and decreasing Mcl-1 expression as a consequence of the DNA damage response (Cuconati, Mukherjee et al. 2003; Flinterman, Mymryk et al. 2007). As 22Rv1 cells have an activated EGF signalling pathway and express Mcl-1 (Kharaziha, Rodriguez et al. 2012), it would be of interest to assess the E1A12S-specific modulation of these pathways with and without p53 knockdown. This may prove useful in defining the significance of p53-independent pathways of cell death, which presumably contribute to AdE1A12S-induced cell death since p53 knockdown did not abrogate cell killing completely.

4.3. Ad5Hey1 induces a G2 cell cycle delay in 22Rv1 cell but not in DU145 cells

Activated p53 in addition to inducing apoptosis, also causes cells to undergo growth arrest and for this reason I investigated whether Ad5Hey1 had an effect on the cell cycle distribution of 22Rv1. In parallel, the effects of Ad5Hey1 on the cell cycle in DU145 cells was also assessed since these cells express mutated p53. In contrast to another study where ectopically expressed Hey1 in Ewing's sarcoma cell line, TC252 induced a p53-dependent G1 cell cycle arrest (Ban, Bennani-Baiti et al. 2008), Ad5Hey1-infected 22Rv1 cells resulted in a dose-dependent decrease in the proportion of cells in G1. It is probable that variation in cell cycle defects between cancer cells account for the contrasting effects of Hey1 on cell cycle regulation between these two studies. Although 22Rv1 cells express both functional pRb and p53, the G1 checkpoint appears to be non-functional and cells infected with either Ad5Hey1 or AdE1A12S showed a signficant increase in G2/M populations.

Cell cycle analysis of 22Rv1 cells infected with increasing doses of Ad5Hey1 resulted in a significant increase in the proportion of cells in G2/M in a dose- and time-dependent manner. This cell cycle distribution was in keeping with the cell cycle profile of U2OS-HEY1 cells where there was a reduction in the proportion

of cells in G1 and an increase in the percentage of cells in S and G2 phase (Villaronga, Lavery et al. 2009). Both the data presented in this thesis and the findings reported by Villaronga *et al*, show a correlation between increased population of cells in G2/M phase and increased p53 activation. Corresponding to the accumulation of G2/M, I observed a dose- and time-dependent increase in cyclin B1 levels. Together, this indicates Hey1 may activate the G2-checkpoint through the accumulation of p53 and in 22Rv1 cells and U2OS cells The importance of p53 in G2 checkpoint control is recognised from earlier studies using isogenic p53 HCT116 cell lines demonstrating p53 was essential for long-term G2-arrest while p53-deficient cells eventually entered mitosis after G2 arrest (Bunz, Dutriaux et al. 1998).

Since I did not see a decrease in cyclin B1 levels up to 72h post-infection, this suggested Ad5Hey1 may delay cell cycle progression into mitosis. It has been reported that cyclin B1, which is in a complex with Cdk1, remains mainly in the cytoplasm during interphase (Pines and Hunter 1991). During mitosis, Cdk1/cyclin B1 complexes are activated on centrosomes and are imported into the nucleus with breakdown of the nuclear envelope coinciding with the activation of the nuclear pool of Cdk1/cyclin B1 (Bailly, Pines et al. 1992; Gavet and Pines 2010). Therefore, since cyclin B1 levels are reported to be still high until degradation begins at the metaphase-anaphase stage of mitosis, I endeavoured to establish whether Ad5Hey1 induced a block in G2 or if an arrest was occurring at the beginning of mitosis. I assessed levels of phospho-Ser10-histone H3 (pH3), which correlates with chromatin condensation at mitosis (Juan, Traganos et al. 1998), for clarification on whether a delay in mitosis was occurring. Concurrent with the increase of cyclin B1 levels, the percentage of Ad5Hey1-infected cells, which were positive for pH3, doubled compared with uninfected and Ad5noHey1-infected cells. To interpret these results, the time at which phosphorylation of histone H3 occurs on the chromosomes requires consideration. Several studies have reported that during chromosome assembly, phosphorylation of histone H3 by aurora A and aurora B kinases occurs in a controlled manner. Phosphorylation in mammalian cells, starts at late G2 phase at the pericentromeric heterochromatin and during mitosis, extends throughout the whole chromosome. Phosphorylation ceases in late prophase but is sustained through metaphase. Dephosphorylation of histone H3 begins in anaphase and ends early telophase (Hans and Dimitrov 2001). From the bivariate analysis of pH3 vs. PI, I observed a large population of cells

arrested in mitosis in the nocodazole-treated sample in agreement with nocodazole arresting at the prometaphase stage in MCF7 cells (Choi, Fukui et al. 2011). In contrast, the pH3 distribution in G2/M for Ad5Hey1- and AdE1A12S-infected cells appeared to reflect an intermediary stage of pH3 staining, between that obtained for nocodazole-treated cells and for control cells. Therefore, I was not able to conclusively deduce whether Ad5Hey1-infected cells are delayed at late G2 or early mitosis. Our current hypothesis is that Ad5Hey1 induces a delay at late G2. A trail of pH3-positive cells can be observed in the cells infected with Ad5Hey1 or AdE1A12S. Since phosphorylation of histone H3 occurs in a stepwise manner, this may reflect cells whose chromosomes have not yet been widely phosphorylated on the histone H3 tails. Therefore, the trail may correspond to cells in a late G2 stage of the cell cycle and are undergoing a delay into mitosis. The population of cells directly above the trail are cells in mitosis and the size and density of this population remains similar between all treatments with the exception of nocodazole.

A more definitive answer to whether Ad5Hey1 stimulates a G2 delay will be to assess activation status of Cdk1 since activation of the Cdk1/cyclin B1 complex triggers transition from interphase to mitosis (Lindqvist, Rodríguez-Bravo et al. 2009). During G2, Wee1 and Myt1 execute inhibitory phosphorylation on tyrosine 15 and threonine 14 of Cdk1 respectively. This preserves Cdk1 activity until DNA replication is completed. Cdk1/cyclin B1 is activated upon abrupt dephosphorylating by Cdc25 phosphatases and drives cells irreversibly into mitosis (Lindqvist, Rodríguez-Bravo et al. 2009). In addition, the subcellular localisation of cyclin B1 may shed more light on the presence of a delay, as cyclin B1 is primarily located in the cytoplasm during G2. It would also be interesting to assess the putative G2 population at later time points to determine their fate – whether they will eventually override the delay that the G2/M checkpoint has imposed or die because of apoptosis. A small >4N DNA content population was observed at the later stages of Ad5Hey1 infection. It is possible the putative G2 delay may supress mitotic catastrophe (cell death that results from abnormal mitosis), which would facilitate the accumulation of polyploidy cells. This usually arises from either mitotic slippage, where a cell escapes mitosis and slips into the next interphase, or through failed cytokinesis after a cell has gone through aberrant mitosis (Yamada and Gorbsky 2006; Vitale, Galluzzi et al. 2011).

For AdE1A12S-infected cells, at the same dose used for Ad5Hey1, I also observed a p53-dependent accumulation of cells in G2/M but the increase was smaller than with Ad5Hey1 and was accompanied by a larger >4N DNA and sub-G1 fraction. The smaller accumulation of cells in G2/M may be a reflection of the observed lower level of activation of p53 by AdE1A12S compared with Ad5Hey1. Furthermore, at 72h both phospho-p53 and cyclin B1 levels were reduced suggesting AdE1A12S was able to overcome the G2/M checkpoint and enter mitosis. The replicating ONYX-015, which does not express E1B55K, similarly resulted in the accumulation of transcriptionally active p53 and was able to overcome the G1 and G2 checkpoints in normal cells resulting in the accumulation of cells with >4N DNA content (Cherubini, Petouchoff et al. 2006). It is probable that AdE1A12S abrogated the spindle checkpoint since enhanced polyploidy is correlated with its deregulation (Suijkerbuijk and Kops 2008). One mechanism through which this checkpoint is hindered is through the overexpression of Mad2, a gene target of E2F transcription, which leads to hyperactivation of the checkpoint (Hernando, Nahlé et al. 2004). MEFs transfected with an E1A vector overexpressed Mad2 which correlated with increased >4N DNA content and an aberrant number of chromosomes (Hernando, Nahlé et al. 2004). In another study, ectopic expression of E1A in chronic myeloid leukaemia K562 cells was reported to overcome G2/M arrest induced by etoposide by promoting the expression and activation of Cdk1 (Stiewe, Parssanedjad et al. 2000). Additionally the polyploidy population could also arise from E1A-mediated inhibition of pRb, which is also required for the p53-dependent, postmitotic spindle checkpoint (Lanni and Jacks 1998).

A strict p53-dependence for Hey1-mediated arrest was reasoned after Ewing's sarcoma cells with mutant p53 failed to reduce the percentage of cells in S phase (Ban, Bennani-Baiti et al. 2008). I also found no major differences in the cell cycle profile of DU145 cells after infection with Ad5Hey1 other than an significant increase in the proportion of cells with >4N DNA. It is therefore possible Ad5Hey1 may, induce mitotic slippage as a result of defective G1 and G2 checkpoints in these cells (DU145; $p53^{mut}$, pRb^{mut}, p16-) (Isaacs, Carter et al. 1991; Skjoth and Issinger 2006). Cells with defective p53 commonly undergo polyploidization compared with their wild-type counterparts resulting in multipolar division of tetraploid cells leading to aneuploidy and genomic instability (Senovilla, Vitale et al. 2009; Vitale, Senovilla et al. 2010). Untreated DU145 cells possess a noticeable proportion of cells with a polyploidy

phenotype compared with 22Rv1 cells. Infection with either Ad5Hey1 or AdE1A12S resulted in a larger proportion of DU145 cells than 22Rv1 cells accumulating with a >4N DNA content suggesting functional p53 in 22Rv1 cells, supresses formation of aneuploidy. A previous study demonstrated that inactivation of p53 in primary rat embryo (REF-52) fibroblasts resulted in tetraploid cells, which did not arrest in G1 and rapidly progressed to aneuploidy (Andreassen, Lohez et al. 2001). Enhanced polyploidy has been linked to chromosomal instability and as a result, the genome of DU145 cells is inherently unstable, carrying numerous chromosomal breaks (Beheshti, Karaskova et al. 2000).

In DU145 cells, significant differences in cell cycle perturbations were observed for cells infected with AdE1A12S at all doses. It should be noted however, that the extent of cell cycle changes induced by AdE1A2S and Ad5Hey1, at doses equivalent to their EC_{50} value (2000 and 8000ppc respectively), were not entirely different - although statistical significance could be attributed to AdE1A12S-mediated effects on G1 and G2/M in addition to the >4N DNA population. E1A binds to numerous cellular proteins to drive cells into S phase. Since pRb is mutated in these cells, E2F is deregulated and hence the pRb-binding function of E1A12S is redundant. However, E1A is still able to stimulate cell cycle progression in non-functional pRb backgrounds. The p400/TRRAP-binding region of E1A has been reported to induce expression and stabilisation of E2F1, independent of pRb-binding through sequestering p400 away from E2F1 in primary transformed retinal cells (Helgason, O'Prey et al. 2010). Furthermore, c-Myc is also a target of E1A-mediated deregulation. E1A binding to both p300 and p400 have been reported to drive c-Myc expression and stabilisation respectively. Sequestration of p300 alleviates the repression exerted by HDAC complexes on the c-Myc promoter while binding to p400 binding site facilitates stabilisation of p400/c-Myc complex enhancing expression of c-Myc target genes (Tworkowski, Chakraborty et al. 2008; Sankar, Kadeppagari et al. 2009). Therefore the attenuated G1 and G2 checkpoints in these cells and the deregulation of c-Myc by AdE1A12S may ultimately result in enhanced polyploidy. It has also been reported that overexpression of c-Myc with the combined loss of p53 is a mechanism of tetraploidization (Yin, Grove et al. 1999).

In conclusion, my data suggests that Ad5Hey1 can abrogate the cell cycle checkpoints in PCa cells and cause only a putative G2 delay in p53-expressing 22Rv1 cells followed by mitotic entry. In DU145 cells, Ad5Hey1 enhanced mitotic slippage resulting in a higher proportion of aneuploid cells with increased genomic instability. This may be a potential mechanism for Ad5Hey1 to sensitise cells to chemotherapeutic drugs leading to enhanced cell death by attenuating cellular checkpoints and enable cells to progress through the cell cycle in the presence of DNA-damage and virus infection.

4.4. Ad5Hey1-mediated cytotoxicity and cooperation with chemotherapeutic drugs by p53-dependent and –independent mechanisms

Together with previous reports and the data presented in this thesis, there is compelling evidence that overexpression of Hey1 results in p53-dependent cell growth inhibition and cell death. However, Ad5Hey1-mediated cytotoxicity and synergy with chemotherapeutic drugs was also observed in DU145 cells which express mutant p53. The p53 isogenic HCT116 cell lines were used to definitively assess the requirement of p53 for Ad5Hey1-dependent cell death and sensitisation. These cells did not express AR therefore circumventing the Hey1-specific regulation of the AR.

No difference in Ad5Hey1-induced potency was observed between the matched cell lines confirming the earlier p53-independent mechanism of action of Ad5Hey1 in DU145 cells. AdE1A12S was more potent in HCT116p53$^{-/-}$ cells than the wild-type counterpart indicating the lack of p53 renders the cells more sensitive to E1A-mediated cell killing. Villaronga and colleagues proposed that upregulation of p53 activity as a consequence of overexpression of Hey1 in U2OS cells was a mechanism by which Hey1 sensitised cells to cisplatin and doxorubicin (Villaronga, Lavery et al. 2009). In agreement with these results and in addition, I have shown that Ad5Hey1 synergised with docetaxel and

mitoxantrone in PCa cell lines both with and without functional AR and p53 pathways. Morover I defined that p53 activation was not a prerequisit for sensitisation as 5-FU and mitoxantrone sensitised HCT116p53$^{-/-}$ cells and HCT115wt cells to Ad5Hey1-mediated cytotoxicity.

An interesting relationship emerged when Ad5Hey1 or AdE1A12S was combined with either 5-FU or mitoxantrone in p53 isogenic HCT116 cells. Results suggested the p53 status of cells and the drug mechanism of action were important for optimal sensitisation to Ad5Hey1 or AdE1A12S-induced cytoxicity. The activity of p53 has previously been found to have a significant impact on the response of cells to chemotherapeutic agents and that the response varies depending on the drug (Bunz, Hwang et al. 1999). Sensitisation by mitoxantrone or 5-FU to Ad5Hey1-mediated cytotoxicity was greater in HCT116wt cells than HCT116p53$^{-/-}$ cells. However, sensitisation by 5-FU to Ad5Hey1 in p53-deficient cells was not decreased significantly suggesting sensitisation by 5-FU to Ad5Hey1 occurred independent of p53. Conversely, when AdE1A12S was combined with 5-FU, optimum sensitisation was observed in HCT116p53$^{-/-}$ whereas minimum sensitisation occurred in HCT116wt cells. Potent sensitisation to AdE1A12S in both cell lines was demonstrated when combined with mitoxantrone.

The therapeutic efficacy of 5-FU derives from its role in inhibiting DNA synthesis and repair as well as incorporation into RNA, inhibiting processing of ribosomal RNA (rRNA) and preventing splicing of pre-mRNA (Zhang, Yin et al. 2008). In accordance with Bunz *et al*, I found HCT116p53$^{-/-}$ cells to be more resistant to 5-FU induced cytotoxicity (Bunz, Hwang et al. 1999) however, at the sub-optimal doses used in this study (wherein 15-30% of cells are killed), p53 status did not significantly affect the potency of 5-FU or mitoxantrone. Later studies reported that 5-FU possesses p53-dependent and –independent mechanisms of action, both of which might contribute to the sensitisation of HCT116 cells to Ad5Hey1-mediated cytotoxicity. As 5-FU affects RNA processing, this results in inhibition of rRNA biogenesis and nucleolar stress activating the p53 pathway thereby keeping deregulated cell growth in check (Zhang and Lu 2009). The resulting ribosomal stress results in liberation of the ribosomal L proteins (L5, L11 and L23), which directly bind to the central acidic region of HDM2 and inhibit HDM2-mediated ubiquitination of p53 in U2OS cells (Sun, Dai et al. 2007). Consequently, sensitisation of HCT116wt cells by 5-FU to Ad5Hey1-dependent

cell killing may be as a result of a convergence of pathways, which together inhibit the HDM2-p53 regulatory loop. Thus, Ad5Hey1 inhibits HDM2 expression leading to p53 activation whereas 5-FU will block the resulting HDM2-p53 feedback circuit by releasing ribosomal proteins, which inhibit the ubiquitin ligase activity of HDM2, and leading to stabilisation of p53. Since Sun *et al* identified that the ribosomal proteins L5, L11 and L23 were involved in mediating 5-FU-induced p53 activation it would be interesting to assess whether knocking down these proteins would desensitise HCT116wt cells to Ad5Hey1 and 5-FU combination treatment.

Earlier reports using normal fibroblast cells demonstrated E1A-dependent sensitisation occurred as a result of E1A-mediated induction of $p19^{ARF}$ (the mouse homologue of human $p14^{ARF}$) through E2F release resulting in p53 stabilisation. A functional $p19^{ARF}$/p53 pathway was required for this since ARF-null cells abrogated this effect (Lowe and Ruley 1993; de Stanchina, McCurrach et al. 1998). The significance of $p14^{ARF}$ in E1A-dependent p53 activation may explain the poor induction of p53 by AdE1A12S in HCT116wt cells since the $p14^{ARF}$ gene is defective in these cells (Burri, Shaw et al. 2001). This also underscores the distinct mechanism by which Ad5Hey1 and AdE1A12S induce p53 activation, Ad5Hey1 by directly inhibiting HDM2 at the transcriptional level while AdE1A12S indirectly regulates posttranslational HDM2 activity through $p14^{ARF}$ upregulation. The sub-optimal stabilisation of p53 by AdE1A12S in these cells may also explain the reduced sensitisation when combined with 5-FU suggesting E1A-binding to p300, HDMX and the 26S proteasome do not efficiently activate p53, in this cell line at least. In 22Rv1 and LNCaP cells, combination treatment with Ad5Hey1 or AdE1A12S enhanced levels of total and/or phospho-ser15-p53 with both docetaxel and mitoxantrone. Greater p53 stabilisation was observed when drugs were combined with Ad5Hey1 than in the presence of AdE1A12S in 22Rv1 cells. Since the levels of expression of Hey1 and E1A were comparable in the 22Rv1 cells under these conditions, these observations support our hypothesis that Ad5Hey1-dependent cytotoxicity and sensitisation is mediated through p53 signalling to a greater extent than AdE1A12S. In contrast, in LNCaP cells, activation of p53 for combination treatments with Ad5Hey1 did not supersede those induced with AdE1A12S combinations possibly as a result of enhanced HDM2 activity.

It was recently shown that treatment of HCT116p53$^{-/-}$ cells with 5-FU resulted in the stabilisation of the proapoptotic isoform of p73, TAp73α and the induction of p53-inducible genes (Vilgelm, Washington et al. 2010). This could be a potential mechanism by which 5-FU sensitises HCT116p53$^{-/-}$ cells to Ad5Hey1-dependent cytotoxicity since induction of TAp73 in a p53-deficient background permits regulation of downstream effectors which overlap with transcriptional targets of p53 in response to cytotoxic stress. Similarly, it is possible that Ad5Hey1 exerts its effects through induction of TAp73 activity in a p53-deficient background. Overexpression of Hey1 in HCT116p53$^{-/-}$ inhibited HDM2 transactivation and decreased HDM2 protein levels indicating regulation of HDM2 in a p53-deficient background (Huang, Raya et al. 2004). HDM2 interacts with other proteins such as CBP/p300, pRb, p73 and E2F1 that regulate the cell cycle, apoptosis and tumourigenesis independently of p53 (Bartel, Taubert et al. 2002). Inhibition of HDM2 by Nutlin-3 was shown to induce apoptosis in HCT116p53$^{-/-}$ cells by relieving HDM2-mediated inhibition of TAp73α (Lau, Nugent et al. 2008). An attractive hypothesis for a mechanism of sensitisation for these agents in HCT116p53$^{-/-}$ cells might be that both agents are targeting HDM2 as proposed in HCT116wt cells. This could potentially explain why sensitisation, irrespective of p53 status is observed for 5-FU in combination with Ad5Hey1. It would therefore be interesting to determine the importance of TAp73 for Ad5Hey1-dependent cytotoxicity and sensitisation as a putative mechanism in p53-deficient cells. In parallel, it would also be appropriate to assess the activity of Ad5Hey1 on E2F1 stabilisation as Nutlin-3a-treated HCT116p53$^{-/-}$ cells enhanced expression of E2F1 and co-immunoprecipitation of HDM2 demonstrated loss of E2F1 binding after Nutlin-3a treatment (Ambrosini, Sambol et al. 2007). E2F1 has also been demonstrated to induce expression of p73, caspases and BH3 proteins of the Bcl-2 family resulting in E2F1-mediated apoptosis through p53-independent mechanisms (Irwin, Marin et al. 2000; Nahle, Polakoff et al. 2002). Therefore if Ad5Hey1 relieves HDM2-mediated inhibition of TAp73 and/or E2F1 resulting in stabilisation of one or both of these proteins this may confer a potential mechanism through which it could cooperate with cytotoxic drugs in p53-deficient cells. In the context of HCT116wt cells, inhibition of HDM2 and subsequent stabilisation of E2F1 would not result in p14^{ARF} expression thereby precluding the additional suppressive effects of p14^{ARF} on HDM2 activity in this cell line.

Antisense therapy to HDM2 in LNCaP, DU145 and PC3 cells have demonstrated broad-spectrum antitumour activity irrespective of p53 status (Zhang, Li et al. 2003). Importantly, when DU145 cells, which overexpress HDM2, were transfected with antisense oligonucleotides directed towards HDM2, the expression of p21 and E2F1 was upregulated, and was accompanied with apoptosis. Antisense towards HDM2 also sensitised cells to cytotoxic agents *in vitro* as well as increasing efficacy of chemotherapeutic agents in a DU145 xenograft model (Wang, Yu et al. 2003; Zhang, Li et al. 2003). Therefore, analogous to Zhang and colleagues knocking down HDM2 expression in DU145 cells, Ad5Hey1-dependent regulation of HDM2 expression might have resulted in deregulation of HDM2 effector proteins in this cell line. Since Ad5Hey1 has no intrinsic cytotoxicity in PC3 cells, which also express HDM2, this may be an auxiliary role of Ad5Hey1-mediated action and not the main mechanism by which Ad5Hey1 executes cell killing in DU145 cells. Putative mechanisms through which Ad5Hey1 might mediate p53-independent inhibition of cell viability are explored in Figure 64. In this thesis I also investigated the potential role of Ad5Hey1 inhibiting STAT3 signalling in DU145 cells which will be discussed later.

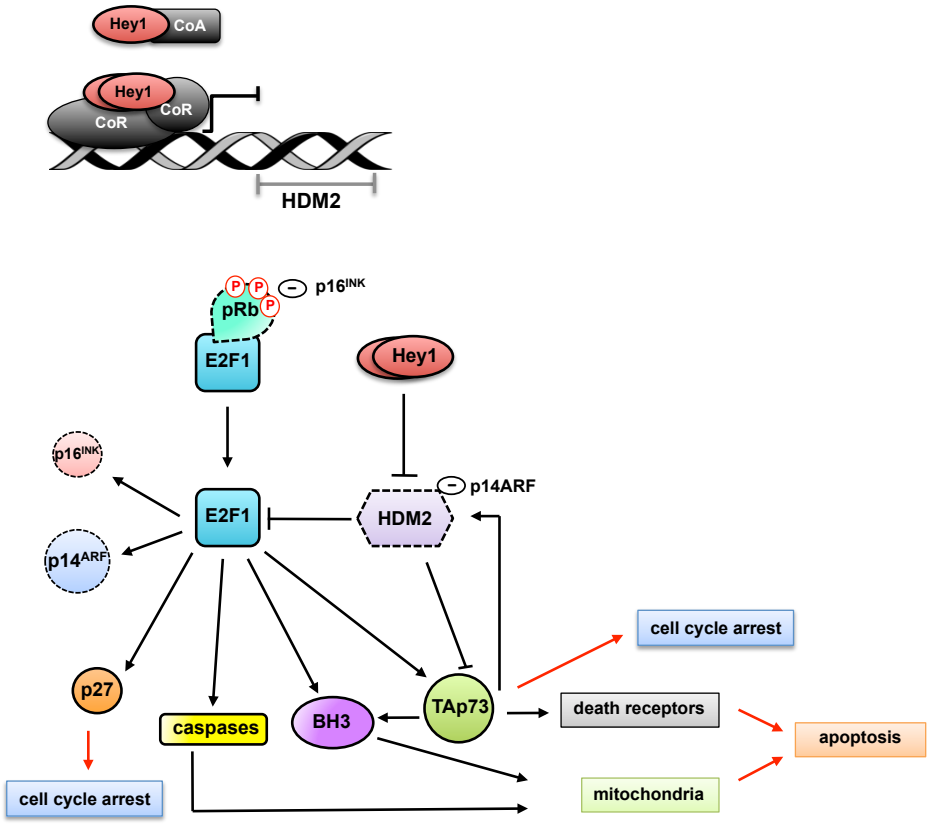

Figure 64. A schematic diagram demonstrating putative mechanisms of Ad5Hey1-mediated cytotoxicity in p53-deficient cell lines.

As demonstrated in cells with functional p53, Hey1 is able to inhibit HDM2 transcription in HCT116p53$^{-/-}$ cells (Huang, Raya et al. 2004). Based on this, I hypothesise that through repression of HDM2 transcription, Hey1 relieves HDM2-mediated inhibition of E2F1 and TAp73. E2F1-dependent apoptotic activities include transactivation of TAp73, caspases and BH3-only proteins (Bax, Noxa, Puma). Due to the functional overlap between TAp73 and p53, TAp73 regulates the expression of some p53-regulated genes leading to cell cycle arrest and apoptosis. Therefore the E2F1-TAp73 pathway may function in place of p53 signalling when p53 is defective underscoring the potential for targeting this pathway in tumours lacking functional p53. The *CDKN2A* and *Rb* loci are defective in HCT116p53$^{-/-}$ and DU145 cells respectively (dashed lines for p16^{INK}, p19^{ARF} and pRb in figure) indicating a deregulated pRb-E2F1 pathway. However these cells remain responsive to HDM2 inhibition by either nutlin-3a (HCT116p53$^{-/-}$) or HDM2 antisense therapy (DU145) leading to increased E2F1 activity and apoptosis (Zhang, Li et al. 2003; Ambrosini, Sambol et al. 2007). This does not exclude the possibility of Hey1 targeting other pathways, which are not amenable to HDM2 regulation. Hey1 may also target the JAK-STAT pathway and both DU145 cells and HCT116 cells express STAT3.

The molecular mechanisms essential for E1A-mediated sensitisation have not been defined owing to numerous cellular pathways regulated by E1A-binding and the molecular alterations of the tumour cells. I have demonstrated that the degree of sensitisation also varies depending on the cytotoxic agent used. In general, the consequence of E1A12S-binding to p300/CBP results in the transcriptional repression of cellular genes (Frisch and Mymryk 2002). Work carried out in our laboratory determined E1A-dependent sensitisation to mitoxantrone and docetaxel was highly dependent on binding to p300/CBP as a non-replicating AdE1A12S mutant defective for p300/CBP binding in the CR1

region failed to sensitise PCa cells to these drugs irrespective of functional p53 status (Miranda, Maya Pineda et al. 2012). In this thesis I have shown that AdE1A12S has a preference of inducing cell death or sensitisation to drugs in a p53-deficient background. However as discussed above, the absence of functional $p14^{ARF}$ in HCT116 cells may have weakened AdE1A12S-mediated cytotoxic effects in the p53-expressing cell line and as a consequence the potency of AdE1A12S alone and in combination with drugs are similar to Ad5Hey1.

I did not characterise the specific mechanisms by which AdE1A12S functioned independently of p53 in HCT116$p53^{-/-}$ cells. A number of studies have shown that E1A mediates proapoptotic and sensitising mechanisms through downregulation of proteins involved in growth and survival and could provide an explanation for our observations. As discussed earlier, E1A has been shown to inhibit transactivation of the EGFR promoter. Epithelial tumour cells frequently overexpress receptors for the EGF family including HCT116 and DU145 cells (Zheng, Ren et al. 2009; van Houdt, Hoogwater et al. 2010). In p53-mutant breast cancer cells overexpressing HER2/neu, E1A and paclitaxel demonstrated synergistic cell killing through E1A-mediated downregulation of HER2/neu expression (Ueno, Yu et al. 1997). E1A also sensitises cells to death receptor-mediated apoptosis. Upon activation of receptors of the TNF superfamily (e.g. Fas receptor; FasR) by they cognate ligand (Fas Ligand; FasL), the adaptor protein, FADD is recruited to intracellular portion of FasR, which in turn associates with monomeric procaspase-8 forming the death-inducing complex (DISC). When c-FLIP levels are high after, for example, TNF receptor 1 activation, procaspase-8 recruits c-FLIP to form caspase-8-c-FLIP heterodimers limiting autocatalytic caspase-8 activation (Elmore 2007). Sensitisation by E1A targets c-FLIP expression by preventing c-FLIP transcription and also promoting ubiquitination and degradation of c-FLIP proteins (Perez and White 2003). This also occurs in unstimulated cells; E1A-mediated inhibition of c-FLIP is sufficient to result in homodimer formation of procaspase-8 resulting in cleavage and autocatalytic activation of caspase-8. Consequently, downstream executioner caspases are cleaved and activated. Caspase-8 also cleaves Bid to generate tBid resulting in oligomerisation of Bak and Bax and subsequent mitochondrial membrane permeabilisation. Thus Bid integrates the extrinsic and intrinsic apoptotic signalling (Elmore 2007). Although not shown in conjunction with cytotoxic agents, E1A also upregulates TAp73 resulting in expression of the

p53/p73 targets, and induction of cell death (Flinterman, Guelen et al. 2005; Klanrit, Flinterman et al. 2008).

4.4.1. Ad5Hey1-mediated targeting of STAT3 in DU145 cells

The potent cell killing by Ad5Hey1 in HCT116p53$^{-/-}$ cells devoid of AR or p53 was in accordance with our observations of Ad5Hey1-mediated cytotoxicity in DU145 cells. Besides crosstalk between Notch and the AR and p53 pathways, Notch signalling also regulates the JAK/STAT pathway. Stimulation of Notch signalling using either an active form of Notch, Hes1 or Hes5 activated STAT3 signalling in neuroepithelial cells and the addition of EGF resulted in synergistic activation (Kamakura, Oishi et al. 2004). Activation of STAT3 occurred through direct binding of the bHLH and Orange domain of Hes1 to STAT3, inducing phosphorylation and activation of STAT3 by recruitment of JAK2 (Kamakura, Oishi et al. 2004). Data from this study suggested Hes proteins might function as scaffold protein that permits JAK2 to phosphorylate STAT3. Although the authors of this study did not demonstrate direct binding of Hey1 with STAT3, Hey1 induced STAT3 phosphorylation and STAT3 transcriptional activity in a COS-1 *in vitro* system (Kamakura, Oishi et al. 2004). I therefore investigated whether Hey1 could regulate constitutively active STAT3 in DU145 cells

The detection of active STAT3 in PCa specimens but not in adjacent tissue has implicated constitutively active STAT3 in contributing to the progression of PCa (Ni, Lou et al. 2000; Barton, Murphy et al. 2001; Barton, Karras et al. 2004). STAT3 is typically activated by an array of ligands including interleukins such as IL-6 through cytokine receptors, growth factor activation of receptor tyrosine kinases (e.g. EGFR) and non-receptor tyrosine kinases (e.g. Src). Upon ligand binding of the receptor, associated JAK kinases mediate tyrosine phosphorylation at the membrane-distal part of the receptor thereby recruiting STAT3. JAK kinases phosphorylate STAT3 at Y705 facilitating homodimerization and translocation to the nucleus. STAT3 is also serine phosphorylated and acetylated with additional modifications in the nucleus, which regulate its activity (Mohr, Chatain et al. 2012). Constitutive activation of STAT3 in DU145 cells is as a consequence of autocrine IL-6 signalling due to expression of IL-6 receptors and secretion of IL-6 (Okamoto, Lee et al. 1997).

STAT3 activation in DU145 cells drives expression of antiapoptotic genes including Bcl-2, Bcl-xL and Mcl-1 contributing to the survival and proliferation of these cells and to a chemotherapy resistant phenotype (Gurumurthy, Vasudevan et al. 2001; Hu, Lee et al. 2008). Inhibition of STAT3 activity was correlated with decrease viability and apoptosis in PCa cell lines making STAT3 a promising target for PCa therapy (Barton, Karras et al. 2004; Gao, Zhang et al. 2005; Shodeinde and Barton 2012).

At 48h post-infection I observed dose-dependent decrease in levels of phospho-STAT3 in response to Ad5Hey1 and AdE1A12S. The decrease was accompanied by a reduction in the STAT3 gene target, cyclin D1. From these results I inferred that Ad5Hey1 could be repressing STAT3 activity thereby reducing the expression of target genes such as cyclin D1. I hypothesise this could occur through one or more of the following mechanisms: Firstly, Hey1 may function as a corepressor of STAT3 activity and inhibit target gene transcription. Secondly, Hey1 could be targeting STAT3 for proteosomal degradation. Thirdly, Hey1 could be preventing STAT3 phosphorylation thereby preventing transcriptional activity with subsequent downregulation of STAT3-inducible gene expression. With regards to E1A-mediated regulation of total and phospho-STAT3 levels, early studies demonstrated E1A binding to p300 inhibited STAT3 transcriptional activity and prevented p300-mediated activation of STAT3 (Takeda, Nakajima et al. 1994; Paulson, Pisharody et al. 1999). The transcriptional activation of STAT3 relies on interaction with coactivator, p300/CBP (Wang, Cherukuri et al. 2005). Therefore, E1A-mediated transcriptional repression of STAT3 may account for the decrease in cyclin D1 and phospho-STAT3 levels. E1A can also directly interact with the C-terminal transactivation domain of STAT1 (Look, Roswit et al. 1998; Chatterjee-Kishore, van Den Akker et al. 2000). Although binding of E1A to STAT3 as yet has not been shown, E1A-mediated inhibition by this mechanism might result in decreased STAT3 activity and reduced target gene expression.

Combining Ad5Hey1 with the small molecule inhibitors, AG490 and AZD1480 in DU145 cells delivered contrasting results. AG490 was able to sensitise cells to Ad5Hey1 and AdE1A12S resulting in significant decreases in the viral EC_{50} values. This was interesting from a therapeutic point of view however due to the less specific nature of AG490 it was likely Ad5Hey1 and AG490 were inhibiting distinct signalling pathways, converging to enhance cell killing. AG490, as well

as inhibiting JAK2 kinase activity also inhibits EGFR and HER2/neu. It is therefore probable that by inhibiting EGF receptors, AG490 is impeding signalling of other pathways such as the MAPK and AKT/PI3K pathways, which are downstream of EGF signalling (Zheng, Ren et al. 2009; Kumar, Srinivasan et al. 2010).

On the other hand, in the presence of the JAK1/2 kinase inhibitor, AZD1480, no sensitisation was observed. Ad5Hey1 and AdE1A12S EC_{50} values increased slightly in the presence of AZD1480. In Ad5Hey1-infected cells, phospho-STAT3 levels were higher than for drug alone when in combination with the low drug dose but were comparable to drug alone at the higher drug dose. Interestingly, phospho-STAT3 levels when AdE1A12S was combined with the higher dose of drug increased and were similar to untreated cells. A possible reason for this might be that Hey1 and E1A in the presence of AZD1480 could be attenuating the transcription and degradation of STAT3 and the observed phospho-STAT3 is not as a result of new phosphorylation but rather, previously formed phospho-STAT3. Further investigations are therefore required to clarify the role of Hey1 in mediating STAT3 signalling.

The precise mechanism as to how Hey1 might act to inhibit the JAK/STAT3 pathway is still to be determined and putative mechanisms are illustrated in Figure 65. Approaches other than using small molecule inhibitors to block STAT3 activity include using oligonucleotides, dominant-negative expression vectors and siRNA against STAT3, which may provide a more specific approach to determine whether Hey1 targets STAT3. Dependent on these results, this study could be extended to assess whether Hey1, as a transcriptional corepressor, represses STAT3 activity. SRC1 has been demonstrated to function as a coactivator of STAT3 together with p300/CBP and co-immunoprecipitated with STAT3 following IL-6 stimulation in hepatoma cells (Giraud, Bienvenu et al. 2002). As Hey1 binds to SRC1, it is possible that it is functioning as a corepressor and inhibiting activation of STAT3. Furthermore, the conserved bHLH and Orange domain might interact with STAT3 providing an additional structural link between these transcription factors. Intriguingly, Hey1 was found to attenuate the cooperative action of Notch and Toll-like receptor-mediated induction of IL-6 in macrophages thus functioning as a feedback inhibitor and repressor of Notch-induced gene activation (Hu, Chung et al. 2008). Suppression of IL-6 expression by Hey1 was mapped to the E-box

binding site within the IL-6 promoter (Hu, Chung et al. 2008). This may provide an indirect mechanism by which Ad5Hey1 reduces STAT3 activity.

Ad5Hey1- and AdE1A12S-mediated reduction in STAT3 activity may reflect a possible mechanism, in part, by which these viruses synergise with docetaxel and mitoxantrone in DU145 cells. As PC3 cells do not express STAT3, this could therefore provide an explanation as to why Ad5Hey1 cannot kill or sensitise these cells to cytotoxic drugs and could be explored in future studies.

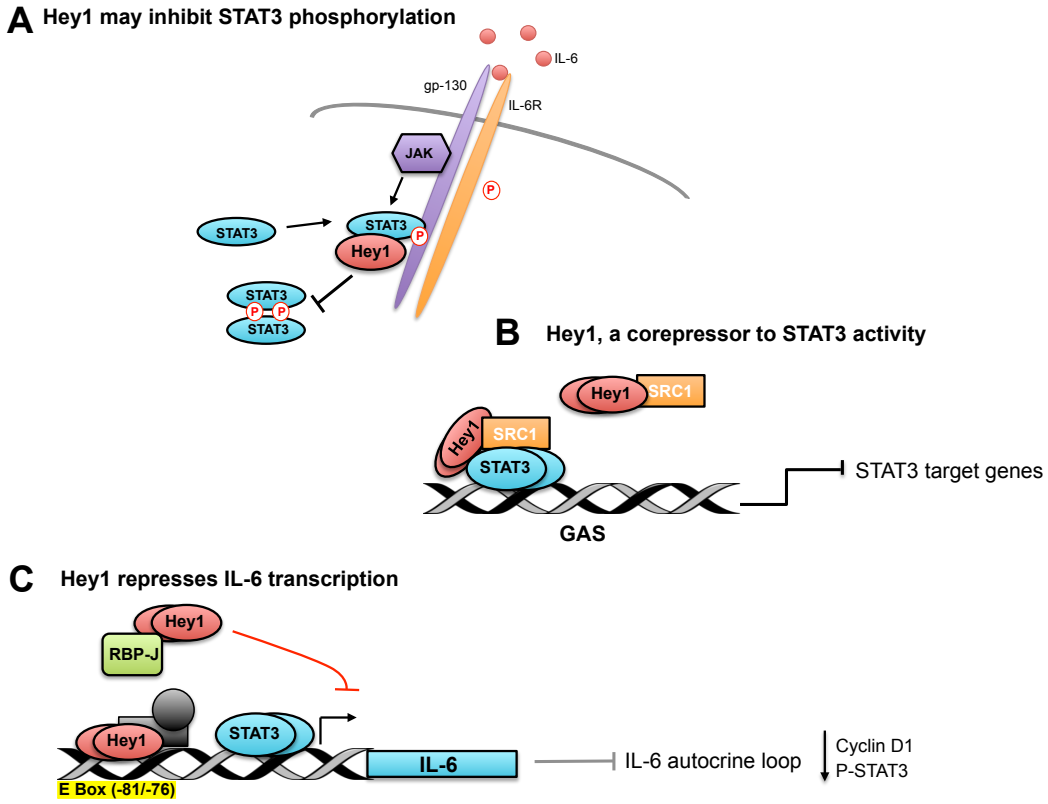

Figure 65. Schematic diagram illustrating the possible mechanisms through which Hey1 might downregulate constitutively active STAT3 in DU145 cells.

A) STAT3 activation is initiated by binding of ligand (IL-6) to gp-130/IL-6R with subsequent dimerization of the receptor and activation of associated JAK kinases. Activated JAK kinases phosphorylate the cytoplasmic region of the receptor and recruit STAT3. Hey1 may bind to STAT3 via the bHLH and orange domain in a similar fashion to Hes1 (Kamakura, Oishi et al. 2004) and prevent JAK kinase-mediated phosphorylation of STAT3 at Y705 thus preventing dimerization of STAT3, translocation to the nucleus and transactivation of STAT3 target genes. B) Alternatively, Hey1 may behave as corepressor to STAT3 by direct interaction with STAT3 and/or binding to SRC1, a coactivator to STAT3-mediated transactivation (Giraud, Bienvenu et al. 2002) thus preventing coactivator recruitment to STAT3 transcription complexes. C) Hey1 may directly bind to an E-box binding site within the proximal promoter of IL-6 and inhibit E box-RBP-J-mediated transcription (Hu, Cheng et al. 2008) thus inhibiting transcription of IL-6 and blocking autocrine stimulation of growth by IL-6 in DU145 cells. Therefore indirect regulation of the JAK/STAT pathway will also culminate in the decrease of STAT3 activity.

4.4.2. Ad5Hey1 and AdE1A12S synergise with docetaxel and mitoxantrone in PCa cells

Using a fixed dose combination approach, sub-optimal dose of either docetaxel or mitoxantrone resulted in synergistic cell killing in combination with Ad5Hey1 in 22Rv1 and DU145 cells. As described previously, AdE1A12S also resulted in synergistic cell death with both drugs in DU145 cells (Miranda, Maya Pineda et al. 2012). However, although Ad5Hey1 and AdE1A12S were shown previously to sensitise LNCaP cells to docetaxel- and mitoxantrone-induced cell death (Cheong *et al*, manuscript in preparation), no synergy was observed at the selected doses for either virus in LNCaP cells. I speculated whether this was as a consequence of drug-induced increases in mitochondrial activity since the MTS viability assay was previously shown to underestimate the antiproliferative effect of the green tea polyphenol, (-)-epigallocatechin-3-gallate (EGCG) in LNCaP cells compared with adenosine triphosphate (ATP), DNA or trypan-blue based assays (Wang, Henning et al. 2010). Furthermore treatment of LNCaP cells with bicalutamide maintained mitochondrial dehydrogenase activity and did not result in $\Delta_{\psi m}$ depolarisation unless in serum-free medium suggesting trophic factors attenuate the process of bicalutamide-dependent $\Delta_{\psi m}$ dissipation (Lee, Zhan et al. 2003). It is possible that the previous sensitisation experiments involving a fixed dose of Ad5Hey1 combined with a dose response to drugs overcame the limitation of the MTS assay. Interestingly when LNCaP cells were treated with either cytotoxic drug, $\Delta_{\psi m}$ hyperpolarisation was detected. In a previous study, $\Delta_{\psi m}$ hyperpolarisation was associated with an increase mitochondrial biomass (McGowan, Alling et al. 2011). The majority of literature report cytotoxic drug treatment results in $\Delta_{\psi m}$ depolarisation. However, drug-induced proliferation of mitochondria has also been cited sporadically in a number of studies including the rat mammary adenocarcinoma cell line (MTLn3) treated with doxorubicin or mitoxantrone (Kluza, Marchetti et al. 2004) confirming a link between apoptosis and changes in the structure and mass of mitochondria. However, despite measuring cell viability with picogreen or sulforhodamine B similar trends in combination treatments were observed in LNCaP cells. Further assessment is therefore necessary to assess whether Ad5Hey1 is able to synergise with these drugs at other selected fixed dose-combinations. As well as testing various dose combinations, the order of the

addition of each agent should also be assessed. Previously in our laboratory, additional dose combinations of replicating Ad5 and docetaxel or mitoxantrone were found to be synergistic in LNCaP cells when the drugs were added 24h before the addition of the virus (Radhakrishnan, Miranda et al. 2010) suggesting p53 induction by cytotoxic drug treatment in certain cell lines may sensitise cells to Ad5-induced cell death.

The therapeutic efficacy of mitoxantrone is primarily through intercalation of DNA and as an inhibitor of topoisomerase IIA, preventing religation of cleaved DNA and causing double-stranded DNA breaks. Docetaxel binds to β-tubulin monomers resulting in microtubule stabilisation, impairing mitosis and driving the cell into mitotic catastrophe, an irreversible state that leads to cell death commonly through apoptosis. Both drugs induce changes in cell cycle progression, induction of oxidative stress and DNA damage, which finally leads to apoptosis. The exact nature of drug-induced deregulation of the cell cycle depends on genetic alterations of the tumour cell and drug dosage resulting in either G1 or G2/M arrest. Using similar doses to those used in this thesis, colleagues in our research group have observed that treatment with mitoxantrone or docetaxel result in an accumulation of cells in G2/M for DU145 and 22Rv1 cells (Radhakrishnan, Miranda et al. 2010; Miranda, Maya Pineda et al. 2012). E1A-dependent increases in p53 activity and p53-independent mechanisms are likely to contribute to synergistic cell killing with cytotoxic drugs. However E1A-dependent effects on cell cycle checkpoints also play a role. Interactions of E1A with p300 and p400 and inactivation of p21 as discussed in section 1.6.3.3.1 and earlier in this chapter promotes cell cycling. Enhanced S phase activity may therefore intensify apoptosis by promoting DNA damage during DNA synthesis in the presence of drugs. A dose-dependent increase in S phase was observed after infection of AdE1A12S in 22Rv1 and DU145 cells indicating E1A12S enhances cell cycle progression. Previously, AdE1A12S was found to increase mitoxantrone-induced accumulation of cells in G2/M in 22Rv1, DU145 and PC3 cells with enhanced polyploidy in combination treatments in DU145 cells (Miranda, Maya Pineda et al. 2012).

No obvious increase in S phase was observed after Ad5Hey1 infection as a single treatment for either cell line. However, studies have implicated the importance of G2/M checkpoint abrogation or arrest in enhancing the effect of DNA damaging drugs (Bucher and Britten 2008). Therefore, the putative delay

in G2 after infection with Ad5Hey1 might contribute to the sensitisation to chemotherapeutic drugs. Cyclin B1 expression in PCa cell lines has been correlated to their responsiveness to treatment with docetaxel (Gomez, de Las Pozas et al. 2007). Future experiments might clarify whether Ad5Hey1 delays drug-treated cells in G2/M and to what extent the Ad5Hey1-mediated G2 delay contributes to this. LNCaP cells expressing high levels of cyclin B1 were more sensitive to apoptosis after treatment with docetaxel compared with DU145 and PC3 cells, which express comparatively low levels of cyclin B1. Cell death was reduced after cyclin B1 knockdown or inhibition of Cdk1 activity (Gomez, de Las Pozas et al. 2007). As a function of doxetaxel-induced G2/M arrest and subsequent mitotic catastrophe-mediated cell death, docetaxel increases cyclin B1 expression and associated Cdk1 activity in PCa cells (Perez-Stable 2006). Consequently, the Ad5Hey1-induced increase in cyclin B1 expression in 22Rv1 cells sensitise cells to treatment with docetaxel. Furthermore overexpression of E2F1 has been correlated with an increase in cyclin B1 and Cdk1 activity resulting in sensitisation to paclitaxel (Russo, Magro et al. 2006). At present this correlates with our knowledge of E1A-dependent release of E2F1 from pRb and suggests AdE1A12S increased cyclin B1 levels as a consequence of E2F1 regulation. Considering that Hey1 might also increase E2F1 stabilisation this could explain Ad5Hey1-mediated increase in cyclin B1 expression. For future studies it will be important to determine how the putative Ad5Hey1-dependent G2 delay contributes to cell cycle deregulation when combined with docetaxel and mitoxantrone and the involvement of Ad5Hey1 in DDR pathway.

Recent studies have reported docetaxel and paclitaxel inhibit AR expression and activity in 22Rv1 and LNCaP cells (Gan, Chen et al. 2009; Kuroda, Liu et al. 2009). The mechanism of reduced AR activity by paclitaxel was attributed to a reduction in AR nuclear translocation possibly as a result of AR binding to tubulin (Zhu, Horbinski et al. 2010). Reduction of AR signalling in docetaxel-treated cells therefore provides an additional targeting mechanism that may be complemented with Ad5Hey1-dependent mechanisms.

It has been reported by members of our laboratory that E1A expressed from AdE1A12S increased in the presence of mitoxantrone in DU145 cells (Dr Enrique Miranda, PhD Thesis, 2009). This could be a function of enhanced transcription of E1A12S from the CMV promoter. I did not assess Hey1 expression after combination treatment however in support of a drug-induced

effect on CMV transcription it was recently shown that doxorubicin-induced response to cellular stress and DNA damage results in activation of NFκB which in turn binds and transactivates the CMV promoter and enhances transgene expression (Kim, Kang et al. 2007). This was also found in the context of adenovirus-mediated gene delivery after treatment with cisplatin-enhanced expression from the CMV promoter as a consequence of persistent DNA damage (Zacal, Francis et al. 2005). Increased transcriptional activation of the CMV promoter has also been associated with docetaxel. In combination with a prostrate-restricted oncolytic virus, docetaxel increased CMV activity and enhanced transgene expression. This was associated with increased p38 MAPK activity and was independent to adenovirus-binding receptors and replication (Li, Liu et al. 2010).

Currently, our intention is to insert Hey1 into the potent, replication-selective AdΔΔ viral vector. In this context Hey1 will be under the control of the viral E3 promoter to ensure early transgene expression independent of viral late gene expression and replication. In addition, it is now recognised that CMV promoters are less suitable *in vivo* because of time-limited transcriptional activity through cytokine-mediated repression of the promoter resulting in reduced transgene expression (Qin, Ding et al. 1997). Previously we have shown that cytotoxic agents including docetaxel and mitoxantrone enhance E1A expressed from the native viral promoter, which together with increased infection and replication rates contributed to synergistic cell killing in a cell line and drug-dependent manner (Cheong, Wang et al. 2008; Radhakrishnan, Miranda et al. 2010). Furthermore, when the drugs enhance E1A-expression, the activity of the E3 promoter would also increase since transcription is partly dependent on E1A in addition to cellular factors such as NFκB. It will be interesting to realize the extent of Hey1 expression in the context of a replication-selective virus (AdΔΔHey1).

4.4.3. Ad5Hey1 primarily enhances drug-induced apoptosis in PCa cells

In 22Rv1, DU145 and LNCaP cells, Ad5Hey1 augmented docetaxel-induced apoptosis. In combination with mitoxantrone, Ad5Hey1 enhanced drug-induced apoptosis in 22Rv1 and LNCaP cells but not in DU145 cells. Apoptosis was

characterised by greater $\Delta_{\psi m}$ depolarisation and increased activation of caspase-3 and caspase-7. In DU145 cells, Ad5Hey1 in combination with mitoxantrone resulted in a reduction in the levels of these apoptotic markers compared with mitoxantrone alone. In all cell lines AdE1A12S enhanced docetaxel and mitoxantrone-induced apoptosis. This is in accordance with a previous study showing AdE1A12S enhanced mitoxantrone-induced $\Delta_{\psi m}$ depolarisation in DU145 cells (Miranda, Maya Pineda et al. 2012). In addition, AdE1A12S enhanced mitoxantrone-induced apoptosis through the mitochondrial pathway in 22Rv1 cells as well which was previously believed not to be involved in AdE1A12S-mediated sensitisation (Miranda, Maya Pineda et al. 2012). This disparity is a result of differences in drug dose and concentration of TMRE used to measure $\Delta_{\psi m}$.

Resistance to apoptosis occurs when a variety of blocks on the apoptotic pathways are imposed. Proteins involved in the regulation of apoptosis such as Bcl-2, Bax and p53 are differentially expressed in the cell lines used in this research (Gurumurthy, Vasudevan et al. 2001; Skjoth and Issinger 2006). This affects their propensity to undergo cell death, the mechanism of which is influenced by the mutational background of the cells as well as the cytotoxic agent and dose used. Therefore, the induction of apoptosis in DU145 cells is independent of p53 status, while 22Rv1 and LNCaP cells, which express functional p53, probably require p53 activation to undergo efficient cell death. This seems the case with regards to Ad5Hey1 and AdE1A12S-mediated cell death in 22Rv1 cells since cell death was reduced after ablation of p53. 22Rv1 overexpress the p53-antagonist, Bcl-2 (Skjoth and Issinger 2006), however, this did not impact on their capacity to undergo apoptosis in response to the viruses and/or drugs. In general, apoptosis was induced to a greater extent in these cells compared with DU145 and LNCaP cells. With regards to virus-induced cell death in 22Rv1 cells, their enhanced permissiveness to adenoviral infection is likely to have contributed to this. Both drugs induced apoptosis to a similar degree in these cells. Furthermore, Ad5Hey1 infection induced greater $\Delta_{\psi m}$ depolarisation and caspase-3 activation compared with an equivalent dose of AdE1A12S. This is not unexpected as it is in line with our observations that Ad5Hey1 induced p53 stabilisation to a greater extent than AdE1A12S. This also suggests that the degree of apoptosis in these cells is dependent on p53 activity. The capacity of 22Rv1 cells to readily undergo $\Delta_{\psi m}$ depolarisation may be as a consequence of a more functional mitochondrial pathway compared with

DU145 and LNCaP cells. p53 activity is known to enhance the propapoptotic activity of Bax either by promoting its expression, repressing transcription of Bcl-2 or Bcl-xL expression or through direct binding of Bcl-2 or Bcl-xL at the outer mitochondrial membrane. Although not assessed, p53 also transactivates BH3-only proapoptotic Bcl-2 family members (e.g. Bid, Puma and Noxa), which mediate mitochondrial membrane permeabilisation (Kroemer, Galluzzi et al. 2007). In addition to the increase in Bax expression after single virus or drug treatment, enhanced expression of a small form of Bax was detected after combination treatments. Proteolytic cleavage of Bax in response to chemotherapeutic agents was previously demonstrated (Yeo, Cha et al. 2002). In another study, Bax cleavage by calpain yielded a p18 Bax product that was more potent in inducing apoptosis compared with full-length Bax. It was proposed that cleavage of Bax might enhance oligomerization in the outer mitochondrial membrane thus serving as an amplification step to accelerate apoptosis (Cao, Deng et al. 2003). I did not verify whether this could be the case in my study. Cell fractionation would clarify whether the product was associated with the mitochondria and hence be putatively correlated with mitochondrial pathway. AdE1A12S-dependent enhancement of drug-induced cell death and sensitisation was similar to that induced by Ad5Hey1 suggesting the transgenes activate similar pathways.

Interestingly, in LNCaP and DU145 cells, I observed $\Delta_{\psi m}$ hyperpolarisation in response to docetaxel and mitoxantrone. Recently, tubulin stabilisation by paclitaxel was found to promote hyperpolarisation whereas tubulin-depolymerizing agent, nocodazole stimulated depolarisation in tumour cells (Maldonado, Patnaik et al. 2010). Tubulin is known to reversibly bind to voltage-dependent anion channel (VDAC), an abundant protein residing in the outer mitochondrial membrane. In the tubulin-blocked state, VDAC is impermeable to ATP/ADP and as a consequence the function of the ATP synthase is inhibited resulting in the accumulation of H^+ in the intermembrane mitochondrial space promoting $\Delta_{\psi m}$ hyperpolarisation (Rostovtseva, Sheldon et al. 2008). Therefore agents that modify the equilibrium between polymerised and dimeric tubulin alter $\Delta_{\psi m}$ potential. Both docetaxel and mitoxantrone have an affinity for tubulin (Ho, Law et al. 1991; Ringel and Horwitz 1991), and in these cells, drug-induced alterations to the microtubule dynamics may account for the $\Delta_{\psi m}$ hyperpolarisation. No $\Delta_{\psi m}$ hyperpolarisation was observed in 22Rv1 cells. The

drug-induced effect on $\Delta_{\psi m}$ may be a consequence of mitochondrial dysfunction and it is possible 22Rv1 cells have a more intact mitochondrial pathway.

DU145 cells do not express Bax and this has been correlated with their resistance to staurosporine-induced cell death and delayed caspases activation and PARP cleavage (Marcelli, Marani et al. 2000; Gurumurthy, Vasudevan et al. 2001). In these cells, mitoxantrone was more efficient at inducing apoptosis through $\Delta_{\psi m}$ depolarisation and caspase-3 and -7 activation than docetaxel and this might reflect the different mechanisms by which these drugs induce cell death. Microtubule stabilisation induced by docetaxel triggers apoptosis through mitotic catastrophe, with the deregulation of tubulin dynamics impacting on mitochondrial function through the phosphorylation and inhibition of Bcl-2 (Fabbri, Amadori et al. 2008). Mitotic catastrophe has been linked to the activation of caspase-2 and in DU145 cells active caspase-2 was detected in response to docetaxel treatment (Fabbri, Amadori et al. 2008). In a separate study, reduction of cell viability by docetaxel was only partially abrogated with a pan caspase inhibitor suggesting docetaxel induces cell death through caspase-independent pathways (Mediavilla-Varela, Pacheco et al. 2009).

In DU145 cells, neither Ad5Hey1 nor AdE1A12S induced obvious changes to $\Delta_{\psi m}$ depolarisation or caspase-3 activation suggesting that the cytotoxicity induced solely by transgene expression occurred through alternative cell death pathways. However, expression levels of active caspase-7 were similar for virus infected cells compared to cells treated with docetaxel suggesting a preference for caspase-7 activation in response to Hey1 or E1A12S expression as opposed to caspase-3 activation. This is in keeping with Walsh *et al*. who determined the activities of these caspases engage in non-redundant roles during apoptosis (Walsh, Cullen et al. 2008). Activation of caspase-7 may not entirely account for the cell death by the viruses and other modes of cell death may be occurring. Necrosis (or necroptosis) is a possibility. Marcelli *et al*. also observed morphological characteristics reflecting necrosis after DU145 cells were treated with stauroporine (Marcelli, Marani et al. 2000).

Whereas Ad5Hey1 increased caspase-dependent cell death in combination with docetaxel in DU145 cells, in combination with mitoxantrone, Ad5Hey1 reduced levels of all apoptotic markers including PARP cleavage. However as the PARP antibody recognised only the 89kDa cleaved form, which is associated with

apoptotic cell death and cathepsin B and D cleavage (Chaitanya, Steven et al. 2010), it is not surprising that PARP cleavage reproduced the caspase-dependent trends detected for this combination treatment. Future studies are required to determine the alternative pathways of cell death that might account for the synergistic cell killing with this Ad5Hey1 drug combination. Alternative cell death mechanisms under consideration for future examination are necroptosis and autophagy.

Although LNCaP cells express wild-type p53, they also possess a deregulated PI3K/AKT pathway due to a loss of PTEN expression (Gurumurthy, Vasudevan et al. 2001; Skjoth and Issinger 2006). Activation of AKT prevents apoptosis by phosphorylating and inhibiting proapoptotic factors Bad, pro-caspase-9 and preventing the expression of Bim (Dijkers, Medema et al. 2000; Gurumurthy, Vasudevan et al. 2001). It also prevents release of cytochrome C thereby preventing the initiation of the caspase cascade (Kennedy, Kandel et al. 1999). Therefore AKT inhibits apoptosis by maintaining mitochondrial integrity. Docetaxel and mitoxantrone had contrasting effects on $\Delta_{\psi m}$ depolarisation in these cells. Docetaxel efficiently induced dissipation of $\Delta_{\psi m}$ while mitoxantrone had no effect. Similarly, Ad5Hey1 and AdE1A12S had no effect on $\Delta_{\psi m}$. Treatment with mitoxantrone or either virus did however induce activation of caspase-3 without $\Delta_{\psi m}$ depolarisation suggesting activation of caspase-3 by the extrinsic pathway. Mitoxantrone and other anthracycline-based agents were found to upregulate expression of FasL in LNCaP cells (Liu, Rubin et al. 1998) indicating the cell death receptor pathway may be activated in response to mitoxantrone treatment which enhances the susceptibility of cells to apoptosis in these cells. The presence of Ad5Hey1 sensitised mitoxantrone-treated cells to enhanced cell death through the mitochondrial pathway. This may be a consequence of p53 activation, which as discussed above results in expression of proapoptotic mitochondrial-associated proteins and inhibition of Bcl-2. This could therefore "prime" the mitochondria for $\Delta_{\psi m}$ depolarisation through the cleavage of Bid by FasR/FasL-mediated activation of procaspase-8. Therefore Ad5Hey1 was able to trigger apoptosis via the mitochondrial pathway in the presence of mitoxantrone which at the dose used, primarily functioned as a cytostatic agent in these cells. Deregulation of E2F activity by E1A is directly coupled to the components of the apoptotic pathway (Nahle, Polakoff et al. 2002). Caspase expression is a direct target of E2F, potentially increasing levels over that of inhibitor of apoptosis (IAP) proteins to trigger caspase activation.

Alternatively. E1A-induced E2F expression could also increase caspase-8 expression and sensitise cells to death-inducing ligands. Thus E1A has an additional method of cooperating with p53-dependent apoptosis to amplify apoptosis (Nahle, Polakoff et al. 2002).

It is evident that the various genetic alterations of the various PCa cell lines resulted in differential outcomes in the specific apoptotic mechanism triggered by Ad5Hey1 and drug treatments. I have demonstrated that Ad5Hey1 in combination with either drug results in supra-additive cell death in all of the PCa cell lines, which were receptive to Ad5Hey1. Ad5Hey1 enhanced apoptosis produced by sub-optimal doses of the drug with the exception of mitoxantrone in DU145 cells where alternative cell death mechanism are presumed to occur as a consequence of this combination treatment. The studies in this thesis therefore demonstrate the potential for Hey1 as a therapeutic transgene in future adenoviral gene therapy studies.

4.5. Ad5Hey1 is efficacious in a translational setting

The majority of CRPC tumours, despite castrate serum levels of testosterone, are still subject to low-level androgen stimulation by conversion of adrenal androgens to testosterone or through intraprostatic *de novo* androgen synthesis. CRPC tumours may overexpress AR or harbour mutant AR with these alterations modifying the response of the cancer cells to ADT therapy. It was therefore important to assess the potency of Ad5Hey1 during androgen stimulation and in the presence of bicalutamide to further validate Hey1 for the treatment of PCa.

Ad5Hey1 decreased cell growth of androgen-responsive LNCaP and VCaP cells when AR signalling was stimulated with mibolerone. In LNCaP cells, growth was inhibited to below basal levels. This result is in agreement with another study, which showed HeyL inhibited growth of androgen-stimulated LNCaP cells stably, expressing inducible HeyL (Lavery, Villaronga et al. 2011). Ad5Hey1 only partially inhibited androgen-stimulated growth in VCaP cells. VCaP cells contain an amplified wild-type AR gene locus, which may explain the enhanced

androgen-stimulated growth compared with LNCaP cells. Therefore it is not unexpected that a more limited growth inhibition by Ad5Hey1 is observed.

Intriguingly, mibolerone sensitised 22Rv1 cells to Ad5Hey1-dependent growth inhibition. 22Rv1 cells differ from the other AR-positive cell lines by expressing androgen-independent AR isoforms. It is attractive to hypothesise that the androgen-independent isoforms in 22Rv1 cells may have additional roles other than androgen-independent transcriptional activity. For example in the LNCaP 104-R1 cells, non-genomic activity of AR has been implicated in promoting AR-mediated translocation of ectopically expressed Bax to the mitochondria of 104-R1 cells (Lin, Kokontis et al. 2006). This effect was potentiated with androgen stimulation while bicalutamide blocked the androgen-specific sensitising effect indicating the transcriptional activity of AR only enhanced the AR-dependent effect on Bax and apoptosis (Lin, Kokontis et al. 2006). In addition, ligand-independent functions related to the apoptotic pathway have been associated with an orphan member of the steroid-thyroid hormone nuclear receptor, Nur77/TR3 which binds Bcl-2 and converts its antiapoptotic role to one of proapoptotic, possibly through the activation of Bax (Kroemer, Galluzzi et al. 2007). In a recent study, induction of mitochondrial fission by Ca^{2+} efflux inhibition in LNCaP cells was further enhanced by pre-treatment with androgen. This was found to be related to the action of the androgen-regulated, dynamin-related protein, Drp1, which is involved in mitochondrial fission (Choudhary, Kaddour-Djebbar et al. 2011). It is therefore conceivable that mibolerone-activation of the AR and/or AR isoforms in 22Rv1 cells could enhance this Ad5Hey1-mediated effects on mitochondrial dysfunction. As the growth stimulatory effects of androgens on LNCaP and VCaP cells are more profound, potential proapoptotic effects by androgens/AR will be offset by cell growth.

The effectiveness of bicalutamide as an antiandrogen is dependent on AR mutation status and copy number. Bicalutamide is converted to a partial agonist when AR is overexpressed leading to alteration in coactivator and corepressor recruitment to the AR transcriptional complex at target genes (Chen, Welsbie et al. 2004). In LNCaP cells overexpressing AR, recruitment of NCoR to the promoters of AR target genes, *PSA* of *KLK2* was reduced or absent respectively after bicalutamide treatment (Chen, Welsbie et al. 2004). This may explain the ineffectiveness of bicalutamide on basal and androgen-stimulated growth in VCaP cells. On the other hand in LNCaP cells, bicalutamide functioned as a

potent AR antagonist. Nevertheless, in VCaP and LNCaP cells, combination of Ad5Hey1 and bicalutamide under mibolerone stimulation resulted in a beneficial effect over uninfected or Ad5GFP-infected cells. Furthermore bicalutamide further sensitised LNCaP cells to Ad5Hey1-mediated growth inhibition. Bicalutamide binds at the AR LBD whereas Ad5Hey1 targets the N-terminal AF-1 domain. The separate binding site for these agents affords the potential of cooperation thereby enhancing Ad5Hey1-mediated inhibition of AR transcriptional activity. However it should be considered that N-terminal mutations within the AR could abrogate Hey1 binding thereby decreasing efficacy. Further studies will be required to assess the effect of Ad5Hey1 and bicalutamide on AR transcriptional activity at the doses used in this study in VCaP and LNCaP cells. Importantly, Ad5Hey1 was able to work in concert with bicalutamide in the presence of androgen stimulation and did not antagonise the effect of bicalutamide. These results indicate Ad5Hey1 is able to inhibit cell growth and furthermore might control for further tumour growth.

An androgen-independent LNCaP progression model (Kokontis, Takakura et al. 1994; Kokontis, Hay et al. 1998; Kokontis, Hsu et al. 2005), which reflects the clinical state of CRPC was employed to assess the potency of Ad5Hey1. It has been demonstrated using tumour xenograft models that 104-R1 and CDXR3 sub-clones reflect an intermediary stage of CRPC. After being subjected to androgenic suppression, these cell clones relapsed as either androgen-stimulated or androgen-independent models respectively. Therefore, CDXR3 cells are thought to imitate a more advanced stage of disease progression than 104-R1 cells (Kokontis, Takakura et al. 1994; Kokontis, Hsu et al. 2005; Chuu, Kokontis et al. 2011). It was encouraging to find that 104-R1 and CDXR3 cell were more susceptible to cell killing by Ad5Hey1 than the parental, 104-S cells. Preliminary data indicates the growth inhibitory effects by Ad5Hey1 in the 104-R1 and particular, CDXR3 cells could be a consequence of an accumulation of cells in G1. It has been previously determined that CDXR3 xenograft tumours relapsed less frequently than 104-R1 tumours after testosterone treatment possibly due to the slower proliferation rate of CDXR3 cells and enhanced apoptosis induced in these cells compared with 104-R1 cells (Kokontis, Hay et al. 1998; Kokontis, Hsu et al. 2005; Chuu, Kokontis et al. 2011). This highlights the differences between 104-R1 and CDXR3 cells in terms of their outcome to androgen treatment, which may also translate to differential outcomes in

response to other treatments. These differences could account for why a greater accumulation of CDXR3 cells in G1 after Ad5Hey1 infection was observed.

Androgenic suppression through the activity of the AR was shown by Kokontis and colleagues to induce a prolonged G1 arrest in 104-R1 cells (Kokontis, Hay et al. 1998). Although CDXR3 cells have not been similarly assessed with respect to complete cell cycle analysis, CDXR3 cells were similarly repressed by androgen in terms of proportion of cells in S phase and cell viability (Kokontis, Hsu et al. 2005). It was not possible to replicate the androgen-induced G1 arrest in 104-R1 and CDXR3 cells in this particular study possibly because of variation in cell culture conditions. Under our conditions, the population of cells in G1 in response to Ad5Hey1 was potentially overriding the suppressive effects of androgen in these cells. Furthermore, an increase in the sub-G1 fraction was observed for Ad5Hey1-infected 104-R1 and CDXR3 cells.

In 104-R1 and CDXR3 cells the androgen-stimulated G1 cell cycle arrest was partly attributed to a sustained expression of p27 (Kokontis, Hay et al. 1998; Kokontis, Hsu et al. 2005) maintained through androgen-dependent downregulation of Skp2, a protein of the SCF ubiquitin ligase complex. Androgen exposure also downregulated c-Myc expression in 104-R1 cells contributing to G1 arrest (Kokontis, Takakura et al. 1994). Therefore, it is possible Ad5Hey1 is mediating an accumulation of cells in G1 through activation of p53 and subsequent p27 induction. I did not see any notable changes in the cell cycle profile of 104-S cells after Ad5Hey1 infection. Androgen treatment of 104-S cells releases cells from an androgen deprivation-induced G1 arrest by upregulating Skp2 expression resulting in an increase in protesomal degradation of p27 and p21 (Kokontis, Takakura et al. 1994; Wang, Sun et al. 2008). Therefore, the androgen-regulated decrease in Cdk inhibitor expression may, to a certain extent, oppose the growth inhibitory effects of Ad5Hey1 which may be why I do not detect an accumulation of 104-S cells in G1. However, Ad5Hey1 infection resulted in an increase in the the fraction of cells in sub-G1 indicating Ad5Hey1 was able to kill these cells. The sub-G1 fraction was further increased in the presence of mibolerone, demonstrating that under certain circumstances androgen stimulation sensitises cells to cytotoxic agents. These studies are ongoing and evaluation of Ad5Hey1 in the LNCaP progression model used in this thesis provides a valuable method of assessing the effect of Ad5Hey1 and in the future, AdΔΔHey1 in a treatment-resistant PCa model.

4.6. Concluding remarks

The data in this thesis have demonstrated that overexpression of the Notch signalling effector protein, Hey1, inhibited growth and confirmed the tumour suppressor role of Hey1 in several PCa cell lines. The multiple modes of action for Ad5Hey1 are likely to have contributed to efficient cell death and highlights the numerous and potentially far-reaching actions of Hey1. In agreement with published results, Ad5Hey1 demonstrated crosstalk with AR, p53 and JAK/STAT signalling demonstrating the effectiveness of ectopically expressed Hey1 in a range of genetic backgrounds. Although not explored in this thesis, it is hypothesised Hey1-mediated inhibition of HDM2 may result in activation of p53-independent mechanisms of cell death through upregulation of E2F1 and TAp73. Combination treatments with chemotherapeutic drugs showed that Ad5Hey1 functioned as a sensitising agent and this upholds the rationale for use of Hey1 as a therapeutic transgene in adenoviral gene therapy. In addition, Ad5Hey1 and bicalutamide treatment of a range of AR-positive PCa cell lines, differing in their responsiveness to bicalutamide treatment, could work together to inhibit mibolerone-induced growth stimulation. Finally, preliminary data using Ad5Hey1 in an androgen-independent LNCaP progression model demonstrated promising findings for inhibiting cell growth. Together, this data reveals the potential use of a transcription cofactor as a therapeutic transgene for the treatment of CRPC.

4.7. Future directions

In light of the crosstalk between the AR and p53 signalling pathways it would be interesting to simultaneously knockdown AR and p53 in 22Rv1 cells to determine whether depletion of both proteins will ablate Ad5Hey1-mediated cytotoxicity. Considering that the stabilisation of p53 by Ad5Hey1 in LNCaP cells was not as pronounced as in 22Rv1 and HCT116wt cells, it would be of interest to repeat the AR and p53 knockdown studies in this cell line. It would also be valuable to assess the activation status of p53 through the detection of phospho (ser15) p53 after Ad5Hey1 infection. Since these cells are more dependent on AR signalling for cell growth, we might expect differential regulation of AR and p53 by Ad5Hey1 compared with 22Rv1 cells. As discussed above, the limited

induction of p53 expression by Ad5Hey1 may be a consequence of AKT-induced inhibition and destabilisation of p53 through AKT-dependent promotion of HDM2 activity. It would therefore be of interest to realise whether inhibition of AKT by RNA interference of selective AKT inhibition would sensitise these cells further to Ad5Hey1-dependent cytotoxicity.

In view of the p53-independent activities of HDM2, in particular inhibition of E2F1 and TAp73α, we propose to explore whether Ad5Hey1-mediated inhibition of HDM2 will enhance the activity of these proteins in HCT116p53$^{-/-}$ cells since these cells express p73 and have a functional pRb/E2F1 pathway. Expression levels of bona fide targets of E2F1 targets, cyclin E and p73 will be assessed in response to Ad5Hey1-infection as well as TAp73α protein levels since the activity of this protein is also under the control of HDM2. The expression status of p73 in DU145 cells has not been established therefore, if we find these cells express p73 we will establish whether p73 activation might play a role in Ad5Hey1-dependent cell killing.

I endeavoured to investigate the AR and p53-independent mechanism of Ad5Hey1 mode of action in DU145 cells in the context of STAT3 signalling. This aspect of Ad5Hey1-mediated regulation requires further analysis. Initial experiments will involve assessing the combined effect of Ad5Hey1 and AZD1480 on phospho-STAT3 and cyclin D1 levels after 48h. Cells will be treated with AZD1480 for a small window of time prior to the end of the time course to allow any potential combined effect on STAT3 signalling with these agents to be observed. RNA interference towards STAT3 in DU145 cells provides an alternative, more specific way of blocking STAT3 activity. If Ad5Hey1 does mediate its effects through inhibition of STAT3 signalling, siRNA towards STAT3 might desensitise cells to Ad5Hey1-dependent cell killing. However alternatively, knocking down STAT3 could sensitise cells to other Ad5Hey1-dependent effects of other Hey1 targets such as inhibition of HDM2. Therefore other detailed studies to elucidate the potential mechanism Hey1 might employ on STAT3 signalling are required. To clarify whether Hey1 could be repressing STAT3 transactivation, the activity of a STAT3-inducible reporter system in the presence of Ad5Hey1 would prove informative. Likewise, co-immunoprecipitation studies between Hey1 and STAT3 might demonstrate a direct relationship. Dependent on the results of these studies we would finally

transfect PC3 cells with STAT3 to investigate whether the presence of STAT3 would sensitise these cells to Ad5Hey1-mediated cytotoxicity.

Further investigation into Ad5Hey1-dependent effects on cell cycle deregulation in 104-R1 and CDXR3 cells is required as well as confirming whether Ad5Hey1-mediated cell death occurs via apoptosis. The molecular mechanisms by which Ad5Hey1 is delaying cell cycle progression will also be explored. To extend the study assessing activity of Ad5Hey1 in response to androgen and bicalutamide treatment in AR-positive PCa cells (section 3.4.1), we plan to assess the response of Ad5Hey1 in 104-R1 and CDXR3 cells in the presence of these agents. It would also be valuable to evaluate AR transcriptional activity using our AR-responsive luciferase reporter plasmid after Ad5Hey1 infection in these cells. Furthermore, it would be of interest to assess the sensitivity of the resistant 104-R1 and CDXR3 cell lines to cytotoxic drug treatment and if found to be more resistant to drugs than 104-S cells, to assess the effect of these cells in combination with Ad5Hey1.

Finally, we also plan to complete construction of AdΔΔHey1 and evaluate against AdΔΔ for efficacy as a single agent and in combination with cytotoxic drugs by assessing cell viability and viral replication *in vitro*. Sensitivity of AdΔΔHey1 to human prostate epithelial cells will also require evaluation to ensure AdΔΔHey1 is attenuated in normal cells. Dependent on *in vitro* findings, we plan to verify the efficacy of AdΔΔHey1 *in vivo* using DU145 and LNCaP androgen-ablation and bicalutamide-resistant xenografts.

5. Appendix

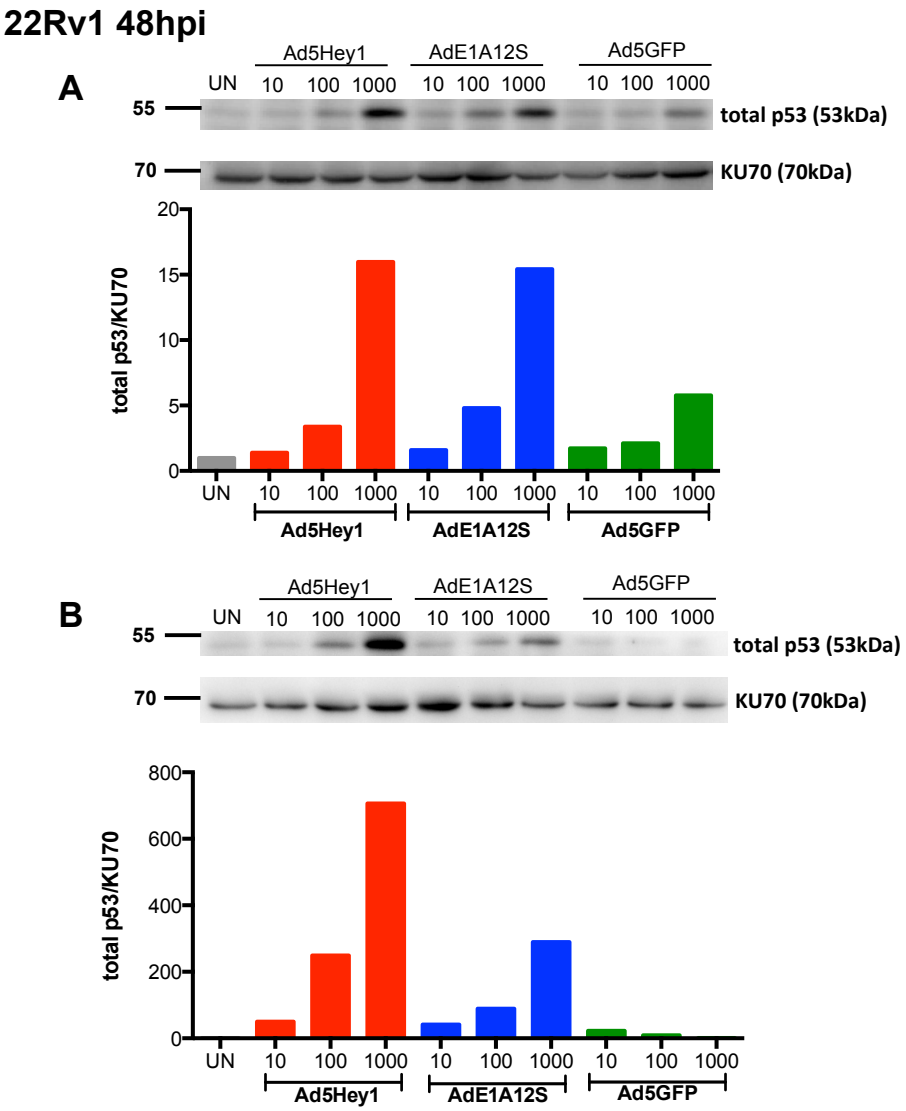

Figure_Apx 1. Ad5Hey1-infection stabilises p53 in 22Rv1 cells at 48h

Cells were infected with Ad5Hey1#2 (A) or Ad5Hey1#3 (B), AdE1A12S#2 and Ad5GFP at 10, 100 and 1000ppc. After 2h, infection medium was removed and replaced with 10% FBS DMEM. Cell lysates were harvested at 48h post-infection and prepared for separation on polyacrylamide gels. 20µg protein was loaded per lane and total p53 blotted. KU70 was used as a loading control. Histogram showing total p53 protein expression normalised to KU70 and expressed relative to uninfected (UN) cells. Results show blots from two independent experiments.

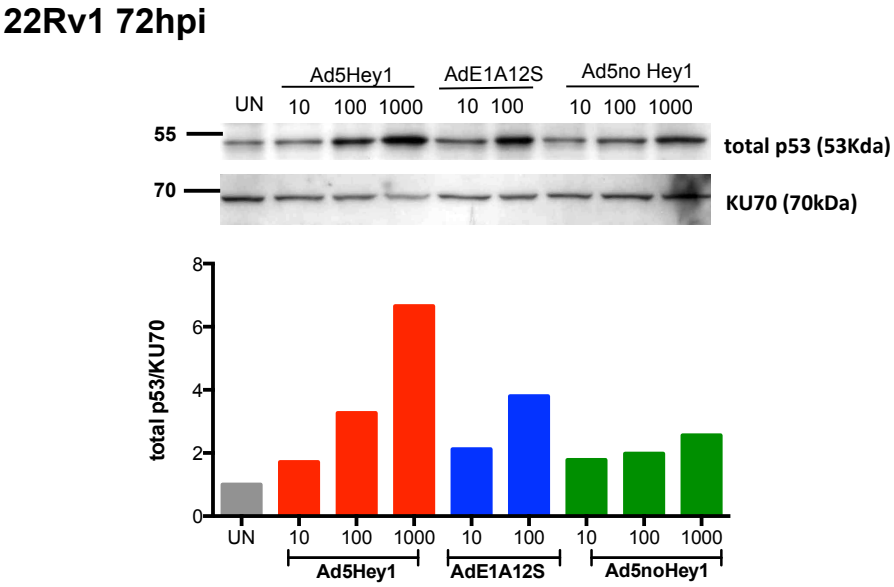

Figure_Apx 2. Ad5Hey1-infection stabilises p53 in 22Rv1 cells at 72h

Cells were infected with Ad5Hey1#2, AdE1A12S#1 and Ad5noHey1 at 10, 100 and 1000ppc. After 2h, infection medium was removed and replaced with 10% FBS DMEM. Cell lysates were harvested at 72h post-infection and prepared for separation on polyacrylamide gels. 20µg protein was loaded per lane and total p53 blotted. KU70 was used as a loading control. Histograms showing total p53 protein expression normalised to KU70 and expressed relative to uninfected (UN) cells. Results are from one experiment.

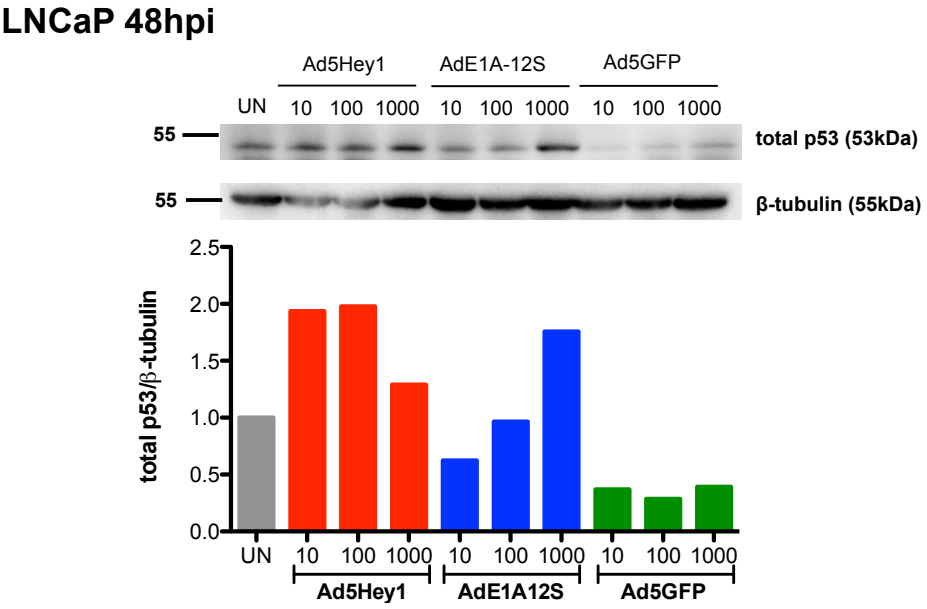

Figure_Apx 3. Ad5Hey1-infection stabilises p53 in LNCaP cells

Cells were infected with Ad5Hey1#3, AdE1A12S#3 and Ad5GFP at 10, 100 and 1000ppc. After 2h, infection medium was removed and replaced with 10%FBS RMPI. Cell lysates were harvested at 48h post-infection and prepared for separation on polyacrylamide gel. 20µg protein was loaded per lane and total p53 blotted. The membrane was stripped and blotted for β-tubulin as a loading control. Histogram showing total p53 expression normalised to β-tubulin and expressed relative to uninfected (UN) cells. Results are from one experiment.

6. References

Aarnisalo, P., H. Santti, et al. (1999). "Transcription activating and repressing functions of the androgen receptor are differentially influenced by mutations in the deoxyribonucleic acid-binding domain." Endocrinology **140**(7): 3097-3105.

Agoulnik, I. U., A. Vaid, et al. (2005). "Role of SRC-1 in the promotion of prostate cancer cell growth and tumor progression." Cancer Res **65**(17): 7959-7967.

Agoulnik, I. U. and N. L. Weigel (2008). "Androgen receptor coactivators and prostate cancer." Adv Exp Med Biol **617**: 245-255.

Alimirah, F, R Panchanathan (2007). "Expression of androgen receptor is negatively regualted by p53." Neoplasia **9**(12**)**: 1152-1159.

Allen, J. M., J. P. O'Shea, et al. (1983). "Advanced carcinoma of the prostate: treatment with a gonadotrophin releasing hormone agonist." Br Med J (Clin Res Ed) **286**(6378): 1607-1609.

Ambrosini, G., E. B. Sambol, et al. (2007). "Mouse double minute antagonist Nutlin-3a enhances chemotherapy-induced apoptosis in cancer cells with mutant p53 by activating E2F1." Oncogene **26**(24): 3473-3481.

Andersen, R. J., N. R. Mawji, et al. (2010). "Regression of castrate-recurrent prostate cancer by a small-molecule inhibitor of the amino-terminus domain of the androgen receptor." Cancer Cell **17**(6): 535-546.

Andreassen, P. R., O. D. Lohez, et al. (2001). "Tetraploid state induces p53-dependent arrest of nontransformed mammalian cells in G1." Mol Biol Cell **12**(5): 1315-1328.

Arnberg, N. (2009). "Adenovirus receptors: implications for tropism, treatment and targeting." Rev Med Virol **19**(3): 165-178.

Arriola, E. L., A. R. Lopez, et al. (1999). "Differential regulation of p21waf-1/cip-1 and Mdm2 by etoposide: etoposide inhibits the p53-Mdm2 autoregulatory feedback loop." Oncogene **18**(4): 1081-1091.

Askew, E. B., S. Bai, et al. (2010). "Transcriptional synergy between melanoma antigen gene protein-A11 (MAGE-11) and p300 in androgen receptor signaling." J Biol Chem **285**(28): 21824-21836.

Azuma, K., K. Nakashiro, et al. (2010). "Anti-tumor effect of small interfering RNA targeting the androgen receptor in human androgen-independent prostate cancer cells." Biochem Biophys Res Commun **391**(1): 1075-1079.

Bailly, E., J. Pines, et al. (1992). "Cytoplasmic accumulation of cyclin B1 in human cells: association with a detergent-resistant compartment and with the centrosome." J Cell Sci **101 (Pt 3)**: 529-545.

Bakkenist, C. J. and M. B. Kastan (2003). "DNA damage activates ATM through intermolecular autophosphorylation and dimer dissociation." Nature **421**(6922): 499-506.

Ban, J., I. M. Bennani-Baiti, et al. (2008). "EWS-FLI1 suppresses NOTCH-activated p53 in Ewing's sarcoma." Cancer Res **68**(17): 7100-7109.

Bartel, F., H. Taubert, et al. (2002). "Alternative and aberrant splicing of MDM2 mRNA in human cancer." Cancer Cell **2**(1): 9-15.

Barton, B. E., J. G. Karras, et al. (2004). "Signal transducer and activator of transcription 3 (STAT3) activation in prostate cancer: Direct STAT3

inhibition induces apoptosis in prostate cancer lines." Mol Cancer Ther **3**(1): 11-20.
Barton, B. E., T. F. Murphy, et al. (2001). "IL-6 signaling by STAT3 participates in the change from hyperplasia to neoplasia in NRP-152 and NRP-154 rat prostatic epithelial cells." BMC Cancer **1**: 19.
Bastus, N. C., L. K. Boyd, et al. (2010). "Androgen-induced TMPRSS2:ERG fusion in nonmalignant prostate epithelial cells." Cancer Res **70**(23): 9544-9548.
Becker, P. B. and W. Horz (2002). "ATP-dependent nucleosome remodeling." Annu Rev Biochem **71**: 247-273.
Beheshti, B., J. Karaskova, et al. (2000). "Identification of a high frequency of chromosomal rearrangements in the centromeric regions of prostate cancer cell lines by sequential giemsa banding and spectral karyotyping." Mol Diagn **5**(1): 23-32.
Belandia, B., S. M. Powell, et al. (2005). "Hey1, a mediator of notch signaling, is an androgen receptor corepressor." Mol Cell Biol **25**(4): 1425-1436.
Bellosillo, B., D. Colomer, et al. (1998). "Mitoxantrone, a topoisomerase II inhibitor, induces apoptosis of B-chronic lymphocytic leukaemia cells." Br J Haematol **100**(1): 142-146.
Bennett, N. C., R. A. Gardiner, et al. (2010). "Molecular cell biology of androgen receptor signalling." Int J Biochem Cell Biol **42**(6): 813-827.
Berk, A. J. (2005). "Recent lessons in gene expression, cell cycle control, and cell biology from adenovirus." Oncogene **24**(52): 7673-7685.
Berthold, D. R., G. R. Pond, et al. (2008). "Docetaxel plus prednisone or mitoxantrone plus prednisone for advanced prostate cancer: updated survival in the TAX 327 study." J Clin Oncol **26**(2): 242-245.
Bevan, C. L., S. Hoare, et al. (1999). "The AF1 and AF2 domains of the androgen receptor interact with distinct regions of SRC1." Mol Cell Biol **19**(12): 8383-8392.
Beverly, L. J., D. W. Felsher, et al. (2005). "Suppression of p53 by Notch in lymphomagenesis: implications for initiation and regression." Cancer Res **65**(16): 7159-7168.
Bhattacharya, S., R. Eckner, et al. (1996). "Cooperation of Stat2 and p300/CBP in signalling induced by interferon-alpha." Nature **383**(6598): 344-347.
Bhattacharyya, M., J. Francis, et al. (2011). "An oncolytic adenovirus defective in pRb-binding (dl922-947) can efficiently eliminate pancreatic cancer cells and tumors in vivo in combination with 5-FU or gemcitabine." Cancer Gene Ther **18**(10): 734-743.
Bill-Axelson, A., L. Holmberg, et al. (2005). "Radical prostatectomy versus watchful waiting in early prostate cancer." N Engl J Med **352**(19): 1977-1984.
Bin Hafeez, B., V. M. Adhami, et al. (2009). "Targeted knockdown of Notch1 inhibits invasion of human prostate cancer cells concomitant with inhibition of matrix metalloproteinase-9 and urokinase plasminogen activator." Clin Cancer Res **15**(2): 452-459.
Bischoff, J. R., D. H. Kirn, et al. (1996). "An adenovirus mutant that replicates selectively in p53-deficient human tumor cells." Science **274**(5286): 373-376.
Bjartell, A. (2006). "Words of wisdom. The 2005 International Society of Urological Pathology (ISUP) Consensus Conference on Gleason Grading of Prostatic Carcinoma." Eur Urol **49**(4): 758-759.
Bookstein, R., J. Y. Shew, et al. (1990). "Suppression of tumorigenicity of human prostate carcinoma cells by replacing a mutated RB gene." Science **247**(4943): 712-715.

Buchanan, G., E. F. Need, et al. (2011). "Corepressor effect on androgen receptor activity varies with the length of the CAG encoded polyglutamine repeat and is dependent on receptor/corepressor ratio in prostate cancer cells." Mol Cell Endocrinol **342**(1-2): 20-31.

Buchanan, G., M. Yang, et al. (2004). "Structural and functional consequences of glutamine tract variation in the androgen receptor." Hum Mol Genet **13**(16): 1677-1692.

Bucher, N. and C. D. Britten (2008). "G2 checkpoint abrogation and checkpoint kinase-1 targeting in the treatment of cancer." Br J Cancer **98**(3): 523-528.

Bunz, F., A. Dutriaux, et al. (1998). "Requirement for p53 and p21 to sustain G2 arrest after DNA damage." Science **282**(5393): 1497-1501.

Bunz, F., P. M. Hwang, et al. (1999). "Disruption of p53 in human cancer cells alters the responses to therapeutic agents." J Clin Invest **104**(3): 263-269.

Burchardt, M., T. Burchardt, et al. (2001). "Reduction of wild type p53 function confers a hormone resistant phenotype on LNCaP prostate cancer cells." Prostate **48**(4): 225-230.

Burd, C. J., L. M. Morey, et al. (2006). "Androgen receptor corepressors and prostate cancer." Endocr Relat Cancer **13**(4): 979-994.

Burri, N., P. Shaw, et al. (2001). "Methylation silencing and mutations of the p14ARF and p16INK4a genes in colon cancer." Lab Invest **81**(2): 217-229.

Cai, C. and S. P. Balk (2011). "Intratumoral androgen biosynthesis in prostate cancer pathogenesis and response to therapy." Endocr Relat Cancer **18**(5): R175-182.

Cai, C., H. H. He, et al. (2011). "Androgen receptor gene expression in prostate cancer is directly suppressed by the androgen receptor through recruitment of lysine-specific demethylase 1." Cancer Cell **20**(4): 457-471.

Callewaert, L., N. Van Tilborgh, et al. (2006). "Interplay between two hormone-independent activation domains in the androgen receptor." Cancer Res **66**(1): 543-553.

Cao, X., X. Deng, et al. (2003). "Cleavage of Bax to p18 Bax accelerates stress-induced apoptosis, and a cathepsin-like protease may rapidly degrade p18 Bax." Blood **102**(7): 2605-2614.

Carver, B. S., C. Chapinski, et al. (2011). "Reciprocal Feedback Regulation of PI3K and Androgen Receptor Signaling in PTEN-Deficient Prostate Cancer." Cancer Cell **19**(5): 575-586.

Castilla, C., B. Congregado, et al. (2006). "Bcl-xL is overexpressed in hormone-resistant prostate cancer and promotes survival of LNCaP cells via interaction with proapoptotic Bak." Endocrinology **147**(10): 4960-4967.

Cawood, R., H. H. Chen, et al. (2009). "Use of tissue-specific microRNA to control pathology of wild-type adenovirus without attenuation of its ability to kill cancer cells." PLoS Pathog **5**(5): e1000440.

Chaitanya, G. V., A. J. Steven, et al. (2010). "PARP-1 cleavage fragments: signatures of cell-death proteases in neurodegeneration." Cell Commun Signal **8**: 31.

Chakraborty, A. A. and W. P. Tansey (2009). "Adenoviral E1A function through Myc." Cancer Res **69**(1): 6-9.

Chan, J. M., P. H. Gann, et al. (2005). "Role of diet in prostate cancer development and progression." J Clin Oncol **23**(32): 8152-8160.

Chandarlapaty, S., A. Sawai, et al. (2011). "AKT inhibition relieves feedback suppression of receptor tyrosine kinase expression and activity." Cancer Cell **19**(1): 58-71.

Chartier, C., E. Degryse, et al. (1996). "Efficient generation of recombinant adenovirus vectors by homologous recombination in Escherichia coli." J Virol **70**(7): 4805-4810.
Chatterjee-Kishore, M., F. van Den Akker, et al. (2000). "Adenovirus E1A down-regulates LMP2 transcription by interfering with the binding of stat1 to IRF1." J Biol Chem **275**(27): 20406-20411.
Chen, C. D., D. S. Welsbie, et al. (2004). "Molecular determinants of resistance to antiandrogen therapy." Nat Med **10**(1): 33-39.
Chen, Y., N. J. Clegg, et al. (2009). "Anti-androgens and androgen-depleting therapies in prostate cancer: new agents for an established target." Lancet Oncol **10**(10): 981-991.
Chène, P. (2003). "Inhibiting the p53-MDM2 interaction: an important target for cancer therapy." Nat Rev Cancer **3**(2): 102-109.
Cheng, H., R. Snoek, et al. (2006). "Short hairpin RNA knockdown of the androgen receptor attenuates ligand-independent activation and delays tumor progression." Cancer Res **66**(21): 10613-10620.
Cheong, S. C., Y. Wang, et al. (2008). "E1A-expressing adenoviral E3B mutants act synergistically with chemotherapeutics in immunocompetent tumor models." Cancer Gene Ther **15**(1): 40-50.
Cherubini, G., T. Petouchoff, et al. (2006). "E1B55K-deleted adenovirus (ONYX-015) overrides G1/S and G2/M checkpoints and causes mitotic catastrophe and endoreduplication in p53-proficient normal cells." Cell Cycle **5**(19): 2244-2252.
Chin, M. T., K. Maemura, et al. (2000). "Cardiovascular basic helix loop helix factor 1, a novel transcriptional repressor expressed preferentially in the developing and adult cardiovascular system." J Biol Chem **275**(9): 6381-6387.
Chmelar, R., G. Buchanan, et al. (2007). "Androgen receptor coregulators and their involvement in the development and progression of prostate cancer." Int J Cancer **120**(4): 719-733.
Choi, H. J., M. Fukui, et al. (2011). "Role of cyclin B1/Cdc2 up-regulation in the development of mitotic prometaphase arrest in human breast cancer cells treated with nocodazole." PLoS One **6**(8): e24312.
Choi, J. W., J. S. Lee, et al. (2012). "Evolution of oncolytic adenovirus for cancer treatment." Adv Drug Deliv Rev **64**(8): 720-729.
Choi, S. and A. K. Lee (2011). "Efficacy and safety of gonadotropin-releasing hormone agonists used in the treatment of prostate cancer." Drug Healthc Patient Saf **3**: 107-119.
Choudhary, V., I. Kaddour-Djebbar, et al. (2011). "Novel role of androgens in mitochondrial fission and apoptosis." Mol Cancer Res **9**(8): 1067-1077.
Chuu, C. P., J. M. Kokontis, et al. (2011). "Androgens as therapy for androgen receptor-positive castration-resistant prostate cancer." J Biomed Sci **18**: 63.
Clark, J., S. Edwards, et al. (2003). "Genome-wide screening for complete genetic loss in prostate cancer by comparative hybridization onto cDNA microarrays." Oncogene **22**(8): 1247-1252.
Cody, J. J. and J. T. Douglas (2009). "Armed replicating adenoviruses for cancer virotherapy." Cancer Gene Ther **16**(6): 473-488.
Comstock, C. E., M. P. Revelo, et al. (2007). "Impact of differential cyclin D1 expression and localisation in prostate cancer." Br J Cancer **96**(6): 970-979.
Cottet-Rousselle, C., X. Ronot, et al. (2011). "Cytometric assessment of mitochondria using fluorescent probes." Cytometry A **79**(6): 405-425.
Coughlan, L., R. Alba, et al. (2010). "Tropism-modification strategies for targeted gene delivery using adenoviral vectors." Viruses **2**(10): 2290-2355.

Cronauer, M. V., W. A. Schulz, et al. (2004). "Inhibition of p53 function diminishes androgen receptor-mediated signaling in prostate cancer cell lines." Oncogene **23**(20): 3541-3549.
Cuconati, A., K. Degenhardt, et al. (2002). "Bak and Bax function to limit adenovirus replication through apoptosis induction." J Virol **76**(9): 4547-4558.
Cuconati, A., C. Mukherjee, et al. (2003). "DNA damage response and MCL-1 destruction initiate apoptosis in adenovirus-infected cells." Genes Dev **17**(23): 2922-2932.
Cuesta, R., G. Laroia, et al. (2000). "Chaperone hsp27 inhibits translation during heat shock by binding eIF4G and facilitating dissociation of cap-initiation complexes." Genes Dev **14**(12): 1460-1470.
Culig, Z., B. Comuzzi, et al. (2004). "Expression and function of androgen receptor coactivators in prostate cancer." J Steroid Biochem Mol Biol **92**(4): 265-271.
Cunha, G. R., S. W. Hayward, et al. (2003). "Role of the stromal microenvironment in carcinogenesis of the prostate." Int J Cancer **107**(1): 1-10.
Damber, J. E. and G. Aus (2008). "Prostate cancer." Lancet **371**(9625): 1710-1721.
Danila, D. C., M. J. Morris, et al. (2010). "Phase II multicenter study of abiraterone acetate plus prednisone therapy in patients with docetaxel-treated castration-resistant prostate cancer." J Clin Oncol **28**(9): 1496-1501.
Darzynkiewicz, Z., G. Juan, et al. (1997). "Cytometry in cell necrobiology: analysis of apoptosis and accidental cell death (necrosis)." Cytometry **27**(1): 1-20.
Davis, R. L. and D. L. Turner (2001). "Vertebrate hairy and Enhancer of split related proteins: transcriptional repressors regulating cellular differentiation and embryonic patterning." Oncogene **20**(58): 8342-8357.
Davison, A. J., M. Benko, et al. (2003). "Genetic content and evolution of adenoviruses." J Gen Virol **84**(Pt 11): 2895-2908.
de Bono, J. S., C. J. Logothetis, et al. (2011). "Abiraterone and increased survival in metastatic prostate cancer." N Engl J Med **364**(21): 1995-2005.
de Launoit, Y., R. Veilleux, et al. (1991). "Characteristics of the biphasic action of androgens and of the potent antiproliferative effects of the new pure antiestrogen EM-139 on cell cycle kinetic parameters in LNCaP human prostatic cancer cells." Cancer Res **51**(19): 5165-5170.
De Leon, J. T., A. Iwai, et al. (2011). "Targeting the regulation of androgen receptor signaling by the heat shock protein 90 cochaperone FKBP52 in prostate cancer cells." Proc Natl Acad Sci U S A **108**(29): 11878-11883.
de Stanchina, E., M. E. McCurrach, et al. (1998). "E1A signaling to p53 involves the p19(ARF) tumor suppressor." Genes Dev **12**(15): 2434-2442.
Debbas, M. and E. White (1993). "Wild-type p53 mediates apoptosis by E1A, which is inhibited by E1B." Genes Dev **7**(4): 546-554.
Debes, J. D., L. J. Schmidt, et al. (2002). "p300 mediates androgen-independent transactivation of the androgen receptor by interleukin 6." Cancer Res **62**(20): 5632-5636.
Dehm, S. M., K. M. Regan, et al. (2007). "Selective Role of an NH2-Terminal WxxLF Motif for Aberrant Androgen Receptor Activation in Androgen Depletion–Independent Prostate Cancer Cells." Cancer Research **67**(20): 10067-10077.

Dehm, S. M., L. J. Schmidt, et al. (2008). "Splicing of a novel androgen receptor exon generates a constitutively active androgen receptor that mediates prostate cancer therapy resistance." Cancer Res **68**(13): 5469-5477.
DeMarzo, A. M., W. G. Nelson, et al. (2003). "Pathological and molecular aspects of prostate cancer." Lancet **361**(9361): 955-964.
Denayer, S., C. Helsen, et al. (2010). "The rules of DNA recognition by the androgen receptor." Mol Endocrinol **24**(5): 898-913.
Deng, J., F. Kloosterbooer, et al. (2002). "The NH(2)-terminal and conserved region 2 domains of adenovirus E1A mediate two distinct mechanisms of tumor suppression." Cancer Res **62**(2): 346-350.
Dewailly, E., G. Mulvad, et al. (2003). "Inuit are protected against prostate cancer." Cancer Epidemiol Biomarkers Prev **12**(9): 926-927.
DeWeese, T. L., H. van der Poel, et al. (2001). "A phase I trial of CV706, a replication-competent, PSA selective oncolytic adenovirus, for the treatment of locally recurrent prostate cancer following radiation therapy." Cancer Res **61**(20): 7464-7472.
Di Lorenzo, G., G. Tortora, et al. (2002). "Expression of epidermal growth factor receptor correlates with disease relapse and progression to androgen-independence in human prostate cancer." Clin Cancer Res **8**(11): 3438-3444.
Dijkers, P. F., R. H. Medema, et al. (2000). "Expression of the pro-apoptotic Bcl-2 family member Bim is regulated by the forkhead transcription factor FKHR-L1." Curr Biol **10**(19): 1201-1204.
Dillard, P. R., M. F. Lin, et al. (2008). "Androgen-independent prostate cancer cells acquire the complete steroidogenic potential of synthesizing testosterone from cholesterol." Mol Cell Endocrinol **295**(1-2): 115-120.
DiPaola, R. S. (2002). "To Arrest or Not to G2-M Cell-Cycle Arrest." Clinical Cancer Research **8**: 4.
Donovan, M. J., I. Osman, et al. (2010). "Androgen receptor expression is associated with prostate cancer-specific survival in castrate patients with metastatic disease." BJU Int **105**(4): 462-467.
Dotto, G. P. (2009). "Crosstalk of Notch with p53 and p63 in cancer growth control." Nat Rev Cancer **9**(8): 587-595.
Duff, J. and I. J. McEwan (2005). "Mutation of histidine 874 in the androgen receptor ligand-binding domain leads to promiscuous ligand activation and altered p160 coactivator interactions." Mol Endocrinol **19**(12): 2943-2954.
Dumaz, N. and D. W. Meek (1999). "Serine15 phosphorylation stimulates p53 transactivation but does not directly influence interaction with HDM2." EMBO J **18**(24): 7002-7010.
Durr, F. E., R. E. Wallace, et al. (1983). "Molecular and biochemical pharmacology of mitoxantrone." Cancer Treat Rev **10 Suppl B**: 3-11.
Edwards, S. J., B. R. Dix, et al. (2002). "Evidence that replication of the antitumor adenovirus ONYX-015 is not controlled by the p53 and p14(ARF) tumor suppressor genes." J Virol **76**(24): 12483-12490.
Edwards, S. M., Z. Kote-Jarai, et al. (2003). "Two percent of men with early-onset prostate cancer harbor germline mutations in the BRCA2 gene." Am J Hum Genet **72**(1): 1-12.
Eeles, R. A., A. A. Olama, et al. (2013). "Identification of 23 new prostate cancer susceptibility loci using the iCOGS custom genotyping array." Nat Genet **45**(4): 385-391.
Ehrenberg, B., V. Montana, et al. (1988). "Membrane potential can be determined in individual cells from the nernstian distribution of cationic dyes." Biophys J **53**(5): 785-794.

Elagib, K. E., M. Xiao, et al. (2004). "Jun blockade of erythropoiesis: role for repression of GATA-1 by HERP2." Mol Cell Biol **24**(17): 7779-7794.
Elmore, S. (2007). "Apoptosis: a review of programmed cell death." Toxicol Pathol **35**(4): 495-516.
Fabbri, F., D. Amadori, et al. (2008). "Mitotic catastrophe and apoptosis induced by docetaxel in hormone-refractory prostate cancer cells." J Cell Physiol **217**(2): 494-501.
Fahrenholtz, C. D., P. J. Beltran, et al. (2013). "Targeting IGF-IR with ganitumab inhibits tumorigenesis and increases durability of response to androgen-deprivation therapy in VCaP prostate cancer xenografts." Mol Cancer Ther.
Feldman, B. J. and D. Feldman (2001). "The development of androgen-independent prostate cancer." Nat Rev Cancer **1**(1): 34-45.
Fischer, A. and M. Gessler (2007). "Delta-Notch--and then? Protein interactions and proposed modes of repression by Hes and Hey bHLH factors." Nucleic Acids Res **35**(14): 4583-4596.
Fischer, A., B. Klamt, et al. (2004). "Phenotypic variability in Hey2 -/- mice and absence of HEY2 mutations in patients with congenital heart defects or Alagille syndrome." Mamm Genome **15**(9): 711-716.
Fischer, A., J. Klattig, et al. (2005). "Hey basic helix-loop-helix transcription factors are repressors of GATA4 and GATA6 and restrict expression of the GATA target gene ANF in fetal hearts." Mol Cell Biol **25**(20): 8960-8970.
Fischle, W., F. Dequiedt, et al. (2002). "Enzymatic activity associated with class II HDACs is dependent on a multiprotein complex containing HDAC3 and SMRT/N-CoR." Mol Cell **9**(1): 45-57.
Fizazi, K., H. I. Scher, et al. (2012). "Abiraterone acetate for treatment of metastatic castration-resistant prostate cancer: final overall survival analysis of the COU-AA-301 randomised, double-blind, placebo-controlled phase 3 study." Lancet Oncol **13**(10): 983-992.
Flinterman, M., L. Guelen, et al. (2005). "E1A activates transcription of p73 and Noxa to induce apoptosis." J Biol Chem **280**(7): 5945-5959.
Flinterman, M. B., J. S. Mymryk, et al. (2007). "p400 function is required for the adenovirus E1A-mediated suppression of EGFR and tumour cell killing." Oncogene **26**(48): 6863-6874.
Fortune, J. M. and N. Osheroff (2000). "Topoisomerase II as a target for anticancer drugs: when enzymes stop being nice." Prog Nucleic Acid Res Mol Biol **64**: 221-253.
Fox, E. J. (2004). "Mechanism of action of mitoxantrone." Neurology **63**(12 Suppl 6): S15-18.
Freytag, S. O., K. N. Barton, et al. (2007). "Replication-competent adenovirus-mediated suicide gene therapy with radiation in a preclinical model of pancreatic cancer." Mol Ther **15**(9): 1600-1606.
Freytag, S. O., B. Movsas, et al. (2007). "Phase I trial of replication-competent adenovirus-mediated suicide gene therapy combined with IMRT for prostate cancer." Mol Ther **15**(5): 1016-1023.
Frisch, S. M. and J. S. Mymryk (2002). "Adenovirus-5 E1A: paradox and paradigm." Nat Rev Mol Cell Biol **3**(6): 441-452.
Fu, M., C. Wang, et al. (2000). "p300 and p300/cAMP-response element-binding protein-associated factor acetylate the androgen receptor at sites governing hormone-dependent transactivation." J Biol Chem **275**(27): 20853-20860.
Fueyo, J., C. Gomez-Manzano, et al. (2000). "A mutant oncolytic adenovirus targeting the Rb pathway produces anti-glioma effect in vivo." Oncogene **19**(1): 2-12.

Fulci, G., N. Dmitrieva, et al. (2007). "Depletion of peripheral macrophages and brain microglia increases brain tumor titers of oncolytic viruses." Cancer Res **67**(19): 9398-9406.
Gaddipati, J. P., D. G. McLeod, et al. (1994). "Frequent detection of codon 877 mutation in the androgen receptor gene in advanced prostate cancers." Cancer Res **54**(11): 2861-2864.
Gallimore, P. H. and A. S. Turnell (2001). "Adenovirus E1A: remodelling the host cell, a life or death experience." Oncogene **20**(54): 7824-7835.
Galsky, M. D., A. Dritselis, et al. (2010). "Cabazitaxel." Nat Rev Drug Discov **9**(9): 677-678.
Gan, L., S. Chen, et al. (2009). "Inhibition of the androgen receptor as a novel mechanism of taxol chemotherapy in prostate cancer." Cancer Res **69**(21): 8386-8394.
Gao, H., X. Ouyang, et al. (2006). "Emergence of androgen independence at early stages of prostate cancer progression in Nkx3.1; Pten mice." Cancer Res **66**(16): 7929-7933.
Gao, L., L. Zhang, et al. (2005). "Down-regulation of signal transducer and activator of transcription 3 expression using vector-based small interfering RNAs suppresses growth of human prostate tumor in vivo." Clin Cancer Res **11**(17): 6333-6341.
Garber, K. (2006). "China approves world's first oncolytic virus therapy for cancer treatment." J Natl Cancer Inst **98**(5): 298-300.
Gavet, O. and J. Pines (2010). "Activation of cyclin B1-Cdk1 synchronizes events in the nucleus and the cytoplasm at mitosis." J Cell Biol **189**(2): 247-259.
Gazit, A., N. Osherov, et al. (1991). "Tyrphostins. 2. Heterocyclic and alpha-substituted benzylidenemalononitrile tyrphostins as potent inhibitors of EGF receptor and ErbB2/neu tyrosine kinases." J Med Chem **34**(6): 1896-1907.
Geoerger, B., G. Vassal, et al. (2004). "Oncolytic activity of p53-expressing conditionally replicative adenovirus AdDelta24-p53 against human malignant glioma." Cancer Res **64**(16): 5753-5759.
Gerritsen, M. E., A. J. Williams, et al. (1997). "CREB-binding protein/p300 are transcriptional coactivators of p65." Proc Natl Acad Sci U S A **94**(7): 2927-2932.
Gessler, M., K. P. Knobeloch, et al. (2002). "Mouse gridlock: no aortic coarctation or deficiency, but fatal cardiac defects in Hey2 -/- mice." Curr Biol **12**(18): 1601-1604.
Giles, G. (2010). Male Reproductive Cancers Epidemiology, Pathology and Genetics. Cancer Genetics. W. D. C. Foulkes, Kathleen A., Springer.
Giono, L. E. and J. J. Manfredi (2007). "Mdm2 is required for inhibition of Cdk2 activity by p21, thereby contributing to p53-dependent cell cycle arrest." Mol Cell Biol **27**(11): 4166-4178.
Giraud, S., F. Bienvenu, et al. (2002). "Functional interaction of STAT3 transcription factor with the coactivator NcoA/SRC1a." J Biol Chem **277**(10): 8004-8011.
Gleave, M., A. Tolcher, et al. (1999). "Progression to androgen independence is delayed by adjuvant treatment with antisense Bcl-2 oligodeoxynucleotides after castration in the LNCaP prostate tumor model." Clin Cancer Res **5**(10): 2891-2898.
Gomez, L. A., A. de Las Pozas, et al. (2007). "Increased expression of cyclin B1 sensitizes prostate cancer cells to apoptosis induced by chemotherapy." Mol Cancer Ther **6**(5): 1534-1543.

Goodrum, F. D. and D. A. Ornelles (1998). "p53 status does not determine outcome of E1B 55-kilodalton mutant adenovirus lytic infection." J Virol **72**(12): 9479-9490.
Gottlieb, B., L. K. Beitel, et al. (2012). "The androgen receptor gene mutations database: 2012 update." Hum Mutat **33**(5): 887-894.
Grand, R. J., M. L. Grant, et al. (1994). "Enhanced expression of p53 in human cells infected with mutant adenoviruses." Virology **203**(2): 229-240.
Gregory, C. W., K. G. Hamil, et al. (1998). "Androgen receptor expression in androgen-independent prostate cancer is associated with increased expression of androgen-regulated genes." Cancer Res **58**(24): 5718-5724.
Gregory, C. W., B. He, et al. (2001). "A mechanism for androgen receptor-mediated prostate cancer recurrence after androgen deprivation therapy." Cancer Res **61**(11): 4315-4319.
Grossman, S. R., M. E. Deato, et al. (2003). "Polyubiquitination of p53 by a ubiquitin ligase activity of p300." Science **300**(5617): 342-344.
Grossman, S. R., M. Perez, et al. (1998). "p300/MDM2 complexes participate in MDM2-mediated p53 degradation." Mol Cell **2**(4): 405-415.
Guo, Z., B. Dai, et al. (2006). "Regulation of androgen receptor activity by tyrosine phosphorylation." Cancer Cell **10**(4): 309-319.
Guo, Z. and Y. Qiu (2011). "A new trick of an old molecule: androgen receptor splice variants taking the stage?!" Int J Biol Sci **7**(6): 815-822.
Gurova, K. V., O. W. Rokhlin, et al. (2003). "Cooperation of two mutant p53 alleles contributes to Fas resistance of prostate carcinoma cells." Cancer Res **63**(11): 2905-2912.
Gurumurthy, S., K. M. Vasudevan, et al. (2001). "Regulation of apoptosis in prostate cancer." Cancer Metastasis Rev **20**(3-4): 225-243.
Haapala, K., E. R. Hyytinen, et al. (2001). "Androgen receptor alterations in prostate cancer relapsed during a combined androgen blockade by orchiectomy and bicalutamide." Lab Invest **81**(12): 1647-1651.
Haelens, A., T. Tanner, et al. (2007). "The hinge region regulates DNA binding, nuclear translocation, and transactivation of the androgen receptor." Cancer Res **67**(9): 4514-4523.
Hakkarainen, T., M. Rajecki, et al. (2009). "Targeted radiotherapy for prostate cancer with an oncolytic adenovirus coding for human sodium iodide symporter." Clin Cancer Res **15**(17): 5396-5403.
Haldar, S., J. Chintapalli, et al. (1996). "Taxol induces bcl-2 phosphorylation and death of prostate cancer cells." Cancer Res **56**(6): 1253-1255.
Halkidou, K., V. J. Gnanapragasam, et al. (2003). "Expression of Tip60, an androgen receptor coactivator, and its role in prostate cancer development." Oncogene **22**(16): 2466-2477.
Hallden, G., R. Hill, et al. (2003). "Novel immunocompetent murine tumor models for the assessment of replication-competent oncolytic adenovirus efficacy." Mol Ther **8**(3): 412-424.
Hallden, G. and G. Portella (2012). "Oncolytic virotherapy with modified adenoviruses and novel therapeutic targets." Expert Opin Ther Targets **16**(10): 945-958.
Hans, F. and S. Dimitrov (2001). "Histone H3 phosphorylation and cell division." Oncogene **20**(24): 3021-3027.
Hara, T., J. Miyazaki, et al. (2003). "Novel mutations of androgen receptor: a possible mechanism of bicalutamide withdrawal syndrome." Cancer Res **63**(1): 149-153.
Hedvat, M., D. Huszar, et al. (2009). "The JAK2 inhibitor AZD1480 potently blocks Stat3 signaling and oncogenesis in solid tumors." Cancer Cell **16**(6): 487-497.

Heidenreich, A. B., P.J.; Bellmunt, J; Bolla, M; Joniau, S; Mason, M.D.; Matveev, V; Mottet, N; van der Kwast, T.H.; Wiegel, T; Zattoni, F (2012). "EAU Guidelines on Prostate Cancer." Eur Urol.

Heise, C., T. Hermiston, et al. (2000). "An adenovirus E1A mutant that demonstrates potent and selective systemic anti-tumoral efficacy." Nat Med **6**(10): 1134-1139.

Heisig, J., D. Weber, et al. (2012). "Target gene analysis by microarrays and chromatin immunoprecipitation identifies HEY proteins as highly redundant bHLH repressors." PLoS Genet **8**(5): e1002728.

Helgason, G. V., J. O'Prey, et al. (2010). "Oncogene-induced sensitization to chemotherapy-induced death requires induction as well as deregulation of E2F1." Cancer Res **70**(10): 4074-4080.

Hellerstedt, B. A. and K. J. Pienta (2002). "The current state of hormonal therapy for prostate cancer." CA Cancer J Clin **52**(3): 154-179.

Hemmati, P. G., D. Guner, et al. (2006). "Bak functionally complements for loss of Bax during p14ARF-induced mitochondrial apoptosis in human cancer cells." Oncogene **25**(50): 6582-6594.

Herbst, R. S. and F. R. Khuri (2003). "Mode of action of docetaxel - a basis for combination with novel anticancer agents." Cancer Treat Rev **29**(5): 407-415.

Hernando, E., Z. Nahlé, et al. (2004). "Rb inactivation promotes genomic instability by uncoupling cell cycle progression from mitotic control." Nature **430**(7001): 797-802.

Ho, C. K., S. L. Law, et al. (1991). "Inhibition of microtubule assembly is a possible mechanism of action of mitoxantrone." Biochem Biophys Res Commun **180**(1): 118-123.

Hobisch, A., I. E. Eder, et al. (1998). "Interleukin-6 regulates prostate-specific protein expression in prostate carcinoma cells by activation of the androgen receptor." Cancer Res **58**(20): 4640-4645.

Hodge, D. R., E. M. Hurt, et al. (2005). "The role of IL-6 and STAT3 in inflammation and cancer." Eur J Cancer **41**(16): 2502-2512.

Hodgson, M. C., I. Astapova, et al. (2005). "The androgen receptor recruits nuclear receptor CoRepressor (N-CoR) in the presence of mifepristone via its N and C termini revealing a novel molecular mechanism for androgen receptor antagonists." J Biol Chem **280**(8): 6511-6519.

Hodgson, M. C., I. Astapova, et al. (2007). "Activity of androgen receptor antagonist bicalutamide in prostate cancer cells is independent of NCoR and SMRT corepressors." Cancer Res **67**(17): 8388-8395.

Hodgson, M. C., L. J. Shao, et al. (2011). "Decreased expression and androgen regulation of the tumor suppressor gene INPP4B in prostate cancer." Cancer Res **71**(2): 572-582.

Hong, S., Q. X. Paulson, et al. (2008). "E2F1 and E2F3 activate ATM through distinct mechanisms to promote E1A-induced apoptosis." Cell Cycle **7**(3): 391-400.

Horoszewicz, J. S., S. S. Leong, et al. (1980). "The LNCaP cell line--a new model for studies on human prostatic carcinoma." Prog Clin Biol Res **37**: 115-132.

Hsiao, P. W., D. L. Lin, et al. (1999). "The linkage of Kennedy's neuron disease to ARA24, the first identified androgen receptor polyglutamine region-associated coactivator." J Biol Chem **274**(29): 20229-20234.

Hu, H., H. J. Lee, et al. (2008). "Penta-1,2,3,4,6-O-galloyl-beta-D-glucose induces p53 and inhibits STAT3 in prostate cancer cells in vitro and suppresses prostate xenograft tumor growth in vivo." Mol Cancer Ther **7**(9): 2681-2691.

Hu, X., A. Y. Chung, et al. (2008). "Integrated regulation of Toll-like receptor responses by Notch and interferon-gamma pathways." Immunity **29**(5): 691-703.
Huang, P., M. Watanabe, et al. (2008). "Direct and distant antitumor effects of a telomerase-selective oncolytic adenoviral agent, OBP-301, in a mouse prostate cancer model." Cancer Gene Ther **15**(5): 315-322.
Huang, Q., A. Raya, et al. (2004). "Identification of p53 regulators by genome-wide functional analysis." Proc Natl Acad Sci U S A **101**(10): 3456-3461.
Huggins, C. S., R.E.; Hodges, C.V. (1941). "Studies on prostatic cancer I. The effect of castration on advanced carcinoma of the prosate gland." Arch Surg **43**: 209-223.
Hulleman, E., M. Quarto, et al. (2009). "A role for the transcription factor HEY1 in glioblastoma." J Cell Mol Med **13**(1): 136-146.
Irvine, R. A., H. Ma, et al. (2000). "Inhibition of p160-mediated coactivation with increasing androgen receptor polyglutamine length." Hum Mol Genet **9**(2): 267-274.
Irwin, M., M. C. Marin, et al. (2000). "Role for the p53 homologue p73 in E2F-1-induced apoptosis." Nature **407**(6804): 645-648.
Isaacs, J. T. and D. S. Coffey (1981). "Adaptation versus selection as the mechanism responsible for the relapse of prostatic cancer to androgen ablation therapy as studied in the Dunning R-3327-H adenocarcinoma." Cancer Res **41**(12 Pt 1): 5070-5075.
Isaacs, W. B., B. S. Carter, et al. (1991). "Wild-type p53 suppresses growth of human prostate cancer cells containing mutant p53 alleles." Cancer Res **51**(17): 4716-4720.
Iso, T., V. Sartorelli, et al. (2001). "HERP, a novel heterodimer partner of HES/E(spl) in Notch signaling." Mol Cell Biol **21**(17): 6080-6089.
Itamochi, H., J. Kigawa, et al. (2007). "Adenovirus type 5 E1A gene therapy for ovarian clear cell carcinoma: a potential treatment strategy." Mol Cancer Ther **6**(1): 227-235.
Iversen, P., C. J. Tyrrell, et al. (2000). "Bicalutamide monotherapy compared with castration in patients with nonmetastatic locally advanced prostate cancer: 6.3 years of followup." J Urol **164**(5): 1579-1582.
Iyer, N. G., H. Ozdag, et al. (2004). "p300/CBP and cancer." Oncogene **23**(24): 4225-4231.
Jemal, A., R. Siegel, et al. (2008). "Cancer statistics, 2008." CA Cancer J Clin **58**(2): 71-96.
Jenster, G., H. A. van der Korput, et al. (1995). "Identification of two transcription activation units in the N-terminal domain of the human androgen receptor." J Biol Chem **270**(13): 7341-7346.
Jiang, Y., J. F. Palma, et al. (2010). "Detection of androgen receptor mutations in circulating tumor cells in castration-resistant prostate cancer." Clin Chem **56**(9): 1492-1495.
Jordan, M. A., K. Wendell, et al. (1996). "Mitotic block induced in HeLa cells by low concentrations of paclitaxel (Taxol) results in abnormal mitotic exit and apoptotic cell death." Cancer Res **56**(4): 816-825.
Juan, G., F. Traganos, et al. (1998). "Histone H3 phosphorylation and expression of cyclins A and B1 measured in individual cells during their progression through G2 and mitosis." Cytometry **32**(2): 71-77.
Kadeppagari, R. K., N. Sankar, et al. (2009). "Adenovirus transforming protein E1A induces c-Myc in quiescent cells by a novel mechanism." J Virol **83**(10): 4810-4822.
Kaighn, M. E., K. S. Narayan, et al. (1979). "Establishment and characterization of a human prostatic carcinoma cell line (PC-3)." Invest Urol **17**(1): 16-23.

Kamakura, S., K. Oishi, et al. (2004). "Hes binding to STAT3 mediates crosstalk between Notch and JAK-STAT signalling." Nat Cell Biol **6**(6): 547-554.
Kang, H. Y., S. Yeh, et al. (1999). "Cloning and characterization of human prostate coactivator ARA54, a novel protein that associates with the androgen receptor." J Biol Chem **274**(13): 8570-8576.
Kelly, W. K. and H. I. Scher (1993). "Prostate specific antigen decline after antiandrogen withdrawal: the flutamide withdrawal syndrome." J Urol **149**(3): 607-609.
Kennedy, S. G., E. S. Kandel, et al. (1999). "Akt/Protein kinase B inhibits cell death by preventing the release of cytochrome c from mitochondria." Mol Cell Biol **19**(8): 5800-5810.
Kharaziha, P., P. Rodriguez, et al. (2012). "Targeting of distinct signaling cascades and cancer-associated fibroblasts define the efficacy of Sorafenib against prostate cancer cells." Cell Death Dis **3**: e262.
Khuri, F. R., J. Nemunaitis, et al. (2000). "a controlled trial of intratumoral ONYX-015, a selectively-replicating adenovirus, in combination with cisplatin and 5-fluorouracil in patients with recurrent head and neck cancer." Nat Med **6**(8): 879-885.
Kim, K. I., J. H. Kang, et al. (2007). "Doxorubicin enhances the expression of transgene under control of the CMV promoter in anaplastic thyroid carcinoma cells." J Nucl Med **48**(9): 1553-1561.
Kim, P. H., J. H. Sohn, et al. (2011). "Active targeting and safety profile of PEG-modified adenovirus conjugated with herceptin." Biomaterials **32**(9): 2314-2326.
Klanrit, P., M. B. Flinterman, et al. (2008). "Specific isoforms of p73 control the induction of cell death induced by the viral proteins, E1A or apoptin." Cell Cycle **7**(2): 205-215.
Klokk TI, K. P., Elbi C, Nagaich AK, Hendarwanto A, and C. C. Slagsvold T, Hager GL, Saatcioglu F 2006 (2006). "Ligand-specific dynamics of the androgen receptor at its response element in living cells." Mol Cell Biol **27**: 1823-1843.
Klotz, L. (2000). "Hormone therapy for patients with prostate carcinoma." Cancer **88**(12 Suppl): 3009-3014.
Kluza, J., P. Marchetti, et al. (2004). "Mitochondrial proliferation during apoptosis induced by anticancer agents: effects of doxorubicin and mitoxantrone on cancer and cardiac cells." Oncogene **23**(42): 7018-7030.
Knudsen, K. E. and W. K. Kelly (2011). "Outsmarting androgen receptor: creative approaches for targeting aberrant androgen signaling in advanced prostate cancer." Expert Rev Endocrinol Metab **6**(3): 483-493.
Koivisto, P., J. Kononen, et al. (1997). "Androgen receptor gene amplification: a possible molecular mechanism for androgen deprivation therapy failure in prostate cancer." Cancer Res **57**(2): 314-319.
Kokontis, J., K. Takakura, et al. (1994). "Increased androgen receptor activity and altered c-myc expression in prostate cancer cells after long-term androgen deprivation." Cancer Res **54**(6): 1566-1573.
Kokontis, J. M., N. Hay, et al. (1998). "Progression of LNCaP prostate tumor cells during androgen deprivation: hormone-independent growth, repression of proliferation by androgen, and role for p27Kip1 in androgen-induced cell cycle arrest." Mol Endocrinol **12**(7): 941-953.
Kokontis, J. M., S. Hsu, et al. (2005). "Role of androgen receptor in the progression of human prostate tumor cells to androgen independence and insensitivity." Prostate **65**(4): 287-298.
Korenchuk, S., J. E. Lehr, et al. (2001). "VCaP, a cell-based model system of human prostate cancer." In Vivo **15**(2): 163-168.

Kotha, A., M. Sekharam, et al. (2006). "Resveratrol inhibits Src and Stat3 signaling and induces the apoptosis of malignant cells containing activated Stat3 protein." Mol Cancer Ther **5**(3): 621-629.
Kovesdi, I., R. Reichel, et al. (1986). "Identification of a cellular transcription factor involved in E1A trans-activation." Cell **45**(2): 219-228.
Kral, M., V. Rosinska, et al. (2011). "Genetic determinants of prostate cancer: a review." Biomed Pap Med Fac Univ Palacky Olomouc Czech Repub **155**(1): 3-9.
Krasnykh, V., I. Dmitriev, et al. (1998). "Characterization of an adenovirus vector containing a heterologous peptide epitope in the HI loop of the fiber knob." J Virol **72**(3): 1844-1852.
Kretsovali, A., T. Agalioti, et al. (1998). "Involvement of CREB binding protein in expression of major histocompatibility complex class II genes via interaction with the class II transactivator." Mol Cell Biol **18**(11): 6777-6783.
Kroemer, G., L. Galluzzi, et al. (2007). "Mitochondrial membrane permeabilization in cell death." Physiol Rev **87**(1): 99-163.
Kumar, R., S. Srinivasan, et al. (2010). "Activating stress-activated protein kinase-mediated cell death and inhibiting epidermal growth factor receptor signaling: a promising therapeutic strategy for prostate cancer." Mol Cancer Ther **9**(9): 2488-2496.
Kuroda, K., H. Liu, et al. (2009). "Docetaxel down-regulates the expression of androgen receptor and prostate-specific antigen but not prostate-specific membrane antigen in prostate cancer cell lines: implications for PSA surrogacy." Prostate **69**(14): 1579-1585.
Lai, E. C. (2004). "Notch signaling: control of cell communication and cell fate." Development **131**(5): 965-973.
Lang, S. E. and P. Hearing (2003). "The adenovirus E1A oncoprotein recruits the cellular TRRAP/GCN5 histone acetyltransferase complex." Oncogene **22**(18): 2836-2841.
Lanni, J. S. and T. Jacks (1998). "Characterization of the p53-dependent postmitotic checkpoint following spindle disruption." Mol Cell Biol **18**(2): 1055-1064.
Lau, L. M., J. K. Nugent, et al. (2008). "HDM2 antagonist Nutlin-3 disrupts p73-HDM2 binding and enhances p73 function." Oncogene **27**(7): 997-1003.
Lavery, D. N. and C. L. Bevan (2011). "Androgen receptor signalling in prostate cancer: the functional consequences of acetylation." J Biomed Biotechnol **2011**: 862125.
Lavery, D. N., M. A. Villaronga, et al. (2011). "Repression of androgen receptor activity by HEYL, a third member of the Hairy/Enhancer-of-split-related family of Notch effectors." J Biol Chem **286**(20): 17796-17808.
Lee, E. C., P. Zhan, et al. (2003). "Antiandrogen-induced cell death in LNCaP human prostate cancer cells." Cell Death Differ **10**(7): 761-771.
Lee, W. P., D. I. Tai, et al. (2003). "Adenovirus type 5 E1A sensitizes hepatocellular carcinoma cells to gemcitabine." Cancer Res **63**(19): 6229-6236.
Leitner, S., K. Sweeney, et al. (2009). "Oncolytic adenoviral mutants with E1B19K gene deletions enhance gemcitabine-induced apoptosis in pancreatic carcinoma cells and anti-tumor efficacy in vivo." Clin Cancer Res **15**(5): 1730-1740.
Leja, J., B. Nilsson, et al. (2010). "Double-detargeted oncolytic adenovirus shows replication arrest in liver cells and retains neuroendocrine cell killing ability." PLoS One **5**(1): e8916.
Lenaerts, L., E. De Clercq, et al. (2008). "Clinical features and treatment of adenovirus infections." Rev Med Virol **18**(6): 357-374.

Leong, K. G. and W. Q. Gao (2008). "The Notch pathway in prostate development and cancer." Differentiation **76**(6): 699-716.
Li, J., J. Fu, et al. (2006). "A role of the amino-terminal (N) and carboxyl-terminal (C) interaction in binding of androgen receptor to chromatin." Mol Endocrinol **20**(4): 776-785.
Li, X., Y. Liu, et al. (2010). "Docetaxel increases antitumor efficacy of oncolytic prostate-restricted replicative adenovirus by enhancing cell killing and virus distribution." J Gene Med **12**(6): 516-527.
Li, Z., C. P. Day, et al. (2004). "Adenoviral E1A targets Mdm4 to stabilize tumor suppressor p53." Cancer Res **64**(24): 9080-9085.
Liao, G., L. Y. Chen, et al. (2003). "Regulation of androgen receptor activity by the nuclear receptor corepressor SMRT." J Biol Chem **278**(7): 5052-5061.
Liao, X., S. Tang, et al. (2005). "Small-interfering RNA-induced androgen receptor silencing leads to apoptotic cell death in prostate cancer." Mol Cancer Ther **4**(4): 505-515.
Liao, Y., D. Yu, et al. (2007). "Novel approaches for chemosensitization of breast cancer cells: the E1A story." Adv Exp Med Biol **608**: 144-169.
Liao, Y., Y. Y. Zou, et al. (2004). "Enhanced paclitaxel cytotoxicity and prolonged animal survival rate by a nonviral-mediated systemic delivery of E1A gene in orthotopic xenograft human breast cancer." Cancer Gene Ther **11**(9): 594-602.
Lin, H. K., Y. C. Hu, et al. (2003). "Suppression versus induction of androgen receptor functions by the phosphatidylinositol 3-kinase/Akt pathway in prostate cancer LNCaP cells with different passage numbers." J Biol Chem **278**(51): 50902-50907.
Lin, Y., J. Kokontis, et al. (2006). "Androgen and its receptor promote Bax-mediated apoptosis." Mol Cell Biol **26**(5): 1908-1916.
Lindqvist, A., V. Rodríguez-Bravo, et al. (2009). "The decision to enter mitosis: feedback and redundancy in the mitotic entry network." J Cell Biol **185**(2): 193-202.
Litvinov, I. V., A. M. De Marzo, et al. (2003). "Is the Achilles' heel for prostate cancer therapy a gain of function in androgen receptor signaling?" J Clin Endocrinol Metab **88**(7): 2972-2982.
Liu, A. Y., E. Corey, et al. (1996). "Prostatic cell lineage markers: emergence of BCL2+ cells of human prostate cancer xenograft LuCaP 23 following castration." Int J Cancer **65**(1): 85-89.
Liu, Q. Y., M. A. Rubin, et al. (1998). "Fas ligand is constitutively secreted by prostate cancer cells in vitro." Clin Cancer Res **4**(7): 1803-1811.
Liu, T. C., G. Hallden, et al. (2004). "An E1B-19 kDa gene deletion mutant adenovirus demonstrates tumor necrosis factor-enhanced cancer selectivity and enhanced oncolytic potency." Mol Ther **9**(6): 786-803.
Livak, K. J. and T. D. Schmittgen (2001). "Analysis of relative gene expression data using real-time quantitative PCR and the 2(-Delta Delta C(T)) Method." Methods **25**(4): 402-408.
Loberg, R. D., L. N. St John, et al. (2006). "Development of the VCaP androgen-independent model of prostate cancer." Urol Oncol **24**(2): 161-168.
Locke, J. A., E. S. Guns, et al. (2008). "Androgen levels increase by intratumoral de novo steroidogenesis during progression of castration-resistant prostate cancer." Cancer Res **68**(15): 6407-6415.
Lockley, M., M. Fernandez, et al. (2006). "Activity of the adenoviral E1A deletion mutant dl922-947 in ovarian cancer: comparison with E1A wild-type viruses, bioluminescence monitoring, and intraperitoneal delivery in icodextrin." Cancer Res **66**(2): 989-998.

Logan, I. R., H. V. McNeill, et al. (2007). "Analysis of the MDM2 antagonist nutlin-3 in human prostate cancer cells." Prostate **67**(8): 900-906.
Lonergan, P. E. and D. J. Tindall (2011). "Androgen receptor signaling in prostate cancer development and progression." J Carcinog **10**: 20.
Look, D. C., W. T. Roswit, et al. (1998). "Direct suppression of Stat1 function during adenoviral infection." Immunity **9**(6): 871-880.
López-Mateo, I., M. Villaronga, et al. (2012). "The transcription factor CREBZF is a novel positive regulator of p53." Cell Cycle **11**(20): 3887-3895.
Lowe, S. W. and H. E. Ruley (1993). "Stabilization of the p53 tumor suppressor is induced by adenovirus 5 E1A and accompanies apoptosis." Genes Dev **7**(4): 535-545.
Lowe, S. W., H. E. Ruley, et al. (1993). "p53-dependent apoptosis modulates the cytotoxicity of anticancer agents." Cell **74**(6): 957-967.
Lu, Y., J. Zhang, et al. (2004). "Osteoblasts induce prostate cancer proliferation and PSA expression through interleukin-6-mediated activation of the androgen receptor." Clin Exp Metastasis **21**(5): 399-408.
Maddison, L. A., W. J. Huss, et al. (2004). "Differential expression of cell cycle regulatory molecules and evidence for a "cyclin switch" during progression of prostate cancer." Prostate **58**(4): 335-344.
Makridakis, N., R. K. Ross, et al. (1997). "A prevalent missense substitution that modulates activity of prostatic steroid 5alpha-reductase." Cancer Res **57**(6): 1020-1022.
Maldonado, E. N., J. Patnaik, et al. (2010). "Free tubulin modulates mitochondrial membrane potential in cancer cells." Cancer Res **70**(24): 10192-10201.
Marcelli, M., M. Ittmann, et al. (2000). "Androgen receptor mutations in prostate cancer." Cancer Res **60**(4): 944-949.
Marcelli, M., M. Marani, et al. (2000). "Heterogeneous apoptotic responses of prostate cancer cell lines identify an association between sensitivity to staurosporine-induced apoptosis, expression of Bcl-2 family members, and caspase activation." Prostate **42**(4): 260-273.
Masiello, D., S. Cheng, et al. (2002). "Bicalutamide functions as an androgen receptor antagonist by assembly of a transcriptionally inactive receptor." J Biol Chem **277**(29): 26321-26326.
Matias, P. M., P. Donner, et al. (2000). "Structural evidence for ligand specificity in the binding domain of the human androgen receptor. Implications for pathogenic gene mutations." J Biol Chem **275**(34): 26164-26171.
McDonald, S., L. Brive, et al. (2000). "Ligand responsiveness in human prostate cancer: structural analysis of mutant androgen receptors from LNCaP and CWR22 tumors." Cancer Res **60**(9): 2317-2322.
McGowan, E. M., N. Alling, et al. (2011). "Evaluation of cell cycle arrest in estrogen responsive MCF-7 breast cancer cells: pitfalls of the MTS assay." PLoS One **6**(6): e20623.
Mediavilla-Varela, M., F. J. Pacheco, et al. (2009). "Docetaxel-induced prostate cancer cell death involves concomitant activation of caspase and lysosomal pathways and is attenuated by LEDGF/p75." Mol Cancer **8**: 68.
Mellinghoff, I. K., I. Vivanco, et al. (2004). "HER2/neu kinase-dependent modulation of androgen receptor function through effects on DNA binding and stability." Cancer Cell **6**(5): 517-527.
Mendiratta, P., E. Mostaghel, et al. (2009). "Genomic strategy for targeting therapy in castration-resistant prostate cancer." J Clin Oncol **27**(12): 2022-2029.
Meydan, N., T. Grunberger, et al. (1996). "Inhibition of acute lymphoblastic leukaemia by a Jak-2 inhibitor." Nature **379**(6566): 645-648.

Mhaidat, N. M., X. D. Zhang, et al. (2007). "Docetaxel-induced apoptosis of human melanoma is mediated by activation of c-Jun NH2-terminal kinase and inhibited by the mitogen-activated protein kinase extracellular signal-regulated kinase 1/2 pathway." Clin Cancer Res **13**(4): 1308-1314.

Miranda, E., H. Maya Pineda, et al. (2012). "Adenovirus-mediated sensitization to the cytotoxic drugs docetaxel and mitoxantrone is dependent on regulatory domains in the E1ACR1 gene-region." PLoS One **7**(10): e46617.

Mita, A. C., L. J. Denis, et al. (2009). "Phase I and pharmacokinetic study of XRP6258 (RPR 116258A), a novel taxane, administered as a 1-hour infusion every 3 weeks in patients with advanced solid tumors." Clin Cancer Res **15**(2): 723-730.

Mohr, A., N. Chatain, et al. (2012). "Dynamics and non-canonical aspects of JAK/STAT signalling." Eur J Cell Biol **91**(6-7): 524-532.

Mongiat-Artus, P. and P. Teillac (2004). "Abarelix: the first gonadotrophin-releasing hormone antagonist for the treatment of prostate cancer." Expert Opin Pharmacother **5**(10): 2171-2179.

Moreno, C. S. (2010). "The Sex-determining region Y-box 4 and homeobox C6 transcriptional networks in prostate cancer progression: crosstalk with the Wnt, Notch, and PI3K pathways." Am J Pathol **176**(2): 518-527.

Morse, D. L., H. Gray, et al. (2005). "Docetaxel induces cell death through mitotic catastrophe in human breast cancer cells." Mol Cancer Ther **4**(10): 1495-1504.

Munro, S., S. M. Carr, et al. (2012). "Diversity within the pRb pathway: is there a code of conduct?" Oncogene **31**(40): 4343-4352.

Nahle, Z., J. Polakoff, et al. (2002). "Direct coupling of the cell cycle and cell death machinery by E2F." Nat Cell Biol **4**(11): 859-864.

Nair, P., K. Somasundaram, et al. (2003). "Activated Notch1 inhibits p53-induced apoptosis and sustains transformation by human papillomavirus type 16 E6 and E7 oncogenes through a PI3K-PKB/Akt-dependent pathway." J Virol **77**(12): 7106-7112.

Nakagawa, O., D. G. McFadden, et al. (2000). "Members of the HRT family of basic helix-loop-helix proteins act as transcriptional repressors downstream of Notch signaling." Proc Natl Acad Sci U S A **97**(25): 13655-13660.

Nemunaitis, J., F. Khuri, et al. (2001). "Phase II trial of intratumoral administration of ONYX-015, a replication-selective adenovirus, in patients with refractory head and neck cancer." J Clin Oncol **19**(2): 289-298.

Ni, Z., W. Lou, et al. (2000). "Inhibition of constitutively activated Stat3 signaling pathway suppresses growth of prostate cancer cells." Cancer Res **60**(5): 1225-1228.

Nicolas, M., A. Wolfer, et al. (2003). "Notch1 functions as a tumor suppressor in mouse skin." Nat Genet **33**(3): 416-421.

Nokisalmi, P., S. Pesonen, et al. (2010). "Oncolytic adenovirus ICOVIR-7 in patients with advanced and refractory solid tumors." Clin Cancer Res **16**(11): 3035-3043.

O'Connor, M. J., H. Zimmermann, et al. (1999). "Characterization of an E1A-CBP interaction defines a novel transcriptional adapter motif (TRAM) in CBP/p300." J Virol **73**(5): 3574-3581.

O'Reilly. D, M. L., Luckow, V (1994). Virus Methods. Baculovirus Expression Vectors: A laboratory Manual, Oxford University Press**:** 132-134.

O'Shea, C. C., L. Johnson, et al. (2004). "Late viral RNA export, rather than p53 inactivation, determines ONYX-015 tumor selectivity." Cancer Cell **6**(6): 611-623.
Oberg, D., E. Yanover, et al. (2010). "Improved potency and selectivity of an oncolytic E1ACR2 and E1B19K deleted adenoviral mutant in prostate and pancreatic cancers." Clin Cancer Res **16**(2): 541-553.
Okamoto, M., C. Lee, et al. (1997). "Interleukin-6 as a paracrine and autocrine growth factor in human prostatic carcinoma cells in vitro." Cancer Res **57**(1): 141-146.
Oliveria, S. A. and P. J. Christos (1997). "The epidemiology of physical activity and cancer." Ann N Y Acad Sci **833**: 79-90.
Pan, H., C. Yin, et al. (1998). "Key roles for E2F1 in signaling p53-dependent apoptosis and in cell division within developing tumors." Mol Cell **2**(3): 283-292.
Patel, P., J. G. Young, et al. (2009). "A phase I/II clinical trial in localized prostate cancer of an adenovirus expressing nitroreductase with CB1954 [correction of CB1984]." Mol Ther **17**(7): 1292-1299.
Paulson, M., S. Pisharody, et al. (1999). "Stat protein transactivation domains recruit p300/CBP through widely divergent sequences." J Biol Chem **274**(36): 25343-25349.
Pelka, P., J. N. Ablack, et al. (2009). "Identification of a second independent binding site for the pCAF acetyltransferase in adenovirus E1A." Virology **391**(1): 90-98.
Pelka, P., J. N. Ablack, et al. (2009). "Transcriptional control by adenovirus E1A conserved region 3 via p300/CBP." Nucleic Acids Res **37**(4): 1095-1106.
Perez, D. and E. White (2003). "E1A sensitizes cells to tumor necrosis factor alpha by downregulating c-FLIP S." J Virol **77**(4): 2651-2662.
Perez-Stable, C. (2006). "2-Methoxyestradiol and paclitaxel have similar effects on the cell cycle and induction of apoptosis in prostate cancer cells." Cancer Lett **231**(1): 49-64.
Perry, S. W., J. P. Norman, et al. (2011). "Mitochondrial membrane potential probes and the proton gradient: a practical usage guide." Biotechniques **50**(2): 98-115.
Pesonen, S., I. Diaconu, et al. (2012). "Integrin targeted oncolytic adenoviruses Ad5-D24-RGD and Ad5-RGD-D24-GMCSF for treatment of patients with advanced chemotherapy refractory solid tumors." Int J Cancer **130**(8): 1937-1947.
Pesonen, S., L. Kangasniemi, et al. (2011). "Oncolytic adenoviruses for the treatment of human cancer: focus on translational and clinical data." Mol Pharm **8**(1): 12-28.
Pesonen, S., P. Nokisalmi, et al. (2010). "Prolonged systemic circulation of chimeric oncolytic adenovirus Ad5/3-Cox2L-D24 in patients with metastatic and refractory solid tumors." Gene Ther **17**(7): 892-904.
Peters, J. M. (2002). "The anaphase-promoting complex: proteolysis in mitosis and beyond." Mol Cell **9**(5): 931-943.
Petre, C. E., Y. B. Wetherill, et al. (2002). "Cyclin D1: mechanism and consequence of androgen receptor co-repressor activity." J Biol Chem **277**(3): 2207-2215.
Petrylak, D. P., C. M. Tangen, et al. (2004). "Docetaxel and estramustine compared with mitoxantrone and prednisone for advanced refractory prostate cancer." N Engl J Med **351**(15): 1513-1520.
Pignon, J. C., B. Koopmansch, et al. (2009). "Androgen receptor controls EGFR and ERBB2 gene expression at different levels in prostate cancer cell lines." Cancer Res **69**(7): 2941-2949.

Pines, J. and T. Hunter (1991). "Human cyclins A and B1 are differentially located in the cell and undergo cell cycle-dependent nuclear transport." J Cell Biol **115**(1): 1-17.
Plosker, G. L. (2011). "Sipuleucel-T: in metastatic castration-resistant prostate cancer." Drugs **71**(1): 101-108.
Pommier, Y., E. Leo, et al. (2010). "DNA topoisomerases and their poisoning by anticancer and antibacterial drugs." Chem Biol **17**(5): 421-433.
Pound, C. R., A. W. Partin, et al. (1999). "Natural history of progression after PSA elevation following radical prostatectomy." JAMA **281**(17): 1591-1597.
Powell, S. M., G. N. Brooke, et al. (2006). "Mechanisms of androgen receptor repression in prostate cancer." Biochem Soc Trans **34**(Pt 6): 1124-1127.
Powell, S. M., V. Christiaens, et al. (2004). "Mechanisms of androgen receptor signalling via steroid receptor coactivator-1 in prostate." Endocr Relat Cancer **11**(1): 117-130.
Powers, J. T., S. Hong, et al. (2004). "E2F1 uses the ATM signaling pathway to induce p53 and Chk2 phosphorylation and apoptosis." Mol Cancer Res **2**(4): 203-214.
Putzer, B. M., T. Stiewe, et al. (2000). "E1A is sufficient by itself to induce apoptosis independent of p53 and other adenoviral gene products." Cell Death Differ **7**(2): 177-188.
Qi, Y., M. A. Gregory, et al. (2004). "p19ARF directly and differentially controls the functions of c-Myc independently of p53." Nature **431**(7009): 712-717.
Qin, L., Y. Ding, et al. (1997). "Promoter attenuation in gene therapy: interferon-gamma and tumor necrosis factor-alpha inhibit transgene expression." Hum Gene Ther **8**(17): 2019-2029.
Querido, E., J. G. Teodoro, et al. (1997). "Accumulation of p53 induced by the adenovirus E1A protein requires regions involved in the stimulation of DNA synthesis." J Virol **71**(5): 3526-3533.
Radhakrishnan, S., E. Miranda, et al. (2010). "Efficacy of oncolytic mutants targeting pRb and p53 pathways is synergistically enhanced when combined with cytotoxic drugs in prostate cancer cells and tumor xenografts." Hum Gene Ther **21**(10): 1311-1325.
Ranganathan, P., K. L. Weaver, et al. (2011). "Notch signalling in solid tumours: a little bit of everything but not all the time." Nat Rev Cancer **11**(5): 338-351.
Reid, A. H., G. Attard, et al. (2010). "Significant and sustained antitumor activity in post-docetaxel, castration-resistant prostate cancer with the CYP17 inhibitor abiraterone acetate." J Clin Oncol **28**(9): 1489-1495.
Ringel, I. and S. B. Horwitz (1991). "Studies with RP 56976 (taxotere): a semisynthetic analogue of taxol." J Natl Cancer Inst **83**(4): 288-291.
Robbins, C., J. B. Torres, et al. (2007). "Confirmation study of prostate cancer risk variants at 8q24 in African Americans identifies a novel risk locus." Genome Res **17**(12): 1717-1722.
Rodriguez, R., E. R. Schuur, et al. (1997). "Prostate attenuated replication competent adenovirus (ARCA) CN706: a selective cytotoxic for prostate-specific antigen-positive prostate cancer cells." Cancer Res **57**(13): 2559-2563.
Rokhlin, O. W., A. F. Taghiyev, et al. (2007). "Calcium/calmodulin-dependent kinase II plays an important role in prostate cancer cell survival." Cancer Biol Ther **6**(5): 732-742.
Rokhlin, O. W., A. F. Taghiyev, et al. (2005). "Androgen regulates apoptosis induced by TNFR family ligands via multiple signaling pathways in LNCaP." Oncogene **24**(45): 6773-6784.

Rostovtseva, T. K., K. L. Sheldon, et al. (2008). "Tubulin binding blocks mitochondrial voltage-dependent anion channel and regulates respiration." Proc Natl Acad Sci U S A **105**(48): 18746-18751.
Rothmann, T., A. Hengstermann, et al. (1998). "Replication of ONYX-015, a potential anticancer adenovirus, is independent of p53 status in tumor cells." J Virol **72**(12): 9470-9478.
Ruizeveld de Winter, J. A., P. J. Janssen, et al. (1994). "Androgen receptor status in localized and locally progressive hormone refractory human prostate cancer." Am J Pathol **144**(4): 735-746.
Russell, P. J., S. Bennett, et al. (1998). "Growth factor involvement in progression of prostate cancer." Clin Chem **44**(4): 705-723.
Russell, W. C. (2000). "Update on adenovirus and its vectors." J Gen Virol **81**(Pt 11): 2573-2604.
Russell, W. C. (2009). "Adenoviruses: update on structure and function." J Gen Virol **90**(Pt 1): 1-20.
Russo, A. J., P. G. Magro, et al. (2006). "E2F-1 overexpression in U2OS cells increases cyclin B1 levels and cdc2 kinase activity and sensitizes cells to antimitotic agents." Cancer Res **66**(14): 7253-7260.
Ryan, C. J., M. R. Smith, et al. (2013). "Abiraterone in metastatic prostate cancer without previous chemotherapy." N Engl J Med **368**(2): 138-148.
Sabbatini, P., J. Lin, et al. (1995). "Essential role for p53-mediated transcription in E1A-induced apoptosis." Genes Dev **9**(17): 2184-2192.
Sack, J. S., K. F. Kish, et al. (2001). "Crystallographic structures of the ligand-binding domains of the androgen receptor and its T877A mutant complexed with the natural agonist dihydrotestosterone." Proc Natl Acad Sci U S A **98**(9): 4904-4909.
Sadar, M. D. (2011). "Small molecule inhibitors targeting the "achilles' heel" of androgen receptor activity." Cancer Res **71**(4): 1208-1213.
Samuelson, A. V., M. Narita, et al. (2005). "p400 is required for E1A to promote apoptosis." J Biol Chem **280**(23): 21915-21923.
Sankar, N., R. K. Kadeppagari, et al. (2009). "c-Myc-induced aberrant DNA synthesis and activation of DNA damage response in p300 knockdown cells." J Biol Chem **284**(22): 15193-15205.
Santagata, S., F. Demichelis, et al. (2004). "JAGGED1 expression is associated with prostate cancer metastasis and recurrence." Cancer Res **64**(19): 6854-6857.
Sauthoff, H., T. Pipiya, et al. (2006). "Modification of the p53 transgene of a replication-competent adenovirus prevents mdm2- and E1b-55kD-mediated degradation of p53." Cancer Gene Ther **13**(7): 686-695.
Sauthoff, H., T. Pipiya, et al. (2002). "Late expression of p53 from a replicating adenovirus improves tumor cell killing and is more tumor cell specific than expression of the adenoviral death protein." Hum Gene Ther **13**(15): 1859-1871.
Schellhammer, P. F., P. Venner, et al. (1997). "Prostate specific antigen decreases after withdrawal of antiandrogen therapy with bicalutamide or flutamide in patients receiving combined androgen blockade." J Urol **157**(5): 1731-1735.
Scher, H. I., K. Fizazi, et al. (2012). "Increased survival with enzalutamide in prostate cancer after chemotherapy." N Engl J Med **367**(13): 1187-1197.
Schroder, F. H., J. Hugosson, et al. (2012). "Prostate-cancer mortality at 11 years of follow-up." N Engl J Med **366**(11): 981-990.
Schulz, W. A., M. Burchardt, et al. (2003). "Molecular biology of prostate cancer." Mol Hum Reprod **9**(8): 437-448.

Schwartz, R. A., S. S. Lakdawala, et al. (2008). "Distinct requirements of adenovirus E1b55K protein for degradation of cellular substrates." J Virol **82**(18): 9043-9055.
Scorey, N., S. P. Fraser, et al. (2006). "Notch signalling and voltage-gated Na+ channel activity in human prostate cancer cells: independent modulation of in vitro motility." Prostate Cancer Prostatic Dis **9**(4): 399-406.
Senovilla, L., I. Vitale, et al. (2009). "p53 represses the polyploidization of primary mammary epithelial cells by activating apoptosis." Cell Cycle **8**(9): 1380-1385.
Shang, Y., M. Myers, et al. (2002). "Formation of the androgen receptor transcription complex." Mol Cell **9**(3): 601-610.
Sharff, K. A., W. X. Song, et al. (2009). "Hey1 basic helix-loop-helix protein plays an important role in mediating BMP9-induced osteogenic differentiation of mesenchymal progenitor cells." J Biol Chem **284**(1): 649-659.
Sharma, A., W. S. Yeow, et al. (2010). "The retinoblastoma tumor suppressor controls androgen signaling and human prostate cancer progression." J Clin Invest **120**(12): 4478-4492.
Shen, J., S. Zhang, et al. (2011). "p14(ARF) inhibits the functions of adenovirus E1A oncoprotein." Biochem J **434**(2): 275-285.
Shen, M. M. and C. Abate-Shen (2010). "Molecular genetics of prostate cancer: new prospects for old challenges." Genes Dev **24**(18): 1967-2000.
Shenk, T. E. (2001). Adenoviridae: The viruses and Their Replication. Fields Virology. P. M. H. D.M. Knipe, D.E. Griffin, R.A. Lamb, M.A. Martin, B. Roizman and S.E. Straus. Philadelphia, PA, USA, Lippincott Williams and Wilkins**:** 2265-2300.
Shiina, M., M. D. Lacher, et al. (2009). "RNA interference-mediated knockdown of p21(WAF1) enhances anti-tumor cell activity of oncolytic adenoviruses." Cancer Gene Ther **16**(11): 810-819.
Shodeinde, A. L. and B. E. Barton (2012). "Potential use of STAT3 inhibitors in targeted prostate cancer therapy: future prospects." Onco Targets Ther **5**: 119-125.
Shou, J., S. Ross, et al. (2001). "Dynamics of notch expression during murine prostate development and tumorigenesis." Cancer Res **61**(19): 7291-7297.
Sim, H. G. and C. W. Cheng (2005). "Changing demography of prostate cancer in Asia." Eur J Cancer **41**(6): 834-845.
Simmons, M. N., A. J. Stephenson, et al. (2007). "Natural history of biochemical recurrence after radical prostatectomy: risk assessment for secondary therapy." Eur Urol **51**(5): 1175-1184.
Skjoth, I. H. and O. G. Issinger (2006). "Profiling of signaling molecules in four different human prostate carcinoma cell lines before and after induction of apoptosis." Int J Oncol **28**(1): 217-229.
Slovin, S. F., C. S. Higano, et al. (2013). "Ipilimumab alone or in combination with radiotherapy in metastatic castration-resistant prostate cancer: results from an open-label, multicenter phase I/II study." Ann Oncol.
Small, E. J., M. A. Carducci, et al. (2006). "A phase I trial of intravenous CG7870, a replication-selective, prostate-specific antigen-targeted oncolytic adenovirus, for the treatment of hormone-refractory, metastatic prostate cancer." Mol Ther **14**(1): 107-117.
Small, E. J., S. Halabi, et al. (2004). "Antiandrogen withdrawal alone or in combination with ketoconazole in androgen-independent prostate cancer patients: a phase III trial (CALGB 9583)." J Clin Oncol **22**(6): 1025-1033.
Smith, C. L., S. A. Onate, et al. (1996). "CREB binding protein acts synergistically with steroid receptor coactivator-1 to enhance steroid

receptor-dependent transcription." Proc Natl Acad Sci U S A **93**(17): 8884-8888.
Sramkoski, R. M., T. G. Pretlow, 2nd, et al. (1999). "A new human prostate carcinoma cell line, 22Rv1." In Vitro Cell Dev Biol Anim **35**(7): 403-409.
Stanbrough, M., G. J. Bubley, et al. (2006). "Increased expression of genes converting adrenal androgens to testosterone in androgen-independent prostate cancer." Cancer Res **66**(5): 2815-2825.
Steidl, C., C. Leimeister, et al. (2000). "Characterization of the human and mouse HEY1, HEY2, and HEYL genes: cloning, mapping, and mutation screening of a new bHLH gene family." Genomics **66**(2): 195-203.
Steinkamp, M. P., O. A. O'Mahony, et al. (2009). "Treatment-dependent androgen receptor mutations in prostate cancer exploit multiple mechanisms to evade therapy." Cancer Res **69**(10): 4434-4442.
Stiewe, T., K. Parssanedjad, et al. (2000). "E1A overcomes the apoptosis block in BCR-ABL+ leukemia cells and renders cells susceptible to induction of apoptosis by chemotherapeutic agents." Cancer Res **60**(14): 3957-3964.
Stone, K. R., D. D. Mickey, et al. (1978). "Isolation of a human prostate carcinoma cell line (DU 145)." Int J Cancer **21**(3): 274-281.
Suijkerbuijk, S. J. and G. J. Kops (2008). "Preventing aneuploidy: the contribution of mitotic checkpoint proteins." Biochim Biophys Acta **1786**(1): 24-31.
Sun, J., C. N. Kamei, et al. (2001). "Regulation of myogenic terminal differentiation by the hairy-related transcription factor CHF2." J Biol Chem **276**(21): 18591-18596.
Sun, S., C. C. Sprenger, et al. (2010). "Castration resistance in human prostate cancer is conferred by a frequently occurring androgen receptor splice variant." J Clin Invest **120**(8): 2715-2730.
Sun, X. X., M. S. Dai, et al. (2007). "5-fluorouracil activation of p53 involves an MDM2-ribosomal protein interaction." J Biol Chem **282**(11): 8052-8059.
Sundqvist, A., K. Sollerbrant, et al. (1998). "The carboxy-terminal region of adenovirus E1A activates transcription through targeting of a C-terminal binding protein-histone deacetylase complex." FEBS Lett **429**(2): 183-188.
Symes, J. C., M. Kurin, et al. (2008). "Fas-mediated killing of primary prostate cancer cells is increased by mitoxantrone and docetaxel." Mol Cancer Ther **7**(9): 3018-3028.
Takata, T. and F. Ishikawa (2003). "Human Sir2-related protein SIRT1 associates with the bHLH repressors HES1 and HEY2 and is involved in HES1- and HEY2-mediated transcriptional repression." Biochem Biophys Res Commun **301**(1): 250-257.
Takeda, T., K. Nakajima, et al. (1994). "E1A repression of IL-6-induced gene activation by blocking the assembly of IL-6 response element binding complexes." J Immunol **153**(10): 4573-4582.
Taki, M., S. Kagawa, et al. (2005). "Enhanced oncolysis by a tropism-modified telomerase-specific replication-selective adenoviral agent OBP-405 ('Telomelysin-RGD')." Oncogene **24**(19): 3130-3140.
Tannock, I. F., R. de Wit, et al. (2004). "Docetaxel plus prednisone or mitoxantrone plus prednisone for advanced prostate cancer." N Engl J Med **351**(15): 1502-1512.
Tannock, I. F., D. Osoba, et al. (1996). "Chemotherapy with mitoxantrone plus prednisone or prednisone alone for symptomatic hormone-resistant prostate cancer: a Canadian randomized trial with palliative end points." J Clin Oncol **14**(6): 1756-1764.

Taplin, M. E., G. J. Bubley, et al. (1999). "Selection for androgen receptor mutations in prostate cancers treated with androgen antagonist." Cancer Res **59**(11): 2511-2515.
Taplin, M. E., G. J. Bubley, et al. (1995). "Mutation of the androgen-receptor gene in metastatic androgen-independent prostate cancer." N Engl J Med **332**(21): 1393-1398.
Taylor, R. A., R. Toivanen, et al. (2010). "Stem cells in prostate cancer: treating the root of the problem." Endocr Relat Cancer **17**(4): R273-285.
Taylor, R. C., S. P. Cullen, et al. (2008). "Apoptosis: controlled demolition at the cellular level." Nat Rev Mol Cell Biol **9**(3): 231-241.
Tepper, C. G., D. L. Boucher, et al. (2002). "Characterization of a novel androgen receptor mutation in a relapsed CWR22 prostate cancer xenograft and cell line." Cancer Res **62**(22): 6606-6614.
Terada, N., Y. Shimizu, et al. (2010). "Antiandrogen withdrawal syndrome and alternative antiandrogen therapy associated with the W741C mutant androgen receptor in a novel prostate cancer xenograft." Prostate **70**(3): 252-261.
Thompson, T., C. Tovar, et al. (2004). "Phosphorylation of p53 on key serines is dispensable for transcriptional activation and apoptosis." J Biol Chem **279**(51): 53015-53022.
Thompson, T. C., S. H. Park, et al. (1995). "Loss of p53 function leads to metastasis in ras+myc-initiated mouse prostate cancer." Oncogene **10**(5): 869-879.
Tollefson, A. E., A. Scaria, et al. (2003). "Mutations within the ADP (E3-11.6K) protein alter processing and localization of ADP and the kinetics of cell lysis of adenovirus-infected cells." J Virol **77**(14): 7764-7778.
Tomlins, S. A., D. R. Rhodes, et al. (2005). "Recurrent fusion of TMPRSS2 and ETS transcription factor genes in prostate cancer." Science **310**(5748): 644-648.
Tovar, C., B. Higgins, et al. (2011). "MDM2 antagonists boost antitumor effect of androgen withdrawal: implications for therapy of prostate cancer." Mol Cancer **10**: 49.
Tran, C., S. Ouk, et al. (2009). "Development of a second-generation antiandrogen for treatment of advanced prostate cancer." Science **324**(5928): 787-790.
Turnell, A. S., R. J. Grand, et al. (2000). "Regulation of the 26S proteasome by adenovirus E1A." EMBO J **19**(17): 4759-4773.
Tworkowski, K. A., A. A. Chakraborty, et al. (2008). "Adenovirus E1A targets p400 to induce the cellular oncoprotein Myc." Proc Natl Acad Sci U S A **105**(16): 6103-6108.
Tyrrell, C. J., A. V. Kaisary, et al. (1998). "A randomised comparison of 'Casodex' (bicalutamide) 150 mg monotherapy versus castration in the treatment of metastatic and locally advanced prostate cancer." Eur Urol **33**(5): 447-456.
Udayakumar, T. S., P. Hachem, et al. (2008). "Antisense MDM2 enhances E2F1-induced apoptosis and the combination sensitizes androgen-sensitive [corrected] and androgen-insensitive [corrected] prostate cancer cells to radiation." Mol Cancer Res **6**(11): 1742-1754.
Ueda, T., N. Bruchovsky, et al. (2002). "Activation of the androgen receptor N-terminal domain by interleukin-6 via MAPK and STAT3 signal transduction pathways." J Biol Chem **277**(9): 7076-7085.
Ueda, T., N. R. Mawji, et al. (2002). "Ligand-independent activation of the androgen receptor by interleukin-6 and the role of steroid receptor coactivator-1 in prostate cancer cells." J Biol Chem **277**(41): 38087-38094.

Ueno, N. T., D. Yu, et al. (1997). "Chemosensitization of HER-2/neu-overexpressing human breast cancer cells to paclitaxel (Taxol) by adenovirus type 5 E1A." Oncogene **15**(8): 953-960.
van Beusechem, V. W., D. C. Mastenbroek, et al. (2003). "Conditionally replicative adenovirus expressing a targeting adapter molecule exhibits enhanced oncolytic potency on CAR-deficient tumors." Gene Ther **10**(23): 1982-1991.
van Beusechem, V. W., P. B. van den Doel, et al. (2002). "Conditionally replicative adenovirus expressing p53 exhibits enhanced oncolytic potency." Cancer Res **62**(21): 6165-6171.
van Bokhoven, A., M. Varella-Garcia, et al. (2003). "Molecular characterization of human prostate carcinoma cell lines." Prostate **57**(3): 205-225.
van de Wijngaart, D. J., H. J. Dubbink, et al. (2012). "Androgen receptor coregulators: recruitment via the coactivator binding groove." Mol Cell Endocrinol **352**(1-2): 57-69.
van Houdt, W. J., F. J. Hoogwater, et al. (2010). "Oncogenic KRAS desensitizes colorectal tumor cells to epidermal growth factor receptor inhibition and activation." Neoplasia **12**(6): 443-452.
van Royen, M. E., W. A. van Cappellen, et al. (2012). "Stepwise androgen receptor dimerization." J Cell Sci **125**(Pt 8): 1970-1979.
Velculescu, V. E. and W. S. El-Deiry (1996). "Biological and clinical importance of the p53 tumor suppressor gene." Clin Chem **42**(6 Pt 1): 858-868.
Veldscholte, J., C. A. Berrevoets, et al. (1992). "The androgen receptor in LNCaP cells contains a mutation in the ligand binding domain which affects steroid binding characteristics and response to antiandrogens." J Steroid Biochem Mol Biol **41**(3-8): 665-669.
Verrijdt, G., A. Haelens, et al. (2003). "Selective DNA recognition by the androgen receptor as a mechanism for hormone-specific regulation of gene expression." Mol Genet Metab **78**(3): 175-185.
Vilgelm, A. E., M. K. Washington, et al. (2010). "Interactions of the p53 protein family in cellular stress response in gastrointestinal tumors." Mol Cancer Ther **9**(3): 693-705.
Villaronga, M. A., D. N. Lavery, et al. (2009). "HEY1 Leu94Met gene polymorphism dramatically modifies its biological functions." Oncogene **29**(3): 411-420.
Vitale, I., L. Galluzzi, et al. (2011). "Mitotic catastrophe: a mechanism for avoiding genomic instability." Nat Rev Mol Cell Biol **12**(6): 385-392.
Vitale, I., L. Senovilla, et al. (2010). "Multipolar mitosis of tetraploid cells: inhibition by p53 and dependency on Mos." EMBO J **29**(7): 1272-1284.
Vogelstein, B., D. Lane, et al. (2000). "Surfing the p53 network." Nature **408**(6810): 307-310.
Walsh, J. G., S. P. Cullen, et al. (2008). "Executioner caspase-3 and caspase-7 are functionally distinct proteases." Proc Natl Acad Sci U S A **105**(35): 12815-12819.
Waltering, K. K., M. A. Helenius, et al. (2009). "Increased expression of androgen receptor sensitizes prostate cancer cells to low levels of androgens." Cancer Res **69**(20): 8141-8149.
Wang, C., R. Qi, et al. (2009). "Notch1 signaling sensitizes tumor necrosis factor-related apoptosis-inducing ligand-induced apoptosis in human hepatocellular carcinoma cells by inhibiting Akt/Hdm2-mediated p53 degradation and up-regulating p53-dependent DR5 expression." J Biol Chem **284**(24): 16183-16190.
Wang, H., Z. Y. Li, et al. (2011). "Desmoglein 2 is a receptor for adenovirus serotypes 3, 7, 11 and 14." Nat Med **17**(1): 96-104.

Wang, H., D. Sun, et al. (2008). "An AR-Skp2 pathway for proliferation of androgen-dependent prostate-cancer cells." J Cell Sci **121**(Pt 15): 2578-2587.
Wang, H., D. Yu, et al. (2003). "Experimental therapy of human prostate cancer by inhibiting MDM2 expression with novel mixed-backbone antisense oligonucleotides: in vitro and in vivo activities and mechanisms." Prostate **54**(3): 194-205.
Wang, J., Y. Cai, et al. (2008). "Pleiotropic biological activities of alternatively spliced TMPRSS2/ERG fusion gene transcripts." Cancer Res **68**(20): 8516-8524.
Wang, L., C. L. Hsu, et al. (2004). "Human checkpoint protein hRad9 functions as a negative coregulator to repress androgen receptor transactivation in prostate cancer cells." Mol Cell Biol **24**(5): 2202-2213.
Wang, P., S. M. Henning, et al. (2010). "Limitations of MTT and MTS-based assays for measurement of antiproliferative activity of green tea polyphenols." PLoS One **5**(4): e10202.
Wang, Q., W. Li, et al. (2009). "Androgen receptor regulates a distinct transcription program in androgen-independent prostate cancer." Cell **138**(2): 245-256.
Wang, R., P. Cherukuri, et al. (2005). "Activation of Stat3 sequence-specific DNA binding and transcription by p300/CREB-binding protein-mediated acetylation." J Biol Chem **280**(12): 11528-11534.
Wang, X., M. Kruithof-de Julio, et al. (2009). "A luminal epithelial stem cell that is a cell of origin for prostate cancer." Nature **461**(7263): 495-500.
Wang, X., C. Su, et al. (2008). "A novel triple-regulated oncolytic adenovirus carrying p53 gene exerts potent antitumor efficacy on common human solid cancers." Mol Cancer Ther **7**(6): 1598-1603.
Wang, X. D., C. C. Leow, et al. (2006). "Notch signaling is required for normal prostatic epithelial cell proliferation and differentiation." Dev Biol **290**(1): 66-80.
Wang, X. D., J. Shou, et al. (2004). "Notch1-expressing cells are indispensable for prostatic branching morphogenesis during development and re-growth following castration and androgen replacement." J Biol Chem **279**(23): 24733-24744.
Wang, Y., G. Hallden, et al. (2003). "E3 gene manipulations affect oncolytic adenovirus activity in immunocompetent tumor models." Nat Biotechnol **21**(11): 1328-1335.
Wang, Z., Y. Li, et al. (2010). "Down-regulation of Notch-1 and Jagged-1 inhibits prostate cancer cell growth, migration and invasion, and induces apoptosis via inactivation of Akt, mTOR, and NF-kappaB signaling pathways." J Cell Biochem **109**(4): 726-736.
Wen, Y., M. C. Hu, et al. (2000). "HER-2/neu promotes androgen-independent survival and growth of prostate cancer cells through the Akt pathway." Cancer Res **60**(24): 6841-6845.
Whelan, J. T., A. Kellogg, et al. (2009). "Notch-1 signaling is lost in prostate adenocarcinoma and promotes PTEN gene expression." J Cell Biochem **107**(5): 992-1001.
Whitacre, D. C., S. Chauhan, et al. (2002). "Androgen induction of in vitro prostate cell differentiation." Cell Growth Differ **13**(1): 1-11.
White, E. (2001). "Regulation of the cell cycle and apoptosis by the oncogenes of adenovirus." Oncogene **20**(54): 7836-7846.
Wiethoff, C. M., H. Wodrich, et al. (2005). "Adenovirus protein VI mediates membrane disruption following capsid disassembly." J Virol **79**(4): 1992-2000.

Williams, N., L. J. Hughes, et al. (2011). "Prostate-specific antigen testing rates remain low in UK general practice: a cross-sectional study in six English cities." BJU Int **108**(9): 1402-1408.
Xia, Z. J., J. H. Chang, et al. (2004). "[Phase III randomized clinical trial of intratumoral injection of E1B gene-deleted adenovirus (H101) combined with cisplatin-based chemotherapy in treating squamous cell cancer of head and neck or esophagus]." Ai Zheng **23**(12): 1666-1670.
Xu, J., R. C. Wu, et al. (2009). "Normal and cancer-related functions of the p160 steroid receptor co-activator (SRC) family." Nat Rev Cancer **9**(9): 615-630.
Xu, K., H. Shimelis, et al. (2009). "Regulation of androgen receptor transcriptional activity and specificity by RNF6-induced ubiquitination." Cancer Cell **15**(4): 270-282.
Xu, P., M. Qiu, et al. (2010). "The oncogenic roles of Notch1 in astrocytic gliomas in vitro and in vivo." J Neurooncol **97**(1): 41-51.
Yamada, H. Y. and G. J. Gorbsky (2006). "Spindle checkpoint function and cellular sensitivity to antimitotic drugs." Mol Cancer Ther **5**(12): 2963-2969.
Yang, J., M. Chatterjee-Kishore, et al. (2005). "Novel roles of unphosphorylated STAT3 in oncogenesis and transcriptional regulation." Cancer Res **65**(3): 939-947.
Yang, J. and R. A. Weinberg (2008). "Epithelial-mesenchymal transition: at the crossroads of development and tumor metastasis." Dev Cell **14**(6): 818-829.
Yang, L., L. Wang, et al. (2003). "Interleukin-6 differentially regulates androgen receptor transactivation via PI3K-Akt, STAT3, and MAPK, three distinct signal pathways in prostate cancer cells." Biochem Biophys Res Commun **305**(3): 462-469.
Yee, A. S., R. Reichel, et al. (1987). "Promoter interaction of the E1A-inducible factor E2F and its potential role in the formation of a multi-component complex." EMBO J **6**(7): 2061-2068.
Yeo, J. K., S. D. Cha, et al. (2002). "Se-methylselenocysteine induces apoptosis through caspase activation and Bax cleavage mediated by calpain in SKOV-3 ovarian cancer cells." Cancer Lett **182**(1): 83-92.
Yin, X. Y., L. Grove, et al. (1999). "C-myc overexpression and p53 loss cooperate to promote genomic instability." Oncogene **18**(5): 1177-1184.
Yuan, Z. L., Y. J. Guan, et al. (2005). "Stat3 dimerization regulated by reversible acetylation of a single lysine residue." Science **307**(5707): 269-273.
Zacal, N. J., M. A. Francis, et al. (2005). "Enhanced expression from the human cytomegalovirus immediate-early promoter in a non-replicating adenovirus encoded reporter gene following cellular exposure to chemical DNA damaging agents." Biochem Biophys Res Commun **332**(2): 441-449.
Zavadil, J., L. Cermak, et al. (2004). "Integration of TGF-beta/Smad and Jagged1/Notch signalling in epithelial-to-mesenchymal transition." EMBO J **23**(5): 1155-1165.
Zayzafoon, M., S. A. Abdulkadir, et al. (2004). "Notch signaling and ERK activation are important for the osteomimetic properties of prostate cancer bone metastatic cell lines." J Biol Chem **279**(5): 3662-3670.
Zhang, J. J., U. Vinkemeier, et al. (1996). "Two contact regions between Stat1 and CBP/p300 in interferon gamma signaling." Proc Natl Acad Sci U S A **93**(26): 15092-15096.
Zhang, N., Y. Yin, et al. (2008). "5-Fluorouracil: mechanisms of resistance and reversal strategies." Molecules **13**(8): 1551-1569.

Zhang, Q., H. Yao, et al. (2000). "Acetylation of adenovirus E1A regulates binding of the transcriptional corepressor CtBP." Proc Natl Acad Sci U S A **97**(26): 14323-14328.
Zhang, Y. and H. Lu (2009). "Signaling to p53: ribosomal proteins find their way." Cancer Cell **16**(5): 369-377.
Zhang, Y., Z. Wang, et al. (2006). "Down-regulation of Jagged-1 induces cell growth inhibition and S phase arrest in prostate cancer cells." Int J Cancer **119**(9): 2071-2077.
Zhang, Z., M. Li, et al. (2003). "Antisense therapy targeting MDM2 oncogene in prostate cancer: Effects on proliferation, apoptosis, multiple gene expression, and chemotherapy." Proc Natl Acad Sci U S A **100**(20): 11636-11641.
Zheng, C., Z. Ren, et al. (2009). "E2F1 Induces tumor cell survival via nuclear factor-kappaB-dependent induction of EGR1 transcription in prostate cancer cells." Cancer Res **69**(6): 2324-2331.
Zhu, M. L., C. M. Horbinski, et al. (2010). "Tubulin-targeting chemotherapy impairs androgen receptor activity in prostate cancer." Cancer Res **70**(20): 7992-8002.
Zhu, P., S. H. Baek, et al. (2006). "Macrophage/cancer cell interactions mediate hormone resistance by a nuclear receptor derepression pathway." Cell **124**(3): 615-629.